MYCOTAXON

THE INTERNATIONAL JOURNAL OF FUNGAL TAXONOMY & NOMENCLATURE

VOLUME 137 (1) JANUARY–MARCH 2022

Claviceps bavariensis sp. nov.
(Liu, Tanaka, Kolařík— FIG. 3, p. 81)

ISSN (PRINT) 0093-4666 https://doi.org/10.5248/137-1 ISSN (ONLINE) 2154-8889
MYXNAE 137(1): 1–172 (2022)

ISSN 0093-4666 (print)

ISSN 2154-8889 (online)

MYCOTAXON

THE INTERNATIONAL JOURNAL OF FUNGAL TAXONOMY & NOMENCLATURE

JANUARY–MARCH 2022

VOLUME 137 (1)

http://dx.doi.org/10.5248/137-1

www.mycotaxon.com &
www.ingentaconnect.com/content/mtax/mt
P.O. BOX 264, ITHACA, NY 14581-0264, USA

MYCOTAXON

VOLUME ONE HUNDRED THIRTY-SEVEN (1) — TABLE OF CONTENTS

Reviewers vi
Nomenclatural novelties & typifications vii
Corrigenda viii
From the Editor ix
2022 submission procedure xi

New genera & species

Phaeocollybia chefensis sp. nov. and new synonyms for *P. rifflipes, P. rufotubulina,* and *P. tibiikauffmanii*
Lorelei L. Norvell, Ronald L. Exeter, Matthew Gordon, Sahra-Taylor Mullineux, Scott A. Redhead 1

Beltrania shenzhenica sp. nov. from Guangdong Province, China
Zhao-Xue Zhang, Tai-Chang Mu, Zhuang Li, Xiu-Guo Zhang, Ji-Wen Xia 31

Termitomyces cryptogamus sp. nov. associated with *Macrotermes natalensis* in Africa
Lennart J.J. van de Peppel, Z. Wilhelm de Beer, Duur K. Aanen, Ben Auxier 41

Clitopiloides prati and *Trichopilus lecythiformis* spp. nov. from Australia
David L. Largent & Molly B. Cribari 51

Neoacrodictys elegans gen. & sp. nov. from Hainan Province, China
Ji-Wen Xia, Tai-Chang Mu, Zhao-Xue Zhang, Zhuang Li, Xiu-Guo Zhang 63

Neotypification of *Claviceps humidiphila* and recognition of *C. bavariensis* sp. nov.
Miao Liu, Eiji Tanaka, Miroslav Kolařík 73

New combination

Passalora golaghati comb. nov. from India
Gargee Singh, Sanjay Yadav, Raghvendra Singh, Shambhu Kumar 89

New ranges/hosts

Stigmatomyces aff. *limnophorae*
on dipteran hosts in Peninsular Malaysia
Natasha Azmi Nur Aliah, Jingyu Liu,
Nurul Azmiera, Chong Chin Heo 95

Pluteus variabilicolor and *Volvopluteus earlei,*
new records for Pakistan
Junaid Khan, Hassan Sher, Aiman Izhar,
Muhammad Haqnawaz, Abdul Nasir Khalid 109

New Turkish records of *Hebeloma excedens* and *H. geminatum,*
and confirmation of *H. celatum*
Ayten Dizkirici, Aysenur Kalmer, İsmail Acar 123

Ganoderma multipileum and *Tomophagus cattienensis*—
new records from Pakistan
Aisha Umar, Shakil Ahmed,
Laura Guzmán-Dávalos, Milay Cabarroi-Hernández 135

Marasmius tageticolor and *M. tucumanus*
from the Dominican Republic
Nicolás Niveiro, Natalia A. Ramírez, Claudio Angelini 153

Mycobiota (Funga) new to the Mycotaxon website
New records of *Chaetomium* and *Chaetomium*-like species
(*Ascomycota, Chaetomiaceae*) on *Syagrus coronata*
from the Raso da Catarina Ecological Station (ESEC),
Caatinga, Bahia, Brazil (summary)
Nilo Gabriel Soares Fortes & Nadja Santos Vitória 171

Reviewers — volume one hundred thirty-seven (1)

The Editors express their appreciation to the following individuals who have, prior to acceptance for publication, reviewed one or more of the papers prepared for this issue.

Mustafa Emre Akçay
Joe Ammirati
Flavia Rodrigues Barbosa
Timothy J. Baroni
Sarah Bergemann
R.F. Castañeda Ruiz
Tobias Guldberg Frøslev
Danny Haelewaters
Egon Horak
Alfredo Justo
Abdullah Kaya
Rachel A. Koch
N'golo Abdoulaye Koné
Jian Ma
Li-Guo Ma
Brandon Matheny
Roger Fagner Ribeiro Melo
Nelson Menolli Jr.
Lorelei L. Norvell
Jadson José Souza de Oliveira
Shaun R. Pennycook
Walter P. Pfliegler
Mario Rajchenberg
Scott A. Redhead
Gerardo Robledo
Michelline Lins Silvério
Adna Cristina Barbosa de Sousa
Joey B. Tanney

Nomenclatural novelties and typifications proposed in Mycotaxon 137(1)

Beltrania shenzhenica Z.X Zhang, J.W. Xia & X.G. Zhang
[MB 839268], p. 36

Claviceps bavariensis M. Kolařík, E. Tanaka & M. Liu
[MB 838352] p. 80

Claviceps humidiphila Pažoutová & M. Kolařík 2015 (neotypified)
[MBT 395372], p. 78

Clitopiloides prati Largent
[IF 558177], p. 53

Neoacrodictys J.W. Xia & X.G. Zhang
[MB 816515], p. 66

Neoacrodictys elegans J.W. Xia & X.G. Zhang
[MB 816516], p. 66

Passalora golaghati (Saikia & Sarbhoy) Gargee Singh, Sanj. Yadav, Raghv. Singh & Sh. Kumar
[MB 835579], p. 90

Phaeocollybia chefensis Norvell & Exeter
[IF 559441], p. 12

Termitomyces cryptogamus van de Peppel
[MB 838129], p. 44

Trichopilus lecythiformis Largent
[IF 558178], p. 56

Corrigenda

Mycotaxon 136(4)

p. v, line 9 FOR: Five new foliicolous micromycete records from Turkey
READ: Additions to the knowledge of foliicolous micromycetes in Turkey

From the Editor-in-Chief

Late again! — Unseasonal snowfalls, power & computer outages at critical times, the Covid Omicron variant in New Zealand, time-consuming medical treatments in Oregon, research obligations, and fewer final submissions (despite a last-minute 25-day extended deadline) have all conspired to delay our 2022 January–March Mycotaxon. Your editors regret the unavoidable delay and heartily thank all authors for their extreme patience. The good news is that nomenclatural reviews are now being returned very quickly by a recovered *Nomenclature Editor* and soon-to-be acknowledged final submissions are arriving at an equally brisk pace. Being realistic, we suspect the April–June issue will probably go out in early (if lucky) July rather than late June, but your two volunteer editors are valiantly trying to bring back the journal to the quick turn-around its founders intended. Welcome to the slim—but mighty—Mycotaxon 137(1).

Our 2022 January–March Mycotaxon may indeed be slender, but it offers a wide variety of truly fascinating papers. There are 13 contributions by 49 authors (representing 16 countries) as revised by 28 expert reviewers and the editors.

The new genera & species section proposes one new genus (*Neoacrodictys* from China) and seven species new to science representing *Beltrania & Neoacrodictys* from China; *Claviceps* from Germany; *Clitopiloides & Trichopilus* from Australia; *Phaeocollybia* from the U.S.A.; and *Termitomyces* from South Africa. We also offer one new combination in *Passalora* from India, and one newly registered neotypification for *Claviceps humidiphila* from its type locality in Japan.

The New ranges/hosts section contains five titles. Species range extensions are reported for [basidiomycetes] *Ganoderma* & *Tomophagus* and *Pluteus* & *Volvopluteus* from Pakistan; *Hebeloma* from Turkey; *Marasmius* from the Dominican Republic; and [laboulbeniomycetes] a possible new *Stigmatomyces* species from Malaysia. New dipteran hosts (*Boettcherisca* and *Hypopygiopsis* [the first for any laboulbenialean species] are cited for *Stigmatomyces*. Mycotaxon 137(1) also provides keys to species in *Neoacrodictys, Passalora,* and *Phaeocollybia* (the last also proposing three long-awaited synonymies). And a first: papers providing conclusions supported by sequence analyses include all seven newly described species (including one cryptospecies diagnosed by sequence data alone—for good reason) and all eleven range extensions.

Our issue concludes with the announcement of a new annotated species list on our mycobiota website, which describes and illustrates six new records and includes a key to *Chaetomium* and *Chaetomium*-like species in one Caatinga ecological research station in Brazil

Warm regards,
Lorelei L. Norvell (*Editor-in-Chief*)
20 April 2022

publication date for volume one hundred thirty-six (4)

MYCOTAXON *for* October–December 2021 (i–xlviii + 693–880)
was issued on February 8, 2022

2022 Mycotaxon submission procedure

Prospective Mycotaxon authors should download the Mycotaxon 2022 guide, review & submission forms, and Mycotaxon sample manuscript by clicking the 'file download page' link on our Instructions to Authors page before preparing their manuscript. This page briefly summarizes our '4-step' submission process.

1—Peer review: Authors first contact peer reviewers (two for journal papers; three for mycobiota/fungae) before sending them formatted text & illustration files and the appropriate 2022 Mycotaxon journal or mycota reviewer comment form. Experts return revisions & comments to both the *Editor-in-Chief* <editor@mycotaxon.com> and authors. All co-authors must correct and *proof-read* their files before submitting them to the *Nomenclature Editor*.

2—Nomenclatural review: Authors email all **error-free** text & illustration files to the *Nomenclature Editor* <PennycookS@LandcareResearch.co.nz>. Place **first author surname** + **genus** + 'Mycotaxon' on the subject line, and (required) attach a completed submission form. The Nomenclature Editor will (i) immediately assign the accession number and (ii) after a few weeks return his notes and suggested revisions to the author(s) and *Editor-in-Chief*.

3—Final submission: All coauthors thoroughly revise and proof-read files to prepare error-free text and images ready for immediate publication. Poorly formatted copy will be rejected or returned for revision. E-mail the final manuscript to the *Editor-in-Chief* <editor@mycotaxon.com>, adding the **accession number** to the message and **all** files, which include a **(i)** revised 2022 submission form, all **(ii)** text files and **(iii)** jpg images, and **(iv)** FN, IF, or MB identifier verifications for each new name or typification. The *Editor-in-Chief* acknowledges submissions within two weeks of final submission but requests authors to wait at least 14 days before sending a follow-up query (without attachments).

4—Final editorial review & publication: The *Editor-in-Chief* conducts a final grammatical and scientific review and returns her editorial revisions to all expert reviewers and coauthors for final author approval. Author-approved files are placed in the publication queue.

The PDF proof and bibliographic & nomenclatural index entries are sent to all coauthors for final inspection. After PDF processing, the *Editor-in-Chief* corrects only PDF editorial/conversion and index entry errors; corrections of all other errors are listed in the Errata of a subsequent issue for no charge. Authors will pay fees for mycobiota uploads, optional open access, and correction of major author errors to the *Business Manager* <subscriptions@mycotaxon.com> at this time.

Mycotaxon ltd— www.mycotaxon.com

The Mycotaxon *Webmaster* <mycotaxon@gmail.com> posts announcements, subscription & publication information, and author forms & templates on the official Mycotaxon site. Our server also hosts the mycobiota web-page for free download of Fungae (regional annotated species lists).

Mycotaxon online— www.ingentaconnect.com/content/mtax/mt

The Mycotaxon journal publishes four quarterly issues per year. Both open access and subscription articles are offered.

MYCOTAXON

ISSN (print) 0093-4666 (online) 2154-8889 Mycotaxon, Ltd. ©2022

January–March 2022—Volume 137, pp. 1–30

https://doi.org/10.5248/137.1

Phaeocollybia chefensis sp. nov. and new synonyms for *P. rifflipes, P. rufotubulina,* and *P. tibiikauffmanii*

Lorelei L. Norvell[1*], Ronald L. Exeter[2], Matthew Gordon[3], Sahra-Taylor Mullineux[4], Scott A. Redhead[4]

[1] *Pacific Northwest Mycology Service, 6720 NW Skyline, Portland OR 97229 USA*

[2] *2477 SW Maplewood Drive, Dallas OR 97338 USA*

[3] *Molecular Solutions, 4216 N. Castle Ave., Portland OR 97217 USA*

[4] *National Mycological Herbarium (DAOM), Agriculture & Agri-Food Canada, 960 Carling Avenue, Ottawa ON K1A 0C6 Canada*

*Correspondence to: *llnorvell@pnw-ms.com*

Abstract—Phylogenetic analyses of ITS and RBP2 sequence data from *Phaeocollybia* collections made at Cascade Head Experimental Forest in Oregon support recognition of a new species, *P. chefensis.* Collections of the new species were previously referred to *P. tibiikauffmanii.* Sequence analyses also establish that *P. tibiikauffmanii* is a synonym of *P. spadicea, P. rifflipes* is a synonym of *P. lilacifolia,* and *P. rufotubulina* is a synonym of *P. californica.* A revised general key to Pacific Northwest *Phaeocollybia* species is provided.

Key words—*Basidiomycota, Hymenogastraceae,* nomenclature, Northwest Forest Plan, taxonomy

Introduction

Phaeocollybia R. Heim (*Agaricomycetes, Hymenogastraceae*) is a genus of brown-spored agarics characterized by conic-campanulate pilei, cartilaginous stipes and pseudorhizae, ornamented 'beaked' basidiospores, sarcodimitic tissue, monovelangiocarpy, and tibiiform diverticula that arise from the mycelium and primordial pellicular remnants (Norvell 1998a,b; Norvell & Exeter 2009). The forests of western North America have provided an exceptionally large number of species in this genus (Murrill 1911; Smith 1937, 1957a,b; Smith & Trappe 1972; Redhead & Norvell 1993; Norvell 1998a,b,

2000, 2002, 2004; Norvell & Redhead 2000, Norvell & Exeter 2007, 2009; Norvell & al. 2010).

In 1995 the first author collected a solitary tawny colored *Phaeocollybia* from Oregon's Cascade Head Experimental Forest (CHEF). Although the specimen's general morphology resembled that of *P. kauffmanii* (A.H. Sm.) Singer, it differed by possessing abundant refractive tibiiform cheilocystidia, prompting application of the provisional name *P. tibiikauffmanii* to the Oregon coast taxon in Norvell's 1998 doctoral dissertation.

The author's research on *Phaeocollybia* coincided with establishment of the Northwest Forest Plan (NWFP; USDA-USDI 1994), which listed 14 phaeocollybias among its 234 fungal species of concern (Castellano & al. 1999, 2003; ORBIC 2021). In 1998 transects were established for surveying epigeous ectomycorrhizal basidiomycetes in Benton County's Bureau of Land Management (BLM) Green Peak Density Management Study and Polk County's BLM Fungal Chronosequence Study (Norvell & Exeter 2004). Numerous gregarious to caespitose clusters of *P. kauffmanii*-like specimens with tibiiform cheilocystidia were collected that matched the solitary 1995 specimen from Lincoln County. After morphological comparison with other specimens from Washington, Oregon, and California, a particularly well-documented collection from the chronosequence 'old growth' study transect (approximately 64 km from the CHEF site) was selected as type for *P. tibiikauffmanii* (Norvell 2004).

In 2008, the U.S. Forest Service (FS) & BLM Interagency Special Status/ Sensitive Species Program initiated a project to generate DNA sequence data for *Phaeocollybia* specimens (Gordon 2009). Since then, 350 sequences for the internal transcribed spacer region (ITS1-5.8S rRNA-ITS2) in the nuclear ribosomal RNA gene cassette and 46 sequences of a portion of the gene encoding the second largest subunit in the DNA-directed RNA polymerase (RPB2) were deposited in GenBank. These data, along with NWFP surveys, have provided several hundred *Phaeocollybia* collections for taxonomic and genetic analysis, and serve as an excellent resource for phylogenetic analyses and specific primer design.

Initial molecular analyses that clustered *P. tibiikauffmanii* and *P. spadicea* sequences within one intermixed clade were received on the same day as the arrival of the galley proofs for *Phaeocollybia* of Pacific Northwest North America (Norvell & Exeter 2009). Although the vital data arrived too late for a thorough publication revision, the authors annotated their keys and commentaries in anticipation of subsequent taxonomic changes.

Additional ITS sequence analyses confirmed the synonymy of *P. spadicea* and *P. tibiikauffmanii* but also supported newly collected material from the original Lincoln County '*tibiikauffmanii*' site as a distinct species, independent of *P. spadicea*.

A revised ITS-based phylogeny of *Phaeocollybia* was presented in the Norvell & al. (2010) poster at the International Mycological Congress in Edinburgh. In this paper we provide additional ITS and RPB2 sequence data that establish *P. chefensis* as a new species and formally publish synonymies for *P. californica* (= *P. rufotubulina*), *P. lilacifolia* (= *P. rifflipes*), and *P. spadicea* (= *P. tibiikauffmanii*).

Materials & methods

Collections

Specimen collection and examination, ultraviolet inspection, and syringaldazine spot tests of fresh material followed procedures outlined in Norvell & Exeter (2009), where morphotaxonomic terms (e.g., tibiiform diverticula, sarcodimitic tissues, pellicular veil, vertical-monopodial, and rhizomorphic pseudorhizae) are also defined. Parenthesized color references from Ridgway (1912: e.g., "Pale Pinkish Cinnamon") accompany colors of fresh specimens described in general non-standardized color names in lower case. Microscopical examinations were made of fresh tissues in H_2O or (for the type material) dried tissues rehydrated in 6% aqueous KOH. Basidiospores were taken from the stipe apex. Dimensions of all anatomical cells follow the format n (number measured): (outlier)low–average–high(outlier) [e.g., basidia n = 19: 25–34.2–41(43) × 6.5–8.1–9.4(9.9) µm].

Collector abbreviations include LLN (Norvell), RLE (Exeter), and SAR (Redhead). Latitude/longitude geographic coordinates were converted and rounded to four decimal places from surveyor input using [for TRS] https://www.earthpoint.us/TownshipsSearchByDescription.aspx and [for UTM] https://www.ngs.noaa.gov/NCAT/.

Vegetation abbreviations follow those used during Northwest Forest Plan surveys and include (in all caps for overstory) ABPR (*Abies procera* Rehder), PISI (*Picea sitchensis* (Bong.) Carr.), PSME (*Pseudotsuga menziesii* (Mirbel) Franco), and TSHE (*Tsuga heterophylla* (Raf.) Sarg.) and (in small caps for understory) BENE (*Berberis nervosa* Pursh = *Mahonia nervosa* (Pursh) Nutt., the preferred synonym), GASH (*Gaultheria shallon* Pursh), OXOR (*Oxalis oregana* Nutt.), POMU (*Polystichum munitum* (Kaulf.) C. Presl), VAOV (*Vaccinium ovatum* Pursh), and VAPA (*Vaccinium parviflorum* Andrews = *Gaylussacia baccata* (Wangenh.) K. Koch, the preferred synonym).

Material cited in the SPECIMENS EXAMINED sections is housed (unless otherwise specified) in Norvell's Pacific Northwest Mycology Service fungarium (PNW) and will be distributed among DAOM, NY, OSC, PNW, and WTU after publication. Herbarium acronyms follow Thiers (2021).

Table 1: PNW *Phaeocollybia* ITS & RPB2 sequence data. (Type data in bold).

Species	Coll./Fung. number	ITS	RGB2	County, State/Prov; Primary collector
ammiratii	**LLN1941028-10-T**	**JN102495**	**—**	**Clackamas, OR; Norvell**
	LLN2051018-01	GQ165629	—	Skamania, WA; Norvell
	OSC 155802	KJ450913	—	Coos, OR; Rodenkirk
	RLE2007-103	(GQ165627)	KU574760	Benton, OR; Exeter
	RLE2007-105	GQ165624	KU574759	Polk, OR; Exeter
	RLE2008-068	KX574502	—	Benton, OR; Exeter
	RLE2009-19	JN102493	KU574787	Benton, OR; Exeter
	RLE2009-31	JN102494	KU574790	Benton, OR; Exeter
	RLE2009-41	KX574503	—	Benton, OR; Exeter
attenuata	LLN2071029-51	JN102501	—	Benton, OR; Norvell
	RLE2007-026	MZ352106	KU574794	Lincoln, OR; Exeter
	RLE2007-090	JN102498	—	Benton, OR; Exeter
	RLE2007-176	(GQ165632)	KU574761	Benton, OR; Exeter
benzokauffmanii	**LLN1921120-01-T**	**GQ165636**	**—**	**Mendocino, CA; Norvell**
	RLE2007-035	GQ165636	—	Benton, OR; Exeter
	RLE2009-15	(JN102502)	KU574785	Benton, OR; Exeter
californica	**MICH 11607-T**	**JN102503**	—	**Del Norte, CA; Smith**
	OSC 109290	EU669240	—	Linn, OR; Smith
	OSC 109332	EU846292	—	Josephine, OR; Friend
	RLE2007-177	GQ165647	KU574764	Benton, OR; Exeter
	RLE2010-05	JN102504		Benton, OR; Exeter
#	**LLN1921116-1 ruf-T**	**GQ165707**	—	**Mendocino, CA; Norvell**
#	SAR7500	GQ165708	—	Mendocino, CA; Redhead
chefensis	**RLE2009-04-T**	**MZ352102**	**KU57484**	**Lincoln, OR; Exeter**
	LLN2091026cc6a	MZ352101	—	Benton, OR; Norvell
	OSC 155803	MK326851	—	Polk, OR; Christensen
	RLE2007-074	MZ352097	KU574779	Lincoln, OR; Exeter
	RLE2007-129	MZ352096	—	Lane, OR; Exeter
dissiliens	OSC 114217	EU846271	—	Coos, OR; Sperling
	RLE2008-138	KF219569	KU574767	Benton, OR; Exeter
fallax	LLN1921007-01	JN102512	—	Vancouver Isl. BC; Redhead
	RLE2004-01	JN102511	—	Benton, OR; Exeter
	RLE2007-140	MZ352103	KU574791	Benton, OR; Exeter
	RLE2007-159	JN102516	KU574795	Benton, OR; Exeter
	RLE2007-175	JN102518	KU574796	Benton, OR; Exeter

Species	Coll./Fung. number	ITS	RGB2	County, State/Prov; Primary collector
gregaria	LLN2091026cg8	JN102520	—	Benton, OR; Norvell
	RLE2007-061	GQ165652	—	Lincoln, OR; Exeter
	RLE2008-026	GQ165654	KU574772	Polk, OR; Exeter
	RLE2013-07b	KJ450915	—	Polk, OR; Exeter
kauffmanii	LLN1931015-02	JN102542	—	Clallam, WA; Leuthy
	RLE2006-10	KF219573	KU574782	Benton, OR; Exeter
	RLE2006-13	JN102547	—	Benton, OR; Exeter
	RLE2007-095	JN102524	—	Polk, OR; Exeter
	RLE2008-027	KF219572	KU574781	Polk, OR; Exeter
	RLE2008-045	JN102526	—	Lane, OR; Exeter
lilacifolia	LLN1921111-06	KF219576	—	Clackamas, OR; Norvell
	LLN2071018-12	GQ165657	KU574763	Lincoln, OR; Exeter
^	RLE2006-43	KF219580	—	Polk, OR; Exeter
^	RLE2013-44	—	KU574803	Lane, OR; Exeter
luteosquamulosa	LLN2071029-33	GQ165668	KU574774	Benton, OR; Norvell
	LLN2071029-43	GQ165667	—	Benton, OR; Norvell
	RLE2007-016	GQ165663	—	Lincoln, OR; Exeter
	WTU-F-003084	JN102528	—	Snohomish, WA; Ammirati
ochraceocana	**RLE2007-033-T**	**GQ165674**	**KU574775**	**Polk, OR; Exeter**
	OSC 134678	GQ165672	—	Benton, OR; Villella
	OSC 134679	GQ165671	—	Tillamook, OR; Paque
	RLE2007-009	GQ165673	—	Polk, OR; Exeter
olivacea	LLN1921015-03	JN102533	—	Jefferson, WA; Norvell
	LLN1921122-04	JN102530	—	Mendocino, CA; Norvell
	LLN1941128-01	JN102532	—	Clackamas, OR; Norvell
	OSC 109501	EU846281	—	Coos, OR; Sperling
	OSC 113875	EU846282	—	Douglas, OR; Kersens
	RLE2007-122	JN102534	KU574798	Benton, OR; Exeter
	RLE2007-133	JN102535	KU574799	Lane, OR; Exeter
	RLE2008-050	MZ352094	KU574766	Lane, OR; Exeter
	RLE2008-051	JN102536	—	Benton, OR; Exeter
	RLE2008-129	GQ165678	KU574776	Benton, OR; Exeter
oregonensis	LLN2001105-01	GQ165681	—	Multnomah, OR; Norvell
	OSC 67425	EU846273	—	Douglas, OR; Goldenberg
	RLE2006-16	GQ165685	—	Lane, OR; Exeter
	RLE2013-42	—	KU574804	Lane, OR; Exeter

Species	Coll./Fung. number	ITS	RGB2	County, State/Prov; Primary collector
phaeogaleroides	**RLE199-064a-T**	**OM065392**	**—**	**Benton, OR; Exeter**
	RLE2009-29a	MF737171	KU57489	Benton, OR; Exeter
	RLE2010-086	KX574499	—	Benton, OR; Exeter
piceae	**MICH 11629-T**	**MF737169**	**—**	**Tillamook, OR; Smith**
	RLE2007-178	(MZ352093)	KU574762	Mendocino CA; Bojantchev
	RLE2009-12	KF219583	—	Benton, OR; Exeter
pleurocystidiata	**LLN1940330-02-isoT**	**GQ165688**	**—**	**Clallam WA; Norvell**
	LLN1930516-01	GQ165686	—	Linn, OR; Bailey
	RLE2008-002	GQ165687	KU574765	Benton, OR; Exeter
pseudofestiva	LLN1921104-10	KF219588	—	Multnomah, OR; Norvell
	RLE2007-069	KF219589	KU574797	Lincoln, OR; Exeter
	RLE2007-070	KF219590	—	Lincoln, OR; Exeter
radicata	OSC 112980	EU846275	—	Coos, OR; Rodenkirk
	RLE2006-19	GQ165696	—	Benton, OR; Exeter
	RLE2008-131	GQ165695	KU574771	Benton, OR; Exeter
redheadii	LLN2071018-17	JN102544	—	Lincoln, OR; Norvell
	LLN2091026cg18	JN102541	—	Benton, OR; Norvell
	RLE2007-106	JN102546	—	Polk, OR; Exeter
	RLE2008-038	MZ352098	KU574783	Lincoln, OR; Exeter
scatesiae	LLN1921015-19	GQ165701	—	Jefferson, WA; McClenaghan
	LLN1931104-09	GQ165703	—	Lincoln, OR; Norvell
	LLN2071029-02	GQ165699	KU574768	Benton, OR; Norvell
	RLE2007-151	GQ165700	KU574769	Benton, OR; Exeter
sipei	LLN1971023-69	EU644706	—	Benton, OR; Norvell
	OSC 96908	EU644707	—	Linn, OR; Bacheller
	RLE2007-123	GQ165704	KU574773	Benton, OR; Exeter
spadicea	OSC 112482	EU697252	—	Benton, OR; Giachini
	OSC 113791	EU669364	—	Douglas, OR; Wetzel
	OSC 134542	MZ352099	—	Douglas, OR; Sperling
	RLE2009-18	JN102550	KU574786	Benton, OR; Exeter
	RLE2009-20	JN102551	KU574788	Benton, OR; Exeter
*	**A2011031ox1 tib-T**	**KF219597**	**KU574780**	Polk, OR; Norvell
*	A2061114o2-O	KF219596	KU574778	Polk, OR; Norvell
*	RLE2007-165	(KF219594)	KU574777	Benton, OR; Exeter
P. sp. 1	OSC 155805	JN102507	KU574793	Lane, OR; Loring
	RLE2010-05	JN102504	—	Benton, OR; Exeter
	RLE2014-01	KU574726	KU574801	Benton, OR; Exeter

Species	Coll./Fung. number	ITS	RGB2	County, State/Prov; Primary collector
P. sp. 2	RLE2009-09	KX574498	—	Benton, OR; Exeter
	RLE2010-109	KX575400	—	Benton, OR; Exeter
P. sp. 3	LLN2071029-53	(KF219598)	KU574770	Benton, OR; Norvell
	RLE2007-100	KX574493	—	Polk, OR; Exeter
	RLE2007-152	KF219600	—	Benton, OR; Exeter
	RLE2015-35	KU574725	KU574800	Benton, OR; Exeter
P. sp. 4	RLE2010-009	MZ352104	KU574792	Benton, OR; Exeter
	RLE2015-01	KX574505	—	Benton, OR; Exeter
	RLE2015-06	KU574727	KU574802	Benton, OR; Exeter
P. sp. 5	OSC 155806	MF957115	—	Josephine, OR; Scelza
	RLE2013-14	KJ450918	—	Benton, OR; Exeter
P. sp. 6	OSC 134575	GQ165677	—	Linn, OR; Nakvasil
	OSC 151647	MH819350	MH823881	Douglas, OR; Scelza

= *P. rufotubulina,* ^ = *P. rifflipes,* and * = *tibiikauffmanii* in Norvell (1998ab, 2002, 2004) and Norvell & Exeter (2004, 2007, 2009).
(**T** = type); ITS sequences enclosed in parentheses not included in Fig. 1.

DNA amplification & sequencing

Standard protocols and published primers were followed for DNA extraction, PCR amplification, and sequencing (White & al 1990, Gardes & Bruns 1993, Liu & al. 1999, Matheny 2005). Amplifications of the ITS region from 350 *Phaeocollybia* collections representing 34 putative species utilized fungal primers ITS1 and ITS4b (Gardes & Bruns 1993). Amplifications of the RPB2 gene region from 46 collections representing 26 putative species utilized the degenerate basidiomycete specific primers bRPB2-6F and bRPB2-7.1R (Matheny 2005). Additionally, a new RPB2 forward primer, RPB2Phf (5′-GCAGAAACACCYGAGGGC-3′, slightly downstream from the bRPB2-6F primer) was designed based on existing *Phaeocollybia* RPB2 sequences and used successfully where the original primer pair failed after multiple attempts. In total 396 (350 ITS + 46 RPB2) new sequences were generated. Additional ITS and RPB2 sequences were added from GenBank to provide a comprehensive phylogeny for *Phaeocollybia* (Norvell & al. 2010, this publication). Table 1 provides collection and sequence data for PNW specimens, and Table 2 provides sequencing information for extralimital taxa and the outgroup cited in Figs 1 and 2.

Separate gene regions were initially aligned with Clustal X (Thompson & al. 1997). Subsequent new sequences were aligned manually in MacClade 4.0 (Maddison & Maddison 2000). Taxa for which gene regions were not sequenced were coded as missing. Sequences were aligned using MAFFT ver. 7 (Katoh & al. 2019) and manually corrected using MEGA X 10.0.0 (Kumar & al. 2018, Stecher & al. 2020). All new sequences were deposited in GenBank.

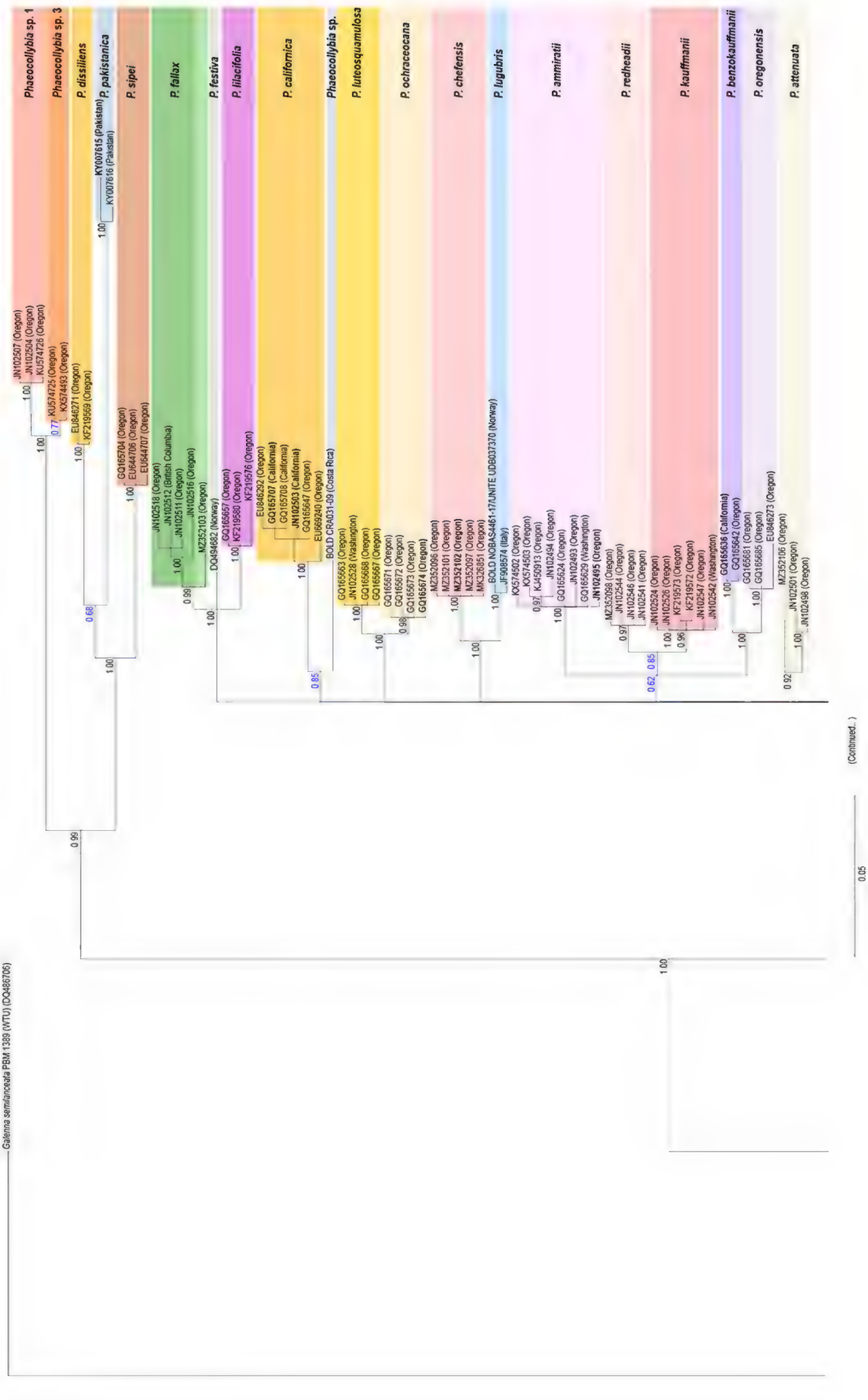
Galerina semilanceata PBM 1389 (WTU) (DQ486706)
0.05
(Continued...)
Phaeocollybia sp. 1
JN102507 (Oregon)
JN102504 (Oregon)
KU574726 (Oregon)
Phaeocollybia sp. 3
KU574725 (Oregon)
KX574493 (Oregon)
P. dissiliens
EU846271 (Oregon)
KF219569 (Oregon)
P. pakistanica
KY007615 (Pakistan)
KY007616 (Pakistan)
P. sipei
GQ165704 (Oregon)
EU844706 (Oregon)
EU844707 (Oregon)
P. fallax
JN102518 (Oregon)
JN102512 (British Columbia)
JN102511 (Oregon)
JN102516 (Oregon)
P. festiva
MZ352103 (Oregon)
DQ494682 (Norway)
P. lilacifolia
GQ165657 (Oregon)
KF219580 (Oregon)
KF219576 (Oregon)
P. californica
EU846232 (Oregon)
GQ165707 (California)
GQ165708 (California)
JN102503 (California)
GQ165647 (Oregon)
EU669240 (Oregon)
Phaeocollybia sp.
BOLD CRA031-09 (Costa Rica)
P. luteosquamulosa
GQ165663 (Oregon)
JN102528 (Washington)
GQ165668 (Oregon)
GQ165667 (Oregon)
P. ochraceocana
GQ165671 (Oregon)
GQ165672 (Oregon)
GQ165673 (Oregon)
GQ165674 (Oregon)
P. chefensis
MZ352096 (Oregon)
MZ352101 (Oregon)
MZ352102 (Oregon)
MZ352097 (Oregon)
MK326851 (Oregon)
P. lugubris
BOLD NOBAS4461-17UNITE UDB037370 (Norway)
JF908574 (Italy)
KX574502 (Oregon)
KX574503 (Oregon)
KJ450913 (Oregon)
P. ammiratii
JN102494 (Oregon)
GQ165624 (Oregon)
JN102493 (Oregon)
GQ165629 (Oregon)
JN102495 (Oregon)
P. redheadii
MZ352098 (Oregon)
JN102544 (Oregon)
JN102546 (Oregon)
JN102541 (Oregon)
P. kauffmanii
JN102524 (Oregon)
JN102526 (Oregon)
KF219573 (Oregon)
KF219572 (Oregon)
JN102547 (Oregon)
JN102542 (Washington)
P. benzokauffmanii
GQ165636 (California)
GQ165642 (Oregon)
P. oregonensis
GQ165681 (Oregon)
GQ165685 (Oregon)
EU846273 (Oregon)
P. attenuata
MZ352106 (Oregon)
JN102501 (Oregon)
JN102498 (Oregon)

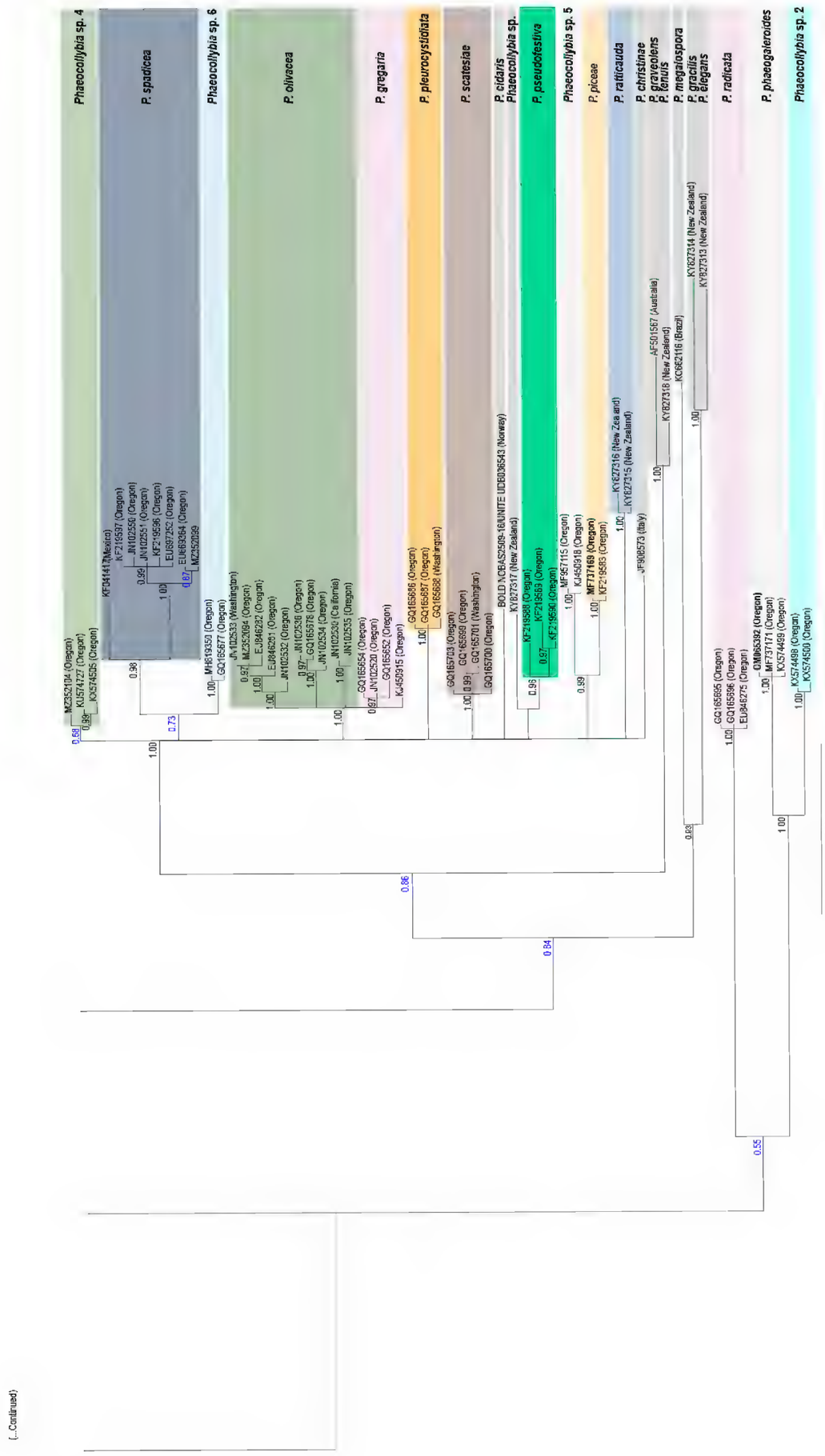

FIG. 1. Phylogenetic analysis of the ITS1-5.8S-ITS2 rDNA region in strains of *Phaeocollybia* spp. Branch lengths were determined using the Bayesian consensus outfile. Nodes with posterior probability values <0.90 are indicated in blue. Type strains are indicated in bold.

Table 2: Sequences from extralimital *Phaeocollybia* spp. and outgroup used in phylogenetic analyses

Species	Fungarium #	GenBank #	Country
christinae	MCVE 3539	JF908573	Italy
cidaris	O-F-252891	UDB036543	Norway
elegans	PDD 72723	KY827313	New Zealand
festiva (ITS)	WTU-F-053245	DQ494682	Norway
— (RPB2)	WTU-F-053245	AY509118	Norway
gracilis	PDD 88665	KY827314	New Zealand
graveolens	PERTH 5311586	AF501567	Australia
lugubris	O-F-253794	UDB037370	Norway
	MCVE 14619	JF908574	Italy
megalospora	SP 445402	KC662116	Brazil
pakistanica-**T**	SWAT 15-1560	KY007615	Pakistan
	SWAT 15-1561	KY007616	Pakistan
ratticauda	PDD 72678	KY827316	New Zealand
	PDD 72544	KY827315	New Zealand
tenuis	PDD 72672	KY827318	New Zealand
Phaeocollybia sp.	TRTC 157723	BOLD CRA031-09	Costa Rica
	AAM A1064	KF041417	Mexico
	PDD 71198	KY827317	New Zealand
Galerina semilanceata	WTU-F-007080	DQ486706	Washington USA
(RPB2 gene)	WTU-F-007080	AY337357	Washington USA

All sequences represent the ITS region unless otherwise indicated.

Sequence analyses

Sequences were analyzed using programs available in Geneious Prime (version 2021.2.2). Sequence data were obtained from NCBI and compiled into a multiple sequence alignment. The original ITS dataset contained 296 sequences identified as *Phaeocollybia* spp. Duplicate sequences were removed. Representative sequences for each taxon were retained and the final dataset, including the outgroup, comprised 129 unique sequences. Sequences were trimmed to remove the CATTA and GACCT motifs. For the analysis of partial RPB2 gene sequences, the dataset was composed of 49 unique sequences.

Sequences were aligned automatically using the Geneious alignment tool, and the alignment was refined manually. Phylogenetic analyses were carried out using the MrBayes 3.2.6 (Huelsenbeck & Ronquist 2001) plugin developed in Geneious. The following parameters were used: substitution model GTR; rate variation gamma; gamma categories 4; 5 million generations; subsampling frequency 1000; burnin

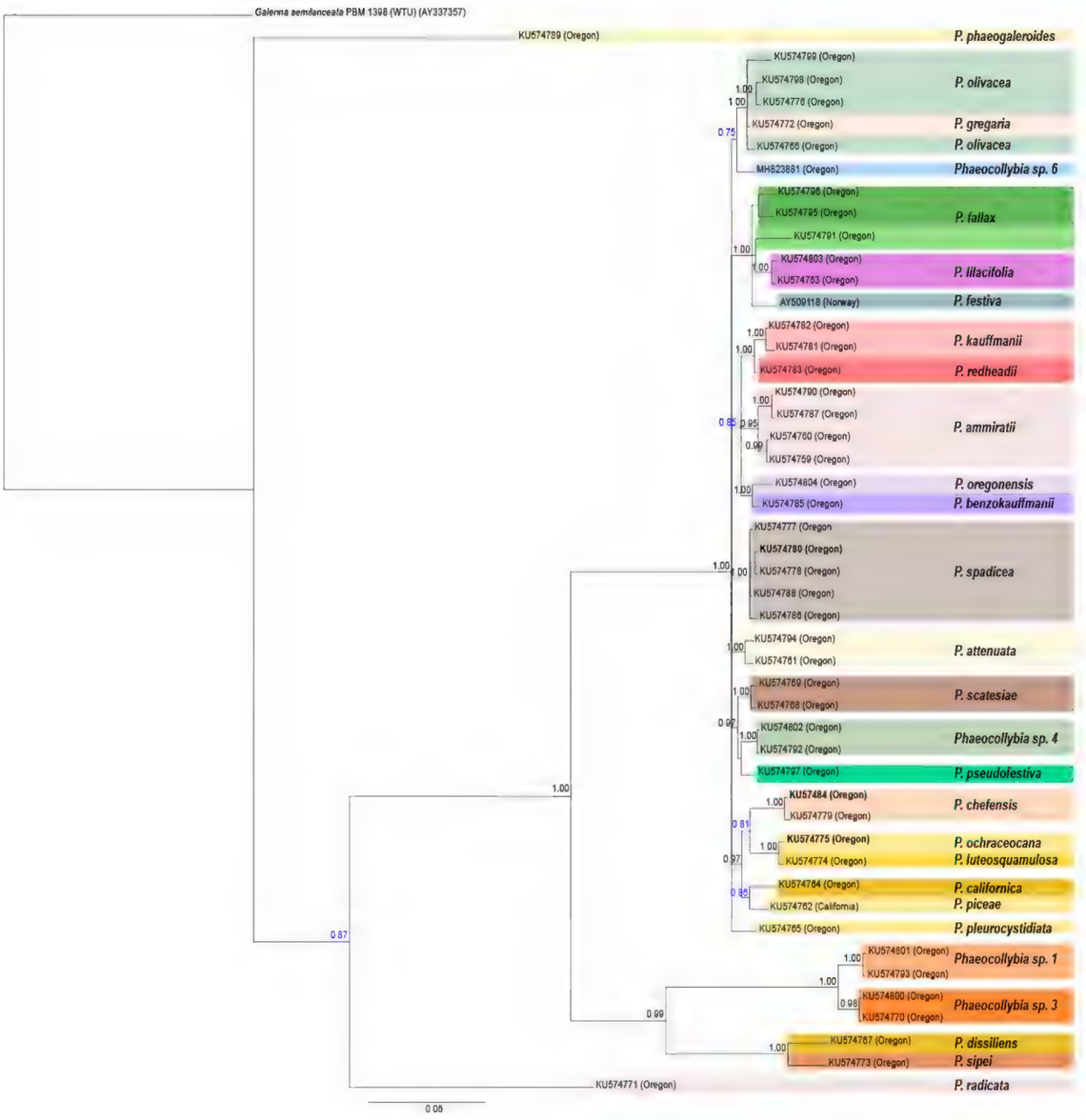

Fig. 2. Phylogenetic analysis of the partial RPB2 gene region in strains of *Phaeocollybia* spp. Branch lengths were determined using the Bayesian consensus outfile. Nodes with posterior probability values <0.90 are indicated in blue. Type strains are indicated in bold.

frequency 50%; heated chains 4; heated chain temperature 0.2; unconstrained branch lengths GammaDir (1, 0.1, 1, 1); and shape parameter exponential (10). The outgroup was *Galerina semilanceata* PBM 1398 (WTU); DQ486706 for the ITS analysis and AY337357 for the RPB2 analysis, respectively). Phylogenetic trees were drawn using the Bayesian consensus outfile and annotations were added using Inkscape 0.92.4.

Phylogenetic results

Figs 1–2

Norvell & al. (2010) presented the first comprehensive ITS phylogeny for the genus based on 300 *Phaeocollybia* sequences (including two from Australia—*P. graveolens* B.J. Rees & K. Syme, *P. ratticauda* E. Horak—and *P. festiva* (Fr.)

R. Heim from Norway) and the outgroup—*Hebeloma radicosum* (Bull.) Ricken, *Psilocybe semilanceata* (Fr.) P. Kumm., *Galerina marginata* (Batsch) Kühner—revealing a cohesive clade of 69 putative taxa with the *Galerina*-like *P. phaeogaleroides* clade in the basal-most position within *Phaeocollybia*. The current ITS tree (pruned to eliminate duplicates) confirms the existence of three synonymies, several difficult species complexes, and six unnamed species (Fig. 1). The three synonymies supported are *P. rifflipes* = *P. lilacifolia* (>99.7% similarity), *P. rufotubulina* = *P. californica* (>99.5% similarity), and *P. tibiikauffmanii* = *P. spadicea* (>99.8% similarity (Figs 1, 2).

The comprehensive ITS phylogeny (not shown) generated from 296 sequences (plus the outgroup *Inocybe pallidicremea* Grund & D.E. Stuntz [as *I. lilacina* (Peck) Kauffman)] and *Galerina semilanceata* (Peck) A.H. Sm. & Singer) and the trimmed 129-sequence ITS tree (Fig. 1) both support 29 PNW species and 14 extralimital putative taxa. A familial relationship between *Phaeocollybia* and *Galerina* is also supported, with both genera now classified in *Hymenogastraceae* (Matheny & al. 2006, Kalichman et al. 2020).

The successful amplification of far fewer (46) RPB2 sequences prohibits generating a robust multigene consensus tree. Nevertheless, both ITS (Fig. 1) and RPB2 (Fig. 2) trees support the same clades. With insufficient coverage across the genus for 28S sequence data and with the two-gene phylogeny well supported by convincing morphological characters, we do not include a 28S-based phylogeny at this time.

Taxonomy

Phaeocollybia chefensis Norvell & Exeter, **sp. nov.** Figs 3–6

IF 559441

Differs from *Phaeocollybia kauffmanii* by its tibiiform cheilocystidia and from *P. spadicea* by its uniformly carrot orange to orange-tawny coloration, larger basidiospores, and solitary to scattered (never gregarious or cespitose) habit.

Type: Oregon, Lincoln County, Cascade Head Experimental Forest, W of Hwy 12, 30 m S Tillamook Co. line, 45.0447°N 123.9153°W, 245 m asl, 27.x.2009, *Tsuga heterophylla* (old and young), *Picea sitchensis, Vaccinium parviflorum, Polystichum munitum,* RLE2009-04 (**holotype** OSC 155804, **isotype** PNW; GenBank MZ352102, KU574784).

Etymology: derived from the acronym (CHEF) for the type locality, Cascade Head Experimental Forest.

Pileus 70–80 mm diam, broadly conic-campanulate with acute papillate umbo, upturned inner margin, down-turned outer margin, and straight edge; glabrous, glutinous in rain with the gluten at times somewhat milky, non-striate, overall brownish orange or foxy brown (Tawny, Orange Cinnamon); dried

Ron Exeter

FIG. 3. *Phaeocollybia chefensis* (Holotype, RLE2009-04). TOP: excavated specimens with intact vertical monopodial pseudorhizae. BOTTOM: Two views of the type collection in situ in Cascade Head Experimental Forest, Lincoln County, Oregon. Five collections of 1–2 specimens were collected from this same site during 1995–2021.

pileus uniformly copper metallic. CONTEXT ~6 mm at the disc and confluent with stipitipith, pale orangish white. ODOR faintly floral with farinaceous overtones; TASTE mild, not distinctive. LAMELLAE nearly free, ventricose, thin with ± even edges, polydymous with 3–7 irregularly interspersed tiers of lamellulae, narrow (4–5 mm, with average length/width ratio 5.5), close, pale orangish buff (Warm Buff) when young, developing darker spots in maturity. VEIL sparse (when present, evident only as occasional darker fibrillose

remnants on stipe apex). Stipe slightly eccentric, terete, 80–90 mm above ground level, overall length including pseudorhiza ≤200 mm, apex 10–12 mm diam, ± equal above, gradually narrowing below toward pseudorhiza; glabrous except for occasional fibrils, moist, finely longitudinally lined, apex pale to deep pinkish orange (Pinkish Cinnamon, Orange Cinnamon) below grading to dull pinkish brown (Fawn Color), 2 mm thick cartilaginous rind surrounding compact fibrillose orangish white stipitipith, rind sometimes with small perpendicular separations producing ~5 mm long recurved rind patches. Pseudorhizal form vertical-monopodial, ≤2/3 overall stipe length, gradually tapering to pale salmon-colored pointed to blunt origin, firm pith brown where water-soaked, otherwise concolorous with stipitipith. Spores in mass dull pinkish brown (Fawn Color).

Basidiospores (n = 64): 8–8.9–10 × (5)5–5.6–5.8 µm, Q = (1.45)1.52–1.65–1.81(1.84), limoniform with a protruding beaked apex in profile, fusoid-elliptical to amygdaliform in face view, apical callus 0.5–1 µm long (occasionally abrupt or more often tapering to end), ornamentation verruculose to verrucose except on smooth apical callus and eccentric apiculus, suprahilar plage an indistinctly bordered area of lowered ornamentation (oil immersion); orangish amber in KOH (ochraceous in H_2O, based on examinations of paratypes). Basidia (n = 19): 4-spored, curved; broadly clavate above narrower base, 25–34.2–41(43) × 6.5–8.1–9.4(9.9) µm, sterigmata 2.0–3.0–3.7 µm long, curved; hyaline to dull orangish brown, guttulate, granular, or uniformly oily. Cheilocystidia 24.2–28.7–34 µm long, diameters (basal septum) 2–2.6–3 × (stomach) 4.9–5.7–6.9 × (neck) 1–1.3–1.6 × (capitulum) 1.5–2.0–2.6 µm (n = 13), abundant, intermixed with basidia, secretory; capitulate tibiiform (primarily) and lageniform, (only occasionally intermixed with thin-walled clavate elements), bases hyaline, necks and capitula refractive, thick-walled, pale amber. Pleurocystidia absent except for isolated cheilocystidia scattered occasionally on the gill face. Lamellar trama hyphae parallel, 65–80 × 3–6 µm, thin-walled, hyaline inflated, subgelatinized, narrowing toward gill edges to 2–3 µm diam and giving rise to the subhymenial layer. Subhymenium c. 25 µm thick, hyphae 2–4 µm diam, tightly packed, parallel, cylindrical, hyaline, gelatinized. Pellicular hyphae: pileipellis a bilaminate ixocutis with a ≥300 µm thick suprapellis with elements tightly compact in freshly dried material (but readily separating in gel matrix after 11 years in fungarium), hyphae >40 × 1.5–5.0 µm, radially aligned, sinuous, long-branching, gelatinized, frequently (spirally) gel encrusted, hyaline; subpellis c. 500 µm thick, gelatinized, vessel

A–C, E–G: *Lorelei Norvell*. D, H, J: *Ron Exeter* ⅄: *Heidi Christensen*.

FIG. 4. *Phaeocollybia chefensis* paratypes. [Lincoln Co.: LLN1951109-16 (A–C), RLE2007-074 (F), RLE2015-21 (H), RLE2021-1 (J); Lane Co.: RLE2007-129 (D, E); Polk Co.: HC2018-LB4 (I); Benton Co.: LLN2091026cc6 (G)]. A–C. Three views of the first specimen from CHEF that fostered the concept for *P. tibiikauffmanii* in 1995. D. Young robust specimens excavated from Lobster Creek. E. Pristine pseudorhizal tissues display strong magenta reaction in syringaldazine after 15 minutes. F. Second specimen retrieved from CHEF in 2007. G. Solitary specimen retrieved from Conner's Camp on Marys Peak. H. Basidiome at the original CHEF site prior to excavation in 2015. I. The first primordium excavated with its more mature partner in 2018 at Boulder Creek. J. Exeter's 2021 negative syringaldazine reaction from this waterlogged solitaire cautions that adverse environmental conditions do disable this usually reliable diagnostic tool.

hyphae with thinner walls; hyphae long, 4–12 µm diam at septa and inflating to ≤25 µm; pigments orange to dark brownish orange, diffuse to occasionally encrusting, soluble in KOH (forming droplets in mountant); small hyaline crystals scattered infrequently throughout. STIPITIPELLIS hyphae 75–100 × 1.5–3(6) µm, parallel aligned, gelatinized, pigments diffuse, pale amber to reddish in places. RHIZOPELLIS cells long × 4–10 µm, pale to dark amber, heavily gel- and/or red-brown pigment-encrusted. TRAMAL TISSUES: lightly (pileus) to noticeably (stipe, pseudorhiza) sarcodimitic, gelatinized, ±hyaline except darkening in pseudorhiza; VESSEL HYPHAE fusoid (sometimes tapering to obtuse end), 25–100 × 3–13 (at septa), rigid walls 1–2 µm thick; FLEXUOUS HYPHAE generally winding or curving around vessels, more or less cylindrical but sometimes appearing flattened, thin-walled, ≤50 µm long, diameters narrowest (1–2 µm) in pileus and broadest (3–5 µm) in stipe; OLEIFEROUS HYPHAE occasional to frequent in tramal tissues throughout, sinuous, aseptate, 3–10 µm diam, thin-walled, contents dull brown, oily. TIBIIFORM DIVERTICULA infrequent on aerial stipe apex, lageniform to (more often) tibiiform, frequent to abundant on rhizopellis, 8–20 µm long, 1–2 at base, narrowing in refractive neck area before expanding when capitula (1–2 µm diam) present; arising directly from hypha and lacking basal septum, secretory, hyaline, refractive to very pale amber. CLAMP CONNECTIONS absent in all tissues.

SYRINGALDAZINE SPOT TEST: strongly positive (pseudorhizal origin dark burgundy in five minutes; stipe (cross-section) and pileus and lamellae leaching magenta after ten minutes). FLUORESCENCE fresh material (of holotype) not tested; dried lamellae dull yellow orange (one small area of one specimen a brilliant orange yellow).

ADDITIONAL SPECIMENS EXAMINED—**UNITED STATES, OREGON, Benton Co.** Conner's Camp, 44.5060°N 123.5565°W, 762 m asl, 200yo PSME TSHE 26.x.2009 LLN2091026cc6 (MZ352101). **Lane Co.** Lobster Valley, 44.2268°N, 123.6148°W, 427 m asl, 200yo PSME young TSHE GASH, 6.xi.2007 RLE2007-129 (MZ352096). **Lincoln Co.** Cascade Head EF, 30 m S Tillamook Co. Line, 45.0447°N 123.9153°W, 245 m asl, ~120yo PISI TSHE VAPA POMU OXOR: 9.xi.1995 LLN1951109-19; 18.x.2007 RLE2007-074

FIG. 5. *Phaeocollybia chefensis* (Holotype, RLE2009-04): A. Colorless suprapellis in gelatinous matrix overlying a pigmented subpellis [400×]. B. Pileipellis under oil [1000×]. C, D. Suprapellis hyphae (gel encrustations detailed in C). E. Lightly sarcodimitic pileus tramal tissues with relatively thin-walled vessel hyphae. F. Oleiferous hyphae in stipititrama (just below pellis hyphae). G. Strongly sarcodimitic pseudorhizal trama with thick-walled vessel hyphae and thin-walled flexuous (arrow) hyphae.

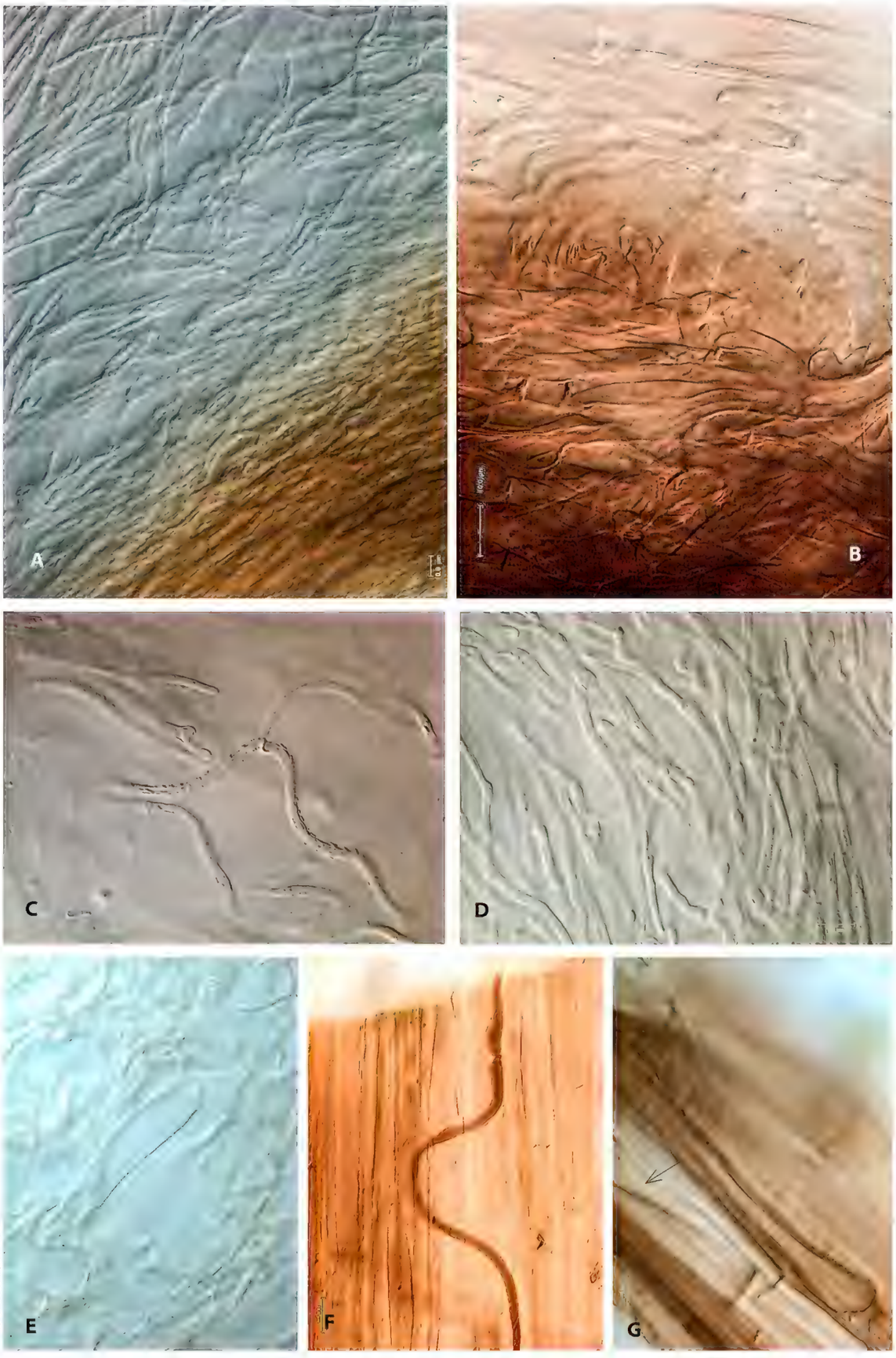

Lorelei Norvell

(MZ352097, KU574779); 2.xi.2015 RLE2015-21 (KX574495); 14.x.2021 RLE2021-01. **Polk Co.** Boulder Creek 44.8983°N 123.4995°W, 823 m asl, ~80yo ABPR PSME TSHE POMU VAPA 10.x.2018 HChristensen HC2018-LB4 (OSC 155803; MK326851).

ECOLOGY & DISTRIBUTION: autumn (October–November); basidiomes solitary or in pairs in needle duff under mature *Abies procera, Tsuga heterophylla, Picea sitchensis* and/or *Pseudotsuga menziesii* with understory of *Gaultheria shallon, Oxalis oregana, Polystichum munitum, Vaccinium ovatum,* and/or *V. parviflorum.* Known thus far from only five sites along the Oregon coast and in the Oregon coast range.

Discussion

Phaeocollybia chefensis

Diagnostic characters include a bright orange to brownish orange viscid conic-campanulate pileus, seemingly robust stature that in age becomes limp or flaccid, stuffed stipe, vertical monopodial pseudorhiza, medium-sized limoniform verrucose basidiospores, thick-walled tibiiform cheilocystidia, and lack of clamp connections. ITS and RPB2 sequence analyses strongly support *P. chefensis* as an independent species (FIGS 1, 2).

Morphologically, all paratypes match the type, except for the smaller (7.5–8–9 × 4–4.5–5.2 µm) basidiospores measured in the immature 1995 specimen (LLN1951109-19), which in part explains why Norvell (2004) did not detect the selection of a *P. spadicea* collection as type until after sequence analyses. The 1995 collection has not been sequenced, but sequences from the four subsequent collections from the identical site strongly support the earlier collection as *P. chefensis*. The molecularly confirmed collections imply *Tsuga heterophylla* as the primary ectomycorrhizal associate; possible secondary associates include *Picea sitchensis* at the type locality (245 m asl), *Pseudotsuga menziesii* at the Lobster Creek (427 m asl) and Conner's Camp (762 m asl) sites, and *Abies procera* and *Pseudotsuga menziesii* at Boulder Creek (823 m asl). Lamellae of fresh specimens examined under UV exhibited the strong yellow fluorescence characteristic of all PNW phaeocollybias except for the uniquely non-fluorescing *P. gregaria* A.H. Sm. & Trappe.

As noted above, *Phaeocollybia chefensis* closely resembles *P. kauffmanii* macroscopically, while microscopically it is quite similar to *P. spadicea* and *P. pseudofestiva* A.H. Sm., *Phaeocollybia chefensis* shares with *P. kauffmanii* a brownish orange viscid pileus, stuffed stipe, vertical-monopodial pseudorhiza, magenta syringaldazine reactivity, and morphologically similar basidiospores, but the presence of refractive thick-walled tibiiform cheilocystidia and

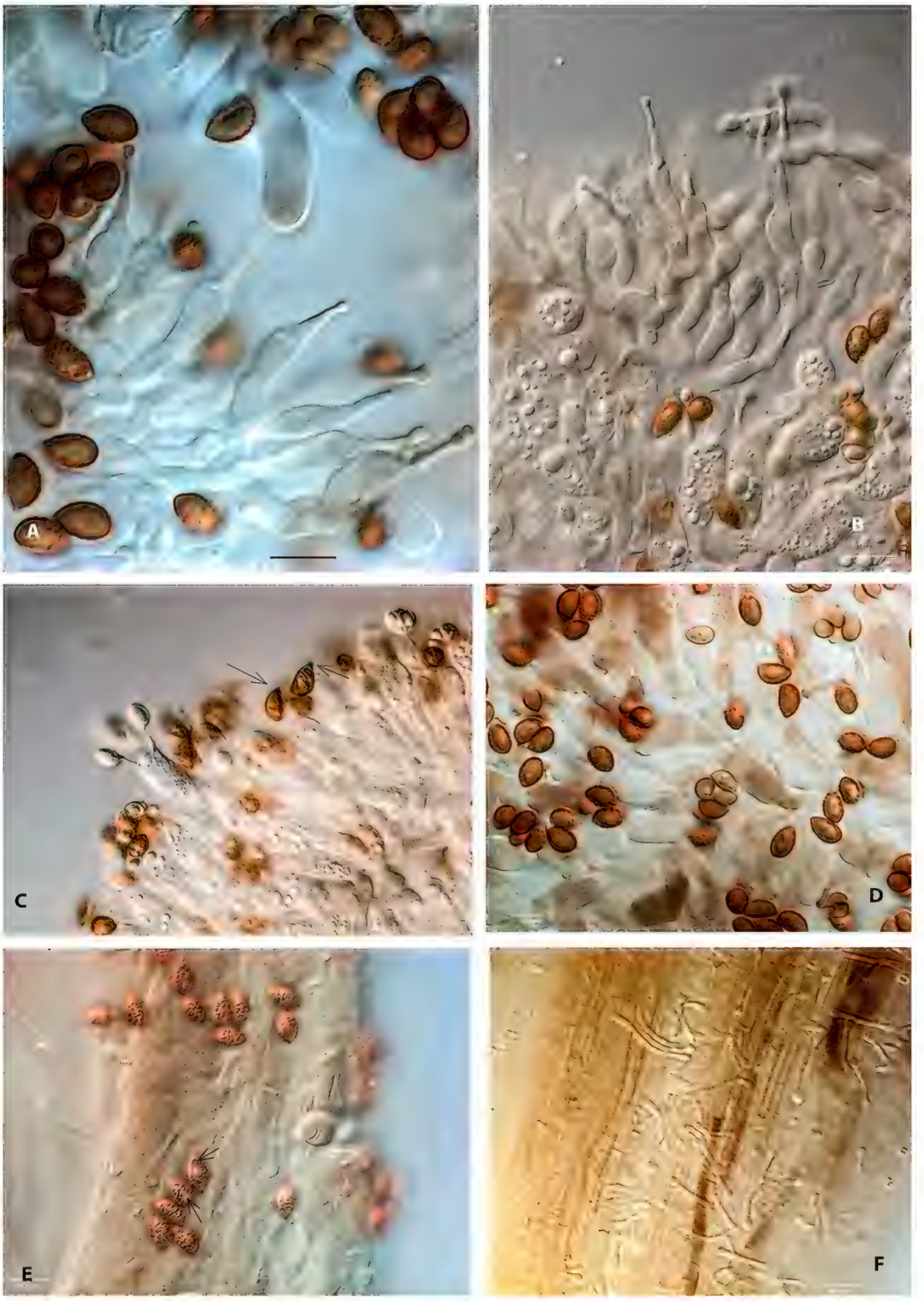

Fig. 6 *Phaeocollybia chefensis* (Holotype, RLE2009-04 (A,D,E); RLE2007-074 (B,C); RLE2007-129 (A,B): A, B. Cheilocystidia. C. Granular basidia, sterigmata, and orangish brown basidiospores with smooth apical beaks (arrow). D. Basidiospores with older basidia lacking guttules or granules. E. Comparison of verrucose spore ornamentation and less ornamented plage regions (arrows). F. Abundant tibiiform diverticula on pseudorhizal pellis.

the absence of heavily gelatinized, strongly sarcodimitic elements in the stipe and less extensive gelatinous matrix in the suprapellis clearly separate *P. chefensis* from *P. kauffmanii*. In the field the much longer-lived *P. kauffmanii* can be distinguished by its larger (at times massive) and more robust stature, sharp farinaceous odor and taste, strongly inrolled mature pileus edge, and frequently gregarious habit.

Phaeocollybia spadicea, sharing many morphological features that led to the selection of an orange form as type for *P. tibiikauffmanii,* differs in its darker tawny ("date-colored") to frequently blackish brown pileus, abundant rough fibrillose patches (invariably covered with tibiiform diverticula) on the stipe apex, closely gregarious habit, and (often) negative reactivity of the pileus and lamellar tissues to syringaldazine. Specimen age and condition may explain the variable syringaldazine reactivity in both *P. chefensis* and *P. spadicea*.

Phaeocollybia pseudofestiva, which shares general basidiospore and cheilocystidial morphology, syringaldazine reactivity, and odor and taste is easily separated from *P. chefensis* by its dark green pileus, smaller size, more prominently beaked basidiospores, cord-like pseudorhiza, and closely gregarious habit.

Phaeocollybia tibiikauffmanii and *P. spadicea*

As noted above, comparisons of ITS and RPB2 sequences from collections designated as either *P. spadicea* or *P. tibiikauffmanii* based on the presence/absence of orange coloration (Norvell 1998a,b,c, 2004; Norvell & Exeter 2009) revealed that all (including the holotype) except one (Fig. 3a) *P. tibiikauffmanii* collection represented *P. spadicea*. Subsequent morphological comparisons have shown that *P. spadicea* pileus colors range along a foxy orange to tawny to deep brown continuum. Additionally, all seven *P. chefensis* collections occurred singly or in pairs in contrast to *P. spadicea,* which typically occurs in closely gregarious to cespitose clusters; Alexander Smith's notes archived in MICH describe an "orange" spadicea that he provisionally named *P. "caespitosa"* (a name he also provisionally applied to what was to become *P. scatesiae* A.H. Sm. & Trappe; Norvell 1995). Thus, we propose the synonymy:

Phaeocollybia spadicea A.H. Sm., Brittonia 9: 215, 1957. Fig. 5

= *Phaeocollybia tibiikauffmanii* Norvell, Mycotaxon 90: 248, 2004.

Specimens confirmed as ***Phaeocollybia spadicea*** (listing those previously cited as *P. tibiikauffmanii* in Norvell (2004) and/or Norvell & Exeter (2004, 2009)—**UNITED STATES. Oregon: Benton Co.** Conner's Camp 44.5060°N 123.5565°W, 762 m asl,

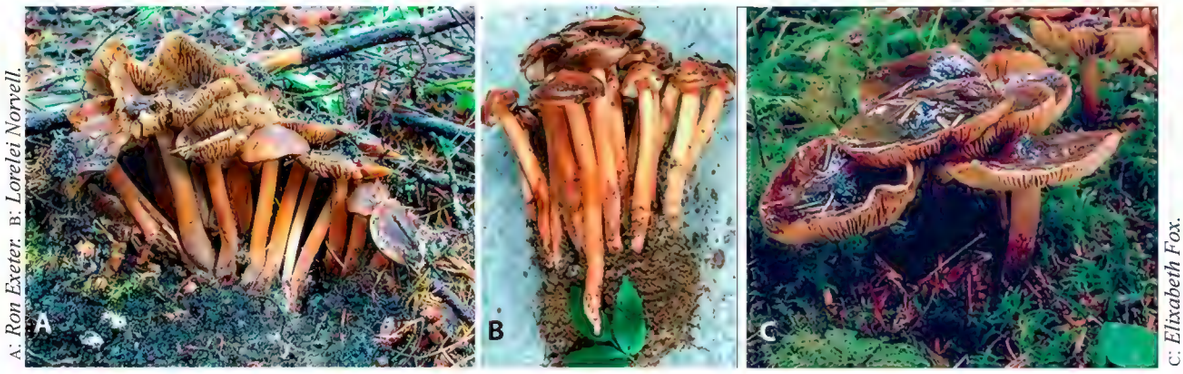

FIG. 7. *Phaeocollybia spadicea* [RLE208-55 (A); A2011031o2-1 (B); LLN1921015-10 (C)]. A. Gregarious cluster on Oregon's Marys Peak (as *P. tibiikauffmanii* in Norvell & Exeter 2009). B. Excavated *P. tibiikauffmanii* holotype from the Polk County Chronosequence Study. C. "Typical" brown-capped *P. spadicea* specimens in Hoh Valley, Olympic National Park.

200yo PSME TSHE, 5.xi.2005 RLE2008-55 (KF219592); Ernest Creek 44.4185°N 123.5165°W, 610m asl, 200yo PSME TSHE 15.xi.2007 RLE2007-165 (KU574777, KF219594); Running Bear 44.4774°N 123.5769°W, 696 m asl, 60yo PSME TSHE, 6.xi.2000 DCalver RLE200-103 (KF219595). **Polk Co.** Pedee Chronosequence Study 44.8113°N 123.5212°W, 460 m asl, 150yo PSME TSHE POMU 4.xi.1998 (all by LLN & RLE) A1981104o1-01, A1981104o2-02–04 (with CHibbler); 5.x.2000 RLE200-045; 18.x.2000 A2001018o1-15,o2-25; 1.xi.2000 RLE200-091, A2001101o2-30; 31.xi.2001 A2011031ox1 (*P. tibiikauffmanii* **holotype**; KF219597, KU574780), A2011031o2-03,04,05,06,08, A2011031ox-02; 14.xi.2011 A2011114o1-01,02,03, A2011114ox-01; 15.x.2002 A2021015o2-01; 13.xi.2002 A2021113o2-01,02,03; 14.xi.2006 A2061114o2-O (KF219596, KU574778), RLE2006-47, 16.x.2007 rle2007-060 (KF219593). WASHINGTON: **Jefferson Co. Hoh Valley @ Twin Creek** 47.8307°N 124.0012°W, 180 m asl, ~400yo PISI TSHE POMU OXOR 15.x.1992 LLN1921015-10 $_{spds1}$ (W SAR) (WTU-F-003698; previously cited and RFLP-confirmed as *P. spadicea*).

ADDITIONAL EXAMINATION NEEDED BUT PROBABLY ALSO ***Phaeocollybia*** **P. —UNITED STATES. OREGON: Benton Co.** Green Peak BLM Density Management Study 44.366°N 123.455°W, (all GP collections by LLN & RLE): Clear-cut transect (pre-treatment)—610m asl, 65yo PSME TSHE POMU 24.xi.1998 GP1981124c1-04 (W TFennell); High Retention transect 579m asl, 65yo PSME TSHE POMU— 8.xii.1999 GP1991208hx.03 (W SAR) (PNW, DAOM), 27.xi.2000 GP2001127hx3; Klickitat BLM Unit-3 44.4406°N 123.5673°W, 60yo PSME TSHE GASH 30.x.2000 RLE200-065; 16.xi.2000 RLE200-252; Klickitat Unit-6 T.S. 44.4548°N 123.5473°W, 50yo PSME TSHE POMU: 30.x.2000 RLE200-082,83,90, 14.xi.2000 RLE200-187b; 44.4260°N 123.5472°W, 60yo PSME TSHE GASH: 30.x.2000 RLE200-070; RUNNING BEAR T.S. 44.4774°N 123.5770°W, 200yo PSME TSHE POMU 9.xi.1998 LLN1981109.108e W RLE, 6.xi.2000 RLE200-103; 28.x.2002 RLE2002-16. **Linn Co.** Keel Flats T.S. 44.5133°N 122.6518°W, PSME BENE POMU 6.xii.1999 KScott RLE199-BK. **Polk Co.** Pedee Crk head waters near Cold Springs 44.8233°N 123.4862°W, 610m asl, 200yo PSME TSHE GASH 26.xi.2001 RLE 2001-112,115. **WASHINGTON: Clallam Co.** Olympic NF Klahanie Campground 47.9657°N 124.3057°W, 250yo PISI TSHE 18.x.1992 STrudell LLN1921018-4 $_{usps3}$ (WTU-F-003646).

Phaeocollybia rufotubulina and *P. californica*

On November 16, 1992, numerous densely gregarious orange phaeocollybias in Jackson State Forest (Mendocino County, California) were collected and referred to *P. californica*. This first highly informative collection contained numerous pin-head primordia that helped establish the presence of a universal veil for all *Phaeocollybia* species and introduced the 'sequential-racemose' pseudorhiza arising from a horizontal 'mother rhizomorph' within the soil (Norvell 1998b, 2004).

Restriction Fragment Length Polymorphism (RFLP) analyses of the ITS region from type materials supported separation of *P. rufotubulina* from *P. californica* and *P. scatesiae* (Norvell 1998a), indicating a new species and supporting the synonymy of *P. scatesiae* under *P. californica* proposed by Horak (1977). The 2009 ITS sequence analyses, however, clustered *P. californica* and *P. rufotubulina* within one intermixed clade well-separated from *P. scatesiae,* a brownish species macroscopically easily distinguishable in the field from the two orange phaeocollybias. *Phaeocollybia scatesiae* is now supported as independent from *P. californica* (Figs 1,2).

Given the difficulty encountered in isolating DNA from the *P. californica* holotype (obtained in 2011), it is probable that the 58-year-old *P. californica* DNA isolated in 1994 was contaminated by DNA isolated in the same run from the much younger *P. scatesiae* isotype. We hereby propose the synonymy:

Phaeocollybia californica A.H. Sm., Brittonia 9: 216, 1957.
= *Phaeocollybia rufotubulina* Norvell, Mycotaxon 90: 243, 2004.

Norvell & Exeter (2009) presented *P. californica* (pp. 63–70) and *P. rufotubulina* (pp. 175–180) as separate species; all material related to *P. rufotubulina* throughout that monograph as well as those in Norvell (1998a,b, 2004) should now be referred to *P. californica.*

Phaeocollybia rifflipes and *P. lilacifolia*

During a two-month long collecting expedition through western North American coastal rainforests 1992, several small lilac-gilled tawny to dark brown-capped phaeocollybias were collected and provisionally determined as *P. lilacifolia.* Except for flaccid small basidiomes and unusually small basidiospores, the specimens morphologically matched Smith's *P. lilacifolia* type from Washington's Mt. Rainier Park (Smith 1957a). However, 1994 restriction digests produced a RFLP profile unique to these collections. Unable to extract DNA from the Washington *P. lilacifolia* holotype or Smith's

Cascade Head Experimental Forest paratype, Norvell (1998a, 2002) proposed the name *P. rifflipes* (honoring its unique RFLP fingerprint) for the specimens that were morphologically separated by unusually small basidiospores and stature.

During 2001–2013, numerous small *P. rifflipes* specimens were collected from the Polk County old growth chronosequence transect; not until 2007, however, was the first recognizable *P. lilacifolia* collected from Lincoln County's Saddle Bag Mountain, c. 25 km southeast of Cascade Head Experimental Forest. The Saddle Bag collections comprised robust healthy specimens with normal-sized basidiospores. In 2009, ITS phylogenetic analyses clustered *P. lilacifolia* sequences and all but one *P. rifflipes* sequences within one clade, a clade supported by our current ITS and RPB2 phylogenies. Disposition of 4592sl (MZ352100), a Loring collection from Josephine County (initially identified as *P. rifflipes*), remains unresolved at this time.

Although we have not yet successfully isolated DNA from Smith's *P. lilacifolia* holotype or paratypes, the small "limp" stature, poor condition, and age of the 1992–1994 collections suggest that their peculiar RFLP profiles resulted from an unknown contaminant. The following synonymy is proposed:

Phaeocollybia lilacifolia A.H. Sm., Sydowia Beih. 1: 59, 1957.
= *Phaeocollybia rifflipes* Norvell, Mycotaxon 81: 102, 2002.

All keys, descriptions, and photos of *P. rifflipes* in Norvell (1998a, 2002) and Norvell & Exeter (2009) should be referred to *P. lilacifolia.*

Revised general key to Pacific Northwest *Phaeocollybia* species

Basidiospore size ranges of measurements taken from holotype specimens are cited for species; means of measurements taken from molecularly confirmed specimens are cited for complexes.

1. Basidiomes small: pileus ≤50 mm diam, and never green or drab; stipe apex usually ≤4 mm diam and never drab 2
1. Basidiomes medium to large: pileus usually ≥50 mm diam; stipe apex usually >5 mm diam 5
2. Basidiospores ellipsoid, ornamentation minutely punctate and small apical callus detectable in 1000× oil immersion; clamp connections present 3
2. Basidiospores limoniform, ornamentation verrucose and protruding apical beak visible without oil immersion lens; clamp connections absent 4

3. Spores small (5–6 × 3–3.5 µm); cheilocystidia lageni-/tibiiform, necks narrow and thick-walled, abundant but inconspicuous, difficult to see in dense gelatinous matrix; basidiome collybioid, stipe pliable ..... ***P. radicata***

3. Spores larger (~10 × 6 µm); cheilocystidia thin walled, narrowly clavate, extending well beyond hymenium; basidiome mycenoid, stipe fragile and easily broken ...***P. phaeogaleroides* complex**

4. Stipe and pseudorhiza fleshy, not shiny or brittle; cheilocystidia tibiiform, necks and capitula refractive and thick-walled; pleurocystidia present and, frequent on gill faces; spores 8–11 × 5–7 µm, tapering to straight beaks; phenology vernal ..... ***P. pleurocystidiata***

4. Stipe polished, corneous, soon hollow; pseudorhiza lateral monopodial, brittle and wire-like (criniform); cheilocystidia clavate, thin-walled; pleurocystidia absent; spores 7–8.5 × 5–5.5 µm, big-bellied with abrupt tilted beaks; phenology autumnal .....***P. attenuata***

5. Young pileus green, rapidly aging to brown or brownish olive **6**

5. Young pileus ochre, orange, tawny, brownish, or drab (never green) **8**

6. Young lamellae violet; spores ~9 × 5.3 µm, moderately beaked, in face view fusoid or naviculate, verrucose to marbled; cheilocystidia clavate, thin-walled, apices swollen to subcapitate, only rarely forming filiform apical outgrowths ..... ***P. fallax* complex**

6. Young lamellae creamy to yellowish buff; spores limoniform with pronounced beak, +/- ovate in face view, rugulose to warty roughened; cheilocystidia clavate or tibiiform **7**

7. Spores 7.5–8 × 4.5–5 µm, with long, projecting beaks; cheilocystidia tibiiform with narrow refractive necks ..... ***P. pseudofestiva***

7. Spores ~10 × 6 µm, 'turtle-backed' with abruptly protruding eccentric refractive beaks; cheilocystidia thin-walled, clavate, filiform apical outgrowths frequent in age ..... ***P. olivacea* complex**

8. Spores ellipsoid, short (<7.5 µm), punctate-roughened; cheilocystidia clavate, thin-walled **9**

8. Spores limoniform, verruculose to warty; cheilocystidia tibiiform or clavate **11**

9. Basidiome drab to gray, robust; stipe ≤20 mm diam, stout, firmly stuffed; pseudorhiza fleshy; taste and odor cucumber-farinaceous; spores 6–7.5 × 4–4.5 µm; all tissues soon deep magenta in syringaldazine ..... ***P. oregonensis***

9. Basidiome orange to auburn colored, fragile; stipe ≤13 mm diam, slender, hollow; pseudorhiza cord-like; taste and odor mild; pileus & lamellae syringaldazine negative **10**

10. Clamp connections abundant; pileus orange with yellowish margin, viscid, conic-campanulate; cheilocystidia filamentous to narrowly clavate; spores 5.5–6.5 × 3.5–4.3 µm ..... ***P. dissiliens***

10. Clamp connections absent; pileus uniformly auburn colored, subviscid, campanulate with a raised blunt umbo; cheilocystidia narrowly clavate with long pedicels and subcapitate apices; spores 5.5–6.5 × 3–4 µm ..... ***P. sipei***

11. Pileipellis 3-layered with colorless gelatinized middle layer between yellow to yellow-orange top and bottom layers; pileus minutely scaly (appressed), dry to subviscid (never glutinous) **12**

11. Pileipellis 2-layered, with colorless top layer and variously pigmented lower layer; pileus bald, smooth (never appressed scaly), subviscid to glutinous **13**

12. Spores large, 9–11 × 5–6.8 µm; pileus dry to greasy, yellowish ochre to ochraceous gold; frequently associated with *Abies* ..... ***P. luteosquamulosa***

12. Spores smaller, 7.2–8.7 × 4.4–5.5 µm; pileus greasy to subviscid, tawny ochraceous or tawny; associated with *Pseudotsuga* or *Tsuga* ..... ***P. ochraceocana***

13. Cheilocystidia tibiiform, broad bases thin-walled, capitula and narrow necks refractive and thick-walled; stipe hollow or stuffed **14**

13. Cheilocystidia variably cylindrical to clavate, filamentous apical secondary growth occasional in older specimens but always lacking refractive thick-walled necks; stipes stuffed with firm pith **17**

14. Mature stipe tubular and hollow; basidiomes closely gregarious to fasciculate, arising from a branching rhizomorphic cord **15**

14. Mature stipe stuffed with firm compact pith; solitary to closely gregarious, arising from unbranched fleshy (not cord-like) pseudorhiza **16**

15. Pileus heavily glutinous, acutely conic-campanulate, yellowish to dark brown; habit in dense fasciculate mounds; suprapellis thick, colorless, hyphae kinked, not spirally pigment-encrusted and with septa obscured by thick gel matrix; spores 8.5–9.5 × 4.5–5.5 µm ..... ***P. scatesiae***

15. Pileus moist to viscid, obtusely convex-campanulate, red orange to tawny; habit in troops, arcs, or (rarely) fasciculate mounds; suprapellis compact, amber to orange, hyphae spirally pigment-encrusted with refractive septa; spores 8.5–10 × 5–6 µm ..... ***P. californica***

16. Pileus foxy orange to orangish brown; stipe apex orange cinnamon colored; habit solitary or paired, never gregarious; all tissues soon magenta in syringaldazine; spores 8–10 × 5–5.8 µm ..... ***P. chefensis***

16. Pileus tawny to dark brown; stipe apex pallid to drab; habit gregarious to fasciculate; only pseudorhiza magenta in syringaldazine; spores 7.5–9 × 4.5–5 µm ..... ***P. spadicea***

17. Clamp connections frequent throughout, most easily seen
in pileus suprapellis and on cheilocystidia;
pileus campanulate with often papillate umbo, tawny ochraceous to tawny;
cheilocystidia cylindrical to narrowly clavate;
spores 8.4–9.2 × 5–6 µm ..... ***P. ammiratii***

17. Clamp connections lacking (rarely in stipitipellis);
pileus shape & color, cheilocystidial shape, and spore size varied **18**

18. Young lamellae whitish, smoky gray, or deep violet;
young pileus colors tawny, brownish-pink or drab;
pileus and lamellae magenta in syringaldazine **19**

18. Young lamellae pinkish, orangish, or yellowish;
young pileus colors rarely pink or drab;
syringaldazine reactivity varied **20**

19. Spores 7.5–9.4 × 4.5–5.5 µm; young lamellae intensely bluish lilac to violet;
pileus tawny to deep brown; taste not distinctive;
pseudorhiza syringaldazine negative ..... ***P. lilacifolia***

19. Spores 9 × 5.5 µm;
young lamellae white (pinkish) or ash gray, never lilac or violet;
pileus pinkish, drab, or purplish brown; taste 'bitter-cucumber' farinaceous;
all tissues soon deep magenta in syringaldazine ..... ***P. benzokauffmanii***

20. Young lamellae never fluorescing under UV;
pileus yellow tan, soon darker (cocoa brown); young stipe ivory tan,
lower stipe staining orange or orange banded at ground level;
habit densely gregarious; syringaldazine negative;
spores 9–10 × 4.5–6 µm ..... ***P. gregaria***

20. Young lamellae fluorescing under UV;
pileus orange or tawny; young stipe apex buff, orange, or pale cinnamon,
lower stipe colors similar to apex, habit scattered to gregarious,
syringaldazein negative or positive; spores 8–12 µm long **21**

21. Basidiome small to moderately large; stipe apex ≤12 mm diam (slender),
stipe stuffed but larval infested, leaving a hollow rind at ground level;
pileus conic umbonate, subviscid, uniformly bright apricot-/peach-colored;
all tissues negative in syringaldazine; pileipellis hyphae colorless,
spirally gel-incrusted, subpellis pigments KOH soluble, diffuse;
spores 8–9.5 × 5–6 µm, beaks short (≤5 µm), straight ..... ***P. piceae***

21. Basidiome large to massive; stipe apex 10–25 mm diam (robust),
stipe long-lived, stuffed with firm, insect-free pith;
pileus campanulate with obtuse umbo, viscid to glutinous, orange to tawny;
all tissues strongly magenta in syringaldazine;
pileus subpellis pigment-encrusted, pigments not KOH soluble;
spores with slightly tilted long (≤1.5 µm) beaks **22**

22. Spores 7.5–10 × 4–6 µm, limoniform, beak forward-tilted;
pileus +/- uniformly orange, tawny, or orangish brown,
typically drying with a burgundy-colored peaked umbo;
lower stipe and pith staining first orange, then orangish brown;
cheilocystidia cylindrical or narrowly to broadly clavate,
rarely pedicellate and subcapitate ..... ***P. kauffmanii***

22. Spores 8.5–12 × 5–7 µm, amygdaliform with long 'belly', beak back-tilted;
young pileus with reddish tawny umbo, amber margin, and tan edge,
eventually uniformly mahogany or dark reddish brown;
lower stipe and pith staining reddish brown;
cheilocystidia clavate to subcapitate with subglobose apices,
pedicellate, catenulate ..... ***P. redheadii***

Research on Pacific Northwest phaeocollybias is ongoing; a fully revised second edition of *Phaeocollybia* of Pacific Northwest North America will be released after several additional taxa have been published.

Acknowledgments

The Pacific Northwest *Phaeocollybia* consortium wishes to acknowledge earlier assistance given by individual collectors, government surveyors and agencies, fungarium curators (BPI, DAOM, F, HSC, MICH, O, OSC, NY, SFSU, TENN, UBC, UC, WTU), technicians, and others cited in full on p. 205 of Norvell & Exeter (2009). We also acknowledge the excellent molecular work by M.N. Louise Lefebvre in 2010 at Agriculture & Agri-Food Canada in Ottawa. Kelli Van Norman (Interagency Special Status/Sensitive Species Program of the Forest Service (Region 6) PNW Region and Oregon/Washington Bureau of Land Management) is thanked for facilitating molecular sampling of government *Phaeocollybia* collections; particular thanks are due Darci Rivers-Pankratz (also of ISSSP) for providing data on specimens inventoried for the Northwest Forest Plan, facilitating microscopical reevaluation, and forwarding Heidi Christensen's Boulder Creek collection for examination. We also thank Dr. Joe Ammirati (University of Washington, Seattle, USA), Dr. Egon Horak (Innsbruck, Austria), and Dr. P. Brandon Matheny (University of Tennessee, Knoxville, USA) for their greatly appreciated expert presubmission reviews. Egon Horak is further thanked for sharing his SEM-based basidiospore measurements for selected type specimens.

Literature cited

Castellano MA, Smith JE, O'Dell T, Cázares E, Nugent S. 1999. Handbook to Strategy 1 fungal species in the Northwest Forest Plan. USDA-FS. PNW-GTR-476. PNW Res. Stn., Portland. https://doi.org/10.2737/PNW-GTR-476

Castellano MA, Cázares E, Fondrick B, Dreisbach T. 2003. Handbook to additional fungal species of special concern in the Northwest Forest Plan. PNW-GTR-572: USDA-FS Pacific Northwest Research Station, Portland OR. https://doi.org/10.2737/PNW-GTR-572

Gardes M, Bruns TD. 1993. ITS primers with enhanced specificity for basidiomycetes—application to the identification of mycorrhizae and rusts. Molecular Ecology 2: 113–118. https://doi.org/10.1111/j.1365-294X.1993.tb00005.x

Gordon M. 2009 (May 7). Molecular marker development for *Phaeocollybia* species. Final report to the Interagency Special Status/Sensitive Species Program. Contract #L08PX02801 for the USDI Oregon/Washington Bureau of Land Management. 21 p. https://www.fs.fed.us/r6/sfpnw/issssp/documents/inventories/inv-rpt-fu-phaeocollybiamolecularmarker-2009.pdf

Gordon M, Van Norman K. 2014. Molecular monitoring of protected fungi: mycelium persistence in soil after timber harvest. Fungal Biology 9: 34–42. https://doi.org/10.1016/j.funeco.2014.01.006

Gordon M, Van Norman K. 2021. Mycelial DNA persistence in a forest soil. Environmental DNA. 2021:3:1208–1213. https://doi.org/10.002/edn3.242

Horak E. 1977 ("1976"). Further additions towards a monograph of *Phaeocollybia*. Sydowia 29: 28–70.

Huelsenbeck JP, Ronquist F. 2001. MrBayes: Bayesian inference of phylogeny. Bioinformatics 17: 754–755. http://dx.doi.org/10.1093/bioinformatics/17.8.754

Kalichman J, Kirk PM, Matheny PB. 2020. A compendium of generic names of agarics and *Agaricales*. Taxon 69: 425–447. https://doi.org/10.1002/tax.12240

Katoh K, Rozewicki J, Yamada KD. 2019. MAFFT online service: multiple sequence alignment, interactive sequence choice and visualization. Briefings in Bioinformatics 20(4): 1160–1066. https://doi.org/10.1093/bib/bbx108

Kumar S, Stecher G, Li M, Knyaz C, Tamura K. 2018. MEGA X: Molecular Evolutionary Genetics Analysis across computing platforms. Mol. Biol. Evol. 35: 1547–1549. https://doi.org/10.1093/molbev/msy096

Liu YJ, Whelen S, Hall BD., 1999. Phylogenetic relationships among *Ascomycetes:* evidence from an RNA polymerase II subunit. Mol. Biol. Evol. 16: 1799–1808. https://doi.org/10.1093/oxfordjournals.molbev.a026092

Maddison D, Maddison W. 2000. MacClade version 4: analysis of phylogeny and character evolution. Version 4.08. Sunderland (MA): Sinauer Associates.

Matheny PB. 2005. Improving phylogenetic inference of mushrooms with RPB1 and RPB2 nucleotide sequences (*Inocybe; Agaricales*). Molecular Phylogenetics and Evolution 35: 1–20. https://doi.org/10.1016/j.ympev.2004.11.014

Matheny PB, Curtis J, Hofstetter V, Aime CA, Moncalvo J-M, Ge Z-W, Yang Z-L & al. 2006. Major clades of *Agaricales:* a multi-locus phylogenetic overview. Mycologia 98(6): 984–997. https://doi.org/10.1080/15572536.2006.11832627

Murrill WA. 1911. *Naucoria.* North American Flora 10(3): 170–176. https://doi.org/10.2307/3753652

Norvell LL. 1995. ROD: Strategy 1—Fungal species Evaluation (30 gilled and non-gilled basidiomycete Strategy 1 species). Unpublished report on file at USFS Forest Sci Lab, Corvallis. 1480 p.

Norvell LL. 1998a. The biology and taxonomy of Pacific Northwest species of *Phaeocollybia* Heim (*Agaricales, Cortinariaceae*). Ph.D. dissertation (Dept. Botany), Seattle: University of Washington. 391 p.

Norvell LL. 1998b. Observations on development, morphology and biology in *Phaeocollybia.* Mycological Research 102: 615–630. https://doi.org/10.1017/S0953756297005431

Norvell LL. 1998c. ROD: Strategy 3—Fungal species evaluation (11 gilled basidiomycete Strategy 3 Species). Parts 1–3. Unpublished report on file at USFS Forest Sci Lab, Corvallis. 1496 p.

Norvell LL. 2000. *Phaeocollybia* in western North America. I. The *Phaeocollybia kauffmanii* complex. Canadian Journal of Botany 78: 1055–1076. https://doi.org/10.1139/b00-082

Norvell LL. 2002. *Phaeocollybia* in western North America 3: New species *P. phaeogaleroides* and *P. rifflipes*, with notes on the *P. festiva* complex. Mycotaxon 81: 95–112. https://www.researchgate.net/publication/255711827

Norvell LL. 2004. *Phaeocollybia* in western North America 4: Two new species with tibiiform cheilocystidia and section *Versicolores* reconsidered. Mycotaxon 90: 241–260. https://www.researchgate.net/publication/255711799

Norvell LL, Exeter RL. 2004. Ectomycorrhizal epigeous basidiomycete diversity in Oregon Coast Range *Pseudotsuga menziesii* forests—Preliminary observations. 159–189, in Fungi in forest ecosystems: systematics, diversity, and ecology (CL Cripps, ed.) The New York Botanical Garden.

Norvell LL, Exeter RL. 2007. *Phaeocollybia* in western North America 5: *P. ochraceocana* sp. nov. and the *P. kauffmanii* complex. Mycotaxon 102: 315–332. https://www.researchgate.net/publication/255711954

Norvell LL, Exeter RL. 2009 ["2008"]. *Phaeocollybia* of Pacific Northwest North America. USDI BLM/OR/WA/GI-08/100-1792. Salem, Oregon. 228 p. Online versions available:

Part 1: https://www.researchgate.net/publication/307601665

Part 2: https://www.researchgate.net/publication/307601721

Part 3: https://www.researchgate.net/publication/307601726

Norvell LL, Exeter RL, Gordon M, Redhead SA. 2010. Species concepts in a molecular age: the *Phaeocollybia* waltz. Abstract in IMC9: The biology of fungi. Oxford abstract disc for 1750 IMC9 delegates. Poster: https://www.researchgate.net/publication/307892378

Norvell LL, Redhead SA. 2000. *Phaeocollybia* in western North America 2: the vernal *P. pleurocystidiata* sp. nov. and *P. carmanahensis* reconsidered. Mycologia 92: 984–991. https://doi.org/10.1080/00275514.2000.12061242

ORBIC 2021 (continually updated). Oregon Biodiversity Information Center), Institute for Natural Resources, Oregon State & Portland State Universities. Accessed 3/1/2021: https://inr.oregonstate.edu/orbic/rare-species/ranking-documentation/fungi-ranks

Redhead SA, Norvell LL. 1993. *Phaeocollybia* in western Canada. Mycotaxon 46: 343–359.

Ridgway R. 1912. Color standards and color nomenclature. Washington, DC: Pub. by author. 43 p., 53 pl.

Smith AH. 1937. New and unusual agarics from the western United States. Mycologia 29: 45–59. https://doi.org/10.1080/00275514.2000.12061242

Smith AH. 1957a. Additional new or unusual North American agarics. Beih. Sydowia. 1: 40–61.

Smith AH. 1957b. A contribution toward a monograph of *Phaeocollybia.* Brittonia 9:195–217. https://doi.org/10.2307/2804723

Smith AH, Trappe JM. 1972. A contribution toward a monograph of *Phaeocollybia.* Brittonia 9: 195–217. https://doi.org/10.2307/2804723

Stamatakis A. 2014. RAxML Version 8: A tool for phylogenetic analysis and post-analysis of large phylogenies. Bioinformatics 30(9): 1312–1313. https://doi.org/10.1093/bioinformatics/btu033

Stecher G. Tamura K, Kumar S. 2020. Molecular Evolutionary Genetics Analysis (MEGA) for macOS. Brief Communications in Mol. Biol. Evol. https://doi.org/10.1093/molbev/msz312

Thiers B. 2021 (updated continuously). Index Herbariorum: A global directory of public herbaria and associated staff. New York Botanical Garden's Virtual Herbarium. [accessed March 2022] http://sweetgum.nybg.org/ih/

Thompson JD, Gibson TJ, Plewniak F, Jeanmougin F, Higgins DG. 1997. The CLUSTAL_X Windows interface: flexible strategies for multiple sequence alignment aided by quality analysis tools. Nucleic Acids Research 25: 4876–4882. https://doi.org/10.1093/nar/25.24.4876

USDA-USDI [USDA-Forest Service, USDI-Bureau of Land Management]. April 1994. Record of decision [ROD] for amendments to Forest Service and Bureau of Land Management planning documents within the range of the Northern Spotted Owl & Standards and guidelines for late-successional and old-growth forest related species within the range of the Northern Spotted Owl. Washington DC: US Govt Printing Office. 75 p + A1–7, B1–32, C1–48, D1–16, E1–21, F1–4.

White TJ, Bruns TD, Lee SB, Taylor JW. 1990. Amplification and direct sequencing of fungal ribosomal RNA Genes for phylogenetics. 315–322, in: MA Innis & al. (eds). PCR-protocols and applications: a laboratory manual. Academic Press, New York. https://doi.org/10.1016/B978-0-12-372180-8.50042-1

MYCOTAXON

ISSN (print) 0093-4666 (online) 2154-8889 Mycotaxon, Ltd. ©2022

January–March 2022—Volume 137, pp. 31–39

https://doi.org/10.5248/137.31

Beltrania shenzhenica sp. nov. from Guangdong, China

Zhao-Xue Zhang, Tai-Chang Mu, Zhuang Li,
Xiu-Guo Zhang, Ji-Wen Xia*

Shandong Provincial Key Laboratory for Biology of Vegetable Diseases and Insect Pests, College of Plant Protection, Shandong Agricultural University, Taian, Shandong 271018, China

* Correspondence to: *xiajiwen1@126.com; xiajw@sdau.edu.cn*

Abstract—During a survey of saprophytic microfungi on dead leaves from Futian Mangrove Nature Reserve in Guangdong Province, China, a new species of asexual ascomycota, *Beltrania shenzhenica*, was identified based on morphology and phylogenetic analyses of partial gene sequences of ITS and LSU. The detailed morphological description, phylogenetic tree, and photographs are provided.

Key words—*Amphisphaeriales,* anamorphic fungi, *Beltraniaceae,* phylogeny, taxonomy,

Introduction

Beltrania Penz., typified by *Beltrania rhombica* Penz. (Penzig 1882), is currently classified in *Beltraniaceae*, *Amphisphaeriales* (Wijayawardene & al. 2020, Zheng & al. 2020). The genus was mainly characterized by mostly unbranched dark setae with radially lobed basal cells, macronematous conidiophores arising from basal cells of setae or from separate radially lobed basal cells, and polyblastic, integrated, terminal, sympodial and denticulate conidiogenous cells that produce solitary acropleurogenous swollen separating cells and biconic, spicate or apiculate conidia with a hyaline equatorial band (Ellis 1971, Seifert & al. 2011, Lin & al. 2017, Hyde & al. 2020). *Beltrania* contains twenty species, of which eight are represented by molecular data (Harkness 1884, Wakefield 1931, Hughes 1951, Pirozynski & Patil 1970, Matsushima 1975, Rao & Varghese 1978, Zhang & Zhang 2003,

Crous & al. 2014, Tibpromma & al. 2018, Bandgar & Patil 2019, Hyde & al. 2020, Zheng & al 2020).

Futian Mangrove Nature Reserve, located northeast of Shenzhen Bay, was officially created in 1984 and designated as a national nature reserve in 1988. It belongs to the East Asian monsoon region with humid subtropical climate. The annual average temperature of 22.4 °C and average annual rainfall of 1700–1900 mm are conducive to the development of various microbial species (Meng & al. 2013). During our ongoing survey of anamorphic fungi associated with mangroves in China, we collected a new species representing *Beltrania* in the reserve.

Materials & methods

Isolation & morphological analysis

Specimens of dead leaves were collected from Futian Mangrove Nature Reserve, Shenzhen, Guangdong Province, China, and returned to the laboratory in plastic bags. The samples were incubated in plastic boxes lined with moistened tissue paper at room temperature for one week. Tissue pieces (5 × 5 mm) were randomly taken from the leaf and surface-sterilized by consecutively immersing in 75% ethanol solution for 1 min, 5% sodium hypochlorite solution for 30 s, and then rinsing three times in sterile distilled water for 1 min. The pieces were dried with sterilized paper towels and then placed on potato dextrose agar (PDA) (Cai & al. 2009). All the PDA plates were incubated at 25 °C for 2–4 d, and subcultures from the colony margins were inoculated

Table 1. Details of strains and sequences of *Beltrania* and related genera included in the phylogenetic analyses. New sequences are in bold; ex-(epi)type isolates are marked with ^{T}.

Species	Voucher	GenBank accession numbers	
		ITS	LSU
Beltrania dushanensis	GZCC18-0020	MN252875	MN252882
Beltrania krabiensis	MFLUCC 16-0257^{T}	MH275048	MH260280
Beltrania pseudorhombica	CPC 23656^{T}	KJ869158	KJ869215
Beltrania querna	CBS 126097	MH864016	MH875474
	CBS 122.51	MH856775	MH868293
Beltrania rhombica	CPC 27482	KX519515	KX519521
	CBS 123.58	MH857718	MH869260
	strain 10353	—	AB496423
	CBS 121.50	—	MH868082
Beltrania shenzhenica	**SAUCC 0061^{T}**	**MW784619**	**MW784621**
	SAUCC 0065	**MW784620**	**MW784622**

Species	Voucher	GenBank accession numbers	
		ITS	LSU
Beltrania sinensis	JS43	MN077366	MN077266
	JS42	MN077365	MN077265
	JS260	MN077364	MN077264
	JS101	MN077363	MN077263
Beltraniella acaciae	CPC 29498^{T}	KY173389	KY173483
Beltraniella botryospora	TUFC 10083^{T}	—	AB496426
Beltraniella brevis	GZCC 18-0081	MN252877	MN252884
	GZCC 18-0082	MN252876	MN252883
Beltraniella carolinensis	IFO 9502	—	DQ810233
Beltraniella endiandrae	CPC 22193^{T}	KJ869128	KJ869185
Beltraniella fertilis	MFLUCC 17-2137	MF580247	MF580254
	MFLUCC 17-2138	MF580248	MF580255
Beltraniella humicola	CBS 203.64	MH858416	MH870044
Beltraniella pandanicola	MFLUCC 18-0121^{T}	MH275049	MH260281
Beltraniella portoricensis	NFCCI 3993	KX519516	KX519522
	CBS 856.70	MH859981	MH871777
Beltraniella pseudoportoricensis	CBS 145547	MK876377	MK876416
Beltraniella ramosiphora	MFLUCC 17-2582^{T}	MG717500	MG717502
Beltraniella thailandica	MFLUCC 16-0377^{T}	MH275050	MH260282
Beltraniopsis longiconidiophora	MFLUCC 17-2139^{T}	MF580249	MF580256
	MFLUCC 17-2140	MF580250	MF580257
Beltraniopsis neolitseae	CPC 22168^{T}	KJ869126	KJ869183
Beltraniopsis sp.	TUFC 10081	—	AB496424
Castanediella couratarii	CBS 579.71	MH860269	MH872031
Hemibeltrania cinnamomi	NFCCI 3695	KT119564	KT119565
	NFCCI 3997	KX519517	KX519523
	MFLUCC 17-2141	MF580251	MF580258
Porobeltraniella porosa	NFCCI 3994	KX519518	KX519524
	NFCCI 3995	KX519519	KX519525
	NFCCI 3996	KX519520	KX519526
Pseudobeltrania cedrelae	COAD 2098^{T}	MG559548	MG559558
	PF 9	MG559552	MG559562
Pseudobeltrania ocoteae	CPC 26219^{T}	KT950856	KT950870
Subramaniomyces fusisaprophyticus	CBS 418.95	EU040241	EU040241
Subsessila turbinata	MFLUCC 15-0831^{T}	KX762288	KX762289

onto new PDA plates. Colonies at 7 d and 15 d were photographed using a PowerShot G7X mark II digital camera. Fungal micromorphological structures were observed and photographed using Olympus SZX10 stereomicroscope and Olympus BX53 microscope, both fitted with Olympus DP80 high definition colour digital cameras. All fungal strains were stored at 4 °C in 10% sterilized glycerin for further studies. The specimens are deposited in the Herbarium of Plant Pathology, Shandong Agricultural University, Taian, Shandong, China (HSAUP). Ex-type cultures are deposited in the Shandong Agricultural University Culture Collection, Taian, Shandong, China (SAUCC).

DNA extraction, PCR amplification, sequencing

Genomic DNA was extracted from colonies grown on PDA based on a modified CTAB method (Doyle & Doyle 1990). The nuclear ribosomal internal transcribed spacer (ITS) was amplified and sequenced using the primer pair ITS4/ITS5 (White & al. 1990), and the large subunit ribosomal RNA gene (LSU) using the primer pair LROR/LR5 (Vilgalys & Hester 1990, Glass & Donaldson 1995).

PCR was performed using an Eppendorf Mastercycler Thermocycler. The DNA was amplified in 25 µL reaction volumes containing 12.5 µL Green Taq Mix, 1 µL of each forward and reverse Biosune primer (10 µM), and 1 µL template genomic DNA in amplifier, and adjusted with distilled deionized water to a total 25 µL volume. PCR parameters followed were 95 °C for 5 min, followed by 35 cycles of denaturation at 95 °C for 30 s, annealing at 55 °C for 30 s, and a 1-min extension at 72 °C and ending with a final 10-min elongation at 72 °C. PCR products were estimated visually by staining with GelRed after 1% agarose gel electrophoresis. Sequencing was performed bi-directionally by BioSune Co. Ltd. (Shanghai). Consensus sequences were obtained using MEGA v. 7 (Kumar & al. 2016). All sequences generated in this study were deposited in GenBank (Table 1).

Sequence alignment & phylogenetic analysis

The quality of our amplified nucleotide sequences was checked and combined by MEGA v. 7 (Kumar & al. 2016), and reference sequences were retrieved from the National Center for Biotechnology Information (NCBI). Sequences were aligned using MAFFT v. 7.310 (Katoh & al. 2019) and manually corrected using MEGA v. 7.

The combined gene regions were phylogenetically analyzed using Maximum-Likelihood (ML) and Bayesian Inference (BI). RaxML analyses (using RaxML v. 8.2.9) and Bayesian analyses (using MrBayes v. 3.2.6) were run on the CIPRES Science Gateway Portal (Miller & al. 2012). Evolutionary models were calculated using MrModeltest v. 2.3 (Nylander 2004) selecting the best-fit model for each data partition according to the Akaike criterion. For ML analyses the default parameters were used and bootstrap support (BS) was carried out using the rapid bootstrapping algorithm with the automatic halt option. Bayesian analyses included two parallel runs of 5,000,000 generations with the stop rule option and a sampling frequency set to each 1000 generations. The 50% majority rule consensus trees and posterior

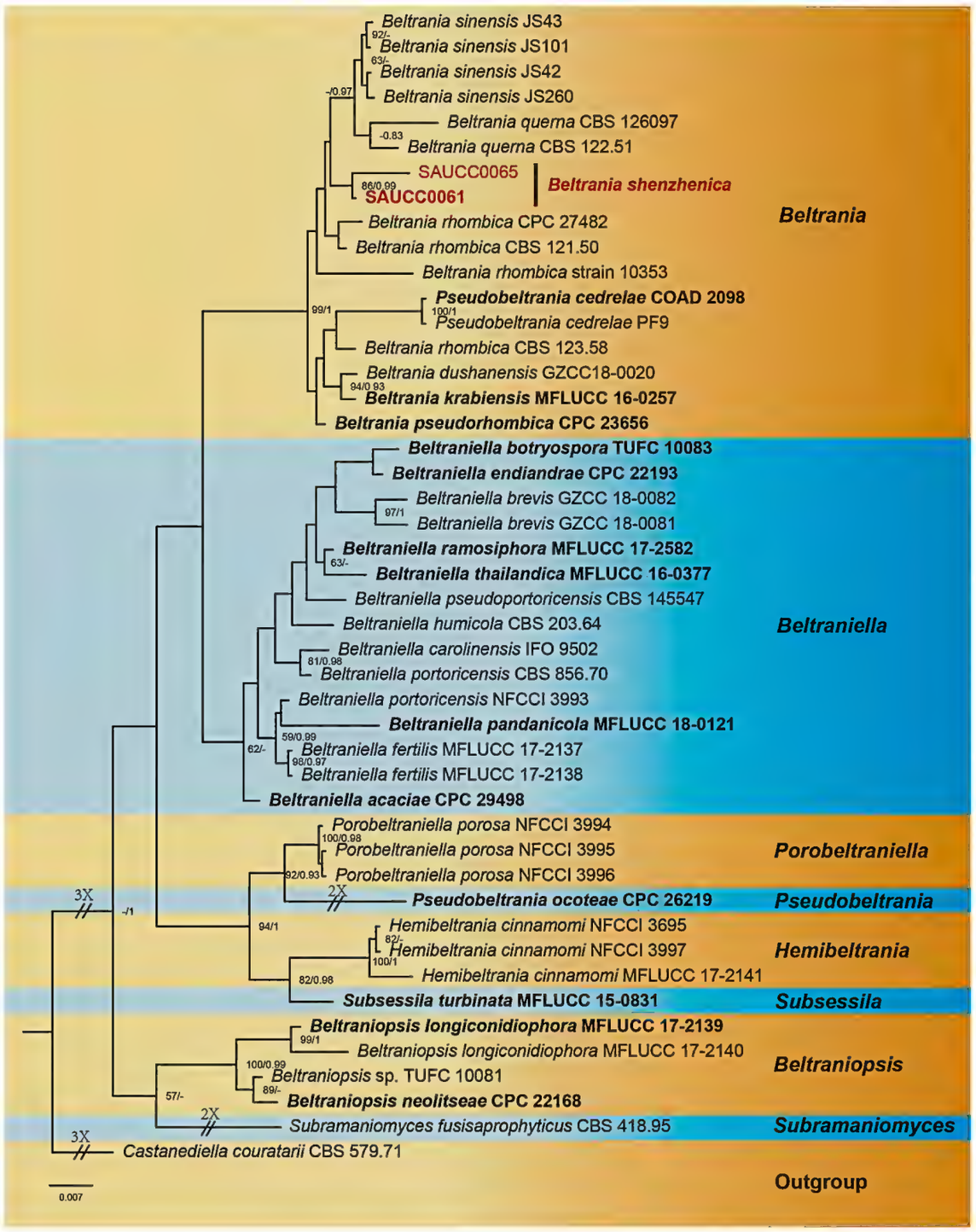

Fig. 1. Phylogram of *Beltrania* and related genera, generated from Bayesian analysis based on combined ITS and LSU sequence genes. Bootstrap support values are shown as ML >50% first, followed by BI >0.90. Some branches were shortened to fit the page – these are indicated by two diagonal lines and a correction factor indicating the full length. Ex-type/ex-epitype strains are in bold. Newly generated sequences are indicated in red.

probability (PP) values were calculated after discarding the first 25% of the samples as burn-in. The resulting trees were plotted using FigTree v. 1.4.2 (http://tree.bio.

ed.ac.uk/software/figtree) and edited with Adobe Illustrator CS v. 5. The individual gene datasets were assessed for incongruence before being concatenated by checking their individual phylogenies for conflicts between clades with significant ML and BI support (Mason-Gamer & Kellogg 1996, Wiens 1998).

Phylogenetic results

The dataset comprised 46 sequences representing 29 species including *Castanediella couratarii* (CBS 579.71) as the outgroup. The final alignment comprised a total of 1549 characters of the combined ITS and LSU including gaps, ITS: 1–940 and LSU: 941–1549. Of these characters, 1256 were constant, 152 parsimony-uninformative and 141 parsimony-informative. For the BI and ML analyses, the substitution model GTR+I+G for ITS and LSU were selected and incorporated into the analyses. The topology of Bayes tree confirmed the tree topologies obtained from the ML analyses, and therefore, only the Bayes tree is presented (Fig. 1). In this tree, our two sequences formed a distinct clade. Therefore, we determined that our strains belonged to a novel species of *Beltrania*.

Taxonomy

Beltrania shenzhenica Z.X Zhang, J.W. Xia & X.G. Zhang, **sp. nov.** Fig. 2

MB 839268

Differs from *Beltrania querna* by its wider conidia and from *B. rhombica* by its longer conidia.

Type: China, Guangdong Province, Shenzhen, Futian Mangrove Nature Reserve, on dead leaves of a broadleaf tree, 14 July 2020, Z.X Zhang (**Holotype**, HSAUP 0061; ex-type living culture SAUCC 0061; GenBank MW784619, MW784621).

Etymology: in reference to the city where the type was found.

Colonies on PDA at 25 °C in darkness, increasing in diameter by 11–15 mm/d, surface greyish white to black, flat, dense, reverse black to dark black. Mycelium partly superficial and partly immersed. Stroma absent. Setae erect, brown, thick-walled, septate, straight to flexuous, conical at the apex, slightly swollen at basal cell. Conidiophores 58–88 × 3–5 μm, aggregated in dense fascicles, pale brown, cylindrical, septate, unbranched, straight to variously curved, proliferating sympodially at apex. Conidiogenous cells terminal, integrated, subhyaline, smooth, holoblastic, polyblastic, with several flat tipped denticles. Separating cells 8–16 × 5–7 μm, subhyaline, finely roughened, with several apical, flat-tipped denticles. Conidia 28–33 × 8.5–12 μm (including apical appendage), biconic, aseptate, solitary, acropleurogenous, subhyaline to pale brown, with distinct granules,

Fig. 2. *Beltrania shenzhenica* (holotype, HSAUP 0061). a, b. Surface and reverse of colony on PDA; c. Mycelium on PDA; d. Setae; e, f. Conidiophores, separating cells, conidiogenous cells, and conidia; g–i. Separating cells; j–l. Conidia. Scale bars: d–l = 10 μm.

without median transverse band, apical appendage 5–9 μm long, tapering to an acutely rounded tip, smooth, without a mucilaginous sheath.

Additional specimen examined: **CHINA**, **Guangdong Province**, **Shenzhen**, Futian Mangrove Nature Reserve, on dead leaves of a broadleaf tree, 14 July 2020, Z.X. Zhang (HSAUP 0065; living culture SAUCC 0065; GenBank MW784620, MW784622).

Comments – Based on phylogenetic analysis, our *Beltrania shenzhenica* sequences grouped together with *B. querna* and *B. rhombica*, but they formed a distinct clade. Morphologically, *B. shenzhenica* is most similar to *B. querna*

and *B. rhombica* in conidial shape, but *B. querna* differs by its narrower conidia (6–8 µm wide; Harkness 1884), and *B. rhombica* differs by its shorter conidia (25–26 µm long; Penzig 1882).

Acknowledgments

The authors express gratitude to Dr. Jian Ma (College of Agronomy, Jiangxi Agricultural University, Nanchang, China) and Dr. Li-Guo Ma (Institute of Plant Protection, Shandong Academy of Agricultural Sciences, Jinan, China) for serving as pre-submission reviewers and to Dr. Shaun Pennycook for nomenclatural review and Dr. Lorelei L. Norvell for editorial review. This work was jointly supported by the National Natural Science Foundation of China (Nos. 31900014, U2002203, 31750001) and National Science and Technology Fundamental Resources Investigation Program of China (2019FY100700).

Literature cited

Bandgar SG, Patil CR. 2019. A new species of *Beltrania* from Western Ghats, India. International Journal of Life Science 7(2): 325–328.

Cai L, Hyde KD, Taylor PWJ, Weir BS, Waller JM, Abang MM & al. 2009. A polyphasic approach for studying *Colletotrichum*. Fungal Diversity 39: 183–204.

Crous PW, Shivas RG, Quaedvlieg W, van der Bank M, Zhang Y, Summerell BA & al. 2014. Fungal planet description sheets: 214–280. Persoonia 32: 184–306. https://doi.org/10.3767/003158514X682395

Doyle JJ, Doyle JL. 1990. Isolation of plant DNA from fresh tissue. Focus 12: 13–15. https://doi.org/10.2307/2419362

Ellis MB. 1971. Dematiaceous hyphomycetes. Commonwealth Mycological Institute, Kew, Surrey, England. 608 p.

Glass NL, Donaldson GC. 1995. Development of primer sets designed for use with the PCR to amplify conserved genes from filamentous ascomycetes. Applied and Environmental Microbiology 61(4): 1323–1330.

Harkness HW. 1884. New species of California fungi. Bulletin of the California Academy of Sciences 1: 29–47.

Hughes SJ. 1951. Studies on micro-fungi. XIII. *Beltrania*, *Ceratocladium*, *Diplorhinotrichum*, and *Hansfordiella* (gen. nov.). Mycological Papers 47. 15 p.

Hyde KD, de Silva NI, Jeewon R, Bhat DJ, Phookamsak R, Doilom M & al. 2020. AJOM new records and collections of fungi: 1–100. Asian Journal of Mycology 3(1): 22–294. https://doi.org/10.5943/ajom/3/1/3

Katoh K, Rozewicki J, Yamada KD. 2019. MAFFT online service: multiple sequence alignment, interactive sequence choice and visualization. Briefings in Bioinformatics 20(4): 1160–1166. https://doi.org/10.1093/bib/bbx108

Kumar S, Stecher G, Tamura K. 2016. MEGA7: Molecular evolutionary genetics analysis version 7.0 for bigger datasets. Molecular Biology and Evolution 33(7): 1870–1874. https://doi.org/10.1093/molbev/msw054

Lin CG, Hyde KD, Lumyong S, Mckenzie EHC. 2017. *Beltrania*-like taxa from Thailand. Cryptogamie, Mycologie 38: 301–319. https://doi.org/10.7872/crym/v38.iss3.2017.301

Mason-Gamer R, Kellogg E. 1996. Testing for phylogenetic conflict among molecular datasets in the tribe *Triticeae* (*Graminae*). Systematic Biology 45: 524–545.

Matsushima T. 1975. Icones microfungorum a Matsushima lectorum. Published by the author, Kobe, Japan.

Meng H, Xue ZQ, Tang J, Lv JH, Ma J. 2013. Soil culturable microorganisms and the activities of enzymes in mangrove sediment from Futian, Shenzhen. Guangdong Agricultural Sciences 1: 53–56. https://doi.org/10.16768/j.issn.1004-874x.2013.01.033

Miller MA, Pfeiffer W, Schwartz T. 2012. The CIPRES science gateway: enabling high-impact science for phylogenetics researchers with limited resources. 1–8, in: C Stewart (ed.). Proceedings of the 1st conference of the extreme science and engineering discovery environment: bridging from the extreme to the campus and beyond. Chicago, IL. New York: Association for Computing Machinery.

Nylander JAA. 2004. MrModeltest v2. program distributed by the author. Evolutionary Biology Centre, Uppsala University.

Penzig AGO. 1882. *Beltrania*, un nuovo genere di ifomiceti. Nuovo Giornale Botanico Italiano 14: 72–75.

Pirozynski KA, Patil SD. 1970. Some setose hyphomycetes of leaf litter in south India. Canadian Journal of Botany 48(3): 567–581. https://doi.org/10.1139/b70-079

Rao VG, Varghese KIM. 1978. Litter-fungi: Two undescribed hyphomycetes from India. National Academy Science Letters 1(2): 49–50.

Seifert KA, Morgan-Jones G, Gams W, Kendrick B. 2011. The genera of hyphomycetes. CBS Biodiversity Series 9. 997 p.

Tibpromma S, Hyde KD, McKenzie EHC, Bhat DJ, Phillips AJL, Wanasinghe DN & al. 2018. Fungal diversity notes 840–928: micro-fungi associated with *Pandanaceae*. Fungal Diversity 93: 1–160. https://doi.org/10.1007/s13225-018-0408-6

Vilgalys R, Hester M. 1990. Rapid genetic identification and mapping of enzymatically amplified ribosomal DNA from several *Cryptococcus* species. Journal of Bacteriology 172(8): 4238–4246. https://doi.org/10.1128/jb.172.8.4238-4246.1990

Wakefield EM. 1931. Fungi exotici. XXVII. Bulletin of Miscellaneous Informations of the Royal Botanical Gardens Kew 1931: 201–206.

White TJ, Bruns T, Lee S, Taylor J. 1990. Amplification and direct sequencing of fungal ribosomal RNA genes for phylogenetics. 315–322, in: MA Innis & al. (eds). PCR Protocols: a guide to methods and applications, Academic Press, San Diego. https://doi.org/10.1016/B978-0-12-372180-8.50042-1

Wiens JJ. 1998. Testing phylogenetic methods with tree congruence: phylogenetic analysis of polymorphic morphological characters in phrynosomatid lizards. Systematic Biology 47: 427–444.

Wijayawardene NN, Hyde KD, Al-Ani LKT, Tedersoo L, Haelewaters D, Rajeshkumar KC & al. 2020. Outline of Fungi and fungus-like taxa. Mycosphere 11(1): 1060–1456. https://doi.org/10.5943/mycosphere/11/1/8

Zhang M, Zhang TY. 2003. A new species of *Beltrania* (hyphomycetes) from China. Mycosystema 22: 520–521

Zheng H, Yang XQ, Deng JS, Xu JP, Yu ZF. 2020. *Beltrania sinensis* sp. nov., an endophytic fungus from China and a key to species of the genus. International Journal of Systematic and Evolutionary Microbiology 70: 1178–1185. https://doi.org/10.1099/ijsem.0.003897

MYCOTAXON

ISSN (print) 0093-4666 (online) 2154-8889 Mycotaxon, Ltd. ©2022

January–March 2022—Volume 137, pp. 41–50

https://doi.org/10.5248/137.41

Termitomyces cryptogamus sp. nov. associated with *Macrotermes natalensis* in Africa

Lennart J.J. van de Peppel[1], Z. Wilhelm de Beer[2], Duur K. Aanen[1]*, Ben Auxier[1]

[1]*Laboratory of Genetics, Wageningen University, 6700 AA, Wageningen, the Netherlands*

[2]*Department of Biochemistry, Genetics and Microbiology, Forestry and Agricultural Biotechnology Institute (FABI), University of Pretoria, Pretoria, South Africa*

Correspondence to: *duur.aanen@wur.nl*

Abstract—A new species of *Termitomyces* symbiotic with the termite *Macrotermes natalensis* is described from Africa. As there are no records of field collected basidiocarps within this lineage, traditional basidiocarp-based morphological taxonomy is not practical. While basidiocarps may be obtained rarely from incubation of fungal comb fragments, their practical use for taxonomical purposes is limited. Therefore, the species is described based on an ITS nucleotide sequence, with comparisons to an asexual culture. Based on samples with similar ITS sequences, this species is likely associated with multiple termite hosts across a large part of Africa.

Key words—*Agaricales*, *Lyophyllaceae*, phylogeny

Introduction

In Africa and Asia, a subfamily of the *Termitidae,* the *Macrotermitinae,* live in obligate symbiosis with members of the basidiomycete genus *Termitomyces* (*Lyophyllaceae*). The fungus resides inside the termite nest in so-called "fungus gardens," with mushroom production being periodically triggered by rain or the potential health of the nest (Koné & al. 2011). The mushrooms vary in size and are generally medium to large, although some species, such as *T. microcarpus* (Berk. & Broome) R. Heim, produce hundreds of small

mushrooms. Traditionally, taxonomy in this genus has been based on basidiocarp morphology, with molecular evidence only recently added (Frøslev 2003, Mossebo & al. 2017).

During research of termites and their associated fungi in Africa, one lineage was found that associates with *Macrotermes bellicosus* and *M. subhyalinus* when found in northern Africa, but only with *M. natalensis* when found in South Africa (Nobre & al. 2011). Surprisingly, sampling over ten years has not resulted in the discovery of mature basidiocarps of this species from any of its termite hosts, frustrating efforts for naming this species. Rarely, while excavating termite mounds, mushroom primordia are recovered (de Fine Licht & al. 2005; Vreeburg & al. 2020) that can occasionally be incubated under laboratory conditions in the absence of termite workers. Presumably due to this laboratory incubation the mushrooms are misshapen, as their appearance is not consistent with other known *Termitomyces* species. This may be similar to development that occurs in the production of "Enoki" mushroom from *Flammulina velutipes* which causes long thin stipes, smaller caps, and pale coloration (Kües & Navarro-González 2015). Despite the need to provide a name for this well-studied fungus, the lack of basidiocarps has prevented comparisons with published literature descriptions (Botha & Eicker 1991b), leading to an argument for using readily obtained asexual cultures as a stable type against which to compare (Makonde & al. 2013).

As extensive comparisons of ITS sequences from herbarium material from South Africa recovered no matches with our *M. natalensis* symbiont (van de Peppel & al., unpublished data), we provide a description based on sequence identity and asexual morphology. While there is a previous description of asexual characteristics from South African *Termitomyces,* only mounds producing basidiocarps were used, with *M. natalensis* mounds apparently not sampled (Botha & Eicker 1991b). As basidiocarp records are lacking, asexual cultures are a logical solution to this taxonomic issue. Three previous publications addressed differences between species in asexual cultures, and while interspecific differences were found, asexual characteristics alone were not considered sufficient to delineate species (Botha & Eicker 1991a,b; Tibuhwa 2012).

Recently an ecological study of *Macrotermes* symbionts in Kenya uncovered results consistent with previous sampling of this lineage (Vesala & al. 2017). Vesala & al. recovered the same fungal species as the one collected from South Africa (Nobre & al. 2011, de Fine Licht & al. 2005; Vreeburg & al.

2020) from mounds of *M. bellicosus, M. herus, M. jeanneli, M. michaelseni,* and *M. subhyalinus.* Vesala & al. (2020), who selected related ITS sequences from GenBank including symbionts of *M. natalensis* and *M. bellicosus*, found that these formed a monophyletic clade. These sequences form two well-supported groups with 97% and 98.5% support, with the exception of a single sequence (GenBank AF357024) isolated from an unidentified *Macrotermes* species. Based on these results we describe the species based on a fungal isolate from South Africa symbiotic with *M. natalensis* for which the fungal genome has been published (Poulsen & al. 2014).

Materials & methods

Samples and Isolates

A heterokaryotic culture, Mn103, was obtained by opening a termite mound and carefully removing nodules containing asexual spores from the fungal combs without soil contamination. These nodules were placed on agar plates without antibiotics to establish hyphal cultures. A homokaryotic culture, P5, was obtained by protoplasting the Mn103 heterokaryotic culture. Additional details regarding sampling, isolation, and subsequent protoplasting of this culture are found in Poulsen & al. (2014) and Nobre & al. (2014). A dried holotype specimen of the Mn103 heterokaryotic culture and a living ex-holotype culture of the P5 homokaryotic culture are conserved at the Westerdijk Fungal Biodiversity Institute, Utrecht, Netherlands (CBS).

DNA extraction, PCR amplification, sequencing

Genomic DNA was extracted from the protoplasted P5 homokaryotic culture using the cetyltrimethylammonium bromide (CTAB) protocol using mycelium and spores scraped from a petri dish. The nuclear ribosomal region containing the ITS1 + 5.8S + ITS2 region (ITS) was amplified using a standard PCR reaction using Promega GoTaq polymerase and the fungal specific primer ITS1F and the general reverse primer ITS4 (White & al. 1990, Gardes & Bruns 1993). The 28S region (LSU) was amplified using primers LR0R and LR5 (Vilgalys & Hester 1990).

As no basidiocarps have been reported from *M. natalensis* termite mounds, we also surveyed herbarium samples from the South African National Collection of Fungi (PREM) and Schweickerdt Herbarium (PRUM) (van de Peppel & al. unpublished data).

Sequence alignment & phylogenetic reconstruction

We used a previously published set of ITS sequences (Vesala & al. 2017), six GenBank sequences from *Termitomyces* symbiotic with *M. natalensis,* and a sequence generated from the specimen we designate here as the type for the new species. Sequences were aligned using the web software MAFFT v. 7 with default settings (Katoh & Standley 2013). Maximum likelihood trees were reconstructed using IQ-TREE v. 2.0.6 with default settings (Trifinopoulos & al. 2016).

Culture & microscopy

Cultures were maintained on MYA (20g Malt Extract, 2g Yeast Extract, 1 L H_2O), and incubated at 25 °C. Microscopical examinations were conducted using a Zeiss Axio Imager A1 with 63X objective lens under DIC optics.

Taxonomy

Termitomyces cryptogamus van de Peppel, **sp. nov.** FIG. 1

MB 838129

Differs from *Termitomyces schimperi* by its clearly separated LSU sequence; there are no useful diagnostic differences in the morphology of the asexual morphs of these species.

TYPE—South Africa, Pretoria, Rietfontein 321-Jr, 25.7292°S 28.2347°E, May 2011, DK Aanen, heterokaryotic isolate (Mn103) obtained from asexual nodules on a fungal comb from a mound of *Macrotermes natalensis* (**Holotype**, CBS H-24752 [metabolically inactive dried culture]; living ex-type culture CBS 147190].

ETYMOLOGY: *cryptogamus*, referring to the hidden marriages of a genetically well-mixed species without recorded basidiocarps in vivo.

SEXUAL STATE—not observed in vivo.

ASEXUAL STATE—Growth of colonies on MYA medium reaching 5–6 cm diam. in 3 weeks at 25 °C (somewhat faster at 30 °C). Growth consisting of white hyphae mostly submerged in agar, with 1–2 mm diam. clusters of asexual spores produced on the agar surface. Conidia highly variable in size (10–100 mm long) and shape, with 2–5 nuclei per spore. Heterokaryotic colonies consistently producing heterokaryotic conidia.

COMMENTS—In the absence of in vivo basidiocarps, *T. cryptogamus* cannot be distinguished readily from closely related *Termitomyces* species based on asexual characters. However, ITS and LSU sequence analyses clearly separate a well-supported clade that includes the holotype of *T. cryptogamus* and several other strains obtained from fungal combs of *Macrotermes natalensis* in South Africa, as well as from those of *M. bellicosus, M. herus, M. jeanneli, M. michaelseni,* and *M. subhyalinus* in Cameroon, Kenya, Senegal, and Ivory Coast.

Phylogenetic results

NCBI GenBank accession numbers were obtained for the nucleotide sequences generated from the protoplasted homokaryotic culture P5: ITS (MW251838), LSU (MW567773), whole genome (GenBank id: GCA_001263195).

The ITS sequence of our isolate P5 places *Termitomyces cryptogamus* inside Group 1 of Vesala & al. (2017). This group includes fungal individuals symbiotic

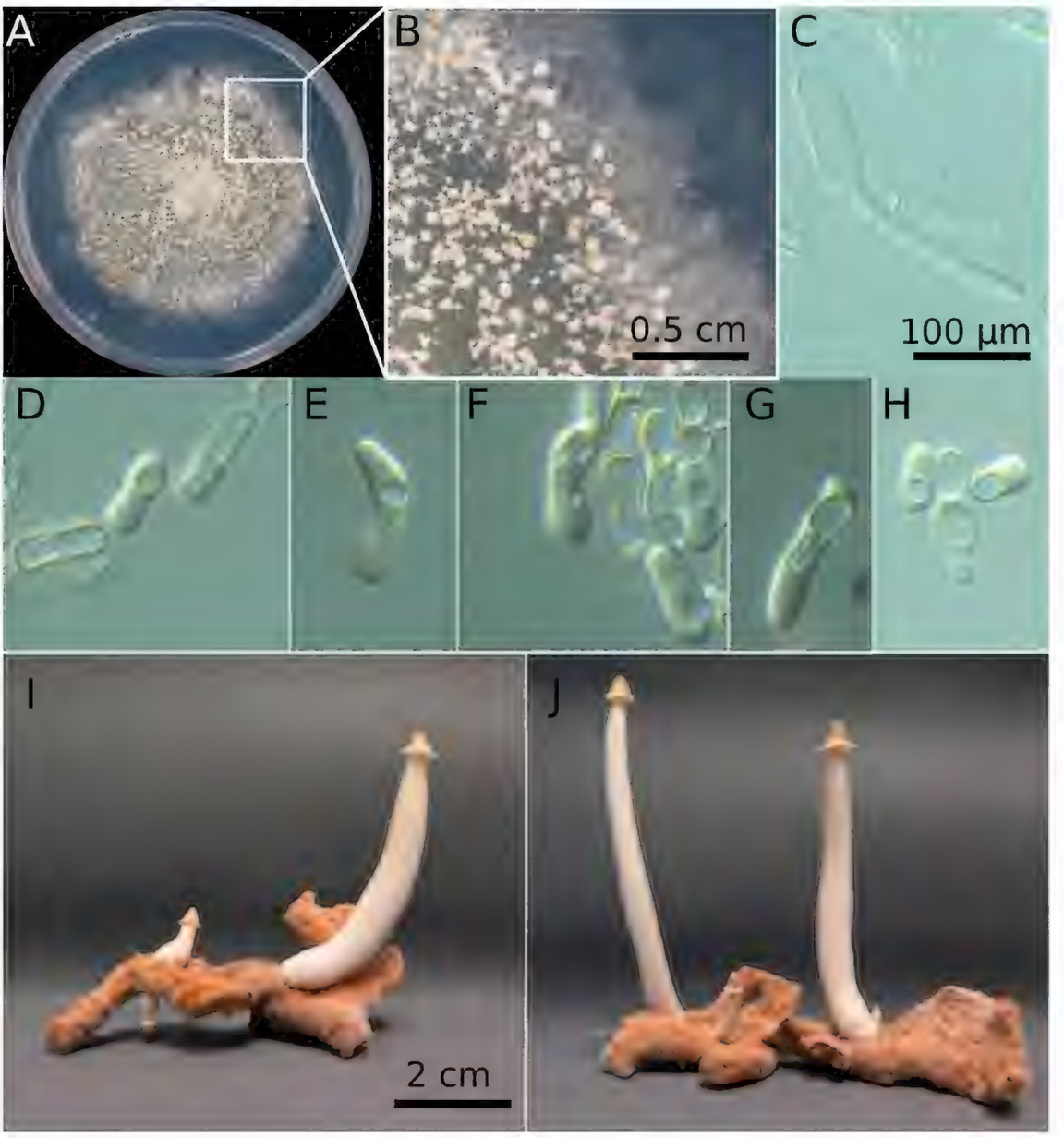

Fig. 1. *Termitomyces cryptogamus*: morphology. A. Growth on Malt Yeast Agar showing abundant nodule formation of asexual conidia; B. Close up view of A; C–H. Variable morphology of conidia; I, J. Morphology of mushrooms on fragments of excavated fungus garden comb produced after incubation for 5–10 days; note the small caps (<1 cm), which produce viable basidiospores.

with *Macrotermes natalensis, M. bellicosus, M. subhyalinus, M. michaelseni, M. herus* and *M. jeanneli* (Fig. 2). Except for *M. natalensis*, these termite species are found with sister species also closely related to *Termitomyces cryptogamus*.

To compare with other common *Macrotermes* mound symbionts, we also extracted DNA from samples of *Termitomyces schimperi* (Pat.) R. Heim. However, repeated PCR amplifications of the ITS region were not successful.

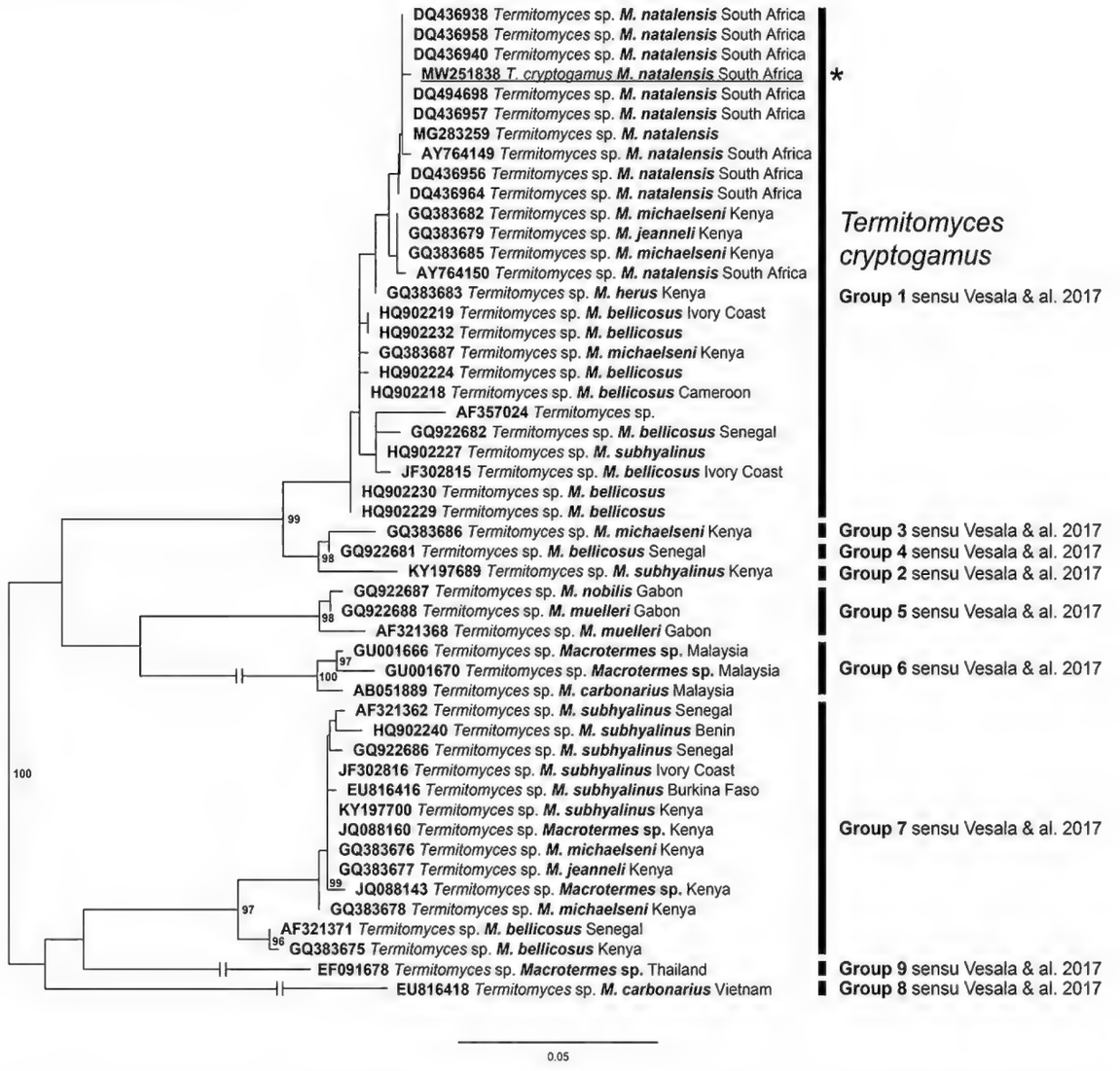

Fig. 2. Maximum likelihood tree based on ITS1-5.8S-ITS2 sequences of *Termitomyces cryptogamus* and allied *Macrotermes* symbionts with their host termite species (in bold) and their collection location. Outgroups were removed to increase readability of the tree. Numbers at the nodes indicate ultrafast bootstrap values, only significant node values >95% are displayed. Species delimitation groups with 97% ITS identity (sensu Vesala & al. 2017) are displayed on the right side of the tree. A sequence of the *T. cryptogamus* ex-type P5 is underlined and indicated by an asterisk.

We were able to amplify LSU sequences from both *T. cryptogamus* and herbarium samples of *T. schimperi* (PREM41964), which were then analysed together with other GenBank LSU sequences of *T. schimperi* and unidentified *M. natalensis* symbionts (Fig. 3). The LSU sequence of our P5 isolate was identical to that from a fungal symbiont of a *M. natalensis* mound. LSU sequences from the commonly recovered *Macrotermes* symbiont, *T. schimperi*, were not monophyletic.

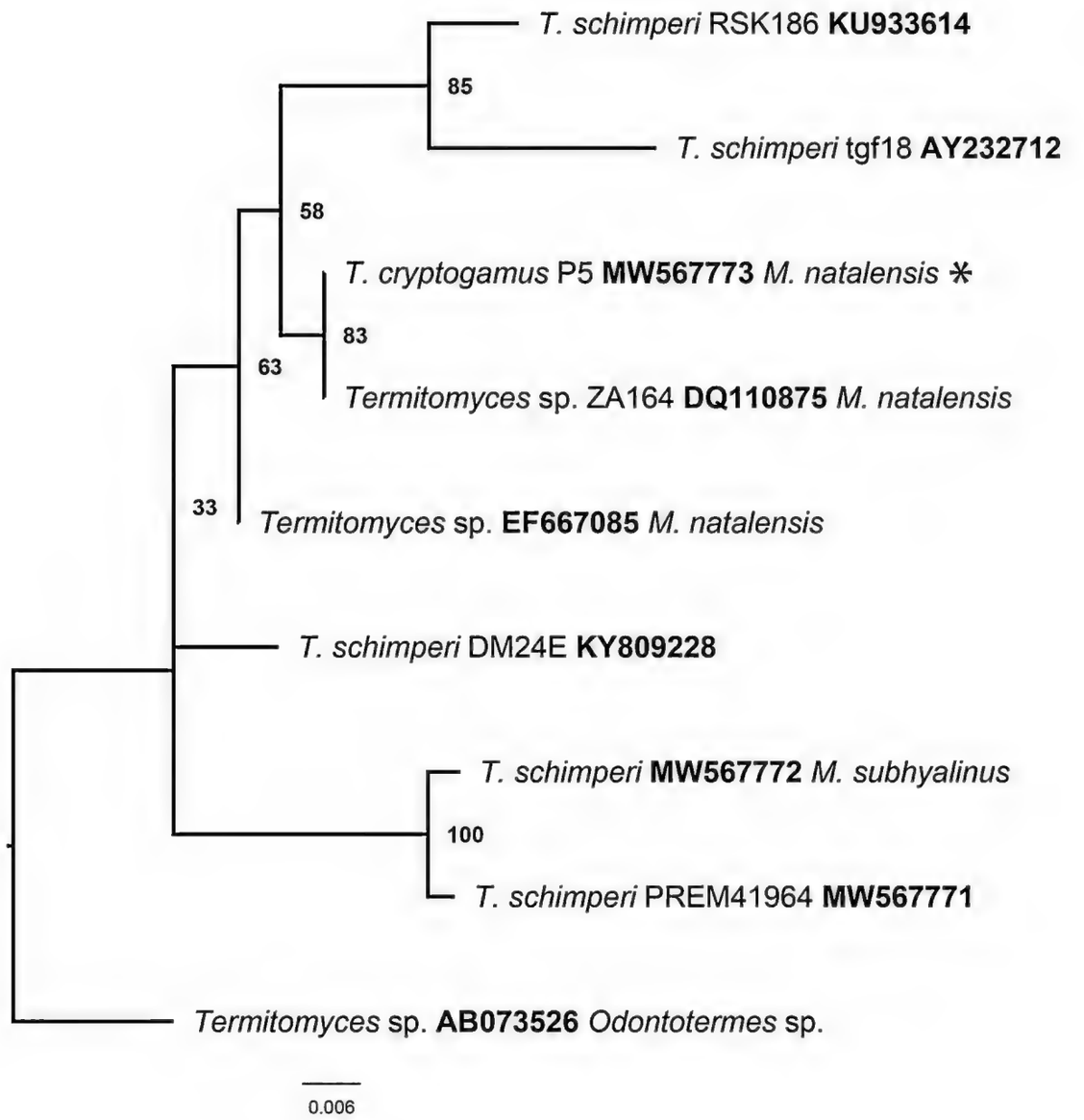

Fig. 3. Phylogenetic tree based on LSU sequences for *Termitomyces cryptogamus*. and publicly available LSU sequences of *T. schimperi*, a common *Macrotermes* symbiont. Sequence of AB073526 used as an outgroup to root the tree. Node values indicate bootstrap support.

Microscopical investigations revealed highly variable morphology of conidia harvested from laboratory grown cultures (Fig. 1c–h), which limits morphological comparison with asexual cultures of other *Termitomyces* species.

Discussion

There is accumulating evidence, both direct and indirect, that sexual reproduction does occur in *T. cryptogamus*. First, sexual reproduction between strains associated with *M. natalensis* was inferred as occurring

sufficiently frequently (at least 100 sexual events per generation) to explain the observed signature of free recombination (de Fine Licht & al. 2006). Second, mating tests between homokaryons retrieved from heterokaryons demonstrated that the *M. natalensis*-associated strains represent a single biological species (Nobre & al. 2014). Finally, strains associated with *M. natalensis* were observed to produce mushrooms and viable basidiospores in vitro (de Fine Licht & al. 2005; Vreeburg & al. 2020). These findings make it all the more surprising that mushrooms have not been found in nature. One hypothesis is that sexual reproduction of this species occurs belowground synchronously with alate dispersal.

Nevertheless, recovery of in-vitro basidiocarps only after prolonged laboratory incubation prevents their use as a morphological type specimen, as presumably incubation conditions greatly influence the resulting morphology. Additionally, the infrequency and unpredictability of these mushroom primordia in nests precludes their use for identification. Further, the asexual spores produced are highly polymorphic, and thus cannot be used for reliable identification with this group. As such, although comparisons of asexual cultures remain valuable, molecular markers provide the only reliable way to identify samples (Lücking & al. 2020). Based on the work of Makonde & al. 2013, it is likely that other *Termitomyces* species exist where the only practical identification markers will be molecular.

Using the 3% ITS similarity threshold, we find one lineage (group 1, sensu Vesala & al. 2017) that is distributed across Africa, with hosts differing geographically, but always within *Macrotermes*. The different termite symbionts combined with geographic isolation may indicate barriers to gene flow. Further study should show whether or not geographically separated populations of *T. cryptogamus,* including populations associated with *Macrotermes* species other than *M. natalensis,* all form a single biological species.

Although comparisons of ITS sequences from *T. cryptogamus* and *T. schimperi* are not currently available, we feel these sequences represent at least two species for two reasons. Firstly, the fact that we are unable to amplify the ITS regions successfully using the ITS1F and ITS4 primers, while we can amplify the LSU sequence indicates that there are likely mutations in the primer binding site not found in *T. cryptogamus* (for which ITS sequences are readily amplified). This suggests that *T. schimperi* likely has fixed substitutions not shared with *T. cryptogamus*. Secondly, the relationships between the LSU sequences generated from *T. schimperi* and *T. cryptogamus*

(Fig. 3) show significant genetic difference, although the backbone nodes of the phylogeny do not receive statistical support of bootstrap values greater than 70. Additionally, the recovery of two clades of *T. schimperi* indicates that *T. schimperi* is potentially paraphyletic and deserves further study.

Acknowledgments

The authors thank Tobias Guldberg Frøslev (Geogenetics, University of Copenhagen, Denmark) and N'golo Abdoulaye Koné (Department of Natural Sciences, Université Nangui Abrogoua, Abidjan, Côte d'Ivoire) for presubmission review. D.K.A., L.J.J.v.d.P., and B.A. were supported by the Netherlands Organization for Scientific Research (D.K.A., L.J.J.v.d.P. by VICI:NWO 86514007; D.K.A. and B.A. by ALWGR.2017.010).

Literature cited

Botha WJ, Eicker A. 1991a. Cultural studies on the genus *Termitomyces* in South Africa. I. Macro- and microscopic characters of basidiome context cultures. Mycological Research 95(4): 435–443. https://doi.org/10.1016/S0953-7562(09)80843-5

Botha WJ, Eicker A. 1991b. Cultural studies on the genus *Termitomyces* in South Africa. II. Macro- and micromorphology of comb sporodochia. Mycological Research 95(4): 444–451. https://doi.org/10.1016/S0953-7562(09)80844-7

de Fine Licht HH, Andersen A, Aanen DK. 2005. *Termitomyces* sp. associated with the termite *Macrotermes natalensis* has a heterothallic mating system and multinucleate cells. Mycological Research 109(3): 314–318. https://doi.org/10.1017/S0953756204001844

de Fine Licht HH, Boomsma JJ, Aanen DK. 2006. Presumptive horizontal symbiont transmission in the fungus-growing termite *Macrotermes natalensis*. Molecular Ecology 15(11): 3131–3138. https://doi.org/10.1111/j.1365-294X.2006.03008.x

Frøslev TG, Aanen DK, Laessøe T, Rosendahl S. 2003. Phylogenetic relationships of *Termitomyces* and related taxa. Mycological Research 107(11): 1277–1286. https://doi.org/10.1017/S0953756203008670

Gardes M, Bruns TD. 1993. ITS primers with enhanced specificity for basidiomycetes – application to the identification of mycorrhizae and rusts. Molecular Ecology 2(2): 113–118. https://doi.org/10.1111/j.1365-294x.1993.tb00005.x

Katoh K, Standley DM. 2013. MAFFT multiple sequence alignment software version 7: improvements in performance and usability. Molecular Biology and Evolution 30(4): 772–780. https://doi.org/10.1093/molbev/mst010

Koné NA, Dosso K, Konaté S, Kouadio JY, Linsenmair KE. 2011. Environmental and biological determinants of *Termitomyces* species seasonal fructification in central and southern Côte d'Ivoire. Insectes Sociaux 58(3): 371–382. https://doi.org/10.1007/s00040-011-0154-1

Kües U, Navarro-González M. 2015. How do agaricomycetes shape their fruiting bodies? 1. Morphological aspects of development. Fungal Biology Reviews 29(2): 63-97. https://doi.org/10.1016/j.fbr.2015.05.001

Lücking R, Aime MC, Robbertse B, Miller AN, Ariyawansa HA, Aoki T, Cardinali G & al. 2020. Unambiguous identification of fungi: where do we stand and how accurate and precise is fungal DNA barcoding? IMA fungus 11(14): [32 p.]. https://doi.org/10.1186/s43008-020-00033-z

Makonde HM, Boga HI, Osiemo Z, Mwirichia R, Stielow JB, Göker M, Klenk HP. 2013. Diversity of *Termitomyces* associated with fungus-farming termites assessed by cultural and culture-independent methods. PLoS ONE 8(2): e56464. https://doi.org/10.1371/journal.pone.0056464

Mossebo DC, Essouman EPF, Machouart M C, Gueidan C. 2017. Phylogenetic relationships, taxonomic revision and new taxa of *Termitomyces* (*Lyophyllaceae*, *Basidiomycota*) inferred from combined nLSU-and mtSSU-rDNA sequences. Phytotaxa 321(1): 71–102. https://doi.org/10.11646/phytotaxa.321.1.3

Nobre T, Fernandes C, Boomsma JJ, Korb J, Aanen DK. 2011. Farming termites determine the genetic population structure of *Termitomyces* fungal symbionts. Molecular Ecology 20(9): 2023–2033. https://doi.org/10.1111/j.1365-294X.2011.05064.x

Nobre T, Koopmanschap B, Baars JJP, Sonnenberg ASM, Aanen DK. 2014 The scope for nuclear selection within *Termitomyces* fungi associated with fungus-growing termites is limited. BMC Evolutionary Biology 14(121): [12 p.]. https://doi.org/10.1186/1471-2148-14-121

Poulsen M, Hu HF, Li C, Chen ZS, Xu LH, Otani A, Nygaard S, Nobre T et al. 2014 Complementary symbiont contributions to plant decomposition in a fungus-farming termite. Proceedings of the National Academy of Sciences of the United States of America 111(40): 14500–14505. https://doi.org/10.1073/pnas.1319718111

Tibuhwa DD. 2012. *Termitomyces* species from Tanzania, their cultural properties and unequalled basidiospores. Journal of Biology and Life Science 3(1): 140–159. https://doi.org/10.5296/jbls.v3i1.1723

Trifinopoulos J, Nguyen LT, von Haeseler A, Minh BQ. 2016. W-IQ-TREE: a fast online phylogenetic tool for maximum likelihood analysis. Nucleic Acids Research 44(W1): W232–W235. https://doi.org/10.1093/nar/gkw256

Vesala R, Niskanen T, Liimatainen K, Boga H, Pellikka P, Rikkinen J. 2017. Diversity of fungus-growing termites (*Macrotermes*) and their fungal symbionts (*Termitomyces*) in the semiarid Tsavo Ecosystem, Kenya. Biotropica 49(3): 402-412. https://doi.org/10.1111/btp.12422

Vilgalys R, Hester M. 1990. Rapid genetic identification and mapping of enzymatically amplified ribosomal DNA from several *Cryptococcus* species. Journal of Bacteriology 172(8): 4238–4246. https://doi.org/10.1128/JB.172.8.4238-4246.1990

Vreeburg SME, de Ruijter NCA, Zwaan BJ, da Costa RR, Poulsen M, Aanen DK. 2020. Asexual and sexual reproduction are two separate developmental pathways in a *Termitomyces* species. Biology Letters 16(20200394): [5 p.]. https://doi.org/10.1098/rsbl.2020.0394

White TJ, Bruns T, Lee S, Taylor J. 1990. Amplification and direct sequencing of fungal ribosomal RNA genes for phylogenetics. 315–322, in: MA Innis & al. (eds). PCR protocols: a guide to methods and applications. Academic Press, San Diego CA. https://doi.org/10.1016/B978-0-12-372180-8.50042-1

MYCOTAXON

ISSN (print) 0093-4666 (online) 2154-8889 Mycotaxon, Ltd. ©2022

January–March 2022—Volume 137, pp. 51–61

https://doi.org/10.5248/137.51

Clitopiloides prati and *Trichopilus lecythiformis* spp. nov. from Australia

David L. Largent* & Molly B. Cribari

Biological Sciences, Humboldt State University, 1 Harpst St, Arcata CA 95521, USA

* Correspondence to: *mrp@humboldt1.com*

Abstract—*Clitopiloides prati* (from northeastern Queensland) and *Trichopilus lecythiformis* (from coastal New South Wales) are described as new entolomatoid species based on morphological characters. Morphological similarities are discussed for these and other closely related species. We also provide nuclear ribosomal RNA repeat (nrITS) and large subunit (nrLSU) sequences where obtained

Key words—*Agaricales, Basidiomycota, Entolomataceae,* taxonomy

Introduction

Agarics are readily recognized as representing *Entolomataceae* (*Agaricales*) by their flesh colored basidiospores that are angular at least in end view; the family has a cosmopolitan distribution and is common in temperate and tropical ecosystems. Within the family, basidiomes exhibit highly diverse morphologies and ecologies. One consequence of this diversity is the acceptance of 1848 species as valid by Kalichman & al. (2020), the second highest of all families classified in the *Agaricales*.

The multigeneric classification of *Entolomataceae* utilized in this paper follows Largent (1994). The reasons for adopting this approach are detailed in Largent (2020), but important points are reiterated here: a) the basionym for nearly every genus in Largent (1994) is identical to the infrageneric basionyms in Romagnesi & Gilles (1979), Noordeloos (1992, 2004), and Noordeloos & Gates (2012); (b) it is relatively easy to distinguish the different genera visually

using this classification in the field; c) although a comprehensive classification based on a phylogenetic and morphological approach in *Entolomataceae* is not yet universally accepted, many segregate entolomatoid genera are supported by phylogenetic analysis (Karstedt & al. 2019, He & al. 2019).

Australian field investigations from 2009–12 within northeastern Queensland's Wet Tropics Bioregion and from 2010–12 in the temperate rainforests of central New South Wales have uncovered several novel species in the *Entolomataceae* (Largent & Abell-Davis 2011; Largent & al. 2011a,b, 2013a,b, 2014, 2016; Bergemann & al. 2013). Here we describe and illustrate two unusual new species from Australia: *Clitopiloides prati* and *Trichopilus lecythiformis*.

Materials & methods

Macro- & micromorphology

Colors were identified subjectively and coded according to Kornerup & Wanscher (1978) with color plates noted in parentheses (E63) in the species description. Common or general names for colors used in this paper are found in the Colour Sample to Colour Name section in the back of the color handbook where each page presents tables flagging technical names for color by * and placing common names in italics; we designate the technical color names using quotation marks (e.g., "Saruk").

Fresh collections were heat dried. Dried basidiomata were sectioned and rehydrated in 3% KOH. A Nikon Eclipse C*i* compound microscope with Lumera Infinity 2 imaging software was used to examine and measure microscopic features following Largent (1994). In the taxonomic descriptions x = mean dimensions, Q = range of length/width ratios from individual structures, Q_m = mean of all individual length/width ratios, and x/y = the total number of structures measured (x) and the total number of collections examined (y). Specimens were deposited in the Plant Pathology Herbarium, Orange Agricultural Institute, Orange, New South Wales, Australia (DAR); or the Fungarium, Biology Department, Humboldt State University, Arcata, Calfornia, USA (HSC).

DNA sequences

Dried basidiomata were pulverized and DNA extracted according to Largent & al. (2011a,b). The ITS region (ITS1, 5.8S and ITS2) of the nuclear ribosomal RNA repeat (nrITS) was amplified with primers ITS1F (Gardes & Bruns 1993) and ITS4 (White Q al. 1990) and the nuclear large subunit (nrLSU) was amplified with primers ctb6 and tw13 (White & al. 1990). PCR reactions of the nrITS and nrLSU were performed in 50 uL reactions following the procedure as outlined in Largent & al. (2011b) and PCR cycling followed the protocol detailed in Bergemann & Garbelotto (2006). PCR products were cleaned using 1 µL of ExoSAP-IT (GE Healthcare) and incubated at 37 °C for 15 min followed by 80 °C for 45 min. Cycle sequencing was performed at MCLAB (South San Francisco CA) using an

ABI3730XL sequencer to obtain bi-directional sequences. Contigs were assembled and edited with Sequencher 4.8.

Taxonomy

Clitopiloides prati Largent, **sp. nov.** FIG. 1

IF 558177

Differs from *Entoloma cyathus* by its greyish brown, appressed fibrillose pileus, equal stipe, encrusting pigments, pileipellis with erect to suberect distal cells, longer cheilocystidia, ammonia-like odor, and habitat in a lawn.

TYPE: Australia, Queensland, Cook Region, Smithfield, 10 Marcia Close, 16.8261°S 145.6857°E, gregarious in lawn, 27 September 2010, Peter Newling 40a (**Holotype** HSC A1429); GenBank MW520128, MW520127)

ETYMOLOGY—the genitive of the Latin *partum*, referring to the habitat in a lawn.

BASIDIOMATA clitocyboid. PILEUS 30–70 mm broad, ≤25 mm high, plano-convex to plane, deeply depressed to infundibuliform; radially appressed-fibrillose at all times; typically with a metallic luster when fresh; at first greyish brown (6E2, "Saruk") fading with age to greyish brown to brown (6E3–4) with the disc area remaining greyish brown; not hygrophanous nor translucent-striate; margin incurved becoming plane, entire then eroded; CONTEXT white to off-white, thickness not measured. LAMELLAE ≤30 mm long, 7–10 mm broad; white at first, flesh colored with spore maturation; uncinate with a decurrent tooth or subdecurrent to decurrent; close; edges smooth then eroded, not denticulate; wavy, concolorous; lamellulae 4–7 mm high, 4–15 mm long. STIPE ≤60 × ≤14 mm, equal; white becoming at the base faintly brownish with handling and age; longitudinally appressed fibrillose; BASAL TOMENTUM absent. ODOR strong, ammonia-like when crushed. TASTE not taken.

BASIDIOSPORES 5 to (rarely) 6 distinct angles in profile and side views, very rarely 4-angled in polar view; in profile view isodiametric to nearly heterodiametric, on average subisodiametric; apex acute, obtuse, or flat; 6.9–8.8 × 5.6–7.6 μm (x= 8.0 ± 0.34 × 6.8 ± 0.4 μm; Q =1.04–1.4; Q_m = 1.2 ± 0.1; x/y = 64/2). BASIDIA clavate, tapered to a narrow or moderately broad base, granules abundant but obscure, 26.6–39.9 × 9.9–12.0 µm (x = 33. ± 3.4 × 11.0 ± 0.65 µm; Q =2.6–3.6; Q_m = 2.6 ± 0.3; x/y = 22/2); 4–sterigmate, sterigma 1.2–5.8 µm long. LAMELLAR EDGE partially sterile. CHEILOCYSTIDIA abundant, but often not on every lamella; appear as terminal cells of tramal hyphae, versiform in shape (clavate, broadly cylindro-clavate, cylindro-clavate, rarely vesiculose, sometimes fusiform), short to long, at times at the end of a long stalk; colorless; 27.6–104.7 × 6.7–28.6 µm (x= 53.8 ± 16.2 × 13.7 ± 4.0 µm;

Q =1.8–9.4; Q_m = 4.2 ±.1.7; x/y = 61/2). Pleurocystidia absent. Lamellar trama when sectioned distinct and 20–30 µm deep, with the mediostratum composed of subparallel, longitudinally entangled, dark colored hyphae bordered by two subhymenia of entangled, colorless, narrow hyphae with non-gelatinized walls; in squash mounts hyphae narrow to very broad and with both ends rounded, 59.8–451.0 × 2.3–23.2 µm (x = 202 ± 110.6 × 10.3 ± 5.1 µm; Q =6.1–54.2; Q_m = 22.4 ± 12.4; x/y = 26/2). Pileipellis ~80 µm deep, a tightly entangled layer of narrow hyphae with distal 1–4 cells erect to suberect; pileocystidia narrowly clavate to cylindric, 23.4–79.0 × 3.0–12.8 µm (x = 44.6 ± 15.7 × 7.6 ± 2.3 µm; Q =2.0–10.6; Q_m = 6.3 ± 2.4; x/y = 27/2). Pileal tramal hyphae in squash sections with distal cells with narrow to broadly acuminate ends, 67.8–261.0 × 8.8–30.6 μm (x = 173.8 ± 67.4 × 16.3 ± 7.2 μm; Q_m = 12.0 ± 5.2; x/y = 11/2). Stipitipellis at the apex 33.0–62.3 µm deep, an entangled layer of hyphae with erect, suberect, or prostrate distal cells; caulocystidia clavate to cylindric, 20.5–91.4 × 4.1–10.8 µm (x = 49.4 ± 18.2 × 6.7 ± 1.7 µm; Q =4.4–12.7; Q =7.7 ± 3.0; x/y = 23/2). Stipe tramal hyphae in longitudinal sections subparallel and entangled, 103–405 × 6.9–36.8 µm (x = 245.2 ± 91.0 × 18.6 ± 8.2 µm; Q = 6.9–25.9; Q_m = 14.4 ± 5.2; x/y = 20/2). Oleiferous hyphae absent in all tramal tissues. Lipid globules absent. Pigmentation slightly to definitely encrusting on lamellar and pileus tramal hyphae; uniform, cytoplasmic, and light brownish in pileocystidia. Clamp connections absent in the pileipellis, typically absent at base of basidia and cheilocystidia, and absent on the hyphae of the pileipellis.

Ecology & Distribution–Gregarious, broadcast over a 10 × 4 m area in a lawn. Spring; early to late September. Known only from type locality.

Additional specimen examined—**AUSTRALIA, Queensland, Cook Region**, Smithfield, 10 Marcia Close, 16.8261°S 145.6857°E, gregarious in lawn, 9 September 2010, **Topotype** Peter Newling

Distinctive characters–Clitocyboid basidiomata with deeply depressed to infundibuliform radially appressed-fibrillose greyish brown pilei that have a metallic luster when fresh, subdecurrent to decurrent close lamellae, an equal stipe that becomes brownish when handled, a strong ammoniac odor, and a lawn habitat. Microscopically distinguished by subisodiametric distinctly angular basidiospores (x = 9 × 7 µm), versiform often long-stalked cheilocystidia, a pileipellis ~80 µm deep with a tightly entangled layer of narrow hyphae with the distal 1–4 cells erect to suberect, cytoplasmic pigmentation in the pileocystidia and encrusting pigment on the walls of the pileal and lamellar tramal hyphae and the presence of caulocystidia.

Fig. 1. *Clitopiloides prati* (holotype HSC A1429; except B): A. basidioma with deeply depressed to nearly infundibuliform pileus; B. (Topotype HSC A1430) overly mature basidiomata with infundibuliform pileus; C. 5-angled basidiospores; D. clavate sterigmate basidium tapered to narrow base; E. cluster of broadly clavate to cylindro-clavate cheilocystidia; F. tightly entangled stipitipellis ~2.4 cm down stipe apex, with semi-erect to prostrate caulocystidia; G. pileipellis from disc with loosely entangled hyphal layer with semi-erect cylindro-clavate pileocystidia. Scale bars: A, B = 14 mm; C = 8 µm; D= 33 µm; E = 15 µm; F = 50 µm; G = 50 µm.

Comments–*Clitopiloides prati* morphologically resembles *C. cyathus* (Romagn. & Gilles) Largent from Gabon and the Ivory Coast in its brownish colored basidiomata, deeply depressed to infundibuliform pileus, decurrent lamellae, presence of cheilocystidia, and 5–6-angled basidiospores measuring 7–9 × 5.7–7.6 μm. However, *C. cyathus* is distinguished by its yellowish brown ("bistre") glabrous, translucent-striate, hygrophanous pileus, denticulated lamellae, clavate stipe, lack of odor or an odor of bitter almonds, cheilocystidia measuring 25–45 × (8.5–)12–16(–24) μm, vacuolar pigmentation, and rainforest habitat (Romagn. & Gilles, 1979). *Entoloma cuboidosporum* (Beeli) E. Horak from Malaysia, Singapore, Zaire, Madagascar, Gabon, and the Congo shares the brownish, deeply depressed to infundibuliform pileus and decurrent lamellae found in *C. prati* but differs in its glabrous pileus, farinaceous odor, and cuboid basidiospores (Horak, 1980).

GenBank's Blastn tool shows the ITS sequence from *C. prati* as 88.63% similar to *Entoloma subclitocyboides* W.M. Zhang (= *E. subinfundibuliforme* T.H. Li & Chuan H. Li) from China. *Entoloma subclitocyboides* differs from *C. prati* in its broader (7.0–8.5 μm) isodiametric basidiospores, dirty yellowish to pale yellow brown pileus, adnexed subventricose lamellae, lack of odor, lack of encrusting pigments in the lamellar trama and pileipellis, presence of clamp connections, and habit on soil in mixed forest (He & al. 2014).

Trichopilus lecythiformis Largent, **sp. nov.** Fig. 2

IF 558178

Differs from *Trichopilus tibiiformis* by its yellowish brown, translucent striate pileus, a stipe that bruises yellow brown, larger basidiospores, and abundant lecythiform cheilocystidia and pleurocystidia.

Type: Australia, New South Wales, North Coast, Myall Lakes National Park, Mungo Brush campground 32.5457°S 152.3094°E, 30 April 2012, DL Largent 10482 (**Holotype,** DAR 81840).

Etymology—*lecythiformis* (Latin) referring to the lecythiform cheilocystidia.

Basidiomata omphalinoid. Pileus 13–14 mm broad × 1.0–1.5 mm tall, convex to plano-convex, shallowly depressed, tomentulose on the disc, glabrous elsewhere; dark yellowish brown (5F4 "sepia brown") in center at all times, elsewhere light yellowish brown (5E4 "hair brown") becoming darker with age and drying (5F7 "coffee"), margin decurved then plane, very slightly crenulate, translucent striate to the disc, moist and wet, not hygrophanous. Lamellae 6 mm long × 2–2.5 mm high, adnate to short decurrent at first, then long decurrent, at first off-white to orange white (5A4), becoming pale orange (5B3) with sporulation, narrow then distant, edge smooth and concolorous;

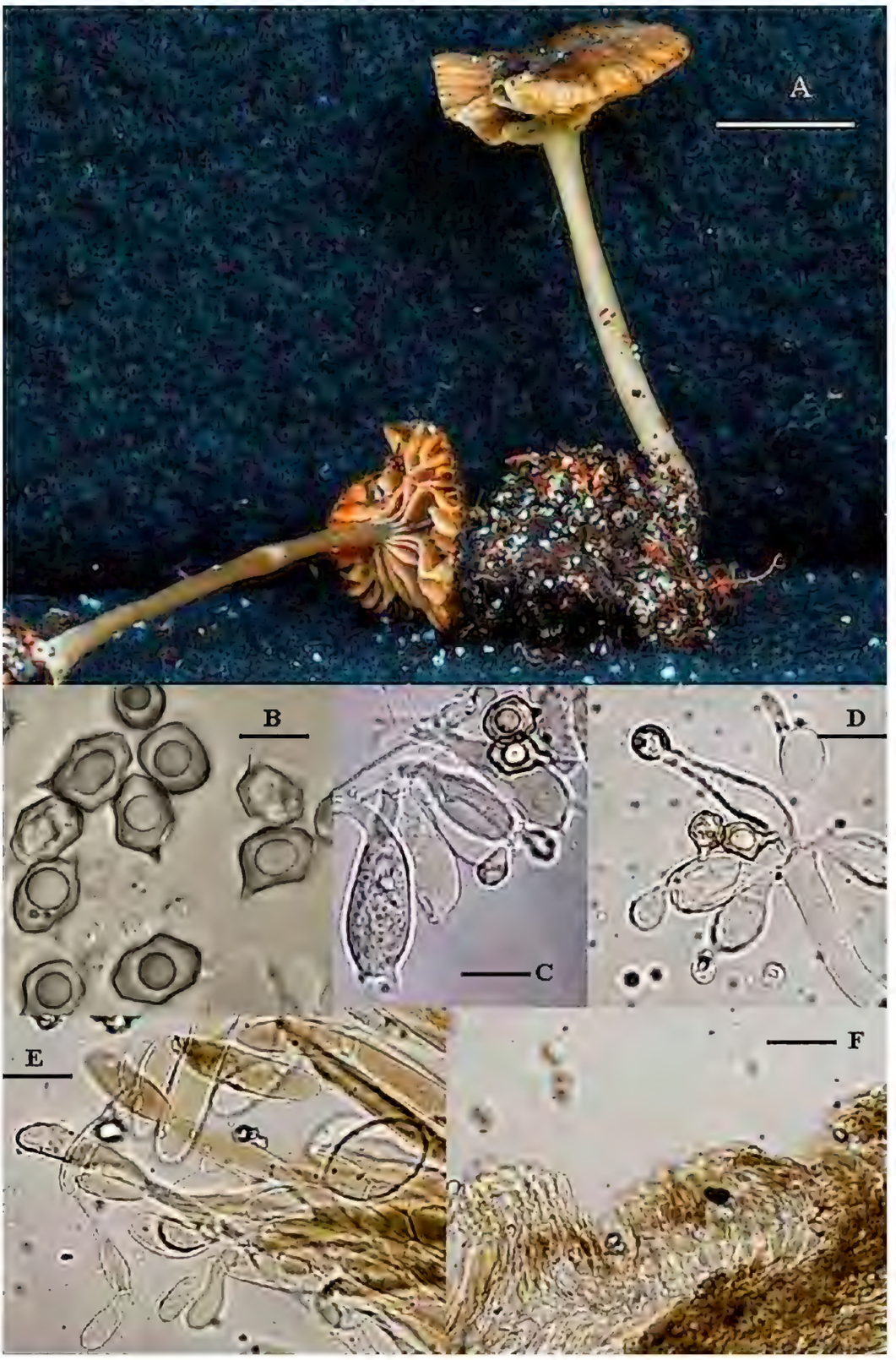

Fig. 2. *Trichopilus lecythiformis.* (holotype DAR 81840): A. basidiomata; B. 6-angled basidiospores in profile view; C. clavate sterigmate basidia tapered to narrow bases; D. tibiiform and lecythiform cheilocystidia; E. clavate pileocystidia with plasmatic brown pigments; F. disc pileipellis showing loosely entangled palisadoderm. Scale bars: A = 14 mm; B = 8 µm; C = 12 µm; D = 14 µm; E = 13 µm; G = 55 µm.

lamellae 2–3 between lamellae, in 2 series (one short, one medium long). Stipe 22–28 × 1.0–1.5 mm, straight, equal, faintly pruinose at the apex, elsewhere glabrous, yellowish white (4A2) to light yellowish grey (5B2 "putty"), bruising yellowish brown (~5E5 "bronze" = "bronze brown"); basal tomentum absent. Odor and Taste mild, not distinctive.

Basidiospores 5–6-angled, angles distinct, hilar appendage large and distinct, apex rarely acute, often obtuse, nearly all spores with single globule, on average heterodiametric, 9.8–14.4 × 6.8–9.9 μm (x = 11.3 ± 1.0 × 8.3 ± 0.67 μm; Q = 1.19–1.55; Q_m = 1.35 ± 0.10; x/y = 53/1). Basidia clavate, narrowly tapered at the very base (7/8 inflated), with granules that are not brilliant; 23.0–36.1 × 11.2–13.8 µm (x = 29.3 ± 2.9 × 12.4 ± 0.85 µm; Q =1.80–2.76; Q_m = 2.38 ± 0.26; x/y = 16/1)); 4-sterigmate, sterigma 2.52–5.79 µm. Cheilocystidia abundant, lamellar edge mostly sterile, tibiiform and lecythiform, colorless, 29.7–57.0 × 10.2–17.4 µm (x = 46.7 ± 7.8 × 14.2 ± 1.5 µm; Q =2.5–4.0; Q_m=3.29±0.45;x/y=19/1);head4.0–9.0µmwide(x/y21/1);neck2.4–6.2µmwide (x/y = 21/1). Pleurocystidia rare at the lamellar edge, similar in shape and size to cheilocystidia. Lamellar tramal hyphae subparallel and in squash mounts rounded at both ends, 55.3–100.9 × 12.2–20.6 μm (x = 78.8 ± 13.9 × 15.1 ± 3.1 μm; Q =3.50–6.75; Q_m = 5.35 ± 1.13; x/y = 7/1). Pileipellis on the disc a distinct palisadoderm with erect hyphal elements attached laterally, distal 4–5 cells inflated, prostrate from the pileus middle to margin; pileocystidia clavate to cylindro-clavate, 27.1–109.3 × 8.25–18.8 µm (x = 56.7 ± 20.4 × 13.9 ± 2.7 µm; Q = 2.62–8.11; Q_m = 4.44 ± 1.44; x/y = 38/1). Pileal tramal hyphae subparallel and entangled, 30.8–56.0 × 5.7–9.5 µm (x = 47.0 ± 8.9 × 8.6 ± 1.5 µm; Q =3.41–8.80; Q =5.66 ± 1.78; x/y = 6/1). Stipitipellis a cutis; caulocystidia absent. Stipe tramal hyphae in longitudinal section, subparallel and entangled; 55.6–273.3 × 7.4–28.5 µm (x = 155.4 ± 59.3 × 15.2 ± 5.0 µm; Q = 4.83–19.40; Q_m = 10.74 ± 4.35; x/y = 15/1). Oleiferous hyphae absent in all tramal tissues. Lipid globules absent. Pigmentation cytoplasmic, uniform, brown in apical cells of the pileipellis, encrusted in the basal cells; basidia containing non-brilliant granules. Clamp connections absent.

Ecology & Distribution– Scattered in grass along the beach track, Myall Lakes National Park, coastal New South Wales, Australia, in late April (autumn). Known only from the type locality.

Comments–*Trichopilus lecythiformis* is known from a single collection of a single basidiome from sandy soil in Myall Lakes National Park in late April. However, this species is distinct from all other Australian entolomatoid fungi due to its combination of small delicate basidiomata, pileus with a

yellowish brown disc, long clavate to cylindro-clavate pileocystidia, 5–6-sided basidiospores measuring ~11.3 × 8.3 μm, tibiiform to lecythiform colorless cheilocystidia and pleurocystidia, palisadoderm pileipellis, and the absence of caulocystidia and clamp connections. As far as I know, this the first report of a *Trichopilus* species in Australia with a small delicate basidiome.

Seven other species might be confused with *T. lecythiformis* due to their small delicate basidiomata and tibiiform/lecythiform cheilocystidia. They can be distinguished from *T. lecythiformis* as follows: *T. tibiiformis* Largent & Aime from Guyana has a dark violet brown shaggy, opaque pileus and smaller (7.6–9.8 × 4.5–6.7 μm) 6–7-angled basidiospores (Aime & Largent 2010). *Entoloma mariae* G. Stev. from New Zealand has smaller (9–11 × 7–8.5 *μm)* basidiospores, larger (35–100 × 10–22 *μm*) cheilocystidia, a pruinose stipe, and clamp connections; *E. perplexum* E. Horak, also from New Zealand, has a brownish grey small (5–10 mm diam) pileus, cinnamon-colored young lamellae, a pileipellis composed of vesiculose or clavate capitate pileocystidia, a weak farinaceous taste and odor, and 5–6-angled basidiospores measuring 10–13 × 7–9 μm (Horak 2008). *Entoloma festivum* Noordel. & al. from the Netherlands has a warm reddish brown hygrophanous pileus with a black disc, smaller (8.5–10.5 × 5.5–7.5 μm) 5–8-angled basidiospores, cheilocystidia with a vacuolar pigment, and clamp connections (Noordel. & al. 2010). *Rhodophyllus capitatus* Romagn. & Gilles has a pinkish white, scaly, translucent striate pileus, pale brownish lamellae, smaller (7–8.5 × 5.7–6.7-μm) 4–5-angled prismatic basidiospores; *R. applanatus* Romagn. & Gilles has a fairly dark pinkish brown, translucent-striate scaly pileus, smaller (7–8.5 × 5.7–6.7 μm) 5–6-angled basidiospores; and *R. lepiotoides* Romagn. & Gilles has a yellow brown opaque pileus with a brown disc and slight umbo and smaller (6.5–7.5 × 5.7–6.5) 4–5-angled basidiospores (Romagn. & Gilles 1979). In the literature cited above, there has only been one collection studied for five of these species and two collections for *R. lepiotoides*, suggesting that these species are either rare or the small basidiomata overlooked in the field.

Unfortunately, because all attempts at obtaining DNA sequences from DLL 10482 (the holotype of *T. lecythiformis*) were unsuccessful, this collection is proposed as a *Trichopilus* species based on morphology alone. However, phylogenetic analyses using four genes demonstrated that *Trichopilus* is a statistically supported genus with bootstrap values of 100%/1 representing a monophyletic group nested deep within the Inocephalus–Cyanula clade. Sequences for all four genes (mtSSU, nLSU, rrpb2, and tef1) were obtained from *T. tibiiformis* with delicate basidiomata in this study (Karstedt & al. 2019).

We are confident that if sequences are obtained from future collections of *T. lecythiformis*, the species will cluster in this well-supported group.

Acknowledgments

Materials required to complete this manuscript were provided by the Largent family trust. The Australian Tropical Herbarium and the School of Marine and Tropical Biology, James Cook University, provided fieldwork and logistical support. The DNA sequences generated in this study were completed and financed by Dr. Sarah Bergemann. Comments by the two expert reviewers, Dr. Sarah Bergemann (Middle Tennessee State University, Murfreesboro, TN, USA) and Dr. Timothy J. Baroni (New York State University at Cortland, NY, USA), and by the Nomenclature Editor, Dr. Shaun Pennycook, were also helpful. We wish to thank Peter Newling for his assistance in collecting in northeastern Queensland and collecting PN40, the holotype collection for *Clitopiloides prati*. We also wish to thank Pam O'Sullivan and Skye Moore for their assistance in collecting in New South Wales. Finally, David and Pamela Largent especially wish to thank Dr. Sandra Abell for being an extraordinary research advisor and contact at James Cook University during the five years of research in northeastern Queensland.

Literature cited

Aime MC, Largent DL, Henkel TW, Baroni TJ. 2010. The *Entolomataceae* of Pakaraima Mountains of Guyana IV: new species of *Calliderma*, *Paraeccilia* and *Trichopilus*. Mycologia 102: 633–649. https://doi.org/10.3852/09-162

Bergemann SE, Garbelotto M. 2006. High diversity of fungi recovered from the roots of mature tanoak (*Lithocarpus densiflorus*) in northern California. Canadian Journal of Botany 84:1380–1394. https://doi.org/10.1139/b06-097

Bergemann SE, Largent DL, Abell-Davis SB. 2013. *Entocybe haastii* from Watagans National Park, New South Wales, Australia. Mycotaxon 126: 61–70. https://doi.org/10.5248/126.61

Gardes M, Bruns TD. 1993. ITS primers with enhanced specificity of basidiomycetes – application to the identification of mycorrhizae and rusts. Molecular Ecology 2: 113–118. https://doi.org/10.1111/j.1365-294X.1993.tb00005.x

He XL, Li TH, Peng WH, Gan BC. 2014. A taxonomic revision of *Entoloma clitocyboides* and *E. subinfundibuliforme* from Hainan Island, South China. Mycoscience 55: 103–107. https://doi.org/10.1016/j.myc.2013.06.002

He XL, Horak E, Wang D, Li TH, Peng WH, Gan BC. 2019. Descriptions of five new species in *Entoloma* subgenus *Claudopus* from China, with molecular phylogeny of *Entoloma* s.l. MycoKeys 61: 1–26. https:// doi.org/10.3897/mycokeys.61.46446

Horak E. 1980. *Entoloma* (*Agaricales*) in Indomalaya and Australasia. Beihefte zur Nova Hedwigia 65. 352p.

Horak E. 2008. Agaricales of New Zealand 1: *Pluteaceae* (*Pluteus*, *Volvariella*); *Entolomataceae* (*Claudopus*, *Clitopilus*, *Entoloma*, *Pouzarella*, *Rhodocybe*, *Richoniella*). Fungal Diversity Research Series 19. 305p.

Karstedt F, Capelari M, Baroni TJ, Largent DL, Bergemann SE. 2019. Phylogenetic and morphological analyses of species of the *Entolomataceae* (*Agaricales*, *Basidiomycota*) with cuboid basidiospores. Phytotaxa 391: 1–27. https://doi.org/10.11646/phytotaxa.391.1.1

Kalichman J, Kirk PM, Matheny PB. 2020. A compendium of generic names of agarics and *Agaricales*. Taxon 69(3): 425–447. https://doi.org/10.1002/taxa.12240

Kornerup A, Wanscher JH. 1978. Methuen handbook of colour 3rd ed. Richard Clay Ltd: Chichester, Sussex. 252 p.

Largent DL. 1994. Entolomatoid fungi of the western United States and Alaska. Mad River Press Inc: Eureka, California. 516 p.

Largent DL. 2020. Nomenclature changes in the "Entolomatoid fungi of western North America and Alaska" (Largent 1994). Mycotaxon 135: 789–794. https://doi.org/10.5248/135.789

Largent DL, Abell-Davis S. 2011 Observations on *Inocephalus virescens* comb. nov. and *Alboleptonia stylophora* from northeastern Queensland. Mycotaxon 116: 231–245. https://doi.org/10.5248/116.231

Largent DL, Abell-Davis SE, Cummings GA, Ryan KL, Bergemann SE. 2011a. Saxicolous species of *Claudopus* (*Agaricales, Entolomataceae*) from Australia. Mycotaxon 116: 253–264. https://doi.org/10.5248/116.253

Largent DL, Bergemann SE, Cummings GA, Ryan, KL, Abell-Davis SE, Moore S. 2011b. *Pouzarella* (*Agaricales, Entolomataceae*) species from New South Wales (Barrington Tops National Park) and northeastern Queensland, Australia. Mycotaxon 117: 435–483. https://doi.org/10.5248/117.435

Largent DL, Bergemann SE, Abell-Davis SE, Kluting KL, Cummings GA. 2013a. Three new *Inocephalus* species with cuboid basidiospores from New South Wales and Queensland, Australia. Mycotaxon 123: 301–319. https://doi.org/10.5248/123.301

Largent DL, Bergemann SE, Abell-Davis SE, Kluting KL, Cummings GA. 2013b. Five *Leptonia* species from New South Wales and Queensland, Australia. Mycotaxon 125: 11–35. https://doi.org/10.5248/125.11

Largent DL, Bergemann SE, Abell-Davis SB. 2014. *Entoloma* species from New South Wales and northeastern Queensland, Australia. Mycotaxon 129(2): 329–359. http://doi.org/10.5248/129.329

Largent DL, Kluting KL, Anderson NM, Bergemann SE. 2016. New leptonioid species from New South Wales and northeastern Queensland, Australia. Mycotaxon 131: 153–176. https://doi.org/10.5248/131.153

Noordeloos ME. 1992. *Entoloma* s.l. Fungi Europaei 5: 1–760.

Noordeloos ME. 2004. *Entoloma* s.l. Fungi Europaei 5a: 761–1378.

Noordeloos ME, Gates GM. 2012. The *Entolomataceae* of Tasmania. Fungal Diversity Research Series 22: 400 p. https://doi.org/10.1007/978-94-007-4679-4

Noordeloos ME, Rommelaars LCAF, Gelderblom JNJ. 2010. *Entoloma festivum*, a new species in subgenus *Trichopilus* from the Netherlands. Mycotaxon 111: 495–499. https://doi.org/10.5248/111.495

Romagnesi H. 1978. Les fondements de la taxinomie des rhodophylles et leur classification. (Tirage à part de "Beiheft 59 zur Nova Hedwigia"). J. Cramer, Vaduz. 79 p.

Romagnesi H, Gilles G. 1979. Les rhodophylles des forêts côtières du Gabon et de la Côte d'Ivoire avec une introduction générale sur la taxinomie du genre. Beihefte zur Nova Hedwigia 59. 649 p.

White TJ, Bruns T, Lee S, Taylor JW. 1990. Amplification and direct sequencing of fungal ribosomal RNA genes for phylogenetics. 315–322, in: MA Innis et al. (eds). PCR protocols: a guide to methods and applications. Academic Press, Inc. New York. http://doi.org/10.1016/B978-0-12-372180-8.50042-1

MYCOTAXON

ISSN (print) 0093-4666 (online) 2154-8889 Mycotaxon, Ltd. ©2022

January–March 2022—Volume 137, pp. 63–71

https://doi.org/10.5248/137.63

Neoacrodictys elegans gen. & sp. nov. from Hainan Province, China

Ji-Wen Xia, Tai-Chang Mu, Zhao-Xue Zhang, Zhuang Li, Xiu-Guo Zhang*

Shandong Provincial Key Laboratory for Biology of Vegetable Diseases and Insect Pests, College of Plant Protection, Shandong Agricultural University, Taian, Shandong 271018, China

* Correspondence to: *sdau613@163.com*

Abstract—A new anamorphic genus and species, *Neoacrodictys elegans*, is illustrated and described from dead branches of an unidentified plant in Hainan Province, China. The genus is characterized by darkly pigmented turbinate to obpyriform muriform conidia produced from monoblastic integrated terminal conidiogenous cells on macronematous unbranched conidiophores.

Key words—asexual *Ascomycota*, hyphomycetes, saprobes, taxonomy

Introduction

During our continuing surveys of dematiaceous hyphomycetes colonizing diverse plant habitats from the forests of Hainan, China, a fungus that does not match any existing genera was collected growing on unidentified dead twigs. Morphological studies and a literature review (Ellis 1971, 1976; Subramanian 1971; Matsushima 1975, 1983, 1985, 1989, 1993, 1995; Castañeda-Ruiz 1986; Castañeda-Ruiz & Kendrick 1990a,b, 1991; Wu & Zhuang 2005; Seifert & al. 2011; Ma & al. 2016, 2021; Xia & al. 2016, 2017; Xu & al. 2020a,b, 2021; Zhang & al. 2020; Niu & al. 2021) indicated that the fungus represents an undescribed genus. Molecular phylogenetic analysis confirmed its morphological identity, and the fungus is described here as a new genus and species.

Materials & methods

Isolates & morphological analysis

Samples of dead branches collected were placed in separate zip-lock plastic bags, taken to the laboratory, and then incubated at 27 °C for more than 2 weeks in an artificial climate box in 9 cm diameter plastic Petri dishes with moistened filter paper. Single-spore cultures of hyphomycetes that could not be identified on natural substrate were isolated from dead branches and incubated on potato-dextrose agar (PDA: 200 g boiled and filtered white potatoes, 20 g dextrose, 15 g agar, 1 L distilled water). All PDA plates were incubated at 25 °C for 1–2 months. The colonies were photographed using a Powershot G7X mark II digital camera. Micromorphological characters were observed using an Olympus SZX10 stereomicroscope and Olympus BX53 microscope, both fitted with Olympus DP80 high definition colour digital cameras. All fungal strains were stored in 10% sterilized glycerin at 4 °C for further studies. The specimens are deposited in the Herbarium of Plant Pathology, Shandong Agricultural University, Taian, Shandong, China (HSAUP). Ex-type cultures are deposited in the Shandong Agricultural University Culture Collection, Taian, Shandong, China (SAUCC).

DNA extraction, PCR amplification, sequencing

Genomic DNA was extracted from colonies grown on PDA, using the CTAB method (Doyle & Doyle 1990). The large subunit ribosomal RNA gene (LSU) was amplified and sequenced by using primers pairs LROR/LR5 (Vilgalys & Hester 1990, Glass & Donaldson 1995).

PCR was conducted using an Eppendorf Master Thermocycler. DNA was amplified in 25-µL volumes containing 12.5 µL Vazyme Green Taq Mix, 1 µL of each forward and reverse primer (10 µM) (Biosune), and 1 µL template genomic DNA adjusted to a total volume of 25 µL with distilled deionized water. PCR parameters were 95 °C for 5 min, followed by 35 cycles of denaturation at 95 °C for 30 s, annealing at 55 °C for 30 s, and extension at 72 °C for 1 min, ending with a final elongation step at 72 °C for 10 min. PCR products were estimated visually by staining with GelRed after 1% agarose gel electrophoresis. Sequencing was done bi-directionally by Biosune Co. Ltd. (Shanghai, China). Consensus sequences were obtained using MEGA 7 (Kumar & al. 2016). All sequences generated in this study were deposited in GenBank (Table 1).

Sequence alignment and phylogenetic analysis

The quality of our amplified nucleotide sequences was checked and combined by MEGA 7 (Kumar & al. 2016), and reference sequences were retrieved from the National Center for Biotechnology Information (NCBI). Sequences were aligned using MAFFT 7.310 (http://mafft.cbrc.jp/alignment/server/index.html) (Katoh & al. 2019), and manually corrected using MEGA 7.

The LSU sequences were analyzed phylogenetically using Maximum-Likelihood (ML) and Bayesian Inference (BI) methods. RaxML and Bayesian analyses were run on the CIPRES Science Gateway portal (Miller & al. 2012) using RaxML 8.2.9 and MrBayes 3.2.6. Evolutionary models were calculated using MrModelTest 2.3 (Nylander

Table 1. Strains and sequences included in the phylogenetic analyses. The new sequence is set in bold.

Taxon	Voucher	GenBank LSU
Acrodictys bambusicola	CGMCC 3.18641	KX033564
Acrodictys elaeidicola	CGMCC 3.18642	KX033568
	CGMCC 3.18643	KX033569
Asterina sp.	SH-2014	KM386978
Botryotinia fuckeliana	AFTOL-ID 59	AY544651
Buelliella physciicola	Ertz 18113 (BR)	KP456147
	Ertz 19173 (BR)	KP456148
Buelliella poetschii	Ertz 18115 (BR)	KP456149
	Ertz 18116 (BR)	KP456150
Junewangia lamma	CGMCC 3.18652	KU751882
	CGMCC 3.18653	KU751883
Junewangia sphaerospora	CGMCC 3.18655	KX033572
Karschia cezannei	Cezanne-Eichler B26 (hb. Diederich)	KP456152
	Cezanne-Eichler 7453 (hb. Diederich)	KP456153
	Ertz 19186 (BR)	KP456154
Karschia talcophila	Diederich 16749 (hb. Diederich)	KP456155
Labrocarpon canariense	Ertz 16308 (BR)	KP456157
	Ertz 16907 (BR)	KP456158
'Melaspilea' lekae	Ertz 17325 (BR)	KP456162
Mycosphaerella pneumatophorae	JK5253B=AFTOL-ID 762	FJ176856
Mycosphaerellaceae sp.	SD-01	JN872645
	KH00300	GU017553
Melaspileopsis cf. *diplasiospora*	Ertz 16247 (BR)	KP456164
	Ertz 16624 (BR)	KP456165
	Ertz 16625 (BR)	KP456166
Melaspileopsis sp.	Ertz 17904 (BR)	KP456167
	Ertz 17913 (BR)	KP456168
Neoacrodictys elegans	**SAUCC H4600**	**MW907608**
Rhexoacrodictys erecta	CGMCC 3.18656	KX033555
	CGMCC 3.18657	KX033556
Rhexoacrodictys fimicola	CGMCC 3.18658	KX033553
	CGMCC 3.18660	KX033554
Stictographa lentiginosa	Ertz 17447 (BR)	KP456169
	Ertz 17570 (BR)	KP456170
	van den Boom 47621 (hb. v.d. Boom)	KP456171

2004) to select the best-fit model for each data partition according to the Akaike criterion. For ML analyses the default parameters were used and bootstrap support (BS) was calculated using the rapid bootstrapping algorithm with the automatic halt option. Bayesian analyses included two parallel runs of 5,000,000 generations, with the stop rule option and a sampling frequency set to each 1000 generations. The 50% majority rule consensus trees and posterior probability (PP) values were calculated after discarding the first 25% of the samples as burn-in. Trees were plotted in FigTree 1.4.2 (http://tree.bio.ed.ac.uk/software/figtree) and edited with Adobe Illustrator CS 5.

Phylogenetic results

The dataset comprised 35 taxa representing 17 named species and four undetermined species including *Botryotinia fuckeliana* (AFTOL-ID 59) as outgroup. The final LSU alignment totaled 1178 characters including gaps. Of these characters, 825 were constant, 89 parsimony-uninformative, and 264 parsimony-informative. For the BI and ML analyses, the substitution model GTR+I+G for LSU was selected and incorporated into the analyses. The topology of the ML tree confirmed the tree topologies obtained from BI analyses, so only the ML tree is presented (Fig. 1). In this tree, our strain formed an independent clade.

Taxonomy

Neoacrodictys J.W. Xia & X.G. Zhang, **gen. nov.**

MB 816515

Differs from *Acrodictys* by its turbinate conidia and oblique septa that are often marked by dark bands.

Type species: *Neoacrodictys elegans* J.W. Xia & X.G. Zhang

Etymology: *Neoacrodictys* = "*neo-*" + "*acrodictys*" (Lat.), referring to its similarity to the genus *Acrodictys*.

Conidiophores macronematous, mononematous, unbranched, septate, brown to dark brown, paler towards the apex, indeterminate with flask-shaped percurrent extensions. Conidiogenous cells monoblastic, integrated, terminal, cylindrical, pale brown to brown, smooth. Conidial secession schizolytic. Conidia solitary, acrogenous, muriform, turbinate to obpyriform, euseptate, with one longitudinal and a few transverse oblique septa usually obscured by dark bands.

Neoacrodictys elegans J.W. Xia & X.G. Zhang, **sp. nov.** Fig. 2

MB 816516

Differs from *Acrodictys* spp. by its turbinate conidia and oblique septa usually obscured by dark bands.

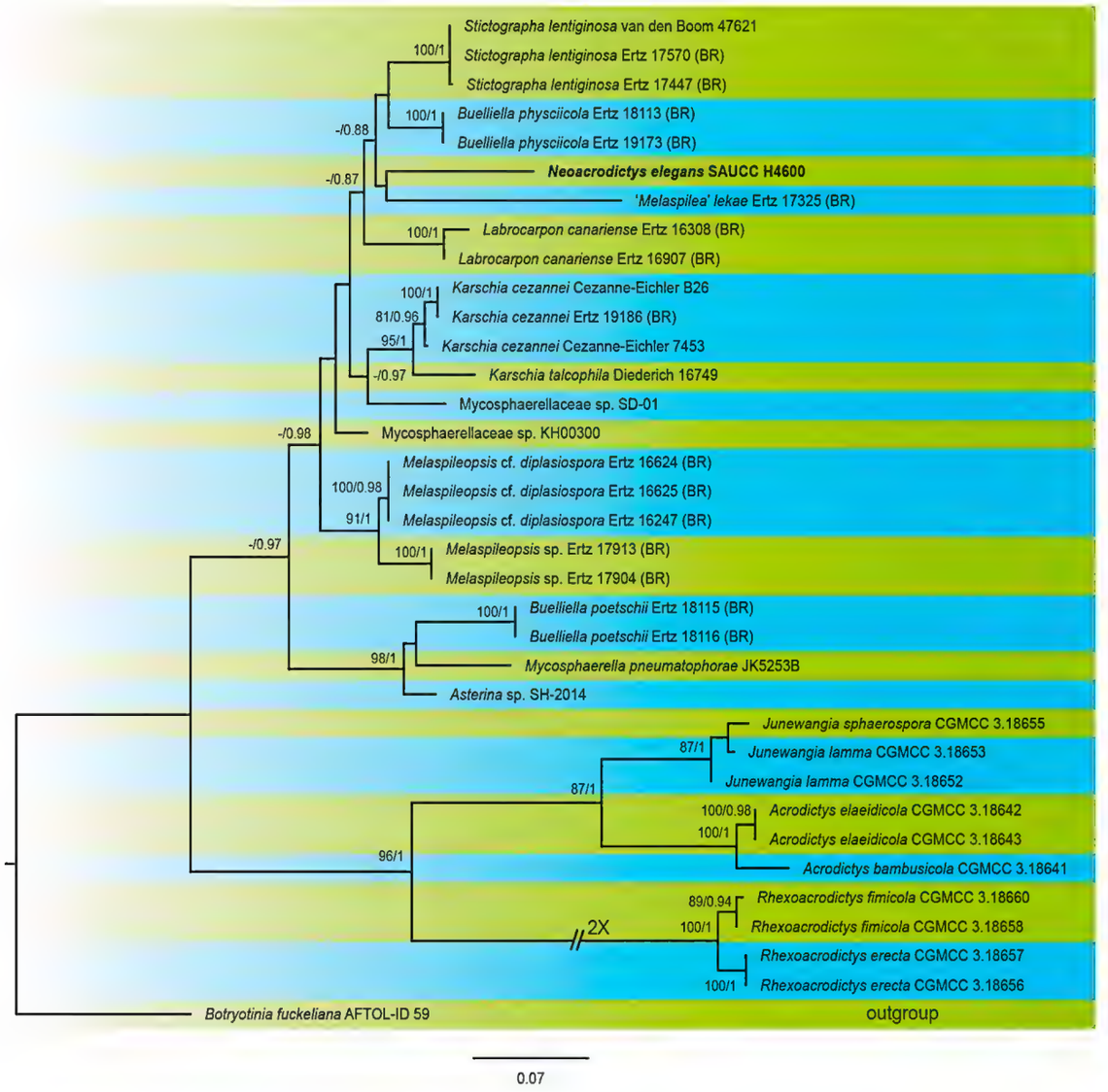

Fig. 1. Phylogram generated from RaxML analysis based on the LSU gene. Bootstrap support values are shown for ML >70% and BI >0.85. Branches shortened to fit the page are indicated by two diagonal lines accompanied by the length reduction factor. The new sequence is indicated in bold.

Type: China, Hainan Province: Ledong, Jianfengling National Forest Park, 18.70°N 108.87°E, on dead branches of an unidentified broadleaf tree, 22 April 2014, Y.R. Ma (**Holotype**, HSAUP H4600; ex-type culture, SAUCC H4600; GenBank MW907608).

Etymology: refers to its conidia that have an elegant appearance.

Colonies effuse, brown, hairy. Mycelium partly superficial, partly immersed in the substrate. Conidiophores macronematous, mononematous, erect, unbranched, straight or flexuous, thick-walled, smooth, dark brown; swollen at the base, narrower and paler toward the apex, 3–7-septate, 54–105 × 4.5–7.5 μm at the broadest part, indeterminate with 1–2 flask-shaped percurrent

extensions. Conidiogenous cells integrated, terminal, cylindrical to doliiform, subhyaline to pale brown, smooth, monoblastic; extending through the scar of the last conidium on the conidiophores. Conidia solitary, muriform, turbinate to obpyriform, 15.5–22.5 × 12–18 µm, with 1 or 2 transverse septa and 1 or 2 longitudinal or oblique septa; septa typically crossing at right angles and usually obscured by a black band. Basal cell funnel-shaped, delimited by a transverse septum, pale brown. Conidial secession schizolytic.

Discussion

Neoacrodictys demonstrates unique morphological and ontogenetic features. It is distinguished by macronematous, mononematous, cylindrical and unbranched conidiophores with holoblastic conidiogenous cells that produce darkly pigmented, muriform, turbinate to obpyriform conidia. A key to *Neoacrodictys* and morphologically similar genera is provided.

Neoacrodictys elegans resembles *Acrodictys bambusicola* M.B. Ellis, *A. elaeidicola* M.B. Ellis, and *A. malabarica* Subram. & Bhat, which differ by conidial shape (Ellis 1961, Subramanian & Bhat 1989, Xia & al. 2017). Also, the genera *Acrodictys* and *Neoacrodictys* belong in different phylogenetic clades (Fig. 1).

Key to *Neoacrodictys* and morphologically similar genera

1. Conidia bicellular ..... *Ityorhoptrum*
1. Conidia muriform 2
2. Conidia with appendages ..... *Pseudoacrodictys*
2. Conidia without appendages 3
3. Conidial secession rhexolytic ..... *Rhexoacrodictys*
3. Conidial secession schizolytic 4
4. Conidia maturing after secession ..... *Acrodictyella*
4. Conidia becoming pigmented and septate prior to secession 5
5. Conidial midpoint attached to the conidiogenous cell ..... *Coleodictyospora*
5. Conidial base attached to the conidiogenous cell 6
6. Conidiophore aseptate, comprising a single conidiogenous cell that extends percurrently after each conidial dehiscence ..... *Junewangia*
6. Conidiophores conspicuously septate, a new conidiogenous cell forming after each conidial dehiscence 7
7. Conidial basal cell inconspicuous, reduced to a short, cylindrical disk ..... *Acrodictys*
7. Conidial basal cell conspicuous, distinctly funnel-shaped and flat at the base ..... *Neoacrodictys*

Fig. 2. *Neoacrodictys elegans* (holotype, HSAUP H4600): a. Colony on PDA (surface and reverse); b. Colony on MEA (surface and reverse); c. Conidia; d–f. Conidiophores, conidiogenous cells, and conidia. Scale bars: c–f = 20 μm.

Acknowledgments

The authors express gratitude to Dr. Jian Ma (College of Agronomy, Jiangxi Agricultural University, Nanchang, Jiangxi, China) and Dr. Li-Guo Ma (Institute of Plant Protection, Shandong Academy of Agricultural Sciences, Jinan, Shandong,

China) for serving as pre-submission reviewers and to Dr. Shaun Pennycook for nomenclatural review and Dr. Lorelei L. Norvell for editorial review. This work was jointly supported by the National Natural Science Foundation of China (Nos. 31900014, U2002203, 31750001) and National Science and Technology Fundamental Resources Investigation Program of China (2019FY100700).

Literature cited

Castañeda-Ruiz RF. 1986. Deuteromycotina de Cuba. Hyphomycetes IV. Instituto de Investigaciones Fundamentales en Agricultura Tropical "Alejandro de Humboldt," Habana, Cuba. 17 p.

Castañeda-Ruiz RF, Kendrick WB. 1990a. Conidial fungi from Cuba: I. University of Waterloo Biology Series 32. 53 p.

Castañeda-Ruiz RF, Kendrick WB. 1990b. Conidial fungi from Cuba: II. University of Waterloo Biology Series 33. 61 p.

Castañeda-Ruiz RF, Kendrick WB. 1991. Ninety-nine conidial fungi from Cuba and three from Canada. University of Waterloo Biology Series 35. 132 p.

Doyle JJ, Doyle JL. 1990. Isolation of plant DNA from fresh tissue. Focus 12: 13–15. https://doi.org/10.2307/2419362

Ellis MB. 1961. Dematiaceous hyphomycetes II. Mycological Papers 79. 23 p.

Ellis MB. 1971. Dematiaceous hyphomycetes. Commonwealth Mycological Institute, Kew, Surrey, England. 608 p.

Ellis MB. 1976. More dematiaceous hyphomycetes. Commonwealth Mycological Institute, Kew, Surrey, England. 507 p.

Glass NL, Donaldson GC. 1995. Development of primer sets designed for use with the PCR to amplify conserved genes from filamentous ascomycetes. Applied and Environmental Microbiology 61(4): 1323–1330.

Katoh K, Rozewicki J, Yamada KD. 2019. MAFFT online service: multiple sequence alignment, interactive sequence choice and visualization. Briefings in Bioinformatics 20(4): 1160–1166. https://doi.org/10.1093/bib/bbx108

Kumar S, Stecher G, Tamura K. 2016. MEGA7: Molecular evolutionary genetics analysis version 7.0 for bigger datasets. Molecular Biology and Evolution 33(7): 1870–1874. https://doi.org/10.1093/molbev/msw054

Ma J, Zhang XG, Castañeda-Ruíz RF. 2016. *Podosporiopsis*, a new genus of synnematous hyphomycetes from China. Mycotaxon 131: 773–780. https://doi.org/10.5248/131.773

Ma J, Ma LG, Cui RQ, Kuang WG, Zhang XG, Castañeda-Ruíz RF. 2021. *Blastophragmia plurisetulosa* gen. & sp. nov. from China. Mycotaxon 136: 163–167. https://doi.org/10.5248/136.163

Matsushima T. 1975. Icones microfungorum a Matsushima lectorum. Published by the author, Kobe, Japan.

Matsushima T. 1983. Matsushima mycological memoirs 3. Published by the author, Kobe, Japan.

Matsushima T. 1985. Matsushima mycological memoirs 4. Published by the author, Kobe, Japan.

Matsushima T. 1989. Matsushima mycological memoirs 6. Published by the author, Kobe, Japan.

Matsushima T. 1993. Matsushima mycological memoirs 7. Published by the author, Kobe, Japan.

Matsushima T. 1995. Matsushima mycological memoirs 8. Published by the author, Kobe, Japan.

Miller MA, Pfeiffer W, Schwartz T. 2012. The CIPRES science gateway: enabling high-impact science for phylogenetics researchers with limited resources. 1–8, in: C Stewart (ed.). Proceedings of the 1st Conference of the Extreme Science and Engineering Discovery Environment: bridging from the extreme to the campus and beyond. Chicago, IL. New York: Association for Computing Machinery. https://doi.org/10.1145/2335755.2335836

Niu ZF, Zhang K, Li DW, Ma J, Castañeda-Ruiz RF. 2021. *Distobactrodesmium* gen. nov. to accommodate *Bactrodesmium rahmii* and notes on *Bactrodesmium*. Mycotaxon 136: 141–158. https://doi.org/10.5248/136.141

Nylander JAA. 2004. MrModeltest v2. program distributed by the author. Evolutionary Biology Centre, Uppsala University.

Seifert K, Morgan-Jones G, Gams W, Kendrick B. 2011. The genera of hyphomycetes. CBS Biodiversity Series 9. 997 p.

Subramanian CV. 1971. Hyphomycetes: an account of Indian species, except cercosporae. The Indian Council of Agricultural Research, New Delhi. 930 p.

Subramanian CV, Bhat DJ. 1989. Hyphomycetes from south India I. Some new taxa. Kavaka 15: 41–74.

Vilgalys R, Hester M. 1990. Rapid genetic identification and mapping of enzymatically amplified ribosomal DNA from several *Cryptococcus* species. Journal of Bacteriology 172(8): 4238–4246. https://doi.org/10.1128/jb.172.8.4238-4246.1990

Wu WP, Zhuang WY. 2005. *Sporidesmium*, *Endophragmiella* and related genera from China. Fungal Diversity Research Series 15. 351 p.

Xia JW, Ma YR, Gao JM, Li Z, Zhang XG. 2016. *Sympodiosynnema*, a new genus of dematiaceous hyphomycetes from southern China. Mycotaxon 131: 45–48. https://doi.org/10.5248/131.45

Xia JW, Ma YR, Li Z, Zhang XG. 2017. *Acrodictys*-like wood decay fungi from southern China, with two new families *Acrodictyaceae* and *Junewangiaceae*. Scientific Reports 7: 7888.

Xu ZH, Qiu L, Kuang WG, Shi XG, Zhang XG, Castañeda-Ruíz RF, Ma J. 2020a. *Varioseptispora chinensis* gen. & sp. nov., *V. apicalis* nom. nov., *V. hodgkissii* comb. nov., and *V. versiseptatis* comb. nov. Mycotaxon 135: 753–759. https://doi.org/10.5248/135.753

Xu ZH, Zhang K, Luo YQ, Zhang XG, Castañeda-Ruíz RF, Ma J. 2020b. *Mesocorynespora sinensis* gen. & sp. nov. from southern China. Mycotaxon 135: 617–622. https://doi.org/10.5248/135.617

Xu ZH, Qiu L, Zhang XG, Castañeda-Ruíz RF, Xia JW, Ma J. 2021. *Teratospermopsis* gen. nov. for *Chaetendophragmia protuberata*, with a taxonomic review of *Teratosperma*. Mycotaxon 136: 85–95. https://doi.org/10.5248/136.85

Zhang K, Guo WH, Heredia G, Delgado-Zúñiga JP, Ma J, Castañeda-Ruíz RF. 2020. *Anasporidesmiella* gen. nov. for an atypical *Sporidesmiella* species and for *A. manifesta* sp. nov. Mycotaxon 135: 719–727. https://doi.org/10.5248/135.719

MYCOTAXON

ISSN (print) 0093-4666 (online) 2154-8889 Mycotaxon, Ltd. ©2022

January–March 2022—Volume 137, pp. 73–87

https://doi.org/10.5248/137.73

Neotypification of *Claviceps humidiphila* and recognition of *C. bavariensis* sp. nov.

Miao Liu[1*], Eiji Tanaka[2*], Miroslav Kolařík[3]

[1]*Ottawa Research and Development Centre, Agriculture and Agri-Food Canada, 960 Carling Ave. Ottawa, Ontario K1A0C6 Canada*

[2] *Ishikawa Prefectural University, 1–308 Suematsu, Nonoichi, Ishikawa 921-8836 Japan*

[3] *Department of Botany Faculty of Science, Charles University, Benatska 2CZ-128 01, Praha 2 Czech Republic*

[*]Correspondence to: *miaomindy.liu@agr.gc.ca; tanakae@ishikawa-pu.ac.jp*

Abstract—*Claviceps humidiphila* [≡ *C. purpurea var. phalaridis*] was previously typified with the holotype collected by Tanda in Japan and an epitype from Bavaria, Germany. Phylogenetic analyses based on translation elongation factor 1-α (TEF1-α) and RNA polymerase II second largest subunit (RPB2) indicated that the previously designated epitype from Germany was not conspecific with the Japanese species. The German specimen is proposed as a new species, *C. bavariensis,* and a specimen collected from the type location (Chiba, Japan) is designated as a neotype for *C. humidiphila*, replacing the lost holotype.

Key words—*Ascomycota*, *Clavicipitaceae*, ergot fungi, *Hypocreales,* taxonomy

Introduction

Claviceps was validly published by Tulasne (1853), as discussed by Donk (1963). *Claviceps purpurea* Tul. was selected as lectotype by Clements & Shear (1931) and accepted by Donk (1963). Tulasne (1853) noted the hosts of *C. purpurea* include cereal crops (e.g., *Avena*, *Secale*, *Triticum*) and grasses (e.g., *Alopecurus*, *Dactylis*, *Lolium*, *Poa*). Thereafter, the reported host range increased to more than 400 species in *Poaceae*. Molecular studies (Pažoutová & al. 2000, Douhan & al. 2008) revealed cryptic speciation within the pre-molecular concept of *C. purpurea* s.lat. Pažoutová & al. (2015) provided

formal taxonomic descriptions for four phylogenetic species to replace *C. purpurea* s.lat.: *C. purpurea* s.str., *C. arundinis*, *C. humidiphila*, and *C. spartinae*.

Claviceps humidiphila was characterized by its frequently larger conidia than *C. purpurea*, sclerotia capable of floating on water, and typical habit on *Calamagrostis*, *Deschampsia caespitosa*, and *Phalaris arundinacea*. Previously, Tanda recognized three varieties: *C. purpurea* var. *alopecuri*, *C. purpurea* var. *dactylidis*, and *C. purpurea* var. *phalaridis*, producing conspicuously larger conidia and on specific host plants. *Claviceps purpurea* var. *alopecuri* was found on *Alopecurus*, but also on *Agrostis clavata*, *A. palustris*, *Calamagrostis epigejos*, *C. hakonensis*, *Holcus lanatus*, *Phleum pratense*, *Poa* spp., *Polypogon fugax*, and *Trisetum bifidum* (Tanda 1978a,b,c, 1979a,c, 1981; Tanda & Kawatani 1980). *Claviceps purpurea* var. *dactylidis* was found on *Dactylis glomerata* and *Calamagrostis epigejos* (Tanda 1980). *Claviceps purpurea* var. *phalaridis* occurred on *Phalaris*, *Calamagrostis epigejos*, and *C. pseudophragmites* (Tanda 1979a).

Pažoutová & al. (2015), who noted that the conidial dimension and host range of *C. purpurea* var. *dactylidis* and *C. purpurea* var. *alopecuri* overlapped with both *C. purpurea* s.str. and *C. humidiphila*, treated the varieties as taxa of uncertain identities. However, *C. purpurea* var. *phalaridis* was considered as representing the same taxon as the species later named *C. humidiphila*. The name *C. purpurea* var. *phalaridis* could not be elevated to species rank as a stat. nov. because this would create an illegitimate later homonym of *C. phalaridis* J. Walker [≡ *Aciculosporium phalaridis* (J. Walker) M. Kolařík & Píchová]. Instead, *Claviceps humidiphila* was proposed as a nom. nov. based on the replaced synonym *Claviceps purpurea* var. *phalaridis*. Tanda (1979b) designated a holotype from Chiba, Japan, now believed to have been lost (see Taxonomy: Comments below, p. 78). Pažoutová & al. (2015) designated an epitype from Bavaria, Germany, but phylogenetic analysis indicates that the epitytpe is not conspecific with Japanese collections. Here, we propose *Claviceps bavariensis* as a new species holotypified by the Bavarian collection and designate a recent specimen from Chiba, Japan, as the neotype of *C. purpurea* var. *phalaridis* [≡ *C. humidiphila*].

Material & methods

DNA extraction, PCR, sequencing, analyses

Axenic cultures were developed for two samples collected from Canada (Alberta) and gDNA extracted following Shoukouhi & al. (2019). For 29 samples from Japan

(Chiba, Gifu, Ishikawa, Kanagawa, Miyagi, Nagano, Niigata, Tochigi, Toyama), axenic cultures were developed from peeled ergots that were surface-disinfected in 2% sodium hypochlorite solution for 1 min; gDNA was extracted according to Izumitsu & al. (2012). Two genomic regions, RPB2 (RNA polymerase II second largest subunit) and TEF1-α (translation elongation factor 1-α), were amplified and sequenced using modified fRPB2-5F (5′-TTTCGTGGTATTGTTCGCAGA-3′) specific for ergot fungi (Pažoutová & al. 2015) and fRPB2-7cR (Liu & al. 1999), and the primer pair EF1-983F and EF1-2218R (Rehner & Buckley 2005). For 29 samples from Japan, the RPB2 regions were amplified and sequenced using Cla-RPB2 (5′-CAGTGAAACCAGAAAGGCCTTC-3′) and modified fRPB2-7cR (5′-CCCATGGCCTGCTTACCCAT-3′). Polymerase chain reactions (PCRs) were performed in 10 µL volumes containing final concentrations of 10× Titanium Taq buffer (with 3.5 mM $MgCl_2$), 0.1 mM dNTPs, 0.08 µM each of forward and reverse primer, 50× Titanium Taq polymerase (Takara Bio, California), 0.01 mg BSA, and 1 µL of DNA template. A touchdown protocol was applied with an initial denaturation at 95 °C for 3 min, followed by 5 cycles of 95 °C for 1 min, annealing at 63 °C (decrease 1 °C per cycle) for 45 s, and extension at 72 °C for 1 min 30 s followed by 30 cycles of 95 °C for 1 min, annealing at 58 °C for 45 s, extension at 72 °C for 1 min 30 s, concluding with a final extension at 72 °C for 8 min. PCR products were sequenced using a ABI BigDye Terminator 3.1 cycling sequencing kit on Applied Biosciences Prism 3130xl Genetic Analyzer.

Fifty-nine reference RPB2 and TEF1-α sequences from previous studies downloaded from GenBank were compiled and aligned with sequences generated in the present study (31 strains) using MAFFT online version 7 (Katoh & al. 2019, https://mafft.cbrc.jp/alignment/server/, accessed in Aug 2020). Alignments of concatenated sequences were generated in Geneious Prime 2020.1.2. (http://www.geneious.com). Maximum parsimony (MP) analyses were performed using PAUP* 4.0b10 (Swofford 2002). Heuristic searches with 200 replicates of random stepwise addition and tree bisection-reconnection branch swapping were conducted with a limit of 1,000,000 re-arrangements for each replicate. Bootstrapping analyses used 2000 replicates of a full heuristic search with random stepwise addition of 20 replicates with limit of 50,000 rearrangements per replicate. Bayesian inference analyses were conducted using MrBayes 3.2 (Ronquist & al. 2012) with a GTR model chosen by a previous study (Liu & al. 2021). Each run was set to four chains of 100,000,000 MCMC generations, sampling frequency was every 2000 generations, terminated when the standard deviation of the average split frequency was lower than 0.01. The BI consensus tree was directly generated after 25% burn-in.

Morphological examination

Specimens were conserved in the Herbarium, Department of Botany, National Museum of Nature and Science, Tsukuba, Japan (TNS) and the Canadian National Mycological Herbarium (DAOM); cultures were conserved in NARO Genebank,

Microorganism Section, Genetic Resources Center, National Agriculture and Food Research Organization, Tsukuba, Japan (MAFF).

Sclerotia were tested for floating ability using the protocol developed by Pažoutová & al. (2000). The shape, size, color, and surface of sclerotia were recorded from observations of available sclerotia. Specimens were photographed using a DFC425 camera and Leica Application Suite 4.12.0 software attached to Leica M165C or Motic SMZ-168-BL stereo microscopes. Colors were characterized using html color HEX codes at the maximum approximation (https://htmlcolorcodes.com/color-names/). Sclerotial tissues were sectioned by hand for microscopical examination. Conidia were washed off from sclerotial surfaces and mounted in water or lactic acid for examination using a Zeiss Axio Scope.A1 microscope with differential interference contrast (DIC) illumination, or Zeiss Imager M2. Microphotographs were taken with either a Jenoptik ProgRes SpeedXTcore 5 digital camera using ProgRes image processing software for CCC samples or with (alternatively) an Axiocam 503 color camera using a Zeiss ZEN (blue edition) 2.6 pro imaging processing for Canadian samples, and for Japanese samples a MicroPublisher 5.0 or 3.3 RTV using QImaging QCapture Pro software or a WRAYCAM-NOA2000 using the Wraymer MicroStudio processing package. Conidiogenesis in sclerotia was observed under a Zeiss Imager M2 by mounting small fragments of internal sclerotial tissue obtained by slicing or picking.

Germinated sclerotia were obtained by chill-treating sclerotia on moistened quartz sand in sealed cups at 4 °C about 3 months followed by incubation under 12 h light/12 h dark condition at 20 °C for a few weeks. Ascostromal sections were prepared as described by Tanaka & al. (2020). Examination and microphotography of asci and ascospores followed the same procedures as used for conidia.

Phylogenetic results

DNA sequences generated in this study were submitted to GenBank. Including 59 reference sequences, the TEF1-α and RPB2 matrices comprised 90 taxa and 918 and 1027 characters. The phylogenetic tree based on the concatenated alignment of TEF1-α and RPB2 placed the specimen collected from the type location of *C. purpurea* var. *phalaridis* (TNS-F-60506 on *Phalaris arundinacea* Chiba) in a different clade, sister to CCC 434 (= DAOMC 251717), the epitype from Germany. Here, we retain the name *C. humidiphila* for the Japanese clade and propose *C. bavariensis* for the German clade. The two are sister species and closely related to *C. arundinis* and *C. perihumidiphila* (Fig. 1). Phylogenetic trees based on the individual genes showed localized low resolution as discussed by Shoukouhi & al. (2019 and Liu & al. (2020).

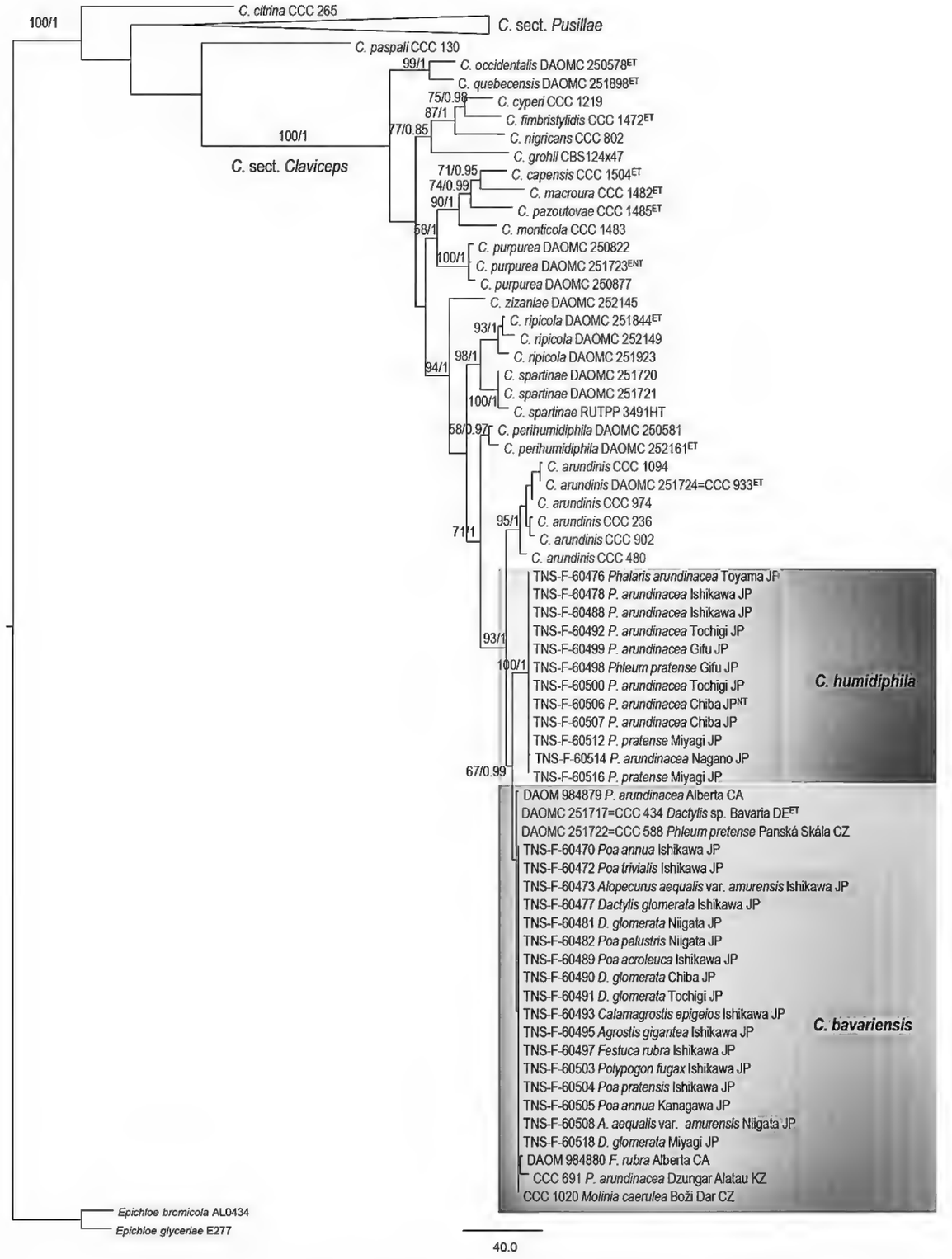

FIG. 1. Phylogenetic tree based on the concatenated sequence alignments of TEF1-α and RPB2 showing the separation and close relationship of *Claviceps humidiphila* and *C. bavariensis*. Reference sequences are in gray font, showing species names and voucher numbers; 24 taxa in *C.* sect. *Pussillae* are abbreviated to a single branch. The labels of the sequences in clades *C. humidiphila* and *C. bavariensis* include voucher numbers, hosts, locations, and country abbreviations: CA Canada; CZ Czech Republican; DE Germany; JP Japan; KZ Kazakhstan. Superscripts ET = ex-type, NT = neotype. Values on branches are bootstrapping values for MP analyses/posterior probability of BI.

Taxonomy

Claviceps humidiphila Pažoutová & M. Kolařík,
Fungal Biol. 119(1): 22 (2015) Fig. 2

≡ *Claviceps purpurea* var. *phalaridis* Tanda, J. Agric. Sci. (Tokyo) 24: 84 (1979).

Holotype (**lost**)—Japan, Chiba, Chiba, Yukijirushi Farm on *Phalaris arundinacea*, Aug 1, 1969, Seinosuke Tanda (TUAMH-PA 921).

Neotype (**here designated**, MBT395372)—Japan, Chiba, Chiba, Inage [= the holotype locality], 35.6672°N 140.1353°E, on *Phalaris arundinacea*, June 23, 2017, Eiji Tanaka (**Neotype**, TNS-F-60506; ex-type culture MAFF 247310; GenBank LC598958, LC598987).

Sclerotia dark purple (#1C0336) to black (#05000A), 4–15 × 0.8–1.4 mm, cylindrical, floating in fresh water. Conidia from sclerotial surface hyaline, aseptate, allantoid, oblong, ovoid, ellipsoid, lunate, 6.0–16.9 × 3.6–5.9 µm, L/W ratio 2.3–2.6.

Ascostromata light orange (#E2C86C) to purplish red (#E6B0AA). Stipe filiform, 6–13 mm long, 0.1–0.4 mm wide. Capitellum 0.5–1.9 mm diam. Perithecia obovoid, slightly fusiform to pyriform, 154–314 × 100–157 µm. Asci cylindrical 50–110 × 2.5–5.5 µm. Ascospores filiform, 85–110 µm long.

Additional specimens examined—**JAPAN**, **Chiba**, **Sakura**, Kodake, 35.7388°N 140.1661°E, on *Phalaris arundinacea*, June 23, 2017, Eiji Tanaka (TNS-F-60507; GenBank LC598959, LC598988), (TNS-F-60525, fruiting bodies derived from TNS-F-60507); **Gifu**, **Takayama**, Hirayu, 36.1917°N 137.5510°E, on *P. arundinacea*, Aug 14, 2016, Kazuhito Tanada (TNS-F-60499; GenBank LC598963, LC598992); 36.1914°N 137.5503°E, on *Phleum pratense*, Aug 14, 2016, Kazuhito Tanada (TNS-F-60498; GenBank LC598967, LC598996); **Ishikawa**, **Nomi**, Nabetani, 36.4189°N 136.5575°E, on *P. arundinacea*, June 30, 2016, Eiji Tanaka (TNS-F-60488; GenBank LC598961, LC598990); **Uchinada**, Kose, 36.6936°N 136.6842°E, on *P. arundinacea*, June 18, 2016, Eiji Tanaka (TNS-F-60478, MAFF 247302; GenBank LC598960, LC598989), (TNS-F-60524, fruiting bodies derived from TNS-F-60478); **Miyagi**, **Ohira**, 38.4683°N 140.8833°E, on *P. pratense*, Aug 10, 2017, Kazuhito Tanada (TNS-F-60512; GenBank LC598968, LC598997); **Nagano**, **Nagano**, Togakushi, 36.7711°N 138.0900°E, on *P. arundinacea*, Aug 1, 2018, Eiji Tanaka (TNS-F-60514; GenBank LC598966, LC598995); **Tochigi**, **Tochigi**, Fujioka, 36.2711°N 139.6567°E, on *P. arundinacea*, July 6, 2016, Kazuhito Tanada (TNS-F-60492, MAFF 247305; GenBank LC598965, LC598994); Nikko, Okukinu, 36.8681°N 139.3947°E, on *P. arundinacea*, Aug 15, 2016, Kazuhito Tanada (TNS-F-60500, MAFF 247310; GenBank LC598964, LC598993); **Toyama**, **Nanto**, Fukumitsu, 36.5636°N 136.8778°E, on *P. arundinacea*, June 16, 2016, Eiji Tanaka (TNS-F-60476, MAFF 247301; GenBank LC598962, LC598991).

Hosts—*Phalaris*, *Phleum*

Comments—In the original description of *C. purpurea* var. *phalaridis* (Tanda 1979b), the specimens TUAMH-PA 820 and TUAMH-PA 921 were listed as the first and second specimens examined followed by the word "Holotype." It is

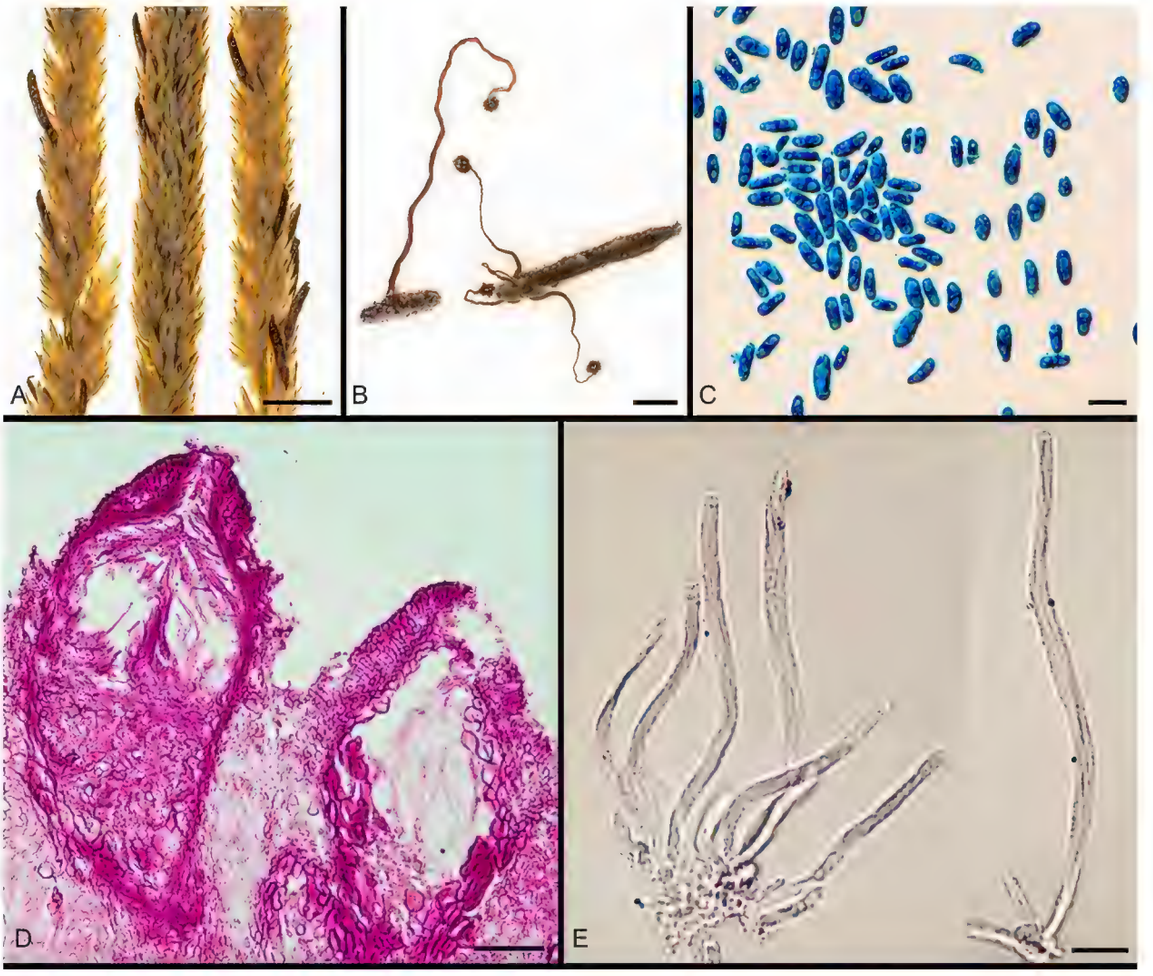

Fig. 2. *Claviceps humidiphila*: A. Sclerotia on *Phalaris arundinacea* (TNS-F-60478); B. Ascostromata (TNS-F-60524) developed from germinated sclerotia (TNS-F-60478); C. Conidia washed off sclerotia (TNS-F-60478); D. Perithecia semi-embedded in stromata; E. Asci with thick caps and filiform ascospores (TNS-F-60524). Scale bars: A = 10 mm; B = 2 mm; D = 50 µm; C, E = 10 µm.

likely that TUAMH-PA 921 was designated as holotype, although PA 820 was recorded as holotype in Pažoutová & al. (2015), possibly because PA 921 was erroneously overlooked. Nevertheless, we searched all of Tanda's research collections (1979b) using several approaches. Firstly, the abbreviation TUAMH is not cited in Index Herbariorum (http://sweetgum.nybg.org/science/ih/) where TUAT is cited as the correct code for Tokyo University of Agriculture Herbarium (Museum); however, TUAT is currently inactive, and its 100,000 specimens were transferred to the National Museum of Nature and Science, Tokyo (TNS) in 2007. We searched the TNS online database (http://db.kahaku.go.jp/webmuseum_en) for *Claviceps purpurea* collected in Japan; of the 18 specimens located, none had been collected from Chiba or

related to TUAMH PA 820 or PA 921. Next, we contacted the herbarium director and curator (Dr. Masanobu Higuchi and Dr. Tsuyoshi Hosoya), who recommended contacting Dr. Keiichi Motohashi at Tokyo University directly. According to a personal communication with Dr. Seinosuke Tanda, Tanda left all his un-submitted specimens in the laboratory at Tokyo University of Agriculture, where Dr. Motohashi checked 6000 specimens that had been collected by Dr. Tanda; 90% represented powdery mildews and the rest were rust fungi; no *Claviceps* specimens were found, possibly because other specimens had been discarded. Based on the collective evidence, it is likely that the specimens linked to the name *C. purpurea* var. *phalaridis* were lost. Therefore, we hereby designate a new specimen from the type location as neotype.

According to Tanda (1979b), the sclerotia were of different sizes. One specimen collected from Asahi-mura, Niigata (PA007), possessed much shorter sclerotia (2.3–7.7 × 0.6–1.3 mm; n = 215), while others had a wider size range (2.2–15.4 × 0.5–1.5 mm; n = 599). The number of stromata developed from sclerotia varied from 1 to 11, for which Tanda (1979b) cited the dimensions of 0.1–1.6 × 0.2–1.9 mm (capitellum), 2–13 × 0.1–0.9 mm (stipe), and 4.4–16.9 × 2.4–5.9 µm [L/W 2.2–2.6] (conidia; n = 1350). Our sclerotial, stromatal, and conidial measurements match those cited by Tanda. In addition, Tanda (1979b) also recorded perithecia at 161–217 × 91–130 µm (a slightly narrower range than our data), asci at 74–133 × 1.8–4.2 µm (slightly longer than our data), and ascospores at 72–129 µm (similar to our data).

Claviceps bavariensis M. Kolařík, E. Tanaka & M. Liu, **sp. nov.** Fig. 3

MB 838352

[≡ "*Claviceps humidiphila*" sensu epitype of Pažoutová & al. 2015, non Tanda 1979.]

Type—Germany, Bavaria, Philippsreut, 48.8564°N 13.6763°E, on *Dactylis* sp., 1988, Pažoutová (**Holotype**, PRM922708 [dried culture on T2 media]; ex-type culture CCC434; GenBank JX083704, JX083635).

= *Claviceps purpurea* var. *alopecuri* Tanda, J. Agric. Sci. (Tokyo) 22: 295 (1977).

= *Claviceps purpurea* var. *dactylidis* Tanda, J. Agric. Sci. (Tokyo) 25: 266 (1980).

Differs from *C. huimidiphila* in amplified TEF1-α region (918 nts) by at least seven sites (*C. humidiphila*/*C. bavariensis* = 271 A/G; 348 A/G; 642 T/C; 675 T/C; 688 C/T; 690 T/C; 860 T/C) that are identical within species.

Etymology—referring to the provenance of the type specimen

Sclerotia purplish brown (#452D2E), dark brown (#2D1E1E) to black (#272424), 3–10 × 0.3–1.4(–1.7) mm, ovoid, obclavate, narrow cylindrical,

Fig. 3. *Claviceps bavariensis*. A. Sclerotia on *Dactylis glomerata* (TNS-F-60477); B. Sclerotia on *Poa annua* (TNS-F-60470); C. Sclerotia on *Alopecurus aequalis* var. *amurensis* (TNS-F-60473); D. Sclerotia on *Festuca rubra* (DAOM 984880); E. Sclerotia on *Phalaris arundinacea* (DAOM984879); F. Sclerotia detached from PRM922708 (holotype); G. Sclerotia detached from DAOM 984880; H. Sclerotia detached from DAOM 984879; I. Longitudinal section near the rind showing textura prismatica (DAOM 984879); J, K. Ascostromata developed from germinated sclerotia from *D. glomerata* (TNS-F-60523), and *A. aequalis* var. *amurensis* (TNS-F-60521); L, M. Cross sections of sclerotia showing the color of inner tissue (DAOM 984879, 984880); N. Asci showing the thick caps with a central pore (TNS-F-60522); O. Conidiogenesis in sclerotia (DAOM 984879, 984880); P. Conidia washed off sclerotia (PRM922708, holotype); Q. Filiform ascospores (TNS-F-60520). Scale bars: A = 5 mm; B, C, F–H, J, K = 2 mm; D, E = 1 mm; L, M = 200 µm; I = 20 µm; N–Q = 10 µm.

curved, or subulate, floating in fresh water, interior white, greyish yellow (#D0CBA0) to olive brown (#4A423B) from center to margin, or vivid yellow (#FEE302) to deep yellow (#FFC40C) in center (3A8–4A8). Conidiogenous cell cylindrical, or obovoid, 12–23(–27) × 5–7 µm. Conidia ovoid, reniform, cylindrical, (5.5–)6.1–13.1(–14.3) × (2.3–)2.4–3.9(–4.4) µm, L/W ratio 2.1–2.2.

Ascostromata pinkish (#FFC0CB) to light brown (#5D4037). Stipe filiform 5–8 mm long. Capitellum 0.5–1 mm diam. Asci cylindrical, 50–155 × 2.8–5.0 µm. Ascospores filiform.

Additional specimens examined—**CANADA**, **Alberta**, **Beaverlodge**, on *Festuca rubra*, Aug. 2019, Henry Klein-Gebbinck (DAOM 984880; GenBank MW411019, MW411021), on *Phalaris arundinacea*, Aug. 2019, Henry Klein-Gebbinck (DAOM 984879; GenBank MW411018, MW411020). **JAPAN**, **Chiba**, **Sakura**, Usuiden, 35.7416°N 140.1850°E, on *Dactylis glomerata*, Jul 4, 2016, Kazuhito Tanada (TNS-F-60490; MAFF 247304; GenBank LC598969, LC598998); **Ishikawa**, **Hakusan**, Shiramine, 36.1150°N 136.6994°E, on *Poa acroleuca*, Jul 1, 2016, Eiji Tanaka (TNS-F-60489; GenBank LC598981, LC599010); Yorishinbo, 36.4770°N 136.5647°E, on *Poa annua*, Apr 29, 2016, Eiji Tanaka (TNS-F-60470; GenBank LC598977, LC599006); **Kanazawa**, Minato, 36.6450°N 136.6631°E, on *Calamagrostis epigejos*, Jul 18, 2016, Eiji Tanaka (TNS-F-60493; MAFF 247306; GenBank LC598985, LC599014); **Komatsu**, Imaemachi, 36.3772°N 136.4492°E, on *Poa trivialis*, May 9, 2016, Eiji Tanaka (TNS-F-60472; GenBank LC598979, LC599008); **Nomi**, Suedera, 36.4442°N 136.5081°E, on *Poa pratensis*, June 9, 2017, Eiji Tanaka (TNS-F-60504; GenBank LC598976, LC599005); **Nonoichi**, Nakabayashi, 36.5064°N 136.5994°E, on *Polypogon fugax*, June 5, 2017, Eiji Tanaka (TNS-F-60503; GenBank LC598986, LC599015); Suematsu, 36.5103°N 136.5967°E, on *Alopecuru. aequalis* var. *amurensis*, May 23, 2016, Eiji Tanaka (TNS-F-60473; culture MAFF 247299; GenBank LC598974, LC599003); (TNS-F-60521, fruiting bodies derived from TNS-F-60473); **Tsubata**, 36.6875°N 136.7589°E, on *F. rubra*, Jul 24, 2016, Eiji Tanaka (TNS-F-60497; GenBank LC598984, LC599013); **Uchinada**, Kose, 36.6758°N 136.6706°E, on *D. glomerata*, June 18, 2016, Eiji Tanaka (TNS-F-60477; GenBank LC598970, LC598999); (TNS-F-60523, fruiting bodies derived from TNS-F-60477); Koyodai, 36.6375°N 136.6300°E, on *Agrostis gigantea*, Jul 24, 2016, Eiji Tanaka (TNS-F-60495; GenBank LC598982, LC599011); **Iwate**, **Miyako**, Kuzakai, 39.6503°N 141.3574°E, on *D. glomerata*, Aug 7, 2019, Eiji Tanaka (TNS-F-60518; GenBank LC598973, LC599002); 39.6512°N 141.3574°E, on *Phleum pratense*, Aug 7, 2019, Eiji Tanaka (TNS-F-60516; GenBank LC598983, LC599012); **Kanagawa**, **Atsugi**, Nurumizu, 35.4347°N 139.3503°E, on *P. annua*, June 16, 2017, Kazuhito Tanada (TNS-F-60505; GenBank LC598978, LC599007); **Niigata**, **Sanjo**, Kamioura, 37.5883°N 139.0124°E, on *A. aequalis* var. *amurensis*, July 3, 2017, Kazuhito Tanada (TNS-F-60508; GenBank LC598975, LC599004); **Tokamachi**, Matsunoyama, 37.1189°N 138.5908°E, on *D. glomerata*, June 24, 2016, Eiji Tanaka (TNS-F-60481; GenBank LC598972, LC599001); 37.0885°N 138.6097°E, on *Poa palustris*, June 24, 2016, Eiji Tanaka (TNS-F-60482; GenBank LC598980, LC599009); **Tochigi**, **Tochigi**, Fujioka, 36.2436°N 136.6614°E, on *D. glomerata*, Jul 6, 2016, Kazuhito Tanada (TNS-F-60491; GenBank LC598971, LC599000).

Hosts—*Alopecurus*, *Agrostis*, *Ammophila*, *Calamagrostis*, *Dactylis*, *Deschampsia*, *Festuca*, *Molinia*, *Phalaris*, *Phleum*, *Phragmites*, *Poa*, *Polypogon*

Comments—In our phylogenetic tree (Fig. 1), two samples on *Alopecurus,* four on *Dactylis,* six on *Poa,* and one on *Polypogon* group in the *Claviceps bavariensis* clade, suggesting that Tanda's two varieties—*C. purpurea* var. *alopecuri* (Tanda 1977), *C. purpurea* var. *dactylidis* (Tanda 1981)—and the samples from *Poa* and *Polypogon* (Tanda 1980; Tanda & Kawatani 1980) might represent this species. In that case, a species name, "*C. alopecuri*" stat. nov., could be coined. However we considered the following: 1) the type specimen of *C. purpurea* var. *alopecuri* designated by Tanda (1977) was lost due to the same reason as *C. purpurea* var. *phalaridis*, therefore it is not possible to verify molecularly that the lost type truly belonged to the clade of *C. bavariensis,* which is essential for species delimitation; 2) the two specimens on *Alopecurus* in this study were not from Suginami, Tokyo, Japan (the type location); 3) the name "*C. alopecuri*" might give the false impression that the species has a host range limited to *Alopecurus*, contrary to the wide host range of the species. Therefore, we avoided elevating the varietal name to species level, proposing instead a new species name, *C. bavariensis*. Normally an epitype can only be replaced via conservation, but in this case the holotype specimen to which the epitype specimen would be attached has been lost, and an epitype no longer has nomenclatural status (Turland & al. 2018, Art. 9.20 Note 8). This allows us to use PRM922708, the epitype for *C. humidiphila* Pažoutová & M. Kolařík, as a holotype for *C. bavariensis*.

Tanda (1977, 1980, 1981) and Tanda & Kawatani (1980) recorded detailed sexual and asexual morphological features of samples from *Alopecurus, Dactylis, Poa,* and *Polypogon*, which could represent *Claviceps bavariensis*. In general, sclerotia are cylindrical with pointed or blunt ends; stromatal stipes are reddish brown, cylindrical or filiform, and curved or straight; capitella are light orange, oblate globose, and verrucose; perithecia are pyriform or ovoid; asci are narrowly cylindrical with thickened caps; ascospores are colorless and filiform; and the conidia are 1-celled, hyaline, and cylindrical or ovoid. The sizes of these characters sclerotia, stromata, perithecia, asci, ascospores and conidia varied significantly from different host plants (Table 1). Pažoutová & al. (2015) also provided more detailed morphological description and comparison with other species for *C. bavariensis* (as *C. humidiphila*). The conidia of *C. bavariensis* tend to be larger than *C. purpurea* s.str. and

Table 1. *Claviceps bavariensis:* observations cited in Tanda (1977; 1980; 1981) and Tanda & Kawatani (1980)

A—Host, sclerotial & ascomal dimensions

Host	Sclerotia (mm)	Stipe (mm)	Capitella* height × diameter (mm)
Alopecurus	1.5–5.1 × 0.3–0.9	1.0–4.0 × 0.3–0.5	0.4–0.9 × 0.6–1.3
Dactylis	3.2–11.7 × 0.6–1.7	1.0–14 × 0.1–1.4	0.3–1.5 × 0.3–2.3
Poa	1.5–5.8 × 0.2–1.5	1.0–9.0 × 0.1–0.7	0.4–1.0 × 0.5–1.9
Polypogon	1.2–4.0 × 0.2–1.0	1.0–7.0 × 0.2–0.6	0.4–1.1 × 0.5–1.4

B—Anatomical dimensions

Perithecia (µm)	Asci (µm)	Ascospore length (µm)	Conidia (µm)	Conidia L/W
151–221 × 77–144	75–138 × 2.5–3.7	74–126	5.0–11.3 × 2.6–5.0	2.1–2.3
154–270 × 88–168	81–151 × 1.8–4.2	74–119	4.0–14.8 × 1.8–4.7	1.9–2.8
147–256 × 60–154	77–158 × 1.8–5.3	63–151	3.2–12.6 × 1.6–5.8	2.0–3.0
119–210 × 56–126	91–133 × 2.5–3.9	84–123	5.0–12.8 × 2.4–5.4	—

C. arundinis, although the size ranges can overlap. Although these three species shared several host genera, population genetic analyses suggested significant genetic differentiation and limited gene flow among them (Pažoutová & al. 2015). The three species also differ in their ergot alkaloid spectra (Pažoutová & al. 2000, Negård & al. 2015) and ergochrome pigments (Flieger & al. 2019). Nevertheless, separation between *C. bavariensis* and *C. humidiphila* relies essentially on molecular evidence (mainly TEF1-α, at least seven constant nucleotide variance). The host species cited by Pažoutová & al. (2015) included 10 genera mainly from Europe (Belgium, Czech Republic, Germany, France, Norway, Poland, Turkey), but also from Central Asia (Kazakhstan, one specimen on *P. arundinacea*) and North America (USA, one specimen on *Ammophila breviligulata*). The present study expanded sample locations and host range by adding Canada (on *Festuca*, *Phalaris*) and Japan (on *Agrostis gigantea*, *Alopecurus aequalis* var. *amurensis*, *Calamagrostis epigejos*, *Dactylis glomerata*, *Festuca rubra*, *Poa acroleuca*, *P. annua*, *P. palustris*, *P. pratensis*, *P. trivialis*, *Polypogon fugax*).

Acknowledgments

We are grateful to MSc Kazuhito Tanada for providing many ergot samples from various regions in Japan and Dr. Henry Klein-Gebbinck for samples from Alberta (Canada). We also thank Drs. Masanobu Higuchi, Tsuyoshi Hosoya, Keiichi Motohashi and Seinosuke Tanda for their efforts in searching for type specimens; Dr. Scott Redhead (DAOM, Agriculture and Agri-Food Canada, Ottawa, ON Canada) for nomenclature advice and pre-submission manuscript review; and Dr. Joey Tanney (DAVP, Pacific Forestry Centre, Victoria, BC, Canada) for pre-submission review. We thank Dr. Shaun Pennycook for the nomenclature review and the meticulous edits that have significantly improved the clarity and efficiency of the presentation. This work was supported by the Japan Society for the Promotion of Science (JSPS) Grants-in-Aid for Scientific Research (KAKENHI) (grant number 16K07238); and Agriculture and Agri-Food Canada STB fungal and bacterial biosystematics J-002272.

Literature cited

Clements FE, Shear CL. 1931. The genera of fungi. New York, The H.W. Wilson Company

Donk MA. 1963. *Claviceps* L. Tul. (1853) not illegitimate. Taxon 12: 264–266.

Douhan GW, Smith ME, Huyrn KL, Westbrook A, Beerli P, Fisher AJ. 2008. Multigene analysis suggests ecological speciation in the fungal pathogen *Claviceps purpurea*. Molecular Ecology 17(9): 2276–2286. https://doi.org/10.1111/j.1365-294X.2008.03753.x

Flieger M, Stodůlková E, Wyka SA, Černý J, Grobárová V, Píchová K, Novák P, Man P, Kuzma M, Cvak L. 2019. Ergochromes: heretofore neglected side of ergot toxicity. Toxins 11: 439. https://doi.org/10.3390/toxins11080439

Izumitsu K, Hatoh K, Sumita T, Kitade Y, Morita A, Gafur A, Ohta A & al. 2012. Rapid and simple preparation of mushroom DNA directly from colonies and fruiting bodies for PCR. Mycoscience 53: 396–401. https://doi.org/10.1007/s10267-012-0182-3

Katoh K, Rozewicki J, Yamada KD. 2019. MAFFT online service: multiple sequence alignment, interactive sequence choice and visualization. Briefings in Bioinformatics 20(4): 1160–1166. https://doi.org/10.1093/bib/bbx108

Liu YJ, Whelen S, Hall BD. 1999. Phylogenetic relationships among ascomycetes: evidence from an RNA polymerase II subunit. Molecular Biology and Evolution 16(12): 1799–1808. https://doi.org/10.1093/oxfordjournals.molbev.a026092

Liu M, Overy DP, Cayouette J, Shoukouhi P, Hicks C, Bisson KR, Spoule A & al. 2020. Four phylogenetic species of ergot from Canada and their characteristics in morphology, alkaloid production and pathogenicity. Mycologia 112: 974–988. https://doi.org/10.1080/00275514.2020.1797372

Liu M, Shoukouhi P, Bisson KR, Wyka SA, Broders KD, Menzies JG. 2021. Sympatric divergence of the ergot fungus, *Claviceps purpurea*, populations infecting agricultural and nonagricultural grasses in North America. Ecology and Evolution 11(1): 273–293. https://doi.org/10.1002/ece3.7028

Negård M, Uhlig S, Kauserud H, Andersen T, Høiland K, Vrålstad T. 2015. Links between genetic groups, indole alkaloid profiles and ecology within the grass-parasitic *Claviceps purpurea* species complex. Toxins 7(5): 1431–1456. https://doi.org/10.3390/toxins7051431

Pažoutová S, Olsovska J, Linka M, Kolinska R, Flieger M. 2000. Chemoraces and habitat specialization of *Claviceps purpurea* populations. Applied and Environmental Microbiology 66(12): 5419–5425. https://doi.org/10.1128/aem.66.12.5419-5425.2000

Pažoutová S, Pešicová K, Chudíčková M, Šrůtka P, Kolařík M. 2015. Delimitation of cryptic species inside *Claviceps purpurea*. Fungal Biology 119(1): 7–26. https://doi.org/10.1016/j.funbio.2014.10.003

Rehner SA, Buckley E. 2005. A *Beauveria* phylogeny inferred from nuclear ITS and EF1-α sequences: evidence for cryptic diversification and links to *Cordyceps* teleomorphs. Mycologia 97(1): 84–98. https://doi.org/10.1080/15572536.2006.11832842

Ronquist F, Teslenko M, van der Mark P, Ayres DL, Darling A, Höhna S, Larget B, Liu L, Suchard MA, Huelsenbeck JP. 2012. MrBayes 3.2: Efficient Bayesian phylogenetic inference and model choice across a large model space. Systematic Biology 61(3): 539–542. https://doi.org/10.1093/sysbio/sys029

Shoukouhi P, Hicks C, Menzies JG, Popovic Z, Chen W, Seifert KA, Assabgui R, Liu M. 2019. Phylogeny of Canadian ergot fungi and a detection assay by real-time polymerase chain reaction. Mycologia 111(3): 493–505. https://doi.org/10.1080/00275514.2019.1581018

Swofford DL. 2002. PAUP*. Phylogenetic analysis using parsimony (*and other methods). version 4.0 b10 (computer program). Sunderland, Massachusetts, Sinauer Associates. https://doi.org/10.1017/cbo9780511819049.010

Tanaka E, Shrestha B, Shivas RG. 2020. *Commelinaceomyces* gen. nov. for four clavicipitaceous species misplaced in *Ustilago* that infect *Commelinaceae*. Mycologia 112: 649–660. https://dx.doi.org/10.1080/00275514.2020.1745524.

Tanda S. 1977. Mycological studies on ergot in Japan (Part 3): a new variety of *Claviceps purpurea* Tul. Parasitic on *Alopecurus aequalis* Sobol. var. *amurensis* Ohwi. Journal of Agricultural Science, Tokyo Nogyo Daigaku 22: 293–299.

Tanda S. 1978a. Mycological studies on ergot in Japan (Part 4): two varieties of *Claviceps purpurea* Tul. parasitic on timothy. *Phleum pratense* L. Journal of Agricultural Science, Tokyo Nogyo Daigaku 23: 141–150.

Tanda S. 1978b. Mycological studies on ergot in Japan (Part 6): a physiologic race of *Claviceps purpurea* Tul. var. *alopecuri* Tanda collected from *Trisetum bifidum* Ohwi. Journal of Agricultural Science, Tokyo Nogyo Daigaku 23: 207–214.

Tanda S. 1978c. Mycological studies on ergot in Japan (Part 7): two varieties of *Claviceps purpurea* Tul. parasitic on *Agrostis* spp. Journal of Agricultural Science, Tokyo Nogyo Daigaku 23: 215–221.

Tanda S. 1979a. Mycological studies on ergot in Japan (Part 8): ergots on *Calamagrostis* spp. Journal of Agricultural Science, Tokyo Nogyo Daigaku 23: 67–78.

Tanda S. 1979b. Mycological studies on ergot in Japan (Part 9): distinct variety of *Claviceps purpurea* Tul. on *Phalaris arundinacea* L. and *P. arundinacea* var. *picta* L. Journal of Agricultural Science, Tokyo Nogyo Daigaku 24: 67–95.

Tanda S. 1979c. Mycological studies on ergot in Japan (Part 10): ergots on velvet grass, *Holcus lanatus* L. Journal of Agricultural Science, Tokyo Nogyo Daigaku 24: 145–148.

Tanda S, Kawatani T. 1980. Mycological studies on ergot in Japan (Part 11): ergots on *Polypogon fugax*. Transactions of the Mycological Society of Japan 21: 97–101.

Tanda S. 1980. Mycological studies on ergot in Japan (Part 16): ergots on orchard grass, *Dactylis glomerata* L. Journal of Agricultural Science, Tokyo Nogyo Daigaku 25: 263–271.

Tanda S. 1981. Mycological studies on ergot in Japan (Part 19): ergots on bluegrasses (*Poa* spp.). Journal of Agricultural Science, Tokyo Nogyo Daigaku 26: 179–192.

Tulasne LR. 1853. Mémoire sur l'ergot des Glumacées. Annales des Sciences Naturelles, Botanique 20: 5–56.

Turland NJ, Wiersema JH, Barrie FR, Greuter W, Hawksworth DL & al. 2018. International Code of Nomenclature for algae, fungi, and plants (Shenzhen Code) adopted by the Nineteenth International Botanical Congress, Shenzhen, China, July 2017. Regnum Vegetabile 159. Glashütten, Koeltz Botanical Books. https://doi.org/10.12705/code.2018

MYCOTAXON

ISSN (print) 0093-4666 (online) 2154-8889 Mycotaxon, Ltd. ©2022

January–March 2022—Volume 137, pp. 89–94

https://doi.org/10.5248/137.89

Passalora golaghati comb. nov. from India

Gargee Singh[1], Sanjay Yadav[2],
Raghvendra Singh[2*], Shambhu Kumar[3]

[1]*Department of Botany, DDU Gorakhpur University, Gorakhpur, U.P., India 273009*

[2] *Centre of Advanced Study in Botany, Institute of Science, Banaras Hindu University, Varanasi, U.P., India 221005*

[3] *Forest Pathology Department, KSCSTE-Kerala Forest Research Institute, Peechi, Thrissur, Kerala, India 680653*

[*] Correspondence to: *drsinghtaxon@gmail.com, singhr.bot@bhu.ac.in*

Abstract—The hyphomycete *Cercospora golaghati* is recombined as *Passalora golaghati* based on critical re-examinations of original type material and a fresh topotypic collection and comparison with closely related species of cercosporoid taxa.

Key words—foliicolous, anamorph, *Mycosphaerellaceae,* nomenclature, taxonomy

Introduction

The significant characteristic that separates the two cercosporoid genera *Cercospora* Fresen. ex Fuckel and *Passalora* Fr. is colouration of conidia. When Crous & Braun (2003) emended the circumscription of *Passalora* based on ITS and 5.8S rDNA sequence analyses, they observed that the formation of single or catenate conidia is not a stable feature for diagnosis at the generic level in cercosporoid hyphomycetes (Crous & al. 2001). Their contributions have confirmed that presence or absence of thickened conidiogenous loci and pigmentation in conidiophores and conidia are important features of taxonomic relevance (Crous & al. 2009, 2013; Videira & al. 2017). During the last decade a large number of cercosporoid fungi have been recombined in the genus *Passalora* (Crous & Braun 2003; Braun

& al. 2013, 2014, 2015a,b, 2016), particularly from India (Kamal 2010). Recently, the addition of several novel taxa of foliicolous cercosporoid fungi described from India (Kumar & Singh 2015a,b, 2016; Awasthi & al. 2016; Singh & al. 2011, 2012, 2013) suggests that cercosporoid diversity is still insufficiently known in this region.

A new collection from the type locality of *Cercospora golaghati* (Saikia & Sarbhoy 1980) confirmed that this species is characterized by thickened scars and coloured conidiophores and conidia, indicating that it should be transferred to *Passalora* (Crous & Braun 2003).

Materials & methods

The holotype [conserved in the Herbarium, Division of Mycology & Plant Pathology, Indian Agricultural Research Institute, New Delhi, India (HCIO)] and a fresh specimen collected from the same host species in the same locality [conserved in the Mycological Herbarium of the Gorakhpur University, Gorakhpur, UP, India (MH-GPU)] were critically analyzed, and slides from infection spots were mounted in distilled water, lactophenol and cotton-blue mixture. Observation of microscopic characters was recorded under an Olympus CH20i-TR compound microscope to understand the exact morphology of the fungus. Measurements of 30 conidia, hila, conidiophores, and conidiogenous cells were recorded with the help of stage and ocular micrometers, and Lucida drawings were also made. The morphology of the fungus was compared with closely related cercosporoid taxa with the help of current literature.

Taxonomy

Passalora golaghati (Saikia & A.K. Sarbhoy) Gargee Singh, Sanj. Yadav, Raghv. Singh & Sh. Kumar, **comb. nov.** Figs 1–4

MB 835579

≡ *Cercospora golaghati* Saikia & A.K. Sarbhoy, Curr. Sci. 49: 830. 1980, as "*golaghatii*".

Infection spots amphigenous, brown to dark blackish brown, initially circular to subcircular, later spreading over the leaf surface to become irregular, 3–15 mm in diam. Colonies hypophyllous and effuse. Mycelium internal. Stromata present, epidermal to subepidermal, pseudoparenchymatous, brown to dark brown, 30–32 × 18–19 µm in diam. Conidiophores fasciculate, macronematous, brown to dark brown, unbranched, cylindrical, erect to procumbent, straight to flexuous, geniculate, smooth, thick-walled, 2–7-septate, (62–)80–102(–152) × 3–5 µm. Conidiogenous cells polyblastic, integrated, terminal, apex often slightly wider than at the base, 20–40 × 3–5 µm, loci thickened and darkened, 2–2.5 µm. Conidia solitary, acropleurogenous, obclavate-cylindrical, simple, dry, straight to slightly

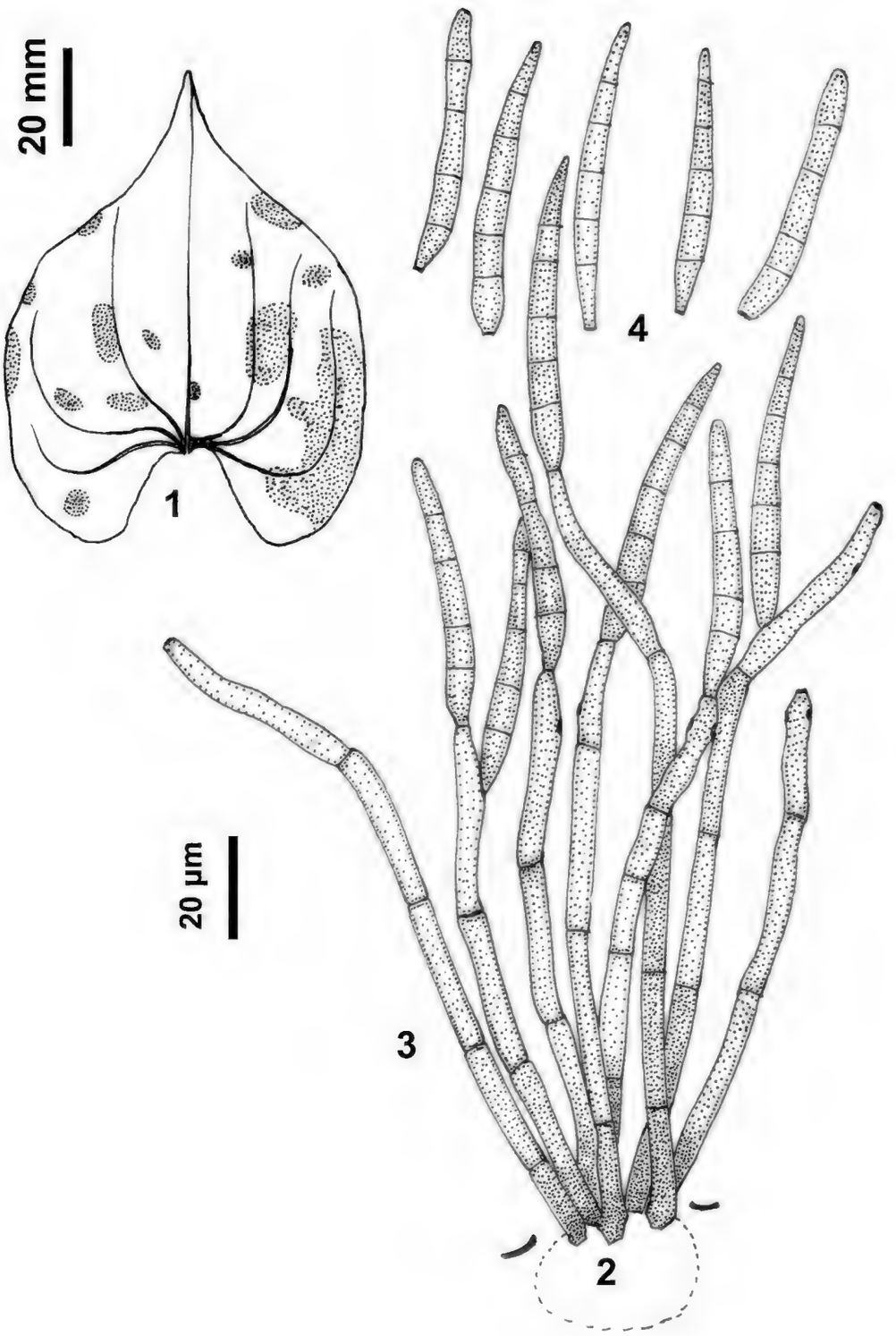

Figs 1–4. *Passalora golaghati* (holotype, HCIO 32660).
1. Symptoms of infection; 2. Stroma; 3. Conidiophores; 4. Conidia.

curved, thin-walled, smooth, brown to mid brown, 3–6-septate, tip acute to sub-obtuse, base obconico-truncate, (35–)50–60(–75) × 2.5–6 µm, hilum protuberant, thickened and darkened, 2–2.5 µm.

Specimens examined: **INDIA, Assam, Golaghat**, Salikihat, on living leaves of *Dioscorea alata* L. (*Dioscoreaceae*), 21 November 1977, leg. U.N. Saikia (HCIO 32660, holotype); 26.5239°N 93.9623°E, on living leaves of *Dioscorea alata*, December 2019, leg. Gargee Singh (MH-GPU 1, topotype).

Discussion

A literature review revealed that seven *Passalora* taxa have been reported on *Dioscoreaceae*: *P. dioscoreae* (Ellis & G. Martin) U. Braun & Crous, *P. dioscoreae-nipponicae* Y.L. Guo, *P. dioscoreae-subcalvae* Y.L. Guo, *P. dioscoreicola* Y.L. Guo, *P. dioscoreigena* U. Braun & Crous, *P. tranzschelii* (Vassiljevsky) U. Braun & Crous var. *tranzschelii*, and *P. tranzschelii* var. *chinensis* Y.L. Guo (Braun & al. 2014, Crous & Braun 2003; Guo 2001, 2011). *Passalora dioscoreae* has been subsequently recombined in *Distocercosporaster* by Videira & al. (2017). *Passalora golaghati* differs distinctly from all the remaining *Passalora* species in its conidiophore and conidial sizes. Morphological comparisons of all *Passalora* species reported on *Dioscoreaceae* are presented in Table 1.

Key to *Passalora* spp. reported on *Dioscoreaceae*

1. Conidial length ≤75 µm **2**
1. Conidial length >75 µm **3**
2. Conidiophores 35–175 × 4–6 µm, conidia 10–55 × 7.5–10 µm, 1–2-septate ..... ***P. dioscoreicola***
2. Conidiophores 80–102 × 3–5 µm, conidia 50–60 × 2.5–6 µm, 3–6-septate ..... ***P. golaghati***
3. Conidiophore length ≤50 µm **4**
3. Conidiophore length >50 µm **5**
4. Conidiogenous loci 1–2 µm diam., conidia 15–90 × 2–5 µm, 0–3-septate ..... ***P. tranzschelii* var. *tranzschelii***
4. Conidiogenous loci 1.5–3 µm diam., conidia 30–125 × 4–7 µm, 3–10-septate ..... ***P. tranzschelii* var. *chinensis***
5. Conidiophore length <100 µm **6**
5. Conidiophore length >100 µm ..... ***P. dioscoreigena***
6. Conidiophores 10–70 × 4–7 µm, conidia 30–125 × 4–6.5 µm, 3–10-septate ..... ***P. dioscoreae-nipponicae***
6. Conidiophores 25–65 × 4.5–6.5 µm, conidia 30–85 × 4.5–6.5 µm, 2–6-septate ..... ***P. dioscoreae-subcalvae***

Table 1. Comparative morphology of *Passalora* taxa reported on *Dioscoreaceae*.

Taxon	Conidiophore size (µm)	Conidia	
		Septation	Size (µm)
P. dioscoreae-nipponicae	10–70 × 4–7	3–10	30–125 × 4–6.5
P. dioscoreae-subcalvae	25–65 × 4.5–6.5	2–6	30–85 × 4.5–6.5
P. dioscoreicola	35–175 × 4–6	1–2	10–55 × 7.5–10
P. dioscoreigena	40–120 × 5–8.5	1–6	25–110 × 4.5–6.5
P. golaghati	80–102 × 3–5	3–6	50–60 × 2.5–6
P. tranzschelii var. *tranzschelii*	5–50 × 3–7	0–3	15–90 × 2–5
P. tranzschelii var. *chinensis*	5–50 × 3–7	3–10	30–125 × 4–7

Acknowledgments

Sincere thanks are due to Curator of the HCIO (New Delhi) for making it possible to examine the holotype collection of *Cercospora golaghati*. We express our deep gratitude to Dr. R.F. Castañeda-Ruiz (INIFAT Alejandro de Humboldt, Habana, Cuba) and Dr. Flavia Rodrigues Barbosa (Universidade Federal de Mato Grosso, Brazil) for presubmission critical review. We express our deep appreciation to Prof. Dr. Kamal (Emeritus Scientist, DST) for his valuable suggestions and kind help. We are also thankful to the Head of the Department of Botany of D.D.U. Gorakhpur University, Gorakhpur, U.P., for providing necessary facilities.

Literature cited

Awasthi N, Singh R, Kumar S. 2016. A new species of *Pseudocercosporella* on *Andrographis paniculata* from Central India. Sydowia 68: 27–33.

Braun U, Nakashima C, Crous PW 2013. Cercosporoid fungi (*Mycosphaerellaceae*) 1. Species on other fungi, *Pteridophyta* and *Gymnospermae*. IMA Fungus 4: 265–345. https://doi.org/10.5598/imafungus.2013.04.02.12

Braun U, Crous PW, Nakashima C. 2014. Cercosporoid fungi (*Mycosphaerellaceae*) 2. Species on monocots (*Acoraceae* to *Xyridaceae*, excluding *Poaceae*). IMA Fungus 5: 203–390. https://doi.org/10.5598/imafungus.2014.05.02.04

Braun U, Crous PW, Nakashima C. 2015a. Cercosporoid fungi (*Mycosphaerellaceae*) 3. Species on monocots (*Poaceae*, true grasses). IMA Fungus 6: 25–97. https://doi.org/10.5598/imafungus.2015.06.01.03

Braun U, Crous PW, Nakashima C. 2015b. Cercosporoid fungi (*Mycosphaerellaceae*) 4. Species on dicots (*Acanthaceae* to *Amaranthaceae*). IMA Fungus 6: 373–469. https://doi.org/10.5598/imafungus.2015.06.02.09

Braun U, Crous PW, Nakashima C. 2016. Cercosporoid fungi (*Mycosphaerellaceae*) 5. Species on dicots (*Anacardiaceae* to *Annonaceae*). IMA Fungus 7: 161–216. https://doi.org/10.5598/imafungus.2016.07.01.10

Crous PW, Braun U. 2003. *Mycosphaerella* and its anamorphs: names published in *Cercospora* and *Passalora*. CBS Biodiversity Series 1. CBS Utrecht, The Netherlands. 571 p.

Crous PW, Kang JC, Braun U. 2001. A phylogenetic redefinition of anamorph genera in *Mycosphaerella* based on ITS rDNA sequence and morphology. Mycologia 93: 1081–1101. https://doi.org/10.1080/00275514.2001.12063243

Crous PW, Summerell BA, Carnegie AJ, Wingfield MJ, Hunter GC, Burgess TI, Andjic V, Barber PA, Groenewald JZ. 2009. Unravelling *Mycosphaerella*: do you believe in genera? Persoonia 23: 99–118. https://doi.org/10.3767/003158509X479487

Crous PW, Braun U, Hunter GC, Wingfield MJ, Verkley GJM, Shin HD, Nakashima C, Groenewald JZ. 2013. Phylogenetic lineages in *Pseudocercospora*. Studies in Mycology 75: 37–114. https://doi.org/10.3114/sim0005

Guo YL. 2001. Studies on *Cercospora* and allied genera in China IX. Mycosystema 20(3): 301–303.

Guo YL. 2011. Studies on *Cercospora* and allied genera of China XIV. Mycosystema 30(6): 865–869.

Kamal. 2010. Cercosporoid fungi of India. Bishan Singh Mahendra Pal Singh Publication, Dehradun (UK), India. 351 p.

Kumar S, Singh R. 2015a. *Passalora musicola* sp. nov. a new Indian hyphomycete. Sydowia 67: 21–23.

Kumar S, Singh R. 2015b. *Pseudocercospora bischofigena*, a new Cercosporoid fungus from northeastern Uttar Pradesh, India. Czech Mycology 67: 39–44. https://doi.org/10.33585/cmy.67105

Kumar S, Singh R. 2016. *Passalora caesalpiniicola* sp. nov. from India on *Caesalpinia bonduc*. Mycotaxon 131: 25–30. https://doi.org/10.5248/131.25

Saikia UN, Sarbhoy AK. 1980. A new species of *Cercospora* from India. Current Science 49: 830–831.

Singh R, Kumar S, Kamal. 2011. Two new species of *Passalora* and *Pseudocercospora* from northeastern Uttar Pradesh, India. Mycotaxon 117: 137–143. https://doi.org/10.5248/117.137

Singh R, Chaurasia B, Shukla K, Upadhyaya PP. 2012. *Passalora aseptata*, a new Cercosporoid fungus from northeastern Uttar Pradesh, India. Mycotaxon 120: 461–463. https://doi.org/10.5248/120.461

Singh R, Kumar S, Saini DC, Upadhyaya PP, Kamal, Braun U. 2013. Diversity of *Passalora* on *Ficus*. Mycological Progress 12: 637–643. https://doi.org/10.1007/s11557-012-0870-6

Videira SIR, Groenewald JZ, Nakashima C, Braun U, Barreto RW, de Wit, PJGM, Crous PW. 2017. *Mycosphaerellaceae* – chaos or clarity? Studies in Mycology 87: 257–421. https://doi.org/10.1016/j.simyco.2017.09.003

MYCOTAXON

ISSN (print) 0093-4666 (online) 2154-8889 Mycotaxon, Ltd. ©2022

January–March 2022—Volume 137, pp. 95–107

https://doi.org/10.5248/137.95

Stigmatomyces aff. *limnophorae* on dipteran hosts in Peninsular Malaysia

Natasha Azmi Nur-Aliah[1], Jingyu Liu[2], Nurul Azmiera[1], Chong Chin Heo[1,3*]

[1] *Department of Medical Microbiology and Parasitology, Faculty of Medicine, Universiti Teknologi MARA Selangor Branch, Sungai Buloh Campus, 47000 Sungai Buloh, Selangor, Malaysia*

[2] *Department of Botany and Plant Pathology, College of Agriculture, Purdue University, West Lafayette IN 47907 U.S.A.*

[3] *Institute for Pathology, Laboratory and Forensic Medicine (I-PPerForM), Universiti Teknologi MARA Selangor Branch, Sungai Buloh Campus, 47000 Sungai Buloh, Selangor, Malaysia*

* Correspondence to: *chin@uitm.edu.my*

Abstract—Flies parasitized by *Laboulbeniales,* captured in Selangor state, were examined and identified as *Boettcherisca javanica, Boettcherisca* sp., and *Hypopygiopsis violacea*. The fungus was identified as *Stigmatomyces* aff. *limnophorae* based on morphology and phylogenetic analysis of sequences of the partial nuclear small and large subunit ribosomal RNA genes. This fungus represents a new record for Malaysia; and these are the first reports of *Boettcherisca* and *Hypopygiopsis* as hosts for any laboulbenialean species.

Key words—*Calliphoridae, Laboulbeniomycetes, Sarcophagidae,* southeastern Asia.

Introduction

Fungi in *Laboulbeniales* (*Ascomycota: Laboulbeniomycetes*) are ectoparasitic fungi that are obligatorily associated with arthropods as ectoparasites (Haelewaters & al. 2012, Melo & Melo 2019, Blackwell & al. 2020). These fungi are characterized by the presence of a three-dimensional thallus (plural: thalli), instead of hyphae with mycelial growth like many other fungi (Blackwell & al. 2020). Representatives of three arthropod subphyla

(*Chelicerata, Myriapoda, Hexapoda*) and various insect orders including *Coleoptera, Diptera, Hemiptera,* and *Hymenoptera* are known as hosts for these fungi (reviewed in Haelewaters & al. 2021). In the past 40 years, only two species *Laboulbeniales* have been reported in Malaysia: *Laboulbenia admirabilis,* found on the body of an unidentified *Spaniocelyphus* (*Diptera*) in Pahang state (Lee & Majewski 1986), and *Diphymyces sabahensis,* on three *Ptomaphaginus* spp. (*Coleoptera*) in Sabah state (Haelewaters & al. 2014).

Stigmatomyces sensu lato is a large, paraphyletic genus of 176 species on dipteran hosts (Haelewaters & al. 2020a; Species Fungorum 2020). Species within this heterogeneous assemblage (sensu lato) are parasites on hosts in many different families—including *Anthomyiidae, Calliphoridae, Chamaemyiidae, Diopsidae, Drosophilidae, Ephydridae, Fanniidae, Muscidae, Nycteribiidae, Sarcophagidae, Sphaeroceridae*, and *Streblidae* (Thaxter 1901, 1905, 1917; Rossi 1998; Hyde & al. 2019; Haelewaters & al. 2018, 2020a). Thus far, five species of *Stigmatomyces* sensu stricto have been reported in Malaysia: *S. dacinus, S. limosinoides, S. tortimasculus*, and *S. venezuelae* in Malaysian Borneo (Thaxter 1915, 1918); and *S. neurochaetae* in Peninsular Malaysia (Sugiyama & Majewski 1985; Rossi & Weir 2007). Note that Thaxter (1915) reported *S. stilici* from Malaysian Borneo and Sugiyama & Majewski (1985) reported *S. orientalis* from Peninsular Malaysia—both associated with staphylinid beetles (*Coleoptera: Staphylinidae*) and both species later recombined in *Zeugandromyces.*

Here, we provide the first records of *Stigmatomyces* aff. *limnophorae* from Malaysia. Our material was studied based on morphological characters and sequence data. The parasitized fly genera are for the first time reported in the literature as hosts for *Laboulbeniales.*

Material & methods

Collection & identification of flies

An entomological survey was conducted in September 2019 in the state of Selangor, Peninsular Malaysia, to investigate the biodiversity of carrion flies. Chicken liver (200 g, 2d old) was used as bait and flies were collected using sweep nets at two different forests in the town of Rawang. Collected adult flies were then placed in a cloth-lid jar and brought back to the Parasitology Laboratory, Institute for Medical Molecular Biotechnology, Universiti Teknologi MARA (UiTM) in Sungai Buloh. The flies were incubated at –4 °C for 15 minutes, after which they were pinned and dried at room temperature. During microscopic examination for species determination, we observed four fly specimens (out of >100 observed) with thalli of

Laboulbeniales. These specimens were carefully examined and photographed using an Olympus SZ51 stereomicroscope equipped with a digital camera and CellD Imaging Software. The parasitized adult flies were identified using Kurahashi & al. (1997) and Kurahashi & Samerjai (2018).

Microscopic study of *Laboulbeniales*

Parasitized flies were shipped to Purdue University for microscopic study of the *Laboulbeniales* (by J.L.). Thalli were taken from the host fly using a BioQuip #1208SA entomological pin dipped in Hoyer's medium (30 g arabic gum, 200 g chloral hydrate, 16 ml glycerol, 50 ml ddH2O). Thalli were mounted in Amann's medium applying a double coverslip technique using Solakryl BMX as outlined in Liu & al. (2020). Microscope mounts were viewed at 200–400× using an Olympus BH2 bright field compound microscope. Line and stipple drawings were made with PITT artist pens based on photomicrographs taken with an Olympus SC30 camera and cellSens 1.18 imaging software. Permanent slides are deposited at PUL (Kriebel Herbarium) under numbers PUL F25943–F25950.

DNA extraction, PCR amplification, sequencing

DNA was extracted from 2–4 thalli of *Stigmatomyces* using the REPLI-g Single Cell Kit with modifications by Haelewaters & al. (2019). The nuclear ribosomal RNA small (SSU) and (LSU) large subunits were amplified using primer pairs NSL1/NSL2 for SSU (Haelewaters & al. 2015), and LR0R/LR5 and LIC24R/LR5 for LSU (Vilgalys & Hester 1990, Hopple 1994, Miadlikowska & Lutzoni 2000). The DNA was amplified using an Eppendorf pro S Mastercycler in 25 µL volumes containing 12.5 µl 2× MyTaq Mix (Bioline, Swedesboro, New Jersey), 9.5 µL ddH2O, 1.0 µL forward and reverse primer, and 1.0 µL DNA. Cycling conditions—for SSU: initial denaturation at 95 °C for 5 min; 40 cycles of denaturation at 95 °C for 30 sec, annealing at 55 °C for 45 sec, extension at 72 °C for 45 sec; and final extension at 72 °C for 1 min and for LSU: initial denaturation at 94 °C for 5 min; 35 cycles of denaturation at 94 °C for 30 sec, annealing at 50 °C for 45 sec, extension at 72 °C for 1 min; and final extension at 72 °C for 7 min. The PCR amplicons were sent to Genewiz (South Plainfield, New Jersey) for purification and sequencing. Raw sequence reads were assembled and edited in Gene Codes Sequencher 5.2.3. Sequences were deposited at the National Center for Biotechnology Information (NCBI) GenBank database; accession numbers MT341792–MT341794 (SSU) and MT341789–MT341791 (LSU). These sequences were then BLAST searched against NCBI's nucleotide collection to establish a rough relationship with existing sequences.

Sequence alignments & phylogenetic analysis

SSU and LSU sequences of *Stigmatomyces* species representing the same clade (clade IV sensu Haelewaters & al. 2020a) were downloaded from GenBank (https://www.ncbi.nlm.nih.gov/genbank/). *Gloeandromyces dickii* was selected as outgroup. Details for all isolates are presented in Table 1. Sequences of both regions

Table 1. Isolates and sequences used in phylogenetic analysis.

Species	Isolate	Country	SSU	LSU	Reference
Gloeandromyces dickii	D.Haelew. 1323b	Panama	MG958011	MH040582	Haelewaters & al. 2018
Stigmatomyces borealis	AW-979	USA	JN835186	—	A. Weir (unpublished)
S. chamaemyiae	D.Haelew. 1137a	Portugal	MH040564	—	Haelewaters & al. 2018
	D.Haelew. 1137c	Portugal	MH040565	—	Haelewaters & al. 2018
S. limnophorae	AW-785	USA	AF407576	—	Weir & Blackwell 2001b
S. aff. *limnophorae*	D.Haelew. 1802c	Malaysia	MT341792	MT341789	This study
	D.Haelew. 1802d	Malaysia	MT341793	MT341790	This study
	D.Haelew. 1820e	Malaysia	MT341794	MT341791	This study
S. protrudens	AW-793	USA	AF298232	AF298234	Weir & Blackwell å2001a
S. rugosus	—	—	AF431759	—	Weir & Hughes 2002
	D.Haelew. 1138a	Portugal	MH040563	—	Haelewaters & al. 2018

were aligned with MUSCLE (Edgar 2004) on the Cipres Science Gateway web portal (Miller & al. 2010). For both datasets, the appropriate nucleotide substitution model was selected by considering the corrected Akaike Information Criterion (AICc) using ModelFinder Plus (Kalyaanamoorthy & al. 2017). Models selected were HKY+F+I (SSU, –lnL = 2420.547) and TIM2+F+I (LSU, –lnL = 1837.675). SSU and LSU aligned datasets were combined using MEGA7 (Kumar & al. 2016). A Maximum likelihood analysis of the concatenated two-locus dataset was performed using IQ-TREE (Nguyen & al. 2015) with partitioned models (Chernomor & al. 2016) and ultrafast bootstrapping with 1000 replicates (Hoang & al. 2018). The best-scoring tree was visualized in FigTree 1.4.3 (http://tree.bio.ed.ac.uk/ software/figtree/) and edited in Adobe Illustrator 24.1.1.

Host identification

The infected insect hosts (n = 4) belonged to two families, *Calliphoridae* (n = 1) and *Sarcophagidae* (n = 3). The calliphorid fly was identified as *Hypopygiopsis violacea* (Fig. 1). Two sarcophagid flies were identified as *Boettcherisca javanica* and the third as *Boettcherisca* sp. (Figs 2, 3). All four specimens bore thalli at their abdominal segments (Table 2).

Fig. 1. Adult fly of *Hypopygiopsis violacea* (*Diptera: Calliphoridae*): A. Habitus of *H. violacea* at 0.8× magnification. B. The silver white facial tomentum. C. *Stigmatomyces* aff. *limnophorae* thalli on 5th tergite (black arrow). D. *Stigmatomyces* aff. *limnophorae* thalli on sternites 3 and 4 (black arrows). Scale bars: A, B = 2 mm; C, D = 1 mm.

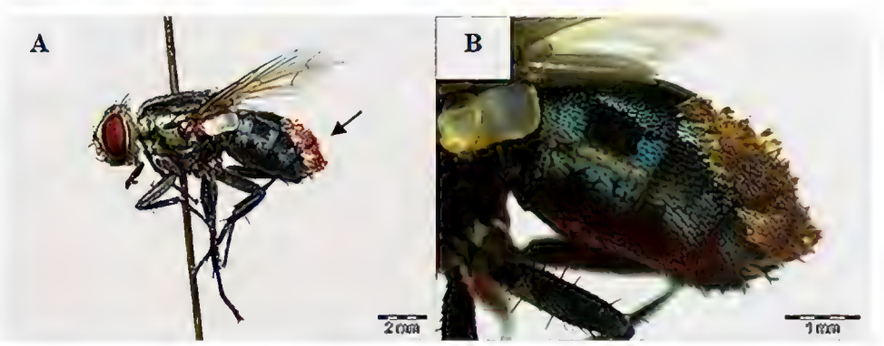

Fig. 2. Adult fly of *Boettcherisca* sp. (*Diptera: Sarcophagidae*): A. Heavy infection with *Stigmatomyces* aff. *limnophorae* at abdominal tergites 4 and 5 (black arrow); B. Close-up view of the parasitized tergites 4 and 5 at 2.5× magnification. Scale bars: A = 2 mm; B = 1 mm.

Fig. 3. Adult fly of *Boettcherisca javanica* (*Diptera: Sarcophagidae*): A. *Stigmatomyces* aff. *limnophorae* thalli on abdominal sternites 4 and 5 (black arrow); B. Tuft of *S.* (aff.) *limnophorae* thalli on abdominal sternites 4 and 5 at 3.2× magnification. Scale bars" A = 2 mm; B = 1 mm.

Table 2. Host specimens examined and position of thalli on the host body.

Dipteran host species	Family	Location of thalli
Hypopygiopsis violacea ♀	*Calliphoridae*	Tergite 5; sternites 3, 4 (Fig. 1C, D)
Boettcherisca sp. ♀	*Sarcophagidae*	Abdominal tergites 3, 4 (Fig. 2)
Boettcherisca javanica ♂	*Sarcophagidae*	Abdominal sternites 4, 5 (Fig. 3)

Taxonomy

Stigmatomyces* aff. *limnophorae Thaxt.,
Proc. Am. Acad. Arts Sci. 36: 400. 1901. Fig. 4

Thallus hyaline, dark amber brown that gradually attenuates as the cell wall thickens; 647 µm long from foot to perithecial tip. Cell II ≤2 times longer than cell I, striate on the cell surface. Cell III longer than wide, rounded externally, not protruding abruptly below basal cell of appendage. Appendage free, slender, elongated, about as long as the perithecial venter; distal portion distinctly curved; bearing a single or multiple antheridia. Antheridia, short, broad, slightly recurved. Perithecium amber brown, 220 × 64 µm; venter relatively small, ellipsoid, subsymmetrical, with wall cells powdered by darker maculation, spirally twisted, separated by corresponding number of well-defined longitudinal ridges, somewhat oblique; neck 96 × 16 µm, abruptly distinguished from venter.

Material examined/sequenced—**PENINSULAR MALAYSIA: Selangor, Gombak District,** Rawang, forested area, 3.281°N 101.261°E, 4 m a.s.l., ex. chicken liver, 11 Sep. 2019, leg. N.A. Nur Aliah & N. Azmiera, on ♀ *Boettcherisca* sp. D. Haelew. 1796 [host label] (slides PUL F25943, PUL F25944, PUL F25945); 3.296°N 101.611°E, 69 m a.s.l., ex. chicken liver, 7 Sep. 2019, leg. N.A. Nur Aliah & N. Azmiera, on ♂ *Boettcherisca javanica* Lopes, D. Haelew. 1801 [host label] (slides PUL F25947, PUL F25948); on ♂ *B. javanica,* D. Haelew. 1802 [host label] (slides PUL F25949, PUL F25950) isolate 1802c [4 mature thalli] GenBank MT341792, MT341789; isolate 1802d [3 mature thalli] GenBank MT341793, MT341790; isolate 1802e [2 perithecia] GenBank MT341794, MT341791); 3.296°N 101.611°E, 101 m a.s.l., ex. chicken liver, 7 Sep. 2019, leg. N.A. Nur Aliah & N. Azmiera, on ♀ *Hypopygiopsis violacea* (Macquart), D. Haelew. 1800 [host label] (slide PUL F25946).

Phylogenetic results

All three newly generated SSU sequences share highest similarity (99.62%) with *Stigmatomyces chamaemyiae* (GenBank MH040565), followed by

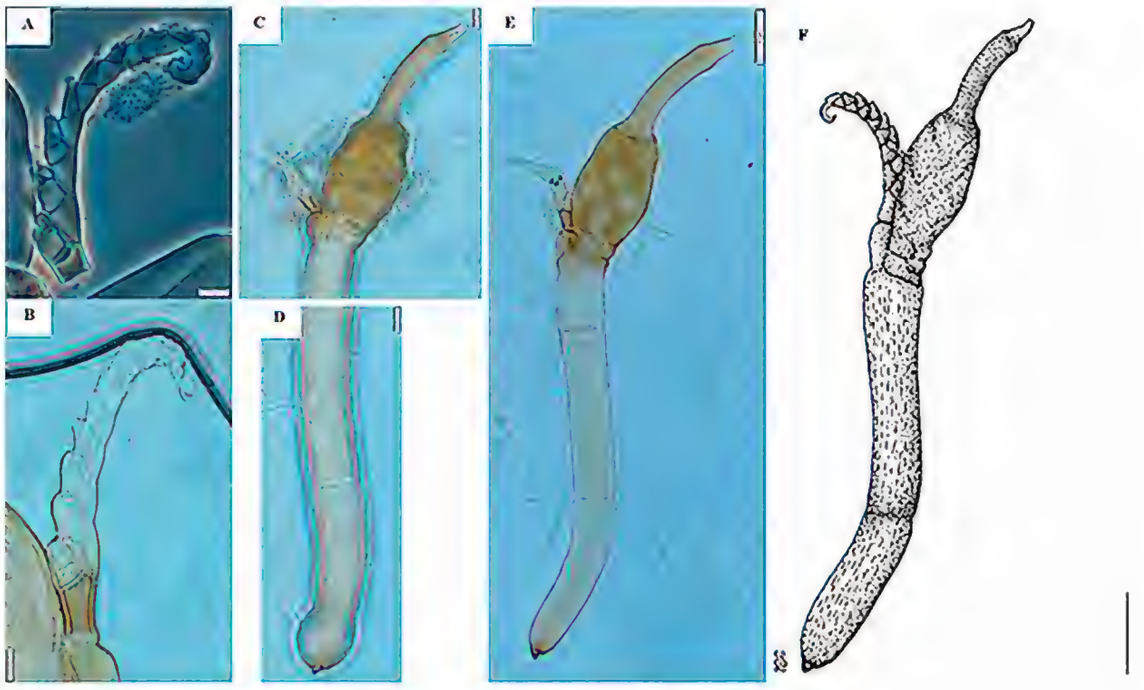

Fig. 4. *Stigmatomyces* aff. *limnophorae:* A [PUL F25945], B [PUL F25948]. Details of primary appendage; C [PUL F25950]. Detail of spirally twisted perithecium; D [PUL F25950]. Receptacular cells I and II with longitudinally striped ornamentation; E [PUL F25950]. Habitus of mature thallus; F. Stipple drawing. Scale bars: A, B = 10 µm; C, D = 20 µm; E = 50 µm; F= 100 µm.

S. rugosus (MH040563) with 98.39–98.54% similarity (Table 1). Based on morphology, we thought the fungus might represent *S. limnophorae*, but that species was not among the BLAST results despite the availability of an SSU sequence in GenBank (AF407576; isolate AW-785). Comparison of our Malaysian SSU sequences with *S. limnophorae* AW-785, however, shows a 99.08–99.36% similarity. All newly generated LSU sequences are most closely related to *Gloeandromyces nycteribiidarum* (MH040566) with 85.78% similarity (Table 1). The highest percentage similarity (87.30%) with any *Stigmatomyces* species is with *S. protrudens* (AF298234), but with only over a 42% query cover.

The three Malaysian isolates group together in a maximum-supported clade that also includes *S. limnophorae* AW-785 and two *S. chamaemyiae* isolates from Portugal. The branch length among the Malaysian isolates and between the USA isolate AW-785 is very short. As a result, we believe the Malaysian fungus may be identified as *S.* aff. *limnophorae*.

Discussion

Fungal thalli were removed from all four fly specimens and subsequently identified as *Stigmatomyces* aff. *limnophorae* based on morphological (Fig. 4)

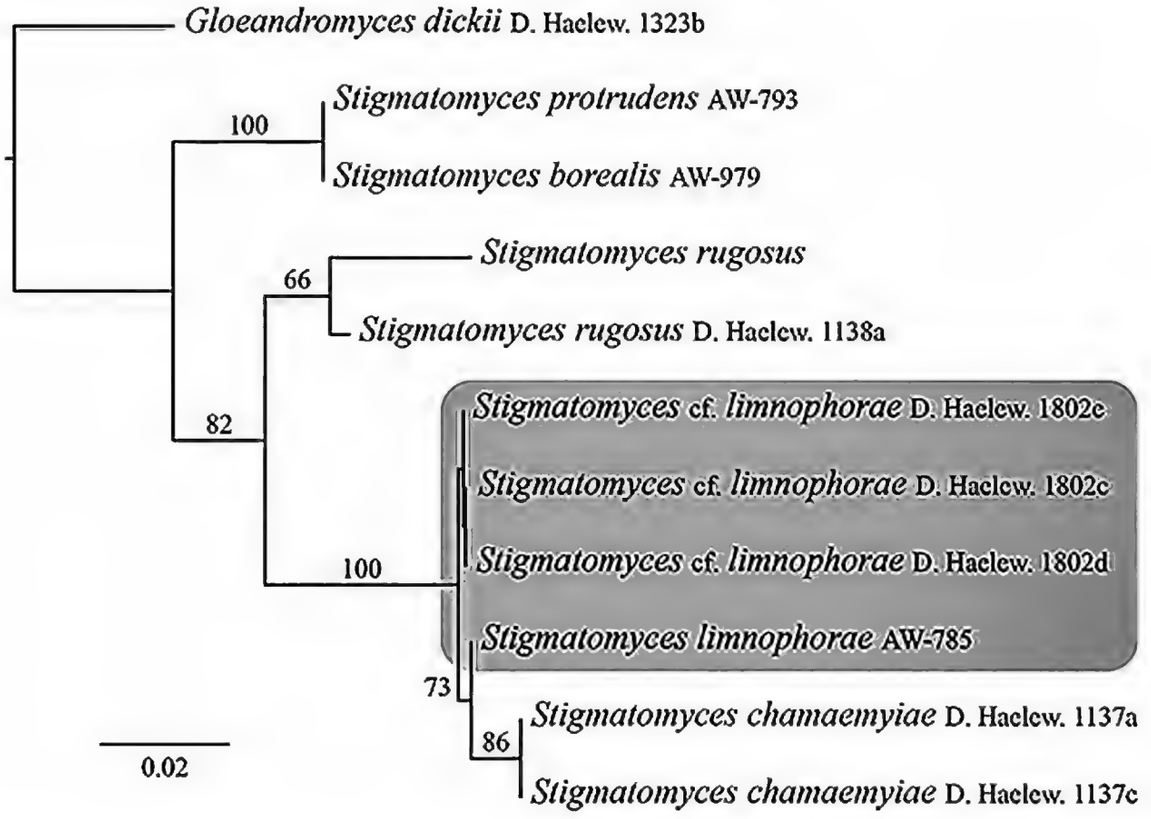

Fig. 5. Phylogeny of *Stigmatomyces* isolates reconstructed from a combined SSU–LSU rDNA dataset, with *Gloeandromyces dickii* as outgroup. Shown is the best-scoring tree (–lnL = 4263.622) as a result of maximum likelihood inference performed with IQ-TREE. For each node, the ML bootstrap (if >60) is presented at the branch leading to that node. *Stigmatomyces* aff. *limnophorae* is highlighted in grayscale.

and phylogenetic (Fig. 5) analyses. The global distribution of *S. limnophorae* is presented in Table 3. *Stigmatomyces limnophorae* was described from a *Limnophora* fly (*Muscidae*) in California, USA. Isolate AW-785 originated from a *Muscidae* gen. sp. indet. collected in Louisiana, USA (Weir & Blackwell 2001b). This isolate will be regarded as representing the species until fungal sequences are obtained from a muscid fly identified to genus-level collected in the type locality of Berkeley, California. Morphologically our material resembles typical *S. limnophorae* morphology (Thaxter 1901, 1908), but our phylogenetic placement of the Malaysian isolates sister to *S. chamaemyiae* + *S. limnophorae* AW-785, suggests that they might represent another species closely related to *S. limnophorae*. Since the vast majority of thalli were heavily damaged, we were unable to describe the material accurately based on all morphological features.

Table 3. World distribution of *Stigmatomyces limnophorae*, with host species and reference of first report.

Continent	Country	Host (family)	First report
North & Central America	Cuba	*Limnophora arcuata (Muscidae)*	Krejzová & Weiser 1968
	Grenada	*Anthomyiidae* gen. sp. *indet.*	Thaxter 1917
	Guatemala	*Limnophora* sp. *(Muscidae)*	Thaxter 1917
	Jamaica	*Leucomelina* sp. *(Muscidae)*	Thaxter 1917
	Mexico	*Onesia* sp. *(Calliphoridae)*	Thaxter 1917
	USA	*Limnophora* sp. *(Muscidae)* [type]	Thaxter 1901
		Anthomyiidae gen. sp. *indet.*	Thaxter 1917
South America	Bolivia	*Limnophora* sp. *(Muscidae)*	Rossi 1998
	Brazil	*Limnophora* sp. *(Muscidae)*	Bergonzo & al. 2004
	Venezuela	*Sarcophaga* sp. *(Sarcophagidae)*	Thaxter 1905
Europe	Portugal	*Limnophora obsignata (Muscidae)*	Rossi & al. 2013
Africa	Cameroon	*Anthomyiidae* gen. sp. indet.	Thaxter 1917
	Canary Islands	*Limnophora obsignata (Muscidae)*	Rossi & al. 2013
	Kenya	*Rhyncomya forcipata (Rhiniidae)*	Rossi & al. 2013
	Morocco	*Limnophora obsignata (Muscidae)*	Rossi & al. 2013
	Sierra Leone	*Lispe desjardinsii (Muscidae)*	Rossi & Leonardi 2018
	Uganda	*Fainia albitarsis (Rhiniidae)*	Rossi & al. 2013
Asia	Indonesia	*Lucilia dux (Calliphoridae)*	Thaxter 1917
	Philippines	*Lucilia dux (Calliphoridae)*	Thaxter 1917
	Thailand	*Heliographa ceylanica (Muscidae)*	Rossi & al. 2013
	Israel	*Limnophora quaterna (Muscidae)*	Rossi & al. 2013
	Saudi Arabia	*Isomyia terminata (Rhiniidae)*	Rossi & al. 2013
		Limnophora quaterna (Muscidae)	Rossi & al. 2013
	Taiwan	*Sumatria flava (Rhiniidae)*	Rossi & al. 2013
	Turkey	*Dasyphora albofasciata (Muscidae)*	Rossi & al. 2013
Australasia	Australia	*Calliphora augur (Calliphoridae)*	Rossi & al. 2013

As a result, for the time being, we refer to the species as *S.* aff. *limnophorae*. Efforts will be ongoing to sample flies using chicken liver and other baits and to collect additional *Stigmatomyces*-infected fly specimens.

Stigmatomyces limnophorae was discovered by Thaxter (1901) as a parasite of *Limnophora* sp. [misspelt as *"Limnophorus"*] (*Muscidae*) in California, USA. The fungus appears to be a very widespread and plurivorous species and has been reported on all continents except Antarctica from hosts in different dipteran families including *Anthomyiidae, Calliphoridae, Muscidae, Rhiniidae,* and *Sarcophagidae* (Table 3). Despite its wide distribution, the fungus has not yet been reported in Malaysia. *Stigmatomyces limnophorae* has, however, been reported in neighbouring countries—Indonesia, the Philippines, Thailand—on different dipteran hosts such as *Chrysomya megacephala* [as *"Lucilia dux"*] (*Calliphoridae*) and *Heliographa ceylanica* (*Muscidae*) (Thaxter 1917, Rossi & al. 2013). Here we report the occurrence of *S.* aff. *limnophorae* in Malaysia on different hosts in *Calliphoridae* and *Sarcophagidae*. While it is not uncommon for *S. limnophorae* to parasitize flies in either of these families (Table 3), the Malaysian hosts are in genera that have not previously been observed with thalli of *Laboulbeniales*.

Thalli of *Stigmatomyces* aff. *limnophorae* were always observed at the abdominal segments, which might indicate the original infection site; however, our observations are based on only three host specimens. Limited data are available on *Laboulbeniales*. For example, the impact of infection on their hosts is still poorly studied (Nalepa & Weir 2007, Riddick 2010, Báthori & al. 2017, Haelewaters & al. 2020b). Further exploration of the diversity of ectoparasitic fungi is required to gain a complete picture of their distribution and interactions with insect hosts.

In summary, we report two new hosts for *Stigmatomyces limnophorae,* a complex species able to infect wide number of species within different genera. This could be caused by evolution and adaption of the fungi for survival in different genera on various continents. As our sample was identified morphologically as *S. limnophorae* but phylogenetically as sister to *S. chamaemyiae* + *S. limnophorae* AW-785 (suggesting a different species), we could postulate that hybridization is occurring between these two species, thereby explaining adaptation of these fungi to different host species and within wide range of genera. Additional research is required to support this hypothesis.

Acknowledgments

We thank the Institute of Medical Molecular Biotechnology (IMMB), Universiti Teknologi MARA, for providing laboratory facilities. Special thanks to Dr. Matthew T. Kasson (West Virginia University, USA) for comments during our early research and to Dr. Danny Haelewaters (Purdue University, USA) for help with phylogenetic

analyses. Dr. Haelewaters and Dr. Walter P. Pfliegler (University of Debrecen, Hungary) are thanked for expert presubmission review.

Literature cited

Báthori F, Rádai Z, Tartally A. 2017. The effect of *Rickia wasmannii* (*Ascomycota, Laboulbeniales*) on the aggression and boldness of *Myrmica scabrinodis* (*Hymenoptera, Formicidae*). Journal of *Hymenoptera* Research 58: 41–52. https://doi.org/10.3897/jhr.58.13253

Bergonzo E, Rossi W, Weir A. 2004. New and interesting *Laboulbeniales* parasitic on Brazilian *Diptera*. Mycologia 96(4): 703–711. https://doi.org/10.1080/15572536.2005.11832918

Blackwell M, Haelewaters D, Pfister DH. (2020). *Laboulbeniomycetes*: Evolution, natural history, and Thaxter's final word. Mycologia, 112(6): 1048-1059. https://doi.org/10.1080/00275514.2020.1718442

Chernomor O, von Haeseler A, Minh BQ. 2016. Terrace aware data structure for phylogenomic inference from supermatrices. Systematic Biology 65: 997–1008. https://doi.org/10.1093/sysbio/syw037

Edgar RC. 2004. MUSCLE: multiple sequence alignment with high accuracy and high throughput. Nucleic Acids Research 32: 1792–1797. https://doi.org/10.1093/nar/gkh340

Haelewaters D, van Wielink P, van Zuijlen JW, Verbeken A, De Kesel A. 2012. New records of *Laboulbeniales* (*Fungi, Ascomycota*) for the Netherlands. Entomologische Berichten 72(3): 175–183.

Haelewaters D, Schilthuizen M, Pfister DH. 2014. On *Diphymyces* (*Laboulbeniales, Ascomycota*) in Malaysian Borneo. Plant Ecology and Evolution 147(1): 93–100. https://doi.org/10.5091/plecevo.2014.912

Haelewaters D, Gorczak M, Pfliegler WP, Tartally A, Tischer M, Wrzosek M, Pfister DH. 2015. Bringing *Laboulbeniales* into the 21st century: enhanced techniques for extraction and PCR amplification of DNA from minute ectoparasitic fungi. IMA Fungus 6(2): 363–372. https://doi/org/10.5598/imafungus.2015.06.02.08

Haelewaters D, Page RA, Pfister DH. 2018. *Laboulbeniales* hyperparasites (*Fungi, Ascomycota*) of bat flies: independent origins and host associations. Ecology and Evolution 8(16): 8396–8418. https://doi.org/10.1002/ece3.4359

Haelewaters D, Pfliegler WP, Gorczak M, Pfister DH. 2019. Birth of an order: comprehensive molecular phylogenetic study reveals that *Herpomyces* (*Fungi, Laboulbeniomycetes*) is not part of *Laboulbeniales.* Molecular Phylogenetics and Evolution 133: 286–301. https://doi.org/10.1016/j.ympev.2019.01.007

Haelewaters D, Dima B, Abdel-Hafiz BII, Abdel-Wahab MA. Abul-Ezz SR & al. 2020a. Fungal Systematics and Evolution 6. Sydowia 72: 231–356

Haelewaters D, Hiller T, Kemp EA, van Wielink PS, Shapiro-Ilan DI, Aime MC & al. 2020b. Mortality of native and invasive ladybirds co-infected by ectoparasitic and entomopathogenic fungi. PeerJ 8: e10110. https://doi.org/10.7717/peerj.10110

Haelewaters D, Blackwell M, Pfister DH. 2021. *Laboulbeniomycetes*: intimate fungal associates of arthropods. Annual Review of Entomology 66: 1–20. https://doi.org/https://doi.org/10.1146/annurev-ento-013020- 013553

Hoang DT, Chernomor O, von Haeseler A, Minh BQ, Vinh LS. 2018. UFBoot2: improving the ultrafast bootstrap approximation. Molecular Biology and Evolution 35: 518–522. https://doi.org/10.1093/molbev/msx281

Hopple JS Jr. 1994. Phylogenetic investigations in the genus *Coprinus* based on morphological and molecular characters. PhD Thesis, Duke University, Durham, North Carolina.

Hyde KD, Tennakoon DS, Jeewon R, Bhat DJ., Maharachchikumbura SSN & al. 2019. Fungal diversity notes 1036–1150: taxonomic and phylogenetic contributions on genera and species of fungal taxa. Fungal Diversity 96: 1–242. https://doi.org/10.1007/s13225-019-00429-2

Kalyaanamoorthy K, Minh BQ, Wong TKF, von Haeseler A, Jermiin LS. 2017. ModelFinder: fast model selection for accurate phylogenetic estimates. Nature Methods 14: 587–589. https://doi.org/10.1038/nmeth.4285

Krejzová R, Weiser J. 1968. *Stigmatomyces limnophorae* Thaxter 1901 (*Ascomycetes, Laboulbeniales*), a new fungus from Cuba with remarks to its morphology. Czech Mycology 22: 220–224

Kumar S, Stecher G, Tamura K. 2016. MEGA7: Molecular Evolutionary Genetics Analysis version 7.0 for bigger datasets. Molecular Biology and Evolution 33(7): 1870–1874. https://doi.org/10.1093/molbev/msw054

Kurahashi H, Samerjai C. 2018. Revised keys to the flesh flies in Thailand, with the establishment of a new genus (*Diptera: Sarcophagidae*). Medical Entomology and Zoology 69: 67–93. https://doi.org/10.7601/mez.69.67

Kurahashi H, Benjaphong N, Omar B. 1997. Blowflies (*Insecta: Diptera: Calliphoridae*) of Malaysia and Singapore. Raffles Bulletin of Zoology (Supp. 5).

Lee YB, Majewski T. 1986. Three new species of *Laboulbeniales* (*Ascomycetes*) from Malaysia. Mycologia 78(3): 401–406. https://doi.org/10.1080/00275514.1986.12025262

Liu J, Haelewaters D, Pfliegler WP, Page RA, Dicke CW, Aime MC. 2020. A new species of *Gloeandromyces* from Ecuador and Panama revealed by morphology and phylogenetic reconstruction, with a discussion of secondary barcodes in *Laboulbeniomycetes* taxonomy. Mycologia 112(6): 1192–1202. https://doi.org/10.1080/00275514.2020.1781496

Melo MPR, Melo RFR. 2019. *Polyandromyces coptosomatis* (*Dimorphomycetaceae, Laboulbeniales*): new records, distribution patterns and host-parasite interactions in Brazil. Sydowia 71: 103–113. https://doi.org/10.12905/0380.sydowia71-2019-0103

Miadlikowska J, Lutzoni F. 2000. Phylogenetic revision of the genus *Peltigera* (lichen-forming *Ascomycota*) based on morphological, chemical, and large subunit nuclear ribosomal DNA data. International Journal of Plant Sciences 161(6): 925–958. https://doi.org/10.1086/317568

Miller MA, Pfeiffer W, Schwartz T. 2010. Creating the CIPRES Science Gateway for inference of large phylogenetic trees. 1–8, in: Proceedings of the Gateway Computing Environments Workshop (GCE), 14 Nov 2010. https://doi.org/10.1109/GCE.2010.5676129

Nalepa CA, Weir A. 2007. Infection of *Harmonia axyridis* (*Coleoptera: Coccinellidae*) by *Hesperomyces virescens* (*Ascomycetes: Laboulbeniales*): role of mating status and aggregation behavior. Journal of Invertebrate Pathology 94(3): 196–203. https://doi.org/10.1016/j.jip.2006.11.002

Nguyen LT, Schmidt HA, von Haeseler A, Minh BQ. 2015. IQ-TREE: A fast and effective stochastic algorithm for estimating maximum likelihood phylogenies. Molecular Biology and Evolution 32: 268–274. https://doi.org/10.1093/molbev/msu300

Riddick EW. 2010. Ectoparasitic mite and fungus on an invasive lady beetle: parasite coexistence and influence on host survival. Bulletin of Insectology 63(1): 13–20.

Rossi W. 1998. New or interesting *Laboulbeniales* parasitic on *Diptera* from Bolivia. Mycologia 90(6): 1047–1054. https://doi.org/10.1080/00275514.1998.12027004

Rossi W, Leonardi M. 2018. New species and new records of *Laboulbeniales* (*Ascomycota*) from Sierra Leone. Phytotaxa 358(2): 91–116. https://doi.org/10.11646/phytotaxa.358.2.1

Rossi W, Weir A. 2007. New species of *Stigmatomyces* from various continents. Mycologia. 99(1):139-143. 10.1080/15572536.2007.11832610

Rossi W, Santamaría S, Andrade R. 2013. Notes on the *Laboulbeniales* (*Ascomycota*) parasitic on *Diptera* from Portugal and other countries. Plant Biosystems 147(3): 730–742. https://doi.org/10.1080/11263504.2012.753132

Species Fungorum. 2020. Search Species Fungorum [online]. Available from http://www.speciesfungorum.org/Names/Names.asp [accessed 12 Jun. 2020].

Sugiyama K. & Majewski T. 1985. The *Laboulbeniomycetes* (*Ascomycotina*) of peninsular Malaysia II. Transactions of the Mycological Society of Japan 26: 449–462

Thaxter R. 1901. Preliminary diagnoses of new species of *Laboulbeniaceae*. – III. Proceedings of the American Academy of Arts and Sciences 36(23): 395–414. https://doi.org/10.2307/20021044

Thaxter R. 1905. Preliminary diagnoses of new species of *Laboulbeniaceae*–VI. Proceedings of the American Academy of Arts and Sciences 41(14): 301–318. https://doi.org/10.2307/20022067

Thaxter R. 1908. Contribution towards a monograph of the *Laboulbeniaceae*. Part II. Memoirs of the American Academy of Arts and Sciences 13: 217–469. https://doi.org/10.2307/25058090

Thaxter R. 1915. New Indo-Malayan *Laboulbeniales*. Proceedings of the American Academy of Arts and Sciences 51(1): 3–51. https://doi.org/10.2307/20025560

Thaxter R. 1917. New *Laboulbeniales,* chiefly dipterophilous American species. Proceedings of the American Academy of Arts and Sciences 52(10): 649–721. https://doi.org/10.2307/20025703

Thaxter R. 1918. Extra-American dipterophilous *Laboulbeniales*. Proceedings of the American Academy of Arts and Sciences 53(9): 697–749. https://doi.org/10.2307/25130007

Vilgalys R, Hester M. 1990. Rapid genetic identification and mapping of enzymatically amplified ribosomal DNA from several *Cryptococcus* species. Journal of Bacteriology 172(8): 4238–4246. https://doi.org/10.1128/jb.172.8.4238-4246.1990

Weir A, Blackwell M. 2001a. Extraction and PCR amplification of DNA from minute ectoparasitic fungi. Mycologia 93(4): 802–806. https://doi.org/10.1080/00275514.2001.12063212

Weir A, Blackwell M. 2001b. Molecular data support the *Laboulbeniales* as a separate class of *Ascomycota, Laboulbeniomycetes*. Mycological Research 105(10): 1182–1190. https://doi.org/10.1016/S0953-7562(08)61989-9

Weir A, Hughes M. 2002. The taxonomic status of *Corethromyces bicolor* from New Zealand, as inferred from morphological, developmental, and molecular studies. Mycologia 94(3): 483–493. https://doi.org/10.1080/15572536.2003.11833213

MYCOTAXON

ISSN (print) 0093-4666 (online) 2154-8889 Mycotaxon, Ltd. ©2022

January–March 2022—Volume 137, pp. 109–121

https://doi.org/10.5248/137.109

Pluteus variabilicolor and *Volvopluteus earlei*, new records for Pakistan

Junaid Khan[1*], Hassan Sher[1], Aiman Izhar[2], Muhammad Haqnawaz[2], Abdul Nasir Khalid[2]

[1] *Center for Plant Sciences and Biodiversity, University of Swat, Mingora, Pakistan*

[2] *Institute of Botany, University of the Punjab, Quaid-e-Azam campus, Lahore, Pakistan*

*Correspondence to: *junaid.botany@gmail.com*

Abstract—*Pluteus variabilicolor* and *Volvopluteus earlei* are reported as new records for the Pakistani funga, with the former representing a new record for South Asia and the latter, a second report from Asia. Morphological descriptions are accompanied by colored photographs of basidiomata and microscopic structures. Identity of both species is confirmed by ITS sequence analyses. Comparison with previous descriptions and data on their distributions are briefly discussed.

Key words—*Agaricales*, phylogeny, *Pluteaceae*, *P.* sect. *Hispidoderma*, taxonomy

Introduction

Pluteaceae Kotl. & Pouzar (*Agaricales*) is a family of saprophytic fungi widely distributed in major parts of the world (Kirk & al. 2008). Molecular reassessment of the family (Justo & al. 2011a) supports two genera: *Pluteus* Fr. and *Volvopluteus* Vizzini & al.

Pluteus, the larger genus, comprises >300 species (Kirk & al. 2008, He & al. 2019), distributed worldwide especially in boreal to tropical forested regions (Menolli & al. 2014). *Pluteus* species are primarily lignicolous and grow on partially or well-rotted angiosperm and gymnosperm wood (Orton 1986, Singer 1986, Vellinga 1990). The presence of free lamellae, pinkish

spore-print, inverse hymenophoral trama, and inamyloid basidiospores and lack of universal veil are some key *Pluteus* characters (Vellinga & Schreurs 1985, Orton 1986, Singer 1986, Vellinga 1990, Heilmann-Clausen 2012). Only eight *Pluteus* species have been reported from Pakistan: *P. ephebeus* (Fr.) Gillet (as *P. murinus* Bres.), *P. escharites* (Berk. & Broome) Sacc., *P. fusconigricans* (Berk. & Broome) Sacc., *P. leoninus* (Schaeff.) P. Kumm., *P. palumbinus* (Berk.) Sacc., *P. pellitus* (Pers.) P. Kumm., *P. petasatus* (Fr.) Gillet, and *P. pulverulentus* Murrill (Ahmad 1980, Iqbal & Khalid 1996, Ahmad & al. 1997).

Volvopluteus, typified by *V. gloiocephalus* (DC.) Vizzini & al., was erected to accommodate some species formerly placed in *Volvariella* (Justo & al. 2011a). The genus is distinguished from *Pluteus* and *Volvariella* by a gelatinous pileipellis that is an ixocutis with relatively narrow hyphae (average ≤15 µm diam.) and average basidiospore length >11 µm (Justo & al. 2011a). Only one *Volvopluteus* species, *V. gloiocephalus*, has been reported from Pakistan (Ahmad 1980 and Iqbal & Khalid 1996, as *Volvariella speciosa* (Fr.) Singer).

This paper, part of a larger project dealing with the exploration of macrofungi in northern Khyber Pakhtunkhwa reports two pluteaceous species as new records for the funga of Pakistan: *Pluteus variabilicolor* and *Volvopluteus earlei*.

Materials and methods

Collection & morphological Studies

Specimens were collected during macrofungal surveys conducted between 2014 and 2019 in different parts of Pakistan. The specimens of *P. variabilicolor* were collected in village Ingaro Dherai, district Swat, Khyber Pakhtunkhwa province. Those of *V. earlei* were collected in the same locality and in the Sheikupura and Muzaffargarh districts of Punjab province. Basidiomata were dug out to the extreme base (to obtain some wood with specimens of *Pluteus* and volva with those of *Volvopluteus*) with a sharp knife. The specimens were photographed in their natural habitat and important macro-morphological characters were noted when fresh. Colors were coded according to soil color chart of Munsell (1975). Terminology for macroscopic and microscopic features follows Vellinga (1988). The specimens were dried in sun and deposited in the herbarium of the University of Swat, Kanju Township, Pakistan (SWAT) and the herbarium of the University of the Punjab, Lahore, Pakistan (LAH).

Microscopic descriptions are based on free-hand sections from dried specimens mounted both in distilled water and in aqueous potassium hydroxide solution (5% w/v), with aqueous Congo red added for contrast. Basidiospore measurements are based on 60 elements randomly selected from all the available basidiomata;

x presents the mean length and width of the basidiospores. The abbreviation Q refers to the length : width (L/W) ratio, with Q_m = the average length : width ratio.

DNA extraction, PCR amplification, sequencing

Genomic DNA from dried herbarium specimens was extracted using modified CTAB method of Gardes & Bruns (1993). The internal transcribed spacer region (ITS = ITS1-5.8S-ITS2) was amplified using the primer pair ITS1F (Gardes & Bruns 1993) and ITS4 (White & al. 1990). Polymerase chain reactions (PCR) were performed in 25 µL volume aliquots. Amplification involved initial 4 minutes denaturation at 94 °C, 40 cycles of 1 minute at 94 °C, 1 min at 55 °C, 1 min at 72 °C, and a final extension of 10 minutes at 72 °C (Naseer & al. 2020). PCR products were visualized in a UV illuminator loaded in 1% agarose gel added with 3 µL ethidium bromide. Purification and sequencing of the PCR amplicons were carried out at Beijing Genomic Institute (BGI) Hong Kong.

Sequence alignment & phylogenetic analysis

The forward and reverse reads were assembled into a consensus sequence using BioEdit software v. 7.2.5 (Hall 1999). The consensus sequences were used for a GenBank search, using the NCBI Basic Local Alignment Search Tool (BLAST) (https://blast.ncbi.nlm.nih.gov/Blast.cgi). Matching sequences, especially those published in Justo & al. (2011b) and Lezzi & al. (2014), were downloaded for further phylogenetic analysis. Separate datasets were used for *Pluteus* and *Volvopluteus*.

Multiple sequences were aligned using online Multiple Alignment using Fast Fourier Transform (MAFFT) algorithm at European Bioinformatics Institute website (https://www.ebi.ac.uk/Tools/msa/mafft/). The phylogenies were inferred by maximum likelihood (ML) analysis using model selection for the best DNA analysis in MEGA6 software (Tamura & al. 2013). Jukes-Cantor model Models with the lowest BIC scores (Bayesian Information Criterion) was considered to describe the substitution pattern the best. Non-uniformity of evolutionary rates among sites were modeled using a discrete gamma distribution (+G) with 5 rate categories and assuming that a certain fraction of sites is evolutionarily invariable (+I). The phylogenetic analyses included 1000 bootstrap replicates.

Phylogenetic results

The final *Pluteus* ITS dataset comprised 37 sequences representing *P.* sect. *Hispidoderma* Fayod including the two sequences from our new Pakistani specimens. *Pluteus diettrichii* Bres. (HM562143) of *P.* sect. *Celluloderma* Fayod was used as outgroup following Lezzi & al. (2014). Maximum likelihood analysis convincingly clustered the Pakistani collections with other sequences of *P. variabilicolor* in the *Leoninus* clade of *P.* sect. *Hispidoderma* with a 100% bootstrap value (Fig. 1).

The ITS consensus sequences from our three new Pakistani *Volvopluteus* collections matched 99–99.5% with multiple *V. earlei* sequences (HM562205,

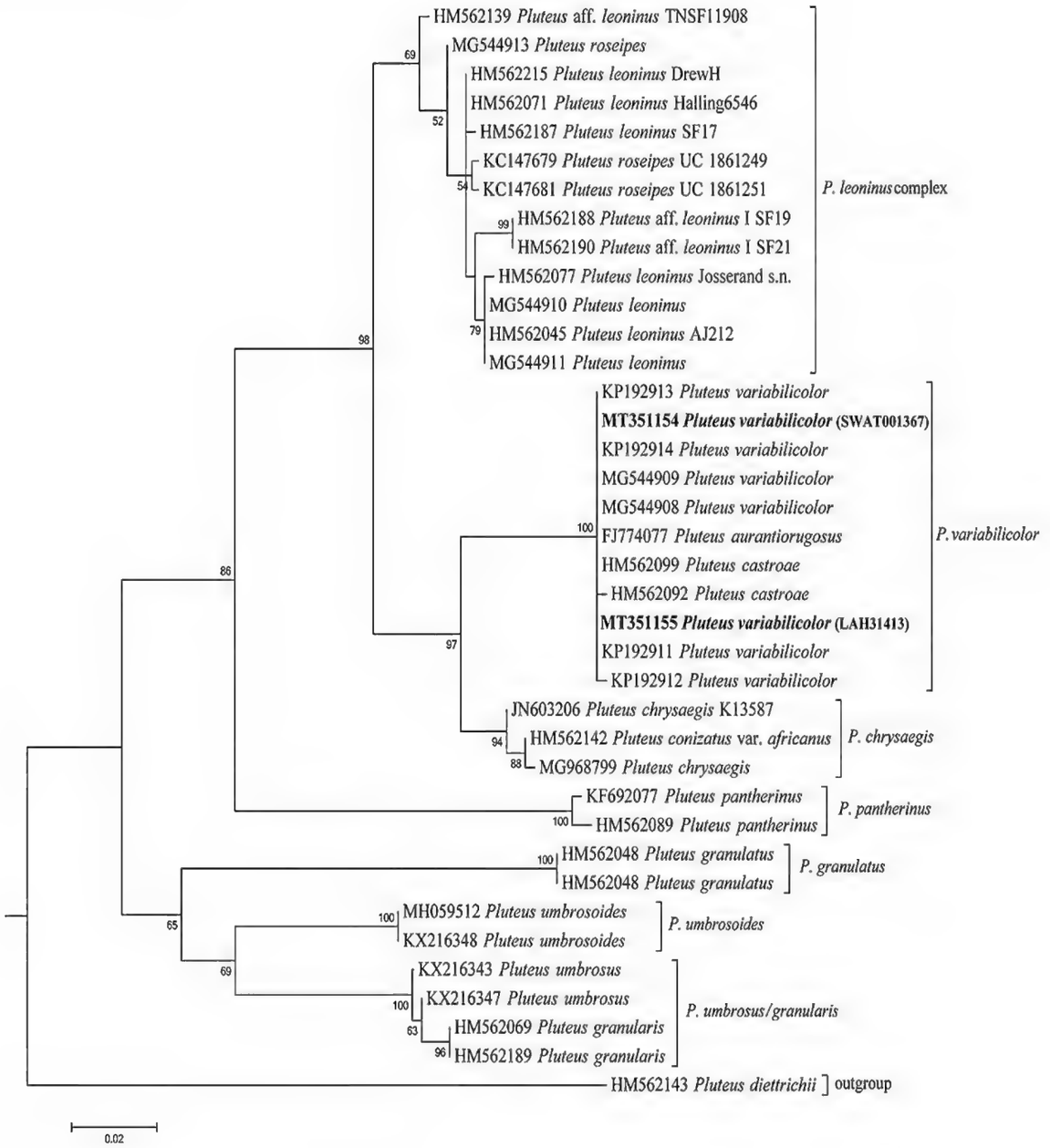

Fig. 1: Maximum likelihood phylogram of *Pluteus variabilicolor* and related species inferred from ITS data. Bootstrap values ≥50% are presented above nodes. Newly generated sequences of *P. variabilicolor* are presented in bold.

HM562205, HM246496, HM246497, HM246498, HM246499, MK204987, MK204989) in GenBank. The final *Volvopluteus* dataset comprises 19 sequences including the three sequences from the new Pakistani specimens and from *Pluteus heteromarginatus* Justo (HM562058) and *P. longistriatus* (Peck) Peck. (HM562082), the outgroup cited in Justo & al. (2011b). Sequences of the Pakistani collections clustered with other sequences of *V. earlei*, confirming their identity (Fig. 2).

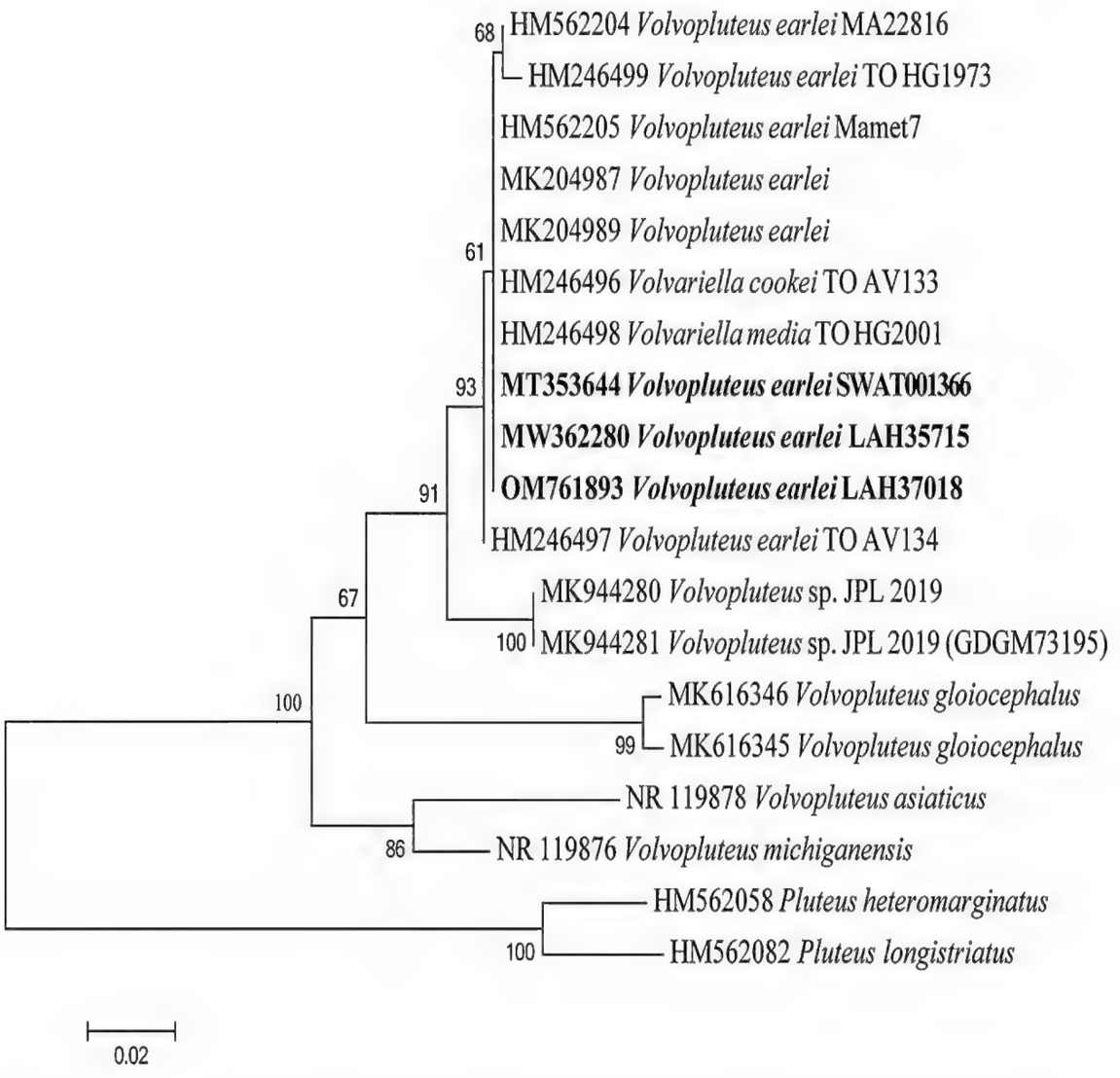

Fig. 2: Maximum likelihood phylogram of *Volvopluteus earlei* and related species inferred from ITS data. Bootstrap values ≥50% are presented above nodes. Newly generated sequences of *V. earlei* are presented in bold.

Taxonomy

Pluteus variabilicolor Babos,
Ann. Hist.-Nat. Mus. Natl. Hung. 70: 93 (1978) Figs 3a–c, 4

Pileus 50–70 mm diam., convex to plano-convex with a central umbo, light orange yellow (10YR 9/8) to dark yellow (2.5Y 9/12), disc darker (2.5Y 7/12); surface smooth, glabrous to lightly velvety, margin striate or not; context concolorous with the pileus just beneath the cuticle, otherwise cream colored, unchanging upon cutting, thin, 2–3 mm at the disc, <1 mm at the margin. Lamellae free, close, sub-ventricose (≤6 mm at the center);

white to pale pink (7.5YR 9/4) when young, pink (7.5R 9/4) when mature; lamellar edge even to slightly undulate; lamellulae present, short to long extending beyond the middle of the lamellae. Stipe 50–80 × 5–7 mm, central, cylindrical to very slightly thickening downward; pinkish (7.5YR 8/4); longitudinally striate in mature specimens, fistulose; context concolorous with the exterior or light yellowish brown (10YR 6/4), unchanging upon cutting.

Basidiospores (5.1–)5.5–6.3(–6.8) × (4.4–)4.8–5.8(–5.9) µm, x = 5.9 × 5.1 µm, Q = 1.1–1.19(–1.2), Q_m = 1.1, mostly sub-globose, rarely ovoid to broadly ellipsoid; smooth, thick-walled (2–3 µm thick), mostly with one central guttula, rarely multi-guttulate. Basidia 20–25 × 6.0–7.0 µm; cylindrical to broadly oblong, with 4 sterigmata. Cheilocystidia 55–90 × 20–30 µm; fusiform with a short appendix at the tip to lageniform. Pleurocystidia 60–120 × 20–40 µm, narrowly utriform to utriform, rare. Pileipellis a hymeniderm composed of clavate to rounded terminal elements, 50–200 × 20–40 µm, without any yellow intracellular pigment. Stipitipellis a cutis composed of narrow branched hyphae, 3.0–5.0 µm diam., with rare claviform caulocystidia, 25–50 × 15–30 µm, usually in clusters extending along the stipe length. Clamp connections absent.

Materials examined: **PAKISTAN, Khyber Pakhtunkhwa, Swat district**, Ingaro Dherai village, 1000 m. a.s.l., on decomposing stump of *Populus nigra* L., 7 August 2014, Junaid Khan ING-32 (SWAT001367; GenBank MT351154); Ingaro Dherai village, 1010 m. a.s.l., on decomposing stump of *Populus nigra*, 27 July 2015, Junaid Khan ING-1507 (LAH31413; GenBank MT351155).

Commentary—*Pluteus variabilicolor*, originally described from Hungary, is characterized by its pileus color varying from yellowish orange to chrome-yellow, pileipellis with morphologically variable elements (a mixture of spheropedunculate-vesiculose and elongated ± cystidioid elements), the presence of caulocystidia, and growth on decaying sawdust (Babos 1978). Our description fits well with previous descriptions (Lohmeyer & al. 1994, Lanconelli & al. 1998, Migliozzi 2011, Lezzi & al. 2014, Kaygusuz & al. 2019).

Lezzi & al. (2014) cite *P. variabilicolor* as widespread but not common. Currently the species has been reported from numerous central and eastern European countries—Hungary (Babos 1978), Austria (Lohmeyer & al. 1994), Italy (Lanconelli & al. 1998, Migliozzi 2011), Germany (Ludwig 2007), central Russia (as *P. castri,* Justo & al. 2011b), Romania (Béres 2012), Slovenia (Jogan & al. 2012), and Moldova (Lezzi & al. 2014). From Asia, the species has been reported from Japan (as *P. castri,* Justo & al. 2011b),

Fig. 3: Field photographs of basidiomata. ***Pluteus variabilicolor***: a–b. (SWAT001367); c. (LAH31413). ***Volvopluteus earlei***: d & f (SWAT001366); e. (LAH37018); g & h. (LAH35715). Scale bars = 10 mm.

and from Turkey and South Korea (Kaygusuz & al. 2019). Here we report *P. variabilicolor* from Pakistan and South Asia for the first time.

Pluteus variabilicolor grows primarily on sawdust deposits and on branches and rotten wood of *Fagaceae*, mainly *Quercus* spp. (Migliozzi 2011, Lezzi & al. 2014). Both Pakistani collections, however, were collected from decaying stumps of *Populus* sp., which agrees with Russian reports of collections growing on *Populus tremula* stumps of (Justo & al. 2011b).

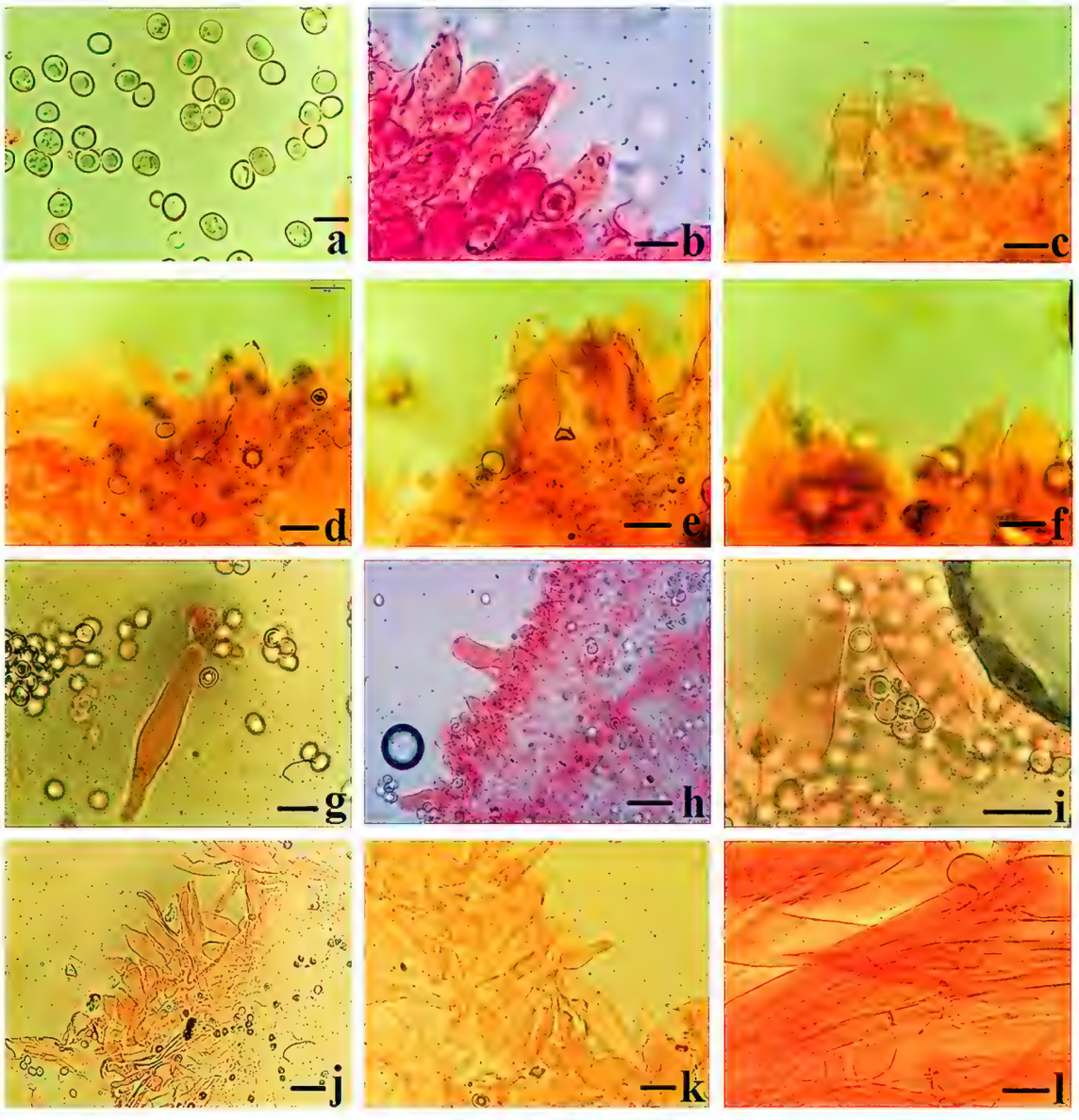

Fig. 4: *Pluteus variabilicolor* (SWAT001367): a. Basidiospores; b. Basidia; c–f. Cheilocystidia; g–i. Pleurocystidia; j, k. Pileipellis elements; l. Stipitipellis elements. Scale bars: a, b = 5 µm; c–i = 20 µm; j–l = 30 µm.

We suggest that *P. variabilicolor* was introduced into Pakistan with the introduction of *Populus nigra.*

Volvopluteus earlei (Murrill) Vizzini, Contu & Justo,
Fungal Biology 115(1): 15 (2011) Figs 3d–h, 5

Pileus 20–40 mm diam.; hemispherical to obtusely conical when young, applanate to plano-concave on maturity; white to greyish white with a greyish disc when young, in maturity white to moderate whitish pink

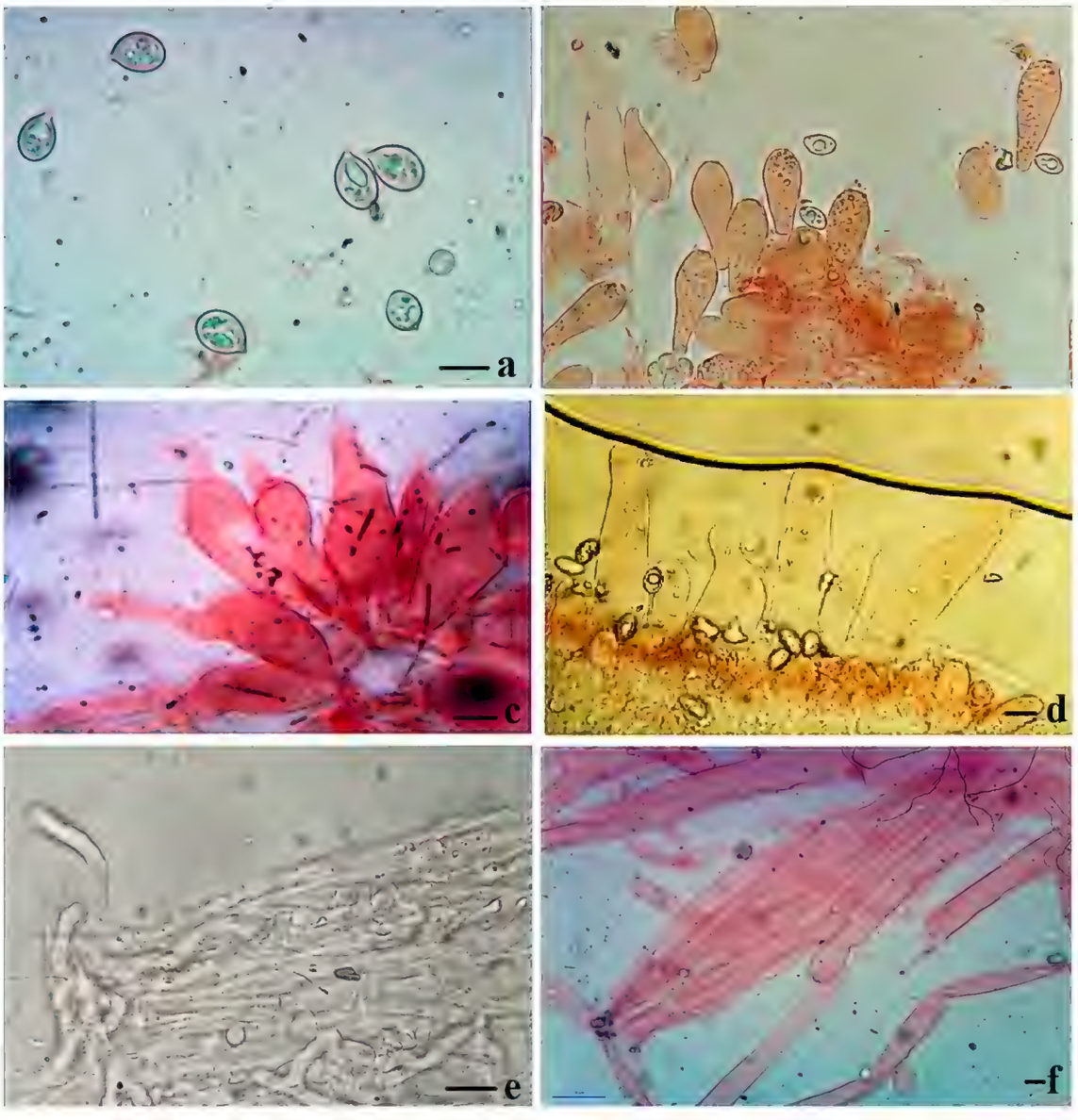

Fig. 5: *Volvopluteus earlei* (LAH35715): a. Basidiospores; b. Basidia; c. Cheilocystidia; d. Pleurocystidia; e. Stipitipellis; f. Pileipellis elements. Scale bars = 10 µm.

(2.5YR 7/4) with reddish pink margins (10R 6/8); surface moist and viscid in young specimens, dry and dull when mature, glabrous; margin striate, striation short (<1/4 of pileus radius); context white, thin, 1–2 mm thick at the disc, ≤1 mm elsewhere. Lamellae free, broad (4–6 mm at the center), sub-crowded to close; white to cream-colored when young, pink (7.5YR 8/8) when mature; lamellulae present. Stipe 70–100 × 4–7 mm; central, tapering upward from slightly flattened base; surface smooth; white to cream colored, turning slightly pinkish (7.5 YR 9/4) upon maturity and handling; volva

present, small (≤8 mm high), membranous, saccate, 2–3 lobed; white to pale gray.

Basidiospores (11.0–)11.5–14.5(–15.0) × (7.0–)7.5–9.6(–10.0) µm, x = 12.8 × 9.1 µm, Q = (1.2–)1.3–1.6(–1.7), Q_m = 1.4; ellipsoid to ovoid, smooth, thick-walled (≤0.5 µm), mostly with one large and many small guttulae. Basidia 30–40 × 10.0–12.0 µm, 4-spored, cylindrical to broadly clavate. Cheilocystidia 35–60 × 8.0–15.0 µm, fusiform to clavate mucronate. Pleurocystidia 80–150 × 15–20 µm, cylindrical to narrowly conical. Pileipellis ixocutis, composed of cylindrical and scattered obovoid to broadly cylindrical and rarely branched terminal elements; 30–35 × 14.0–18.0 µm. Stipitipellis hyphae 7–10 µm diam., ± parallel, caulocystidia cylindrical to narrowly clavate, 40–55 × 8–11 µm. Clamp connections absent.

Material Examined: **PAKISTAN, Khyber Pakhtunkhwa, Swat district**, Ingaro Dherai village, 1000 m. a.s.l., among grasses in humus rich wet soil in the paddy fields, 27 June 2016, Junaid Khan ING-1501 (SWAT001366; GenBank MT353644); **Punjab, Sheikhupura district,** 236 m. a.s.l., solitary on muddy rich soil of a graveyard, 16 July 2017, Aiman Izhar SKP03 (LAH35715; GenBank MW362280); **Muzaffargarh district,** surrounding head Taunsa barrage, 65 m. a.s.l., in scattered groups on humus rich soil, 13 August 2019, Muhammad Haqnawaz TM04 (LAH37018; GenBank OM761893).

Commentary—*Volvopluteus earlei*, originally described from Cuba (Murrill 1911), is characterized by its dry to sub-viscid relatively small (25–45 mm) white pileus, narrowly cylindrical stipe with a small white basal volva, rare or absent broadly clavate pleurocystidia, rostrate cheilocystidia, and large (averaging >12.5 µm long) basidiospores (Shaffer 1957, Desjardin & Hemmes 2001, Contu 2007, Justo & al. 2011a). Murrill (1911) described only basidiospores in his description; other microscopical details were later provided by Coker (1947) and Shaffer (1957). Descriptions from different parts of the world (Pathak 1975, Heinemann 1975, Desjardin & Hemmes 2001, Contu 2007, Vizzini & Contu 2010, Justo & al. 2011a) cite highly diverse cystidial forms for *V. earlei.* For instance, no cystidial forms were reported for the African (Pathak 1975) and Italian (Vizzini & Contu 2010) collections of *V. earlei* [= *Volvariella acystidiata* N.C. Pathak]. Elsewhere, Justo & Castro (2010) reported only cheilocystidia in the Spanish collection, while Shaffer (1957) report both cheilocystidia and pleurocystidia for the North American collections We observed both cheilocystidia and pleurocystidia in the Pakistani collection, which agrees with descriptions of the American collections (Shaffer 1957, Desjardin & Hemmes 2001).

Volvopluteus earlei is known from the U.S.A (Murrill 1911; Coker 1947; Desjardin & Hemmes 2001), Mexico (Vázquez & al. 1989), Africa (Heinemann 1975, as *Volvariella acystidiata*), Sardinia (Contu 2007, as *Volvariella earlei* (Murrill) Shaffer), Spain (Justo & Castro 2010), and India (Amandeep & al. 2015; Atri & al. 1996, as *Volvariella earlei*). This is the first report of this species from Pakistan and the second record from Asia.

Acknowledgments

We are grateful to Dr. Alfredo Justo (Curator of Botany and Mycology, New Brunswick Museum, Saint John, Canada) and Dr. Nelson Menolli Jr., (Professor, Federal Institute of Education, Science and Technology, São Paulo, Brazil) for reviewing this manuscript.

Literature cited

Ahmad S. 1980. A contribution to the *Agaricales* of Pakistan. Bulletin of Mycology (Faisalabad) 1(1): 35–90.

Ahmad S, Iqbal S, Khalid AN. 1997. Fungi of Pakistan. Sultan Ahmad Mycological Society of Pakistan, Lahore. 248 p.

Amandeep K, Atri NS, Munruchi K. 2015. A checklist of coprophilous agarics of India. Current Research in Environmental & Applied Mycology 5(4): 322–348. https://doi.org/10.5943/cream/5/4/3

Atri NS, Saini SS, Kaur G. 1996. Three species of agarics from Patiala. Mushroom Research 5(2): 77–80.

Babos M. 1978. *Pluteus* studies, I. (*Basidiomycetes*, *Pluteaceae*). Annales Historico-Naturales Musei Nationalis Hungarici 70: 93–97.

Béres M. 2012. Macromycete species included in Bern Convention Appendix in the Red List for Romania, and rare presence in historical Maramures area (Romania). Acta Oecologica Carpatica 5: 19–38.

Coker WC. 1947. North Carolina species of *Volvaria*. Journal of the Elisha Mitchell Scientific Society 63: 220–230. https://www.jstor.org/stable/24333992

Contu M. 2007. *Volvariella earlei* (*Basidiomycota*, *Pluteaceae*) nuova per l'Europa, e note sulla tassonomia di *Volvariella* media sensu J.Lange. Micologia e Vegetazione Mediterranea 21(29): 101–106.

Desjardin DE, Hemmes DE. 2001. *Agaricales* of the Hawaiian Islands—7. Notes on *Volvariella*, *Mycena* sect. *Radiatae*, *Physalacria*, *Porpoloma* and *Stropharia*. Harvard Papers in Botany 6(1): 85–103. https://www.jstor.org/stable/41761629

Gardes M, Bruns TD. 1993. ITS primers with enhanced specificity for basidiomycetes – application to identification of mycorrhizae and rusts. Molecular Ecology 2(2): 113–118. https://doi.org/10.1111/j.1365-294x.1993.tb00005.x

Hall TA. 1999. BioEdit: a user-friendly biological sequence alignment editor and analysis program for Windows 95/98/NT. Nucleic Acids Symposium Series 41: 95–98.

He MQ, Zhao RL. Hyde KD, Begerow D, Kemler M, Yurkov A, McKenzie EHC & al. 2019. Notes, outline and divergence times of *Basidiomycota*. Fungal Diversity 99: 105-367.

Heilmann-Clausen J. 2012. *Pluteus* Fr. 386–395, in: H. Knudsen, J Vesterholt (eds). Funga Nordica: agaricoid, boletoid, clavarioid, cyphelloid and gastroid genera, 2nd edition. Copenhagen: Nordsvamp.

Heinemann P. 1975. Flore illustrée des champignons d'Afrique centrale, fasc. 4: *Volvariella*. National Botanical Garden of Belgium, Meise. pp. 73–84.

Iqbal SH, Khalid AN. 1996. Material for the fungus flora of Pakistan. I. Checklist of agarics, their distribution and association with the surrounding vegetation. Science International (Lahore) 8: 51–64

Jogan N, Bačič T, Strgulc-Krajšek S. 2012. Tujerodne in invazivne rastline v Sloveniji. 161–182, in: N Jogan & al. (eds). Neobiota Slovenije, končno poročilo projekta. Oddelek za biologijo, Biotehniška fakulteta, Univerza v Ljubljani, Ljubljana.

Justo A, Castro ML. 2010. The genus *Volvariella* in Spain: *V. dunensis* comb. & stat. nov. and observations on *V. earlei*. Mycotaxon 112: 261–270. https://doi.org/10.5248/112.261

Justo A, Vizzini A, Minnis AM, Menolli Jr. N, Capelari M, Rodríguez O, Malysheva E & al. 2011a. Phylogeny of *Pluteaceae* (*Agaricales*, *Basidiomycota*): taxonomy and character evolution. Fungal Biology 115: 1–20. https://doi.org/10.1016/j.funbio.2010.09.012

Justo A, Minnis AM, Ghinone S, Menolli Jr. N, Capelari M, Rodríguez O, Malysheva E & al. 2011b. Species recognition in *Pluteus* and *Volvopluteus* (*Pluteaceae*, *Agaricales*): morphology, geography and phylogeny. Mycological Progress 10: 453–479. https://doi.org/10.1007/s11557-010-0716-z

Kaygusuz O, Türkekul I, Knudsen H, Çolak ÖF. 2019. New records of *Pluteus* section *Hispidoderma* in Turkey based on morphological characteristics and molecular data. Phytotaxa 413(3): 175–206. https://doi.org/10.11646/phytotaxa.413.3.1

Kirk PM, Cannon PF, Minter DW, Stalpers JA. 2008. Dictionary of the Fungi: 10th edn. CAB International, Wallingford, UK. 771 p.

Lanconelli L, Ballanti F, Rava M. 1998. Funghi del Lughese. Edit Faenza, Faenza. 416 p.

Lezzi T, Vizzini A, Ercole E, Migliozzi V, Justo A. 2014. Phylogenetic and morphological comparison of *Pluteus variabilicolor* and *P. castri* (*Basidiomycota*, *Agaricales*). IMA Fungus 5(2): 415–423. https://doi.org/10.5598/imafungus.2014.05.02.06

Lohmeyer TR, Christan J, Gruber O. 1994. Ein Nachweis von *Pluteus variabilicolor* in Oberösterreich. Österreichische Zeitschrift für Pilzkunde 3: 95–100.

Ludwig E. 2007. Pilzkompendium, Band 2. Beschreibungen. Fungicon–Verlag, Berlin. 723 p.

Menolli Jr. N, Justo A, Arrillaga P, Pradeep CK, Minnis AM, Capelari M. 2014. Taxonomy and phylogeny of *Pluteus glaucotinctus* sensu lato (*Agaricales*, *Basidiomycota*), a multicontinental species complex. Phytotaxa 188(2): 78–90. https://doi.org/10.11646/phytotaxa.188.2.2

Migliozzi V. 2011. *Pluteus variabilicolor*, specie frequente nella cerreta di Macchiagrande di Manziana (RM). Parliamo di Funghi 19(1): 3–9.

Munsell AH. 1975. Munsell soil color charts. Baltimore: Munsell Color Inc.

Murrill WA. 1911. The *Agaricaceae* of tropical North America. Mycologia 3: 271–282. https://doi.org/10.1080/00275514.1911.12017682

Naseer A, Garrido-Benavent I, Khan J, Ballarà J, Mahiques R, Khalid AN, Sher H. 2020. *Cortinarius pakistanicus* and *C. pseudotorvus*: two new species in oak forests in the Pakistan Himalayas. MycoKeys 74:91–108. https://doi.org/10.3897/mycokeys.74.49734

Orton PD. 1986. British Fungus Flora: Agarics and Boleti. Vol. 4. *Pluteaceae*: *Pluteus* & *Volvariella*. Edinburgh: Royal Botanic Garden Edinburgh.

Pathak NC. 1975. New species of *Volvariella* from Central Africa. Bulletin du Jardin Botanique National de Belgique 45: 195–196.

Shaffer RL. 1957. *Volvariella* in North America. Mycologia 49(4): 545–579. https://doi.org/10.1080/00275514.1957.12024669

Singer R. 1986. The *Agaricales* in modern taxonomy (4th revised edition). Koeltz Scientific Books. Koenigstein.

Vázquez LS, Guzmán-Dávalos L, Guzmán G. 1989. Contribution to the knowledge of the species of the genus *Volvariella* in the state of Jalisco. Revista Mexicana de Micología 5: 169–179.

Vellinga EC. 1988. Glossary. 54–64, in: C Bas & al. (eds). Flora Agaricina Neerlandica, vol. 1. A.A. Balkema Publishers, Amsterdam/Brookfield.

Vellinga EC. 1990. *Pluteus*. 31–55, in: C Bas & al. (eds). Flora Agaricina Neerlandica, vol. 2. A.A. Balkema. Rotterdam.

Vellinga EC, Schreurs J. 1985. *Pluteus* Fr. in West Europe. Persoonia 12(4): 337–373.

Vizzini A, Contu M. 2010. *Volvariella acystidiata* (*Agaricomycetes*, *Pluteaceae*), an African species new to Europe, with two new combinations in *Volvariella*. Mycotaxon 112: 25–29. https://doi.org/10.5248/112.24

White T, Bruns TD, Lee S, Taylor J. 1990. Amplification and direct sequencing of fungal ribosomal RNA genes for phylogenetics. 315–322, in: MA Innis & al. (eds). PCR protocols: a guide to methods and applications. San Diego: Academic Press. https://doi.org/10.1016/b978-0-12-372180-8.50042-1

MYCOTAXON

ISSN (print) 0093-4666 (online) 2154-8889 Mycotaxon, Ltd. ©2022

January–March 2022—Volume 137, pp. 123–134

https://doi.org/10.5248/137.123

New Turkish records of *Hebeloma excedens* and *H. geminatum*, and confirmation of *H. celatum*

Ayten Dizkirici[1], Aysenur Kalmer[1], İsmail Acar[2*]

[1] *Department of Molecular Biology and Genetics, Van Yüzüncü Yıl University, 65080, Van, Turkey*

[2] *Department of Organic Agriculture, Başkale Vocational High School, Van Yüzüncü Yıl University, 65080, Van, Turkey*

* Correspondence to: *iacar2011@gmail.com*

Abstract—*Hebeloma excedens* and *H. geminatum* are reported as new records and *H. celatum* is confirmed for the Turkish mycota, on the basis of morphological and phylogenetic data. Morphological descriptions, illustrations, and comparisons with closely related taxa are provided.

Key words—*Agaricales*, *Basidiomycota*, *Hymenogastraceae*, ITS, phylogeny

Introduction

Hebeloma (Fr.) P. Kumm. (*Hymenogastraceae, Agaricales*) is a genus of ectomycorrhizal and mostly poisonous basidiomycetes primarily distributed in temperate, boreal, arctic, and alpine habitats (Vesterholt 2005, Beker & al. 2016, Cripps & al. 2019). The genus is characterized by a mostly two coloured convex to plano-convex pileus, dull brown lamellae, presence of a veil, and morphologically distinctive cheilocystidia (Beker & al. 2016).

Identification of *Hebeloma* at the species level is considerably challenged by morphological similarities and infrequent or transient characters (Eberhardt & al. 2012). Therefore, species determination and classification and their phylogenetic relationships within the genus have come to rely upon DNA genomic sequences such as the nuclear ribosomal DNA internal

transcribed spacer (nrDNA ITS) region. One advantage of selecting the ITS region for analysis is the many *Hebeloma* sequences available in GenBank. Moreover, the availability of universal primers, high rate of PCR success, and superior resolution at infrageneric levels are other important advantages of the ITS region (Aanen & al. 2000, 2001; Vesterholt & al. 2014; Eberhardt & al. 2015a,b).

Twenty-eight *Hebeloma* species have been recorded from Turkey (Sesli & Denchev 2014; Güngör & al. 2015; Sesli & al. 2015, 2018; Solak & al. 2015; Doğan & Kurt 2016; Dizkirici & al. 2019). Beker & al. (2016) investigated seven Turkish specimens (representing six species, including *H. celatum* and *H. subtortum*) using molecular data but did not provide morphological details; subsequently Dizkirici & al. (2019) provided detailed descriptions of Turkish *H. subtortum*. *Hebeloma celatum,* which has been widely reported from Europe, known from Turkey only by a single 2008 collection from Adana province (Grilli & al. 2015). Here, we provide full descriptions and phylogenetic results for *Hebeloma excedens*, *Hebeloma geminatum*, and *Hebeloma celatum*.

Hebeloma excedens is placed in *H.* sect. *Hebeloma,* characterized by the visible cortina seen in young basidiomes and cheilocystidia that are always lageniform or ventricose; *H. geminatum* belongs to *H.* sect. *Denudata,* characterized by cheilocystidia that are primarily clavate-stipitate or clavate-ventricose and basidiospores that are weakly dextrinoid; and *H. celatum* is placed in *H.* sect. *Velutipes,* characterized by a velutinate stipe, clavate cheilocystidia, strongly dextrinoid basidiospores, and absence of cortina (Vesterholt 2005, Beker & al. 2016, Grilli & al. 2015).

In the present study, we used morphological and ITS sequence analyses to identify *H. excedens* and *H. geminatum* as new Turkish records and confirm the existing Turkish record of *H. celatum*.

Materials & methods

Taxon sampling & morphological studies

Fresh basidiomata of *H. excedens*, *H. geminatum*, and *H. celatum* were collected during 2017–18 fieldwork in south-eastern Turkey. Collected specimens were photographed in situ using a Canon (EOS 60D) camera equipped with a Tokina 100 mm macro lens. Macromorphological characters were determined based on field notes and colour photographs of fresh fruiting bodies. Dried specimens were examined microscopically after sectioning and rehydration following procedures in Vesterholt (2005) and Beker & al. (2016). Structures were observed using a Leica DM500 research microscope and measured with the Leica Application Suite v.3.4.0.

The samples were dried and deposited as voucher specimens in the Fungarium of Van Yüzüncü Yıl University, Van, Turkey (VANF). Abbreviations include: x = average length × width and Q = length/width ratio of basidiospores calculated based on the number (n) of spores measured. At least 100 spores, 30 basidia, and cheilocystidia from four samples were measured in distilled water and Melzer's reagent for each specimen. Additional potentially diagnostic characters were abbreviated according to Vesterholt (2005) with "D" indicating the degree of basidiospore dextrinoidity in Melzer's, "P" the degree of loosening of the basidiospore perisporium in Melzer's, and "O" the degree of ornamentation on the basidiospore surface.

DNA isolation, amplification, sequencing

Genomic DNA was extracted and purified directly from dried basidiomata using a modified CTAB protocol (Doyle & Doyle 1987). The purity and quantity of extracted DNA were determined by using a NanoDrop2000c UV–Vis Spectrophotometer and 0.8% agarose gel electrophoresis. Isolated stock DNA was stored at –20°C prior for further studies.

Two different samples were amplified for each *Hebeloma* species to increase reliability of the sequences. DNA was amplified in 25 µl volume mixtures containing genomic DNA (10 ng/µl), 10X PCR Buffer, $MgCl_2$ (25 mM), dNTP mixture (10 mM), the primer pair (10 µM), Taq polymerase (5u/µl) and sterile water. The primer pair N-nc18S10 5′AGGAGAAGTCGTAACAAG3′ / C26A 5′GTTTCTTTTCCTCCGCT3′ (Wen & Zimmer 1996) was used to amplify the ITS1-5.8S-ITS2 region. Amplicons were checked in 1% TAE agarose gel stained with Gelred dye. The PCR products were sequenced with forward and reverse primers in an ABI 3730XL automated sequencer. Sequences generated in the current study were submitted to GenBank.

Sequence alignment and phylogenetic analysis

All sequence chromatograms were opened using Finch TV (http://www.geospiza.com/finchtv/) and checked for reading errors, using the Q-Quality value to assess the accuracy of each base. BLAST analysis was performed using the UNITE (http://unite.ut.ee/) and NCBI (http://www.ncbi.nlm.nih.gov/) databases. Following a preliminary BLAST search that supported our newly amplified sequences in *Hebeloma*, we prepared a combined dataset containing sequences scoring the greatest number of BLAST hits.

Sixty-three sequences representing different *Hebeloma* sections were downloaded from the database and aligned with the newly amplified sequences. The final alignment was trimmed, with the data retained for further phylogenetic analyses. *Galerina pruinatipes* (AJ585510) and *G. pseudocamerina* (AJ585508) were chosen as outgroup.

The nucleotide evolutionary model for phylogenetic analyses was determined using MEGA 6.0 (Tamura & al. 2013), with the model with the lowest BIC (Bayesian Information Criterion) score selected. MrBayes v.3.2.6 (Ronquist & al. 2012) was employed for Bayesian phylogenetic analysis using the Markov chain Monte Carlo (MCMC) method (Yang & Rannala 1997) under K2P model. Two independent runs

with 4 chains each were run for 2 million generations, with trees sampled every 1000 generations. Analyses continued until the average standard deviation of split frequencies was <0.01. A Bayesian inference 50% majority rule tree and posterior probability values were estimated from the samples after discarding the first 25% of sampled trees and viewed with Figtree (Rambaut 2010).

Taxonomy

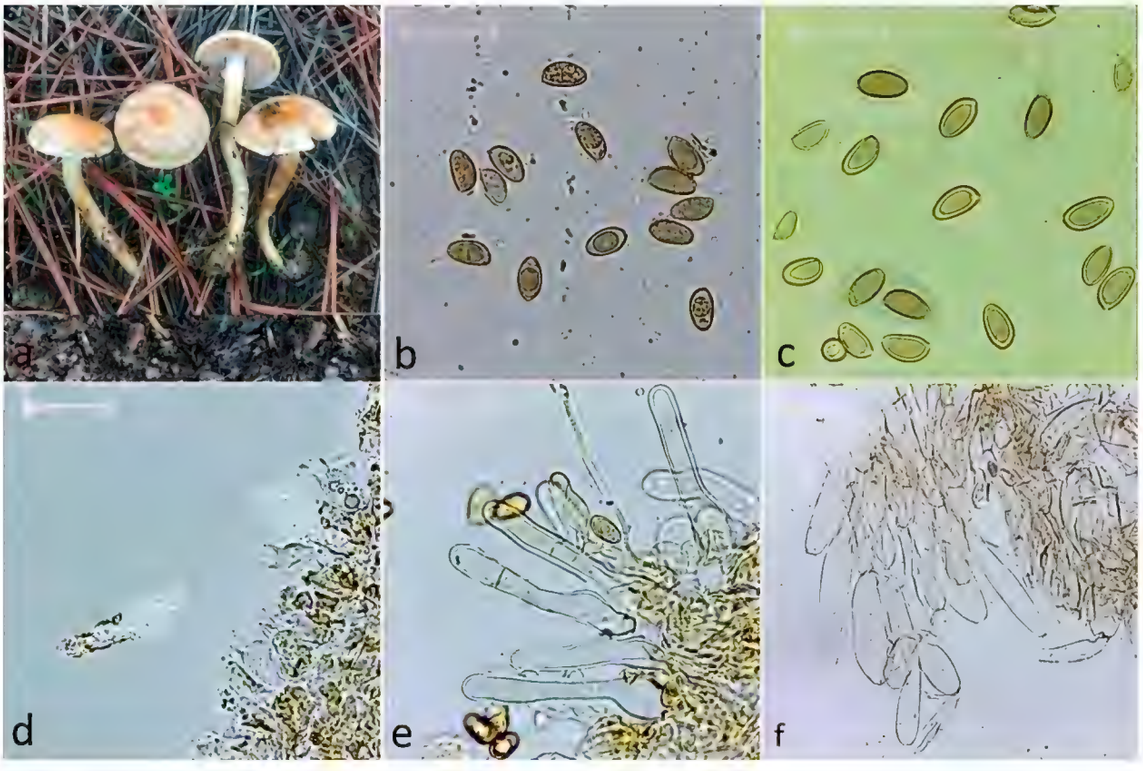

Fig 1. *Hebeloma excedens* [VANF1051]: a. Basidiomata; b. Basidiospores in distilled water; c. Basidiospores in Melzer's reagent; d. Basidia; e. Cheilocystidia; f. Pileipellis. Scale bars: a–e = 20 µm; f = 50 µm.

Hebeloma excedens (Peck) Sacc.,
Syll. Fung. 5: 806 (1887) Fig. 1

Pileus 15–25 mm, convex then almost flat and slightly umbonate, darker in the center (cocoa brown, yellow brown, or cream brown when young; later darkening), pale brown on most of the pileus, lighter at margin and with/without white velar remnants on the edges. Cortina present. Lamellae sinuate, subdecurrent, whitish cream when young, then pale brown, wider and eroded in age. Stipe 30–60 × 3–5 mm, cylindrical, equal, slightly curved, pale cream to light brown, pruinose above cortina zone, lower parts dirty and pale brown, with zones of brown fibrils.

Basidiospores 7.8–11(–12) × 4.1–6.3 µm, x = 9.8 × 5.2 µm, (n = 40; Q = 1.8–1.9), light yellow-yellow brown, elliptical, slightly ovoid, slightly roughened (O1), non- to slightly dextrinoid (D0; D1), perispore not loosening (P0). Basidia 19.7–31 × 7–9.8 µm, clavate, 4-spored. Pleurocystidia absent. Cheilocystidia 35–58 × 5–7 × 4.6–6.8 × 5.6–11 µm, ventricose, cylindrical apex, swollen at the base, rarely fully cylindrical, sometimes septate. Pileipellis an exocutis, ≤45 µm thick, slightly brownish, encrusted.

Specimen examined—**TURKEY, Bitlis, Van-Bitlis roadway**, under *Populus* sp., 38.3625°N 42.7614°E, 1952 m asl, 15.05.2018, Acar 1051 (VANF1051; GenBank MW544166, MW544167).

Hebeloma geminatum Beker, Vesterh. & U. Eberh., Persoonia 35: 122 (2015) Fig. 2

Pileus 25–110 mm, usually convex, occasionally umbonate or flattened, edges generally smooth, slightly incurved or wrinkled when young, when young sticky or moist, usually uniformly coloured (occasionally bi-coloured), cream to beige or (sometimes) light yellow, whitish toward margin. Cortina absent. Lamellae close, adnate to emarginate, notched, finely serrate at margin, droplets on margin when young or in humid conditions, color light pinkish-grey. Stipe 30–100 × 4–12 mm, flocculose, cylindrical to clavate (slightly swollen toward base), whitish.

Basidiospores 10–11.8 × 5.5–6.5 µm, x = 7.6 × 11.5 (n = 40; Q = 1.7–1.8), amygdaloid, non- to very slightly dextrinoid (D0,D1), ornamentation distinct

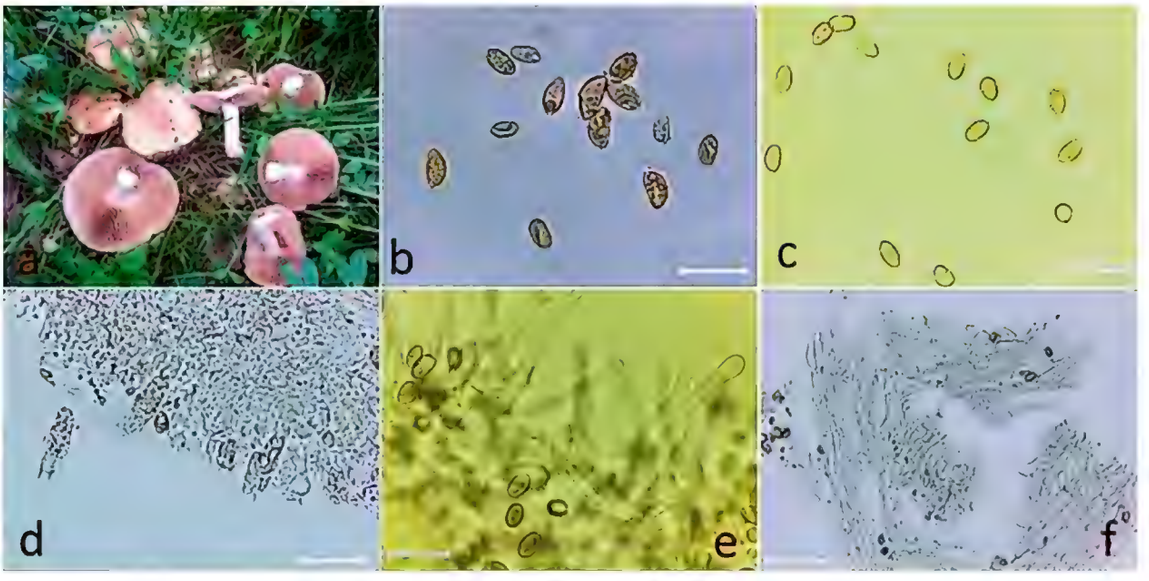

Fig 2. *Hebeloma geminatum* [VANF1116]: a. Basidiomata; b. Basidiospores in distilled water; c. Basidiospores in Melzer's reagent; d. Basidia; e. Cheilocystidia in Melzer's reagent; f. Pileipellis. Scale bars: a–e = 20 µm; f = 50 µm.

verrucose (O2,O3), perispore loosening (P0,P2). Basidia 31 × 8 µm, 4-spored (rarely 2-spored). Pleurocystidia absent. Cheilocystidia 50–85 × 7.2–11 × 4–5.6 × 3.3–4.5 µm, clavate-stipitate, spathulate, sometimes clavate-lageniform or sometimes capitate/bifurcate, septate, sinuate. Pileipellis an ixocutis; with a medium thick epicutis 110–180 µm thick, tramal hyphae beneath subcutis cylindrical, ellipsoid, sausage-shaped and inflating from septa ≤15 µm diam.

Specimen examined—**TURKEY, Bingöl, Elmalı village,** under *Populus* sp., 39.0256°N 40.7339°E, 1234 m, asl 20.05.2017, Acar 1116 (VANF1116; GenBank MW544168, MW544169).

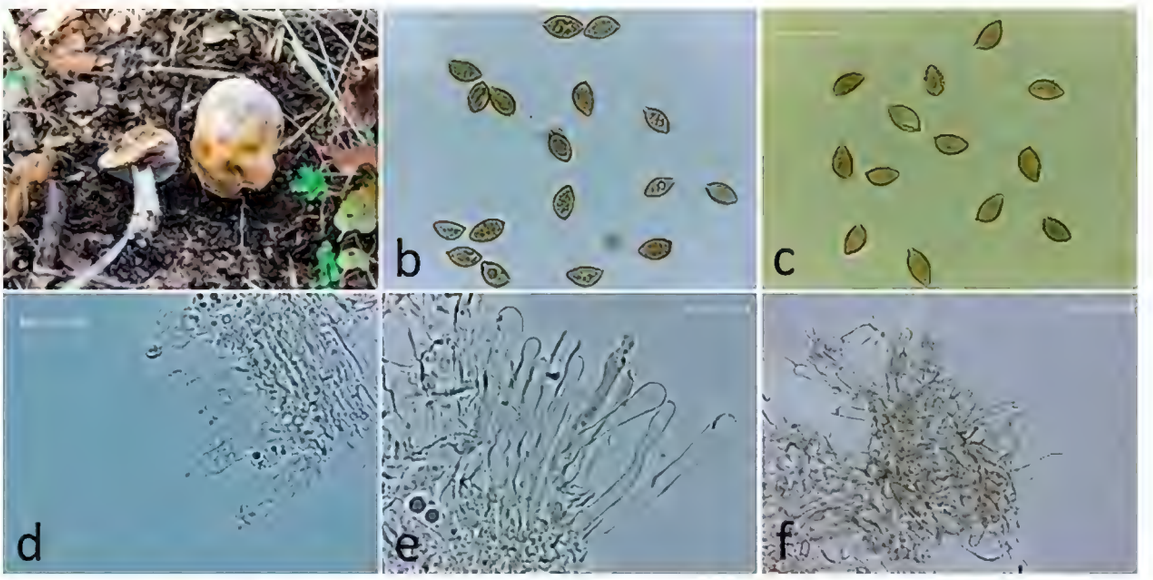

Fig 3. *Hebeloma celatum* [VANF1132]: a. Basidiomata; b. Basidiospores in distilled water; c. Basidiospores in Melzer's reagent; d. Basidia; e. Cheilocystidia; f. Pileipellis. Scale bars: a–e = 20 µm; f = 50 µm.

Hebeloma celatum Grilli, U. Eberh. & Beker,
Mycol. Progr. 15(5): 23. 2015 ["2016"] Fig. 3

Pileus 30–70 mm, convex, occasionally wrinkled, margin involute when young, sometimes smooth or wavy when mature, glutinous when damp, spotting variable, mono- or bi-coloured, cream, clay-buff, ochraceous or yellowish brown. Cortina absent. Lamellae adnexed to emarginate, white fimbriate margin usually present. Stipe 30–70 × 6–10(12) mm, white to light cream, surface with white powdery granules, fibrils, or floccules; cylindrical, clavate with bulbous base, rarely tapering, stuffed when young, later hollow.

Basidiospores 9–15.2 × 5.5–8.5 µm, x = 11.3 × 5.2 µm, (n = 40; Q = 1.6–1.8), amygdaloid, limoniform, yellow, yellowish brown, light yellow, reddish yellow to brown, apiculus distinct, guttulate, ornamentation distinct

verrucose (O2–O4), strongly dextrinoid (D2–D4), perispore loosening (P0–P2). Basidia 25–38 × 7–9.8 µm, cylindrical or clavate, 4-spored, rarely 2-spored. Pleurocystidia absent. Cheilocystidia 32–75 × 4–10 × 4–6.8 × 4–11.2 µm; cylindrical, clavate, clavate-lageniform, or ventricose, sometimes subcapitate, septate. Pileipellis an ixocutis; epicutis 70–95 µm thick, tramal hyphae beneath subcutis angular, ellipsoid, sausage-shaped, inflating from septa ≤18 µm diam. Clamp connections occasionally present on cheilocystidia.

Specimen examined—TURKEY, **Hakkâri**, Şemdinli, Derya village, under *Quercus* sp., 37.3383°N 44.5322°E, 1616 m, 15.10.2018, Acar 1132 (VANF1132; GenBank MW544170, MW544171).

Phylogenetic results

Phylogenetic analyses were performed on the ITS dataset comprising 71 sequences, of which six were derived from our Turkish samples and two represented the outgroup. The 5′ and 3′ends were trimmed from the ~680 bp sequence alignment and of the 631 bp included in the final analysis, 130 were variable and 87 parsimony informative. Of the variable sites, the ITS1 possessed 72, the 5.8S gene only one, and the ITS2 57. BLAST and UNITE results of ITS sequences indicated 99% identity value for each sample.

Our Bayesian phylogenetic tree (Fig. 4) outlines the phylogenetic relationships and taxonomic positions among the species selected. Our *Hebeloma excedens* samples (VANF1051A,B) clustered with *H. excedens*, *H. mesophaeum*, and *H. subtortum* in *H.* sect. *Hebeloma* with strong support (PP = 0.97). The two *H. excedens* sequences grouped together with a PP = 1 value, expected because no nucleotide variation was observed between them. Differences between our and the database sequences were noted at ITS1 base 150 (C to T) and ITS2 base 530 T to C).

Our *Hebeloma geminatum* (VANF1116A, B) samples grouped closely with the database representatives in *H.* sect. *Denudata* (PP = 1), with *H. geminatum* closely related to *H. alpinum* (J. Favre) Bruchet, *H. aanenii* Beker & al., *H. crustuliniforme* (Bull.) Quél., *H. eburneum* Malençon, *H. salicicola* Beker & al., and *H. minus* Bruchet (Fig. 4). *Hebeloma geminatum* cannot be easily separated from its sister species based on ITS sequence data alone; here morphological characters are helpful. Eberhardt & al. (2015a) observed that a specimen almost certainly represents *H. geminatum* when the average width of the cheilocystidial apex exceeds 9 µm. The average cheilocystidial width in our material was 8–9 µm but its range extending to 11 µm supports its identification as *H. geminatum*.

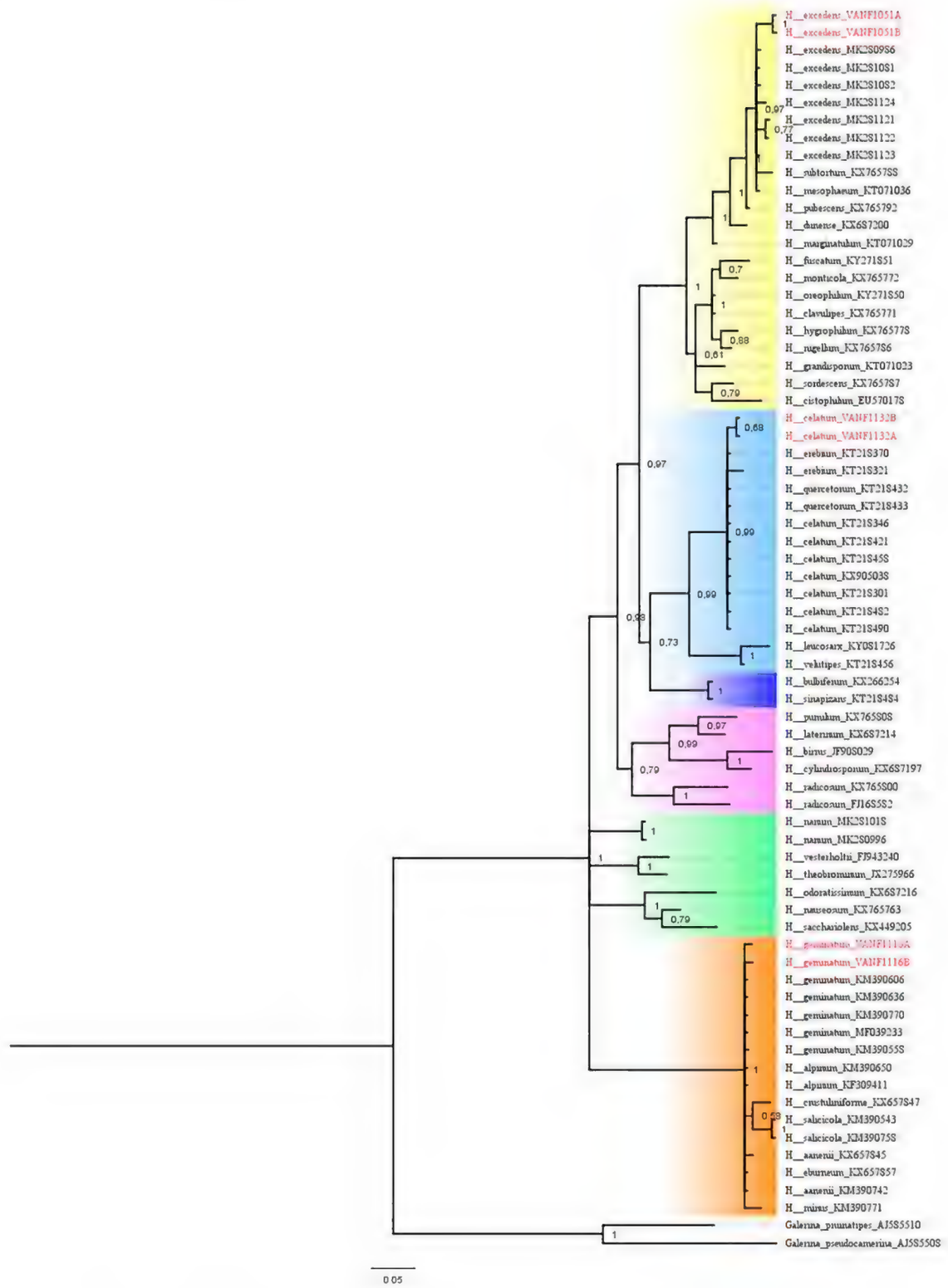

Fig 4. The Bayesian 50% majority rule consensus tree inferred from ITS region. PP> 0.5 are indicated above branches. Sequences from studied specimens are marked with red colour. *Hebeloma* sections are indicated with colours: yellow = *Hebeloma*, pale blue = *Velutipes*, dark blue = *Sinapizantia*, pink = *Scabrispora* & *Myxocybe*, green = *Sacchariolentia* & *Theobromina*, and orange = *Denudata*. Topology is rooted with *Galerina pseudocamerina* and *G. pruinatipes*.

Our *Hebeloma celatum* sequences (VANF1132A, B) clustered in *H.* sect. *Velutipes* (PP = 0.99) with *H. celatum, H. erebium* (Huijsman) Beker & U. Eberh., and *H. quercetorum* Quadr. (Fig. 4). This close phylogenetic relationship can be expected since these species are also morphologically very similar. Our *H. celatum* sequences were phylogenetically separated from representatives retrieved from the database due to nucleotide variations observed at base 497 (A to G).

Discussion

Hebeloma excedens and *Hebeloma geminatum* are recorded for the first time from Turkey, and *Hebeloma celatum,* previously reported for Turkey by Grilli & al. (2015), is confirmed for the country.

Hebeloma excedens and *H. mesophaeum* are not easily separated from each other because of their close morphological and ecological similarities. Nonetheless, the differences in pileus morphology are useful for distinguishing the species. The pileus of *H. excedens* is less yellow brown overall and less brown at the disc, and its margin extends over the lamellae. Also, *H. excedens* has fibrils on the stipe surface that are not observed in *H. mesophaeum* (Cripps & al. 2019, Beker & al. 2016). Our *H. excedens* material produced evenly coloured basidiomes that are more slender than customary for *H. mesophaeum* and cheilocystidia that are generally swollen at the base. Molecular data also supported subtle differences between the two species. Nucleotide variations observed at bases 453 (A to G) and 512 (C to T) support the two species as independent.

Hebeloma geminatum can be confused with *H. alpinum* and *H. aanenii.* Morphologically, the easiest way to separate *H. geminatum* from close relatives is through basidiospore and cheilocystidial comparison (Eberhardt & al. 2015a). The average basidiospore dimensions cited for *H geminatum* is <11 µm long and 6 µm diam. The basidiospores in our collections of *H. geminatum* measured 10–11.8 × 5.5–6.5 µm, while the cheilocystidia were generally swollen in the lower half but appeared spathulate. Eberhardt & al. (2015a) noted that they regarded specimens with cheilocystidial apices with an average width >9 µm to represent *H. geminatum;* our cheilocystidia measured ≤11 µm at the apex, meeting their morphological criterion. Molecular data supported this morphological identification, with nucleotide variations at bases 140 (G to A), 220 (indel), 562 (A to G) and 565 (G to A) bases separating *H. geminatum* from two close relatives.

Grilli & al. (2015) selected a large number of collections from throughout Europe to infer species diversity and evolutionary history in the two main *Hebeloma* sections, *Sinapizantia* and *Velutipes*. They included one *H. celatum* sample (KT218421) collected from Turkey in 2008 in their study, but as there was no mention of *H. celatum* in the Turkish mycobiota since then, we reevaluated *H. celatum* through morphological comparisons and molecular analyses. *Hebeloma celatum,* which produces mature basidiomes that greatly resemble those of *H. erebium* and *H. quercetorum,* can be distinguished by its floccose stem and raphanoid odor. More robust basidiomes with larger stipes help separate *H. celatum* from *H. erebium* (Grilli & al. 2015, Cripps & al. 2019), and the Turkish *H. celatum* specimens were robust. Likewise, the clearly clavate and sometimes subcapitate cheilocystidia distinguish our *H. celatum* from *H. quercetorum,* which is characterized by more regularly ventricose to cylindrical cheilocystidia. *Hebeloma celatum* associates with a variety of trees, among which the most commonly recorded is *Quercus* (Cripps & al. 2019); our specimens from Turkey were associated with *Quercus* species. Sequence variations at bases 140 (A to G) and 475 (A to G) also support separation of *H. celatum* from its two close relatives.

The above data well illustrate that macrofungal molecular analyses aid species identification and that the ITS region is particularly helpful in understanding the taxonomy and phylogeny of *Hebeloma.* Two *Hebeloma* species, *Hebeloma excedens* and *H. geminatum,* have been recorded as new for Turkey, increasing and the total species from twenty-eight to thirty. Moreover, our research confirmed the presence of *H. celatum* in Turkey.

Acknowledgements

This study was financially supported by Van Yüzüncü Yıl University (Scientific Research Project Foundation, FBA-2017-6132), Van, Turkey. We thank the Editor-in Chief Lorelei L. Norvell and Nomenclature Editor Shaun R. Pennycook for their critical reading and corrections. We also thank the pre-submission reviewers Dr Abdullah Kaya (Gazi University, Ankara, Turkey) and Dr Mustafa Emre Akçay (Van Yüzüncü Yıl University, Van, Turkey) for their valuable suggestions.

Literature cited

Aanen DK, Kuyper TW, Boekhout T, Hoekstra RF. 2000. Phylogenetic relationships in the genus *Hebeloma* based on ITS1 and 2 sequences, with special emphasis on the *Hebeloma crustuliniforme* complex. Mycologia 92: 269–281. https://doi.org/10.1080/00275514.2000.12061154

Aanen DK, Kuyper TW, Hoekstra RF. 2001. A widely distributed ITS polymorphism within a biological species of the ectomycorrhizal fungus *Hebeloma velutipes*. Mycological Research 105: 284–290. https://doi.org/10.1017/s0953756201003628

Beker HJ, Eberhardt U, Vesterholt J. 2016. *Hebeloma* (Fr.) P. Kumm. Fungi Europaei 14. Edizioni Technografica. 1218 p.

Cripps CL, Eberhardt U, Schütz N, Beker HJ, Evenson VS, Horak E. 2019. The genus *Hebeloma* in the Rocky Mountain Alpine Zone. MycoKeys 46: 1–54. https://doi.org/10.3897/mycokeys.46.32823

Dizkirici A, Acar A, Kalmer A, Uzun Y. 2019. Morphological and molecular characterization of *Hebeloma subtortum* (*Hymenogastraceae*), a new record macrofungus from Bingöl province, Turkey. Kastamonu Univ., Journal of Forestry Faculty 19(1): 1–10. https://doi.org/10.17475/kastorman.543375

Doğan HH, Kurt F. 2016. New macrofungi records from Turkey and macrofungal diversity of Pozantı-Adana. Turkish Journal of Botany. 40: 209–217. https://doi.org/10.3906/bot-1501-22.

Doyle JJ, Doyle JL. 1987. A rapid DNA isolation procedure for small quantities of fresh leaf tissue. Phytochemical Bulletin 19: 11–15.

Eberhardt U, Beker HJ, Vesterholt J, Dukik K, Walther G, Vila J, Fernández Brime S. 2012. European species of *Hebeloma* section *Theobromina*. Fungal Diversity 58(1): 103–126. https://doi.org/10.1007/s13225-012-0188-3

Eberhardt U, Beker HJ, Vesterholt J. 2015a. Decrypting the *Hebeloma crustuliniforme* complex: European species of *Hebeloma* section *Denudata* subsection *Denudata* (*Agaricales*). Persoonia 35: 101–147. https://doi.org/10.3767/003158515x687704

Eberhardt U, Ronikier A, Schütz N, Beker HJ. 2015b. The genus *Hebeloma* in the alpine belt of the Carpathians including two new species. Mycologia 107(6): 1285–1303. https://doi.org/10.3852/15-097

Grilli E, Beker HJ, Eberhardt U, Schütz N, Leonardi M, Vizzini A. 2015 ["2016"]. Unexpected species diversity and contrasting evolutionary hypotheses in *Hebeloma* (*Agaricales*) sections *Sinapizantia* and *Velutipes* in Europe. Mycological Progress 15(5): [46 p.]. https://doi.org/10.1007/s11557-015-1148-6

Güngör H, Solak MH, Allı H, Işıloğlu M, Kalmış E. 2015. New records for Turkey and contributions to the macrofungal diversity of Isparta Province. Turkish Journal of Botany 39: 867–877. https://doi.org/10.3906/bot-1406-28

Rambaut A. 2010. FigTree v1.3.1. Institute of Evolutionary Biology, University of Edinburgh, Edinburgh.

Ronquist F, Teslenko M, Mark PVD, Ayres DL. 2012. MrBayes 3.2: efficient Bayesian phylogenetic inference and model choice across a large model space. Systematic Biology 61: 539–542. https://doi.org/10.1093/sysbio/sys029

Sesli E, Denchev CM. 2014. Checklists of the myxomycetes, larger ascomycetes, and larger basidiomycetes in Turkey. 6th edn. Mycotaxon Checklists Online. 136 p. (http://www.mycotaxon.com/resources/checkl ists/sesli-v106-checklist.pdf).

Sesli E, Contu M, Vila J, Moreau PA, Battistin E. 2015. Taxonomic studies on some agaricoid and boletoid fungi of Turkey. Turkish Journal of Botany 39: 134–146. https://doi.org/10.3906/bot-1403-63.

Sesli E, Örtücü S, Aytaç E. 2018. Türkiye mikotası için yeni kayıtlar (*Basidiomycota Agaricales*). Bağbahçe Bilim Dergisi5(1): 15–20.

Solak MH, Işıloğlu M, Kalmış E, Allı H. 2015. Macrofungi of Turkey checklist (2nd ed.) Üniversiteliler Ofset, İzmir.

Tamura K, Stecher G, Peterson D, Filipski AM, Kumar S. 2013. MEGA 6: molecular evolutionary genetics analysis, version 6.0. Molecular Biology and Evolution 30(12): 2725–2729. https://doi.org/10.1093/molbev/mst197

Vesterholt J. 2005. The genus *Hebeloma*. Fungi of Northern Europe. Vol. 3. Svampetryk, Tilst, Denmark. 146 p.

Vesterholt J, Eberhardt U, Beker HJ. 2014. Epitypification of *Hebeloma crustuliniforme*. Mycological Progress 13: 553–562. https://doi.org/10.1007/s11557-013-0938-y

Wen J, Zimmer EA. 1996. Phylogeny and biogeography of *Panax* L. (the ginseng genus, *Araliaceae*): inferences from ITS sequences of nuclear ribosomal DNA. Molecular Phylogenetics and Evolution 6: 167–177. https://doi.org/10.1006/mpev.1996.0069

Yang Z, Rannala B. 1997. Bayesian phylogenetic inference using DNA sequences: a Markov chain Monte Carlo method. Molecular Biology and Evolution 14: 717–724. https://doi.org/10.1093/oxfordjournals.molbev.a025811

MYCOTAXON

ISSN (print) 0093-4666 (online) 2154-8889 Mycotaxon, Ltd. ©2022

January–March 2022—Volume 137, pp. 135–151

https://doi.org/10.5248/137.135

Ganoderma multipileum and *Tomophagus cattienensis*—new records from Pakistan

Aisha Umar[1]*, Shakil Ahmed[1],
Laura Guzmán-Dávalos[2], Milay Cabarroi-Hernández[2]*

[1] *Department of Botany, University of the Punjab, Quaid-e-Azam Campus, Lahore, Pakistan*

[2] *Department of Botany and Zoology, University of Guadalajara, Apdo. Postal 1–139, Zapopan, Jal., C.P. 45147, Mexico*

* Correspondence to: *ash.dr88@gmail.com cabarroi80@gmail.com*

Abstract—New records of *Ganoderma multipileum* and *Tomophagus cattienensis* collected from Changa Manga Forest and Lahore, Pakistan, are presented based on morphological and nuclear rDNA ITS sequence data from fresh basidiomata. Specimens previously treated as *G. lucidum* from Pakistan were reviewed and found to represent different species, among them *G. multipileum*. Specimens of *T. cattienensis* determined for the first time from Pakistan presented morphological features similar to *T. colossus* but corresponded molecularly to *T. cattienensis;* the morphological description for *T. cattienensis* is expanded accordingly.

Key words—*Ganodermataceae,* morphology, Punjab, taxonomy

Introduction

Ganodermataceae, a monophyletic polypore family with ganodermatoid basidiospores (Costa-Rezende & al. 2020) previously included in *Polyporaceae* (Justo & al. 2017, He & al. 2019), is characterized by its shelf-like basidiomes, poroid hymenophores, and complex-walled basidiospores. *Amauroderma* Murrill, *Amaurodermellus* Costa-Rezende & al., *Cristataspora* Robledo & Costa-Rezende, *Foraminispora* Robledo & al., *Furtadoa* Costa-Rezende & al., *Ganoderma* P. Karst., *Haddowia* Steyaert, *Humphreya* Steyaert, and *Tomophagus* Murrill are some genera currently included in *Ganodermataceae* (Murrill 1905; Moncalvo 1996; Moncalvo &

Ryvarden 1997; Ryvarden 2004; Kirk & al. 2008; Costa-Rezende & al. 2017, 2020).

Several species of fungi with ganodermatoid basidiospores (specifically in *Ganoderma*) have been used as medicine in Asia for more than 2000 years where they have been cultivated on an industrial scale (Wasser & Weis 1997). Despite of their significance, this group of fungi remains poorly studied in many regions of the world such as in Pakistan, where *Ganoderma ahmadii* Steyaert, *G. applanatum* (Pers.) Pat., *G. australe* (Fr.) Pat., *G. boninense* Pat., *G. chalceum* (Cooke) Steyaert, *G. curtisii* (Berk.) Murrill, *G. flexipes* Pat., *G. lipsiense* (Batsch) G.F. Atk., *G. lucidum* (Curtis) P. Karst., *G. perzonatum* Murrill, *G. philippii* (Sacc.) Bres., *G. praelongum* Murrill, *G. multicornum* Ryvarden, *G. multiplicatum* (Mont.) Pat., *G. resinaceum* Boud., *G. tornatum* (Pers.) Bres., *G. tsugae* Murrill, and *Tomophagus colossus* (Fr.) Murrill [≡ *G. colossus* (Fr.) C.F. Baker] have been recorded (Ahmad 1956, 1972, Steyaert 1972, Irshad & al. 2012, Fakhar-ud-Din & Mukhtar 2019). These species were determined primarily based on morphological concepts; however, there is much uncertainty regarding which morphological criteria should be used to assign species to *Ganodermataceae* and specifically to *Ganoderma* (Moncalvo & Ryvarden 1997, Welti & Courtecuisse 2010).

Clarification on the placement of species in *Ganoderma* or related genera is essential, not only for taxonomic reasons, but also to investigate the economical and pharmacological importance of the species that actually grow in the tropics. The aim of this study was to use morphological and molecular analyses to show that some specimens previously identified as *G. lucidum* in Pakistan actually represent *G. multipileum*, reported here as a first record for the country. We also report *Tomophagus cattienensis* from Pakistan for the first time.

Materials & methods

Collections & ecology

Fungal specimens were collected in Punjab, Pakistan, during 2018 by the first author and deposited in the Herbarium of the Institute of Botany, University of the Punjab, Lahore, Pakistan (LAH). The material was collected in [1] Changa Manga Forest in the Kasur District, dominated by *Dalbergia sissoo* DC. and *Vachellia nilotica* (L.) P.J.H. Hurter & Mabb. (*Fabaceae*) and with an average annual rainfall of 1232 mm and average 24 °C temperature (Ahmad & al. 2014) and [2] the New Campus, University of the Punjab in Lahore, covered by *D. sissoo* with many rotting trunks and with an average annual rainfall of 607 mm and average 24 °C temperature (Shirazi & al. 2019). Additionally, a specimen from XAL was re-examined.

Table 1. Sequences of *Ganoderma*, *Tomophagus*, and *Perenniporiella* outgroup included in the analyses. [T] ex-type sequences.

Species	Voucher/strain	Locality	GenBank ITS1/ITS2	Reference
G. ahmadii	FWP 14329 [T]	Pakistan	Z37047/ Z37098	Moncalvo & al. 1995
G. curtisii	CBS 100132	USA	JQ781848	Cao & al. 2012
	UMNGA1	USA	MG654117	Loyd & al. 2018
G. leucocontextum	AY2B	Pakistan	MN134012	Unpublished
	GDGM 40400 [T]	China	KF011548	Li & al. 2015
G. lingzhi	Cui 9166(67)	China	MH109560	Unpublished
	Dai 12574	China	KJ143908	Zhou & al. 2015
G. lucidum	K 175217	UK	KJ14391	Zhou & al. 2015
	MUCL 35119	France	MK554779	Cabarroi-Hernández & al. 2019
	CWN01740	Taiwan	EU021461	Wang & al. 2009
	BCRC36123	India	EU021459	Wang & al. 2009
G. martinicense	LIP SW-Mart08-44/ MUCL:GSP44	Martinique	KF963257	Welti & al. 2015
	LIP SW-Mart08-55/ MUCL:GSP55 [T]	Martinique	KF963256	Welti & al. 2015
G. mizoramense	UMN-MZ5	India	KY643751	Crous & al. 2017
	UMN-MZ4	India	KY643750	Crous & al. 2017
G. multipileum	CM10	Pakistan	MW349830	This study
	CM110	Pakistan	MW349829	This study
	CWN 04670	China	KJ143913	Zhou & al. 2015
	Dai 9447	China	KJ143914	Zhou & al. 2015
	HMAS242384	China	JF915409	Wang & al. 2012
G. multiplicatum	MN14091107	Myanmar	MK345439	Hapuarachchi & al. 2019
	Dai 13710	China	KU572489	Unpublished
	Dai 12320	China	K00U572490	Unpublished
	JFL 10004081328	China	MH106879	Hapuarachchi & al. 2018
	SPC9	Brazil	KU569553	Bolaños & al. 2016
	SPC5	Brazil	KU569549	Bolaños & al. 2016
G. parvulum	MUCL 47096	Cuba	MK554783	Cabarroi-Hernández & al. 2019
	MUCL 53123	French Guiana	MK531814	Cabarro0i-Hernández & al. 2019
	URM80765	Brazil	JX310822	De Lima Jr & al. 2014
	URM2948	Brazil	JX310821	De Lima Jr & al. 2014

Species	Voucher/strain	Locality	GenBank ITS1/ITS2	Reference
G. resinaceum	CBS 194.76	Netherlan0ds	KJ143916	Zhou & al. 2015
	MUCL 52253	France	MK554786	Cabarroi-Hernández & al. 2019
G. sichuanense	HMAS251146	China	JF915401	Wang & al. 2012
G. valesiacum	CBS 282.33	UK	Z37081/ Z37056	Moncalvo & al. 1995
Ganoderma sp.	AU-2019a/HP12	Pakistan	MN006955	Unpublished
P. chaquenia	MUCL 47648	Argentina	FJ411084	Robledo & al. 2009
P. pendula	MUCL 47129	Cuba	FJ411082	Robledo & al. 2009
T. cattienensis	CATPU120	Pakistan	MW737424	This study
	CATPU121	Pakistan	MW737425	This study
	CT119	Vietnam	JN184398	Le & al. 2012
	CT99 [T]	Vietnam	JN184397	Le & al. 2012
T. colossus	255FL	USA	MG654427	Loyd & al. 2018
	CGMCC5.763	Philippines	JQ081068	Wang & al. 2012
	UMNFL151	USA	MG654431	Loyd & al. 2018
	URM80450	Brazil	JX310825	De Lima Jr & al. 2014
	URM83330	Brazil	JQ618247	De Lima Jr & al. 2014
	TC-02	Vietnam	KJ143923	Zhou & al. 2015
Tomophagus sp.	BAB-4989	India	KR155077	Unpublished
	AUMC 14536	Egypt	MW186858	Unpublished

Morphology

Size, shape, and color of basidiomata were noted from fresh material. Color descriptions follow Munsell (1975). For microscopical analyses, basidiome cross sections were soaked in 3% KOH, stained with 1% Congo red, and examined under 100× magnification using a Meiji MX4300H compound light microscope. At least 30 basidiospore measurements (face and side view, excluding the apical umbo) were recorded and rounded to the nearest 0.5 µm; dimensions are presented as length × width (Nagy & al. 2010). Microscopical terms follow, in part, Torres-Torres & Guzmán-Dávalos (2012). Color descriptions follow Munsell (1975).

DNA extraction, amplification, and sequencing

Total genomic DNA was extracted from dried specimens following a modified CTAB procedure (Doyle & Doyle 1987). The ITS1+5.8S+ITS2 rDNA region (ITS) was amplified using primers ITS1 & ITS2 (White & al. 1990). Reaction mixtures (20 µl) containing 0.5 µl template DNA, 8.5 ml distilled water, 0.5 µl of each primer, and 10 ml DreamTaqGreen PCR Master Mix (2 X) ran 35 cycles of 95 °C for 30 s, 52 °C for 30 s, and 72 °C for 1 min, followed by a final extension at 72 °C for 10 min. The PCR amplicons were purified and sequenced by Tsingke Co. Ltd. (Tianjin, China)

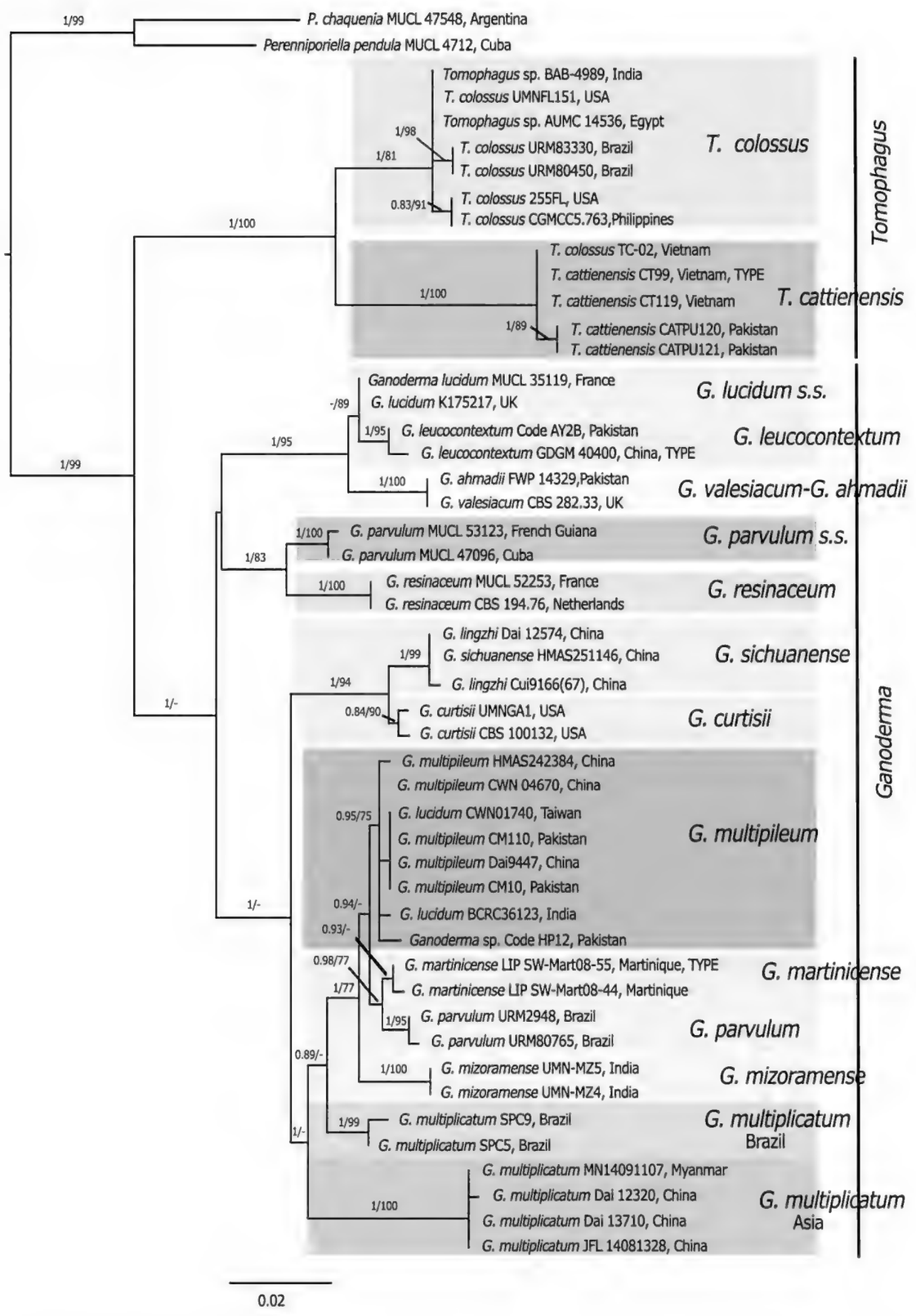

FIG. 1. Phylogenetic tree of *Ganoderma* and *Tomophagus* based on ITS rDNA sequences generated by maximum likelihood. *Perenniporiella pendula* and *P. chaquenia* were chosen as outgroup. Posterior probabilities (>0.85) and bootstrap values (>75%) are shown at the branches.

Phylogenetic analysis

The data set comprised four DNA sequences from Pakistani material and 45 ITS sequences downloaded from GenBank (www.ncbi.nlm.nih.gov/genbank/) (Table 1). The ITS data set was subdivided into three parts: ITS1, 5.8S, and ITS2. *Perenniporiella chaquenia* Robledo & Decock and *P. pendula* Decock & Ryvarden were selected as outgroup (Costa-Rezende & al. 2017).

All sequences were automatically aligned with MUSCLE (Edgar 2004) and manually adjusted using PhyDe® (Müller & al. 2010). JModelTest (Posada & Crandall 1998) was used to determine the best evolutionary model using the corrected Akaike information criterion (AICc). Maximum Likelihood (ML) analyses were conducted using RAxML 7.0.4 (Stamatakis 2006) and Bayesian Inference (BI) analyses were conducted using MrBayes v.3.2.2 (Ronquist & Huelsenbeck 2003). In the ML analysis, the default priors were used, performing 1000 replicates under the GTRGAMMA model. BI analyses were run on CIPRES Science Gateway (Miller & al. 2010). Two independent runs, with 2,000,000 generations each, were carried out with a sampling frequency every 1000 generations and a burn-in of 25%. A 50% majority rule consensus tree with posterior probabilities (PP) was obtained. Convergence of the Markov chains to a stationary distribution was assessed by visual examination of the log likelihood values in the program Tracer v1.7.1 (Rambaut & al. 2018). Nodes were considered supported when bootstrap values (BS) were ≥75% and the PP was ≥0.85. The final alignments were deposited in TreeBASE (www.treebase.org).

Phylogenetic results

The evolutionary models that best fit the individual dataset according to the AICc were ITS1 = GTR+G, 5.8S = K80, ITS2 = GTR+G. In BI analyses, the average standard deviation of split frequencies was 0.007460. Phylogenetic analysis of the ITS region indicated that our specimens represent *Ganoderma multipileum* and *Tomophagus cattienensis* (Fig. 1). All sequences of *G. multipileum*, including the Pakistani collections CM10 and CM110, are supported in one clade (PP = 0.95; BS = 75%). This clade, which included sequences of specimens from China, India, and Taiwan, also clustered with sequences from "*G. lucidum*" specimens and formed a sister group with *G. martinicense* Welti & Courtec. and *G. parvulum* Murrill (0.94 PP; 68% BS). The other two Pakistani sequences (from CATPU120 and CATPU121) clustered in the strongly supported *Tomophagus* group (PP = 1; BS = 100). The Pakistani sequences and the holotype of *T. cattienensis* (CT99) formed a monophyletic group with another *T. cattienensis* sequence from Vietnam and sequence TC–02 (as *T. colossus*, surely a misdetermination), also from Vietnam.

Taxonomy

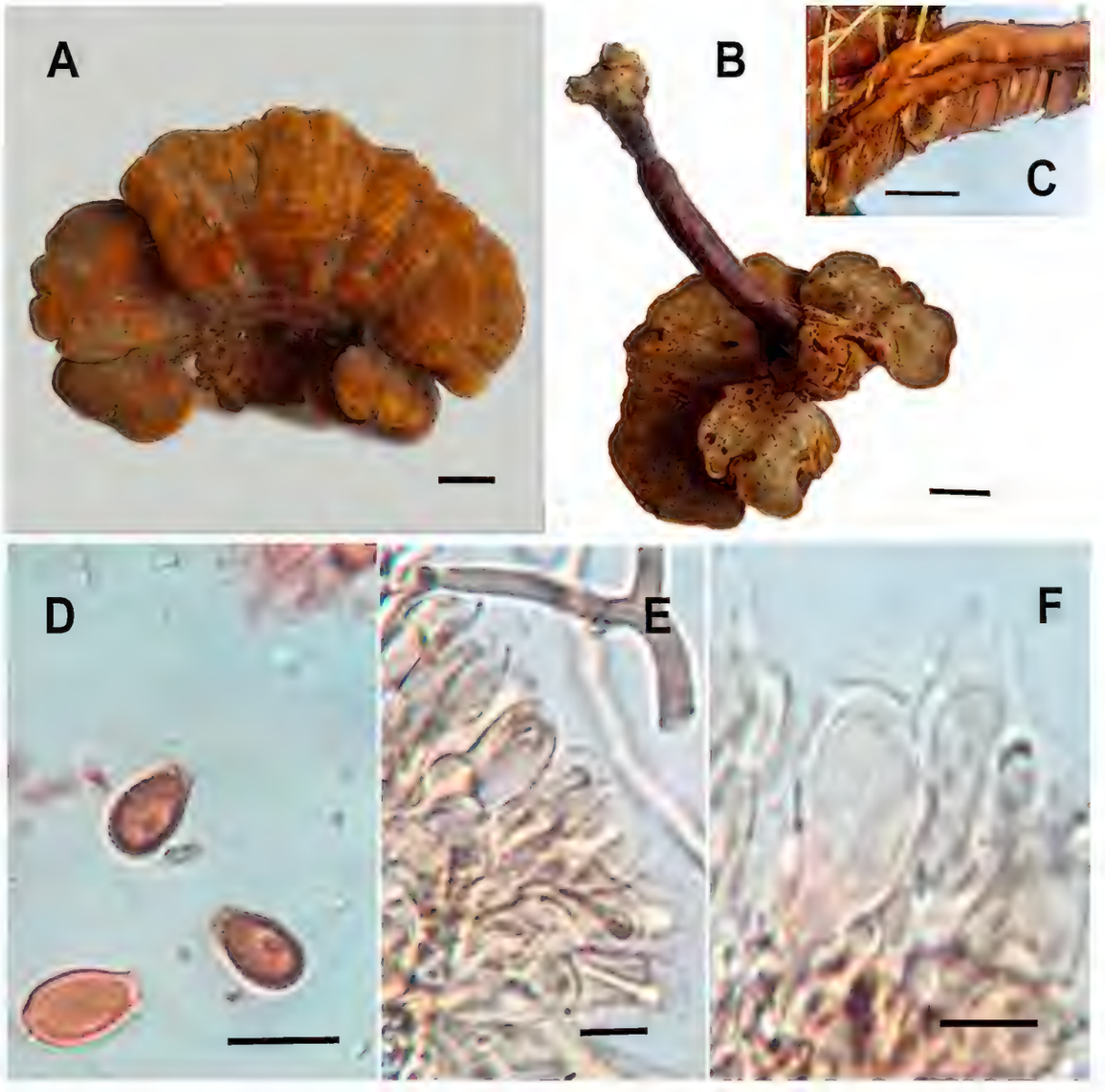

Fig. 2. ***Ganoderma multipileum*** (LAH36825). A. Pileus; B. Pore surface and stipe; C. Section of context and tubes; D. Basidiospores; E. Cells of crustohymeniderm; F. Basidium. Scale bars: A–C = 2 cm; D–F = 10 μm.

Ganoderma multipileum Ding Hou [as *'multipilea'*],
Quart. J. Taiwan Mus. 3: 101 (1950) Fig. 2

Basidiomata annual; stipitate, solitary, single or with a group of 3–4 pilei growing from the same stipe, light in weight, corky. Pileus projecting ≤12 cm, 12.2 cm wide, and ≤2.9 cm thick at the base; reniform, dimidiate to flabelliform, laccate, sulcate, with concentric growing zones; crust thin, yellowish brown (2.5YR4/8) to brown (10R4/6); margin 0.2–0.3 cm thick, entire, obtuse, orange-brown (10YR6/8) to brown (5YR 5/8). Stipe 9–9.6 ×

3–4.1 cm, sub-cylindrical, eccentric to lateral, strongly laccate, woody, maroon-brown (2.5YR3/6). Pores 6–7 per mm, 110–140 µm diam., sub-round to round, straw cream (7.5YR8/4) to brown when bruised (2.5YR4/6). Tubes ≤1.3 cm long, brown (10YR4/6) to pale brown (2.5YR 8/4). Context ≤1.7 cm thick, with concentric growth zones, brown (7.5YR6/8) to yellowish-brown (5YR 5/8), with melanoid incrustations.

Hyphal system dimitic: 1) generative hyphae 3.5–5 µm diam., thin-walled, hyaline, clamped; 2) arboriform skeleto-binding hyphae 2.5–7 µm diam., thick-walled, red-brown to yellow brown. Pileipellis a crustohymeniderm; cells 15–60 × 4.5–12.5 µm, clavate, thick-walled. Basidia 20.5–29 × 5.5–8.5 µm, claviform, hyaline. Basidiospores 8.0–13.2 × 5.5–7.4 µm, ellipsoid to ovoid, apex truncate, brown, double walled with endosporic ornamentation as solid, thin, free pillars or column-like projections.

Specimens examined—**PAKISTAN, Punjab, Kasur district**, Changa Manga Forest, 31.05°N 73.4072°E, 200 m a.s.l., gregarious on decayed hardwood, *Dalbergia sissoo* and *Vachellia nilotica*, 10 July 2018, Aisha Umar CM10 (LAH36826, GenBank MW349830). **Lahore district**, Lahore, New Campus, University of the Punjab, 31.4981°N 73.3044°E, 217 m a.s.l., gregarious on hardwood, on living tree trunk of *V. nilotica*, 10 April 2018, Aisha Umar CM110 (LAH36825, GenBank MW349829).

Distribution: China, India, Nepal, Pakistan, Philippines, Taiwan, Thailand.

Tomophagus cattienensis X.T. Le & Moncalvo,
Mycol. Prog. 11: 777 (2012) Fig. 3a–e

Basidiomata annual, sessile, bulky, light in weight, spongy. Pileus projecting ≤9.2 cm, 10.2 cm wide, and ≤7.8 cm thick at the base, dimidiate to flabelliform, laccate, surface friable, rugose, golden (10YR7/8), yellow-brown (10YR8/8), orange-brown (10YR6/8), colors patchy and not on a gradient; margin 3.4–4 cm, very thick, entire to lobulated, obtuse, rugose, whitish, white creamy (10YR8/3) to pale yellow brown (10YR7/6). Pores 2–3 (–4) per mm, angular to round, creamy (7.7YR8/4) to brown (10YR3/4) when bruised. Tubes 0.9–1.2 cm long., golden yellow (10YR7/8). Context 3.8–7.6 cm thick, thick at the base, homogeneous, light, soft, creamy white (2.5YR8/4) when fresh to pale brown (10YR4/6) when dry, powdery.

Hyphal system dimitic: 1) generative hyphae 2.5–3 µm diam., thin-walled, clamped, hyaline; 2) skeletal hyphae 2–3 µm diam., thick-walled, hyaline. Pileipellis a crustohymeniderm; cells 40–80 × 7–15 µm, narrowly clavate, thick-walled, apically ornamented. Chlamydospores 22–24.5 µm diam., globose, double walled, endosporic ornamentation with thick cylindrical projections, yellowish brown. Basidia not seen. Basidiospores

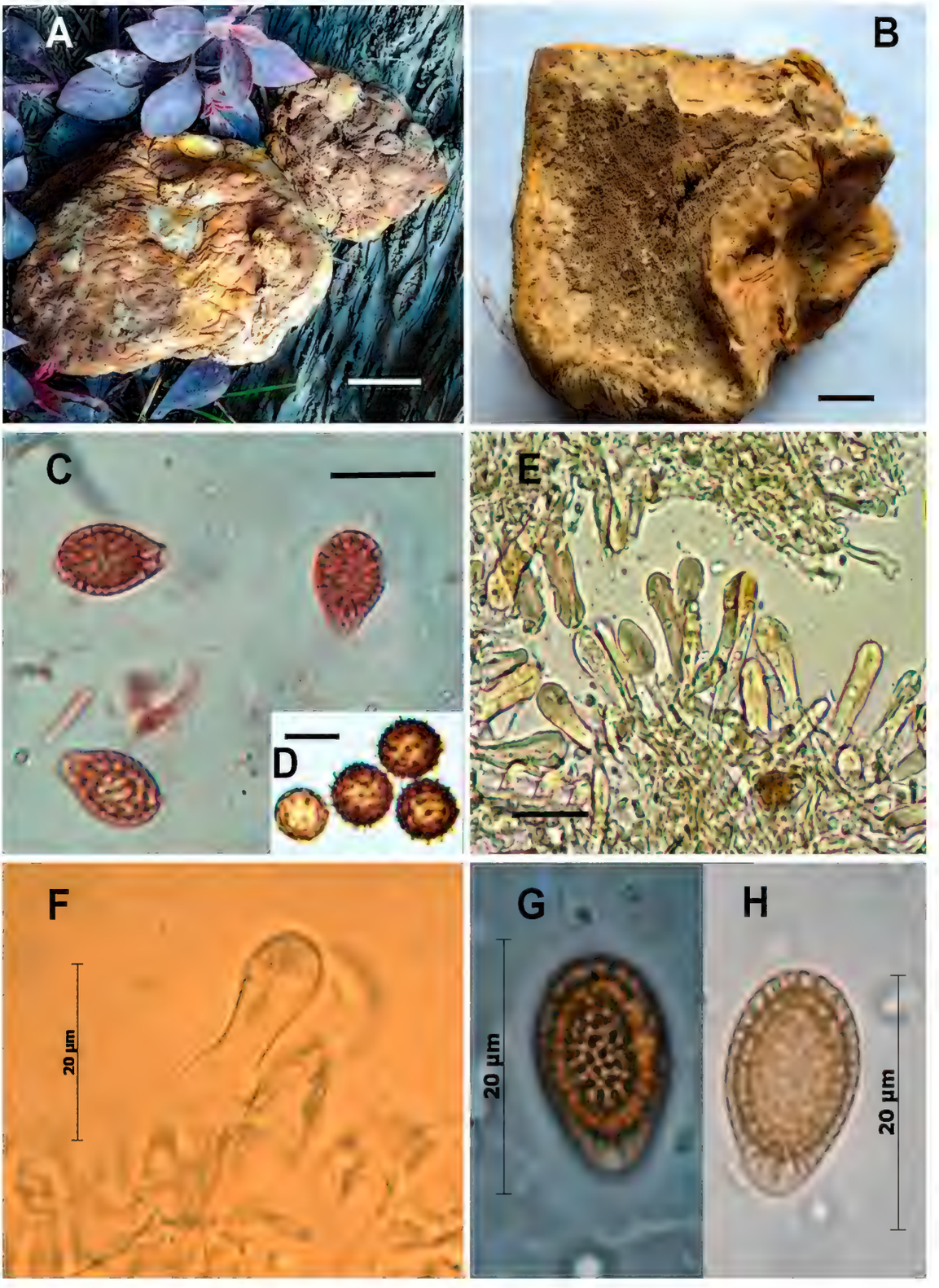

Fig. 3. ***Tomophagus cattienensis*** (LAH36830). A. Pileus; B. Pore surface and context; C. Basidiospores; D. Chlamydospores; E. Crustohymeniderm cells. ***Tomophagus colossus*** (XAL-Guzmán 35708). F. Crustohymeniderm cell; G, H. Basidiospores. Scale bars: A = 2 cm; B = 1 cm; C, D = 20 µm.

17.4–21.3 × 11.3–14.6 µm, ellipsoid to ovoid, apex acute or subacute, or when collapsed then shortly truncated or even concave, reddish brown, double-walled with endosporic ornamentation as thick, partially reticulate pillars, apex hyaline.

Specimens examined—**PAKISTAN, Punjab, Lahore district**, Lahore, New Campus, University of the Punjab, 31.4981°N 73.3044°E, 217 m a.s.l., gregarious on hardwood, on living tree trunk of *Dalbergia sissoo*, 10 April 2018, Aisha Umar CATPU120 (LAH36830, GenBank MW737424). **Kasur district**, Changa Manga Forest, 31.05°N 73.4072°E, 200 m a.s.l., gregarious on decayed hardwood, *Vachellia nilotica*, 10 July 2018, Aisha Umar CATPU121 (LAH36839, GenBank MW737425).

Distribution: Pakistan, Vietnam.

Additional specimen examined (Fig. 3f–h)—***Tomophagus colossus***: **MEXICO, Veracruz,** Guzmán 35708 (XAL) [as *Ganoderma* "*colossum*"].

Discussion

Our morphological and molecular analyses confirm the presence of two polypores of *Ganodermataceae* from Pakistan: *Ganoderma multipileum* and *Tomophagus cattienensis*.

For many years, the name *Ganoderma lucidum* has been misapplied to *Ganoderma* specimens from tropical Asia that represent other species (Wang & al. 2009, Hennicke & al. 2016, Raja & al. 2017). Collections labeled as '*G. lucidum*' from world regions outside Europe (where *G. lucidum* was described) have appeared in several different lineages in numerous phylogenetic analyses (Moncalvo & al. 1995, Gottlieb & al. 2000, Smith & Sivasithamparam 2000, Hong & Jung 2004). *Ganoderma multipileum* is one species confused with *G. lucidum* that is now recognized as representing a different species (Wang & al. 2009) first described over a half century ago by Hou (1950).

Loyd & al. (2018) showed that the "multipileum clade" is sister to the "curtisii clade," with the "multipileum clade" split into two subclades, one clustering specimens of *G. multipileum* from China and the other clustering specimens of *G. martinicense* from Martinique (type specimen) and from North America. *Ganoderma multipileum,* originally described from Taiwan (Wang & al. 2009), has been recorded from India, China, Nepal, and Philippines (Wang & al. 2012, Fryssouli & al. 2020). Welti & Courtecuisse (2010) suggested that *G. martinicense* might represent a "vicariant from the Caribbean area" of *G. multipileum*. Our phylogeny, although based on a single DNA marker, agrees with that of Loyd & al. (2018) based on four markers and supports a relationship between *G. multipileum* and *G. martinicense*.

However, our phylogeny also includes two sequences of *G. parvulum* (De Lima Jr & al. 2014) as sister taxon of *G. martinicense*. Cabarroi-Hernández & al. (2019) suggested that the sequences of *G. parvulum* sensu De Lima Jr. & al. (2014) might represent *G. bibadiostriatum* Steyaert, a species described from Nicaragua (Steyaert 1962) and phylogenetically unrelated to *G. parvulum* s.str. (Cabarroi-Hernández & al. 2019).

Our "multipileum clade" comprises sequences of specimens from China, India, and Taiwan and CM10 and CM110 (previously labeled *G. lucidum*) from Pakistan. The clade also includes the sequences BCRC36123 from India and CWN01740 from Taiwan, both referenced at GenBank as *G. lucidum* but identified as *G. multipileum* by Wang & al. (2009), as well as the sequence Code HP12 referenced at GenBank as *Ganoderma* sp. from Pakistan (very probably representing *G. multipileum*). The ITS tree corroborates our morphology-based identification and supports extending the distribution of *G. multipileum* to Pakistan. Furthermore, we suggest that *G. lucidum* s.str. is not present in that country.

Wang & al. (2009) concluded that, based on morphological characters and their ITS phylogeny, "*G. lucidum*" from tropical Asia is divided into two clades, both of separated from the European *G. lucidum* s.str. One clade contained tropical collections (labeled *G. multipileum*) while a second "unknown" clade clustered specimens from China and Japan (Wang & al. 2009). Wang & al. (2012) later recognized the "unknown" clade as *G. sichuanense* J.D. Zhao & X.Q. Zhang, while Cao & al. (2012) noted that *G. multipileum* also occurred in India and the Philippines.

Ganoderma multipileum is recognized morphologically based on three features: basidiomes with pilei or with some stipes and pilei growing together, mostly regular clavate crustohymeniderm cells, and truncated ellipsoid basidiospores with free fine pillars (Wang & al. 2009, Zhou & al. 2015). According to Cao & al. (2012) *G. multipileum* inhabits fabaceous hosts and is distinguished from *G. sichuanense* (as *G. lingzhi* Sheng H. Wu & al.) by its "distinct concentric growth zones in context at maturity, and finely echinulate basidiospores." These primary diagnostic features are also seen in the Pakistani specimens of *G. multipileum* (Fig. 2). Furthermore, our specimens were collected growing gregariously on decayed hardwood of *Dalbergia* and *Vachellia* (*Fabaceae*).

The other Pakistani specimens studied here nested in the *Tomophagus* clade. Murrill (1905), who proposed the genus, characterized *Tomophagus* by its very lightweight basidiome with a pale soft spongy context and a

"labyrinthine" basidiospore surface (Le & al. 2012), as noted in both species covered here (Fig. 3c,g,h). *Tomophagus* was typified by *Polyporus colossus* Fr. (Murrill 1905). Furtado (1962, 1965), who described the neotype specimen as having "*Ganoderma*-type basidiospores," accepted the species as *G. colossus*.

Moncalvo's (2000) phylogeny revealed an unclassified basal group composed of *G. colossus*, *G. tsunodae* (Lloyd) Sacc. & Trotter, and other taxa. Subsequent molecular phylogenetic studies confirmed the genus as a well-established group independent of *Ganoderma* (Hong & Jung 2004, Le & al. 2012, Xing & al. 2018, He & al. 2019, Costa-Rezende et al 2017, 2020).

Tomophagus cattienensis and *T. colossus* have been distinguished primarily by color of the pileal surface and ITS sequence analyses (Le & al. 2012). *Tomophagus cattienensis* was distinguished from *T. colossus* by its "red-brown or red-coffeate" (instead of yellow) pileal surface and by its harder crust and context that "turns pale brown upon drying (instead of remaining creamy white)" (Le & al. 2012). However, Pakistani specimens have yellow, yellow-brown, orange-brown pilei and lighter crusts (somewhat similar to *T. colossus* or intermediate between the two species) whereas the color change of the context agrees with that described for *T. cattienensis* (Fig. 2a). Another character distinguishing *T. cattienensis* and *T. colossus* are the thick-walled crustohymeniderm cells, present in the Pakistani specimens of *T. cattienensis* but not previously described for this species. *Tomophagus colossus* characteristically has thin-walled cuticular cells (Ryvarden 2000) observed in the specimen of *T. colossus* from Mexico (Guzmán 35708, XAL) (Torres-Torres & al. 2015).

Our observations of the Pakistani specimens therefore expand the morphological description of *T. cattienensis*. In our phylogeny, the ITS sequences of the Pakistani specimens showed only one nucleotide difference from ITS sequences of the *T. cattienensis* type specimen in contrast to the six-nucleotide difference with *T. colossus*.

Our phylogeny included sequences labelled *G. multiplicatum* in GenBank, which separated into two different clades. One clade (PP 1/BS 100) clustered specimens from China and Myanmar, and the other (PP 1/BS 99) clustered specimens from Brazil. Morphologically, *G. multiplicatum* is distinguished from *G. multipileum* primarily by its cuticular cells with up to 14 lateral or apical protuberances (Torres-Torres & Guzmán-Dávalos 2012, Bolaños & al. 2016). Originally described from French Guyana, *G. multiplicatum* was subsequently found in other parts of South America, Africa, and Asia (Steyaert 1980, Zhao 1989), including India (Bhosle & al. 2010), Pakistan

(Fakhar-ud-Din & Mukhtar 2019), and Taiwan (Wang & Wu 2008). The Asian specimens identified as *G. multiplicatum* should be re-evaluated and more DNA regions must be included, to define their taxonomical status.

In this study, we combined macro and microscopic morphological characters, ecological aspects, as well as molecular data to determine two species of *Ganodermataceae* from Pakistan. This is the first report of the occurrence of *G. multipileum* and *T. cattienensis* in this country. Our results suggest that some species with ganodermatoid basidiospores previously registered from Pakistan (e.g., *G. ahmadii, G. applanatum, G. australe, G. boninense, G. chalceum, G. curtisii, G. flexipes, G. lipsiense, G. lucidum, G. praelongum, G. multicornum, G. multiplicatum, G. resinaceum, G. tornatum, G. tsugae,* and *T. colossus*) need thorough re-evaluation of both morphology and molecular data before their presence in the country or taxonomic status can be confirmed.

Acknowledgments

The authors thank Mario Rajchenberg (Centro de Investigación y Extensión Forestal Andino Patagónico, Chubut, Argentina) and Gerardo Robledo (Universidad Nacional de Cordoba, Ciudad Universitaria, Argentina) for helpful comments and their pre-submission expert reviews. MCH gratefully acknowledges financial support received from CONACYT, Mexico (Postdoc Scholarship). MCH and LGD thank the University of Guadalajara, Mexico for supporting their research.

Literature cited

Ahmad S. 1956. Fungi of West Pakistan. Biological Society of Pakistan, Monograph no. 1. Lahore, Biological Laboratories, Government College.

Ahmad S. 1972. Basidiomycetes of West Pakistan. Biological Society of Pakistan, Monograph no. 6. Lahore, Biological Laboratories, Government College.

Ahmad SS, Erum S, Khan SM, Nawaz M. 2014. An appraisal of ecological distribution of herbaceous flora at Changa Manga Park Lahore, Pakistan. Pakistan Journal of Botany 46: 19–25.

Bhosle S, Ranadive K, Bapat G, Garad S, Deshpande G, Vaidya J. 2010. Taxonomy and diversity of *Ganoderma* from the western parts of Maharashtra (India). Mycosphere 1: 249–262.

Bolaños AC, Bononi VLR, Gugliotta AM, Muñoz JE. 2016. New records of *Ganoderma multiplicatum* (Mont.) Pat. (*Polyporales*, *Basidiomycota*) from Colombia and its geographic distribution in South America. Check List 12(4): 1948. https://dx.doi.org/10.15560/12.4.1948

Cabarroi-Hernández M, Villalobos-Arámbula AR, Torres-Torres MG, Decock C, Guzmán-Dávalos L. 2019. The *Ganoderma weberianum–resinaceum* lineage: multilocus phylogenetic analysis and morphology confirm *G. mexicanum* and *G. parvulum* in the Neotropics. MycoKeys 59: 95–131. https://doi/10.3897/mycokeys.59.33182

Cao Y, Wu SH, Dai YC. 2012. Species clarification of the prize medicinal *Ganoderma* mushroom "lingzhi". Fungal Diversity 56: 49–62. https://doi.org/10.1007/s13225-012-0178-5

Costa-Rezende DH, Robledo GL, Góes-Neto A, Reck MA, Crespo E, Drechsler-Santos ER. 2017. Morphological reassessment and molecular phylogenetic analyses of *Amauroderma s.lat.* raised new perspectives in the generic classification of the *Ganodermataceae* family. Persoonia 39: 254–269. https://doi.org/10.3767/persoonia.2017.39.10

Costa-Rezende DH, Robledo GL, Drechsler-Santos ER, Glen M, Gates G, & al. 2020. Taxonomy and phylogeny of polypores with ganodermatoid basidiospores (*Ganodermataceae*). Mycological Progress 19: 725–741. https://doi.org//10.1007/s11557-020-01589-1

Crous PW, Wingfield MJ, Burgess TI, Hardy GEStJ, Barber PA, Alvarado P, Barnes C & al. 2017. Fungal Planet description sheets: 558–624. Persoonia 38: 240–384. https://doi.org/10.3767/003158517X698941

De Lima Jr NC, Gibertoni TB, Malosso E. 2014. Delimitation of some neotropical laccate *Ganoderma* (*Ganodermataceae*): molecular phylogeny and morphology. Revista de Biología Tropical 62: 1197–1208. https://doi.org/10.15517/RBT.V62I3.12380

Doyle JJ, Doyle JL. 1987. A rapid DNA isolation procedure for small quantities of fresh leaf tissue. Phytochemical Bulletin 19: 11–15.

Edgar RC. 2004. MUSCLE: multiple sequence alignment with high accuracy and high throughput. Nucleic Acids Research 32: 1792–1797. https://doi.org/10.1093/nar/gkh340

Fakhar-ud-Din, Mukhtar T. 2019. Morphological characterization of *Ganoderma* species from Murree Hills of Pakistan. Plant Protection 3(2): 73–84. https://doi.org/10.33804/pp.003.02.0128

Fryssouli V, Zervakis GI, Polemis E, Typas MA. 2020. A global meta-analysis of ITS rDNA sequences from material belonging to the genus *Ganoderma* (*Basidiomycota*, *Polyporales*) including new data from selected taxa. MycoKeys 75: 71–143. https://doi.org/10.3897/mycokeys.75.59872

Furtado JS. 1962. Structure of the spore of the *Ganodermoideae*. Rickia 1: 227–242.

Furtado JS. 1965. *Ganoderma colossum* and the status of *Tomophagus*. Mycologia 57: 979–984. https://doi.org/10.2307/3756901

Gottlieb AM, Ferrer E, Wright JE. 2000. rDNA analyses as an aid to the taxonomy of species of *Ganoderma*. Mycological Research 104: 1033–1045. https://doi.org/10.1017/S095375620000304X

Hapuarachchi KK, Elkhateeb WA, Karunarathna SC, Cheng CR, Bandara AR & al. 2018. Current status of global *Ganoderma* cultivation, products, industry and market. Mycosphere 9: 1025–1052. https://doi.org/10.5943/mycosphere/9/5/6

Hapuarachchi KK, Karunarathna SC, McKenzie EHC, Wu XL, Kakumyan P & al. 2019. High phenotypic plasticity of *Ganoderma sinense* (*Ganodermataceae*, *Polyporales*) in China. Asian Journal of Mycology 2: 1-47. https://doi.org/10.5943/ajom/2/1/1

He MQ, Zhao RL, Hyde KD, Begerow D, Kemler M, Yurkov A, McKenzie EHC & al. 2019. Notes, outline and divergence times of *Basidiomycota*. Fungal Diversity 99: 105–367. https://doi.org/10.1007/s13225-019-00435-4

Hennicke F, Cheikh-Ali Z, Liebisch T, Maciá-Vicente JG, Bode HB, Piepenbring M. 2016. Distinguishing commercially grown *Ganoderma lucidum* from *Ganoderma lingzhi* from Europe and East Asia on the basis of morphology, molecular phylogeny, and triterpenic acid profiles. Phytochemistry 127: 29–37. https://doi.org/10.1016/j.phytochem.2016.03.012

Hong SG, Jung HS. 2004. Phylogenetic analysis of *Ganoderma* based on nearly complete mitochondrial small-subunit ribosomal DNA sequences. Mycologia 96: 742–755. https://doi.org/10.1080/15572536.2005.11832922

Hou D. 1950. A new species of *Ganoderma* from Taiwan. Quarterly Journal of the Taiwan Museum 3: 101–105.

Imazeki R. 1939. Studies on *Ganoderma* of Nippon. Bulletin of the National Science Museum, Tokyo 1: 29–52.

Irshad M, Anwar Z, Gulfraz M, Butt HI, Ejaz A, Nawaz H. 2012. Purification and characterization of α-amylase from *Ganoderma tsugae* growing in waste bread medium. African Journal of Biotechnology 11: 8288–8294. https://doi.org/10.5897/AJB11.3643

Justo A, Miettinen O, Floudas D, Ortiz-Santana B, Sjökvist E, Lindner D, Nakasone K & al. 2017. A revised family-level classification of the *Polyporales* (*Basidiomycota*). Fungal Biology 121: 798–824. https://doi.org/10.1016/j.funbio.2017.05.010

Kirk PM, Cannon PF, Minter DW, Stalpers JA. 2008. Ainsworth & Bisby's dictionary of the fungi. 10th ed. Wallingford, CAB International. https://doi.org/10.1079/9780851998268.0000

Le XT, Le QHN, Pham ND, Duong VH, Dentinger BTM, Moncalvo JM. 2012. *Tomophagus cattienensis* sp. nov., a new *Ganodermataceae* species from Vietnam: evidence from morphology and ITS DNA barcodes. Mycological Progress. 11: 775–780. https://doi.org/10.1007/s11557-011-0789-3

Li TH, Hu HP, Deng WQ, Wu SH, Wang DM, Tsering T. 2015. *Ganoderma leucocontextum*, a new member of the *G. lucidum* complex from southwestern China. Mycoscience 56: 81–85. https://doi.org/10.1016/j.myc.2014.03.005

Loyd AL, Barnes CW, Held BW, Schink MJ, Smith ME, Smith JA, Blanchette RA. 2018. Elucidating "lucidum": distinguishing the diverse laccate *Ganoderma* species of the United States. PloS One 13(7): e0199738. https://doi.org/10.1371/journal.pone.0199738

Miller MA, Pfeiffer W, Schwartz T. 2010. Creating the CIPRES Science Gateway for inference of large phylogenetic trees. 1–8, in: Gateway Computing Environments Workshop (GCE), New Orleans. https://doi.org/10.1109/GCE.2010.5676129

Moncalvo JM. 1996. A cladistic approach to biodiversity in the *Ganodermataceae*. 75–89, in: DJ Royse (ed.). Mushroom biology and mushroom products. USA, Pennsylvania State University.

Moncalvo JM. 2000. Systematics of *Ganoderma*. 23–45, in: J Flood & al. (eds). *Ganoderma* diseases of perennial crops. Wallingford, CABI. https://doi.org/10.1079/9780851993881.0023

Moncalvo JM, Ryvarden L. 1997. A nomenclatural study of the *Ganodermataceae* Donk. Synopsis Fungorum 11. 114 p.

Moncalvo JM, Wang HF, Hseu RS. 1995. Gene phylogeny of the *Ganoderma lucidum* complex based on ribosomal DNA sequences. Comparison with traditional taxonomic characters. Mycological Research 99: 1489–1499. https://doi.org/10.1016/S0953-7562(09)80798-3

Müller J, Müller K, Neinhuis C, Quandt D. 2010. PhyDe® Phylogenetic Data Editor. http://www.phyde.de

Munsell. 1975. Munsell soil color charts. Baltimore, Munsell Color Co., Inc.

Murrill WA. 1905. *Tomophagus* for *Dendrophagus*. Torreya 5: 197.

Nagy LG, Vágvölgyi C, Papp T. 2010. Type studies and nomenclatural revisions in *Parasola* (*Psathyrellaceae*) and related taxa. Mycotaxon 112: 103–141. https://doi.org/10.5248/112.103

Posada D, Crandall KA. 1998. MODELTEST: testing the model of DNA substitution. Bioinformatics 14: 817–818. https://doi.org/10.1093/bioinformatics/14.9.817

Raja HA, Baker TR, Little JG, Oberlies NH. 2017. DNA barcoding for identification of consumer-relevant mushrooms: a partial solution for product certification? Food Chemistry 214: 383–392. https://doi.org/10.1016/j.foodchem.2016.07.052

Rambaut A, Drummond AJ, Xie D, Baele G, Suchard MA. 2018. Posterior summarisation in Bayesian phylogenetics using Tracer 1.7. Systematic Biology 67: 901–904. https://doi.org/10.1093/ sysbio/syy032

Robledo GL, Amalfi M, Castillo G, Rajchenberg M, Decock C. 2009. *Perenniporiella chaquenia* sp. nov. and further notes on *Perenniporiella* and its relationships with *Perenniporia* (*Poriales*, *Basidiomycota*). Mycologia 101: 657–673. https://doi.org/10.3852/08-040

Ronquist F, Huelsenbeck JP. 2003. MrBayes 3: Bayesian phylogenetic inference under mixed models. Bioinformatics 19: 1572–1574. https://doi.org/10.1093/bioinformatics/btg180

Ryvarden L. 2000. Studies in neotropical polypores 2: a preliminary key to neotropical species of *Ganoderma* with a laccate pileus. Mycologia 92: 180–191. https://doi.org/10.1080/00275514.2000.12061142

Ryvarden L. 2004. Neotropical polypores, part 1. Introduction, *Ganodermataceae* & *Hymenochaetaceae*. Synopsis Fungorum 19. 229 p.

Shirazi SA, Liaqut A, Shakrullah K. 2019. Analysis of temperature and precipitation trends observed at some selected districts of Punjab, Pakistan. International Journal of Economic and Environmental Geology 10(4): 51–58. https://doi.org/10.46660/ijeeg.Vol10.Iss4.2019.353

Smith BJ, Sivasithamparam K. 2000. Internal transcribed spacer ribosomal DNA sequence of five species of *Ganoderma* from Australia. Mycological Research 104: 943–951. https://doi.org/10.1017/S0953756200002458

Stamatakis A. 2006. RAxML-VI-HPC: maximum likelihood-based phylogenetic analyses with thousands of taxa and mixed models. Bioinformatics 22: 2688–2690. https://doi. org/10.1093/bioinformatics/btl446

Steyaert RL. 1962. Genus *Ganoderma* (*Polyporaceae*). Taxa nova 2. Bulletin du Jardin Botanique de l'État à Bruxelles 32: 89–104. https://doi.org/10.2307/3667315

Steyaert RL. 1972. Species of *Ganoderma* and related genera mainly of the Bogor and Leiden herbaria. Persoonia 7: 55–118.

Steyaert RL. 1980. Study of some *Ganoderma* species. Bulletin du Jardin Botanique National de Belgique 50: 135–186. https://doi.org/10.2307/3667780

Torres-Torres MG, Guzmán-Dávalos L. 2012. The morphology of *Ganoderma* species with a laccate surface. Mycotaxon 119: 201–216. https://doi.org/10.5248/119.201

Torres-Torres MG, Guzmán-Dávalos L, Ryvarden L. 2015. *Ganoderma* subgenus *Ganoderma* in Mexico. Revista Mexicana de Micología 41: 27–45.

Wang DM, Wu SH. 2008. A taxonomic revision of the *Ganodermataceae* reported from Taiwan. Mycotaxon 104: 297–308.

Wang DM, Wu SH, Su CH, Peng JT, Shih YH, Chen LC. 2009. *Ganoderma multipileum*, the correct name for '*G. lucidum*' in tropical Asia. Botanical Studies 50: 451–458.

Wang XC, Xi RJ, Li Y, Wang DM, Yao YJ. 2012. The species identity of the widely cultivated *Ganoderma*, '*G. lucidum*' (Ling-zhi), in China. PLoS One 7(7): e40857. https://doi.org/10.1371/journal.pone.0040857

Wasser SP, Weis AL. 1997. Medicinal mushrooms: *Ganoderma lucidum* (Curtis: Fr.) P. Karst., reishi mushroom. Haifa, Pedelfus Publishing House.

Welti S, Courtecuisse R. 2010. The *Ganodermataceae* in the French West Indies (Guadeloupe and Martinique). Fungal Diversity 43:103–126. https://doi.org/10.1007/s13225-010-0036-2

Welti S, Moreau PA, Decock C, Danel C, Duhal N, Favel A, Courtecuisse R. 2015. Oxygenated lanostane-type triterpenes profiling in laccate *Ganoderma* chemotaxonomy. Mycological Progress 14(45): 1-15. https://doi.org/10.1007/s11557-015-1066-7

White TJ, Bruns T, Lee S, Taylor J. 1990. Amplification and direct sequencing of fungal ribosomal RNA genes for phylogenetics. 315–322, in: MA Innis & al. (eds). PCR protocols, a guide to methods and applications. New York, Academic Press. https://doi.org/10.1016/B978-0-12-372180-8.50042-1

Xing JH, Sun YF, Han YL, Cui BK, Dai YC. 2018. Morphological and molecular identification of two new *Ganoderma* species on *Casuarina equisetifolia* from China. MycoKeys 34: 93–108. https://doi.org/10.3897/mycokeys.34.22593

Zhao JD. 1989. Studies on the taxonomy of *Ganodermataceae* in China. IX. Subgen. *Ganoderma* sect. *Ganoderma*. Acta Mycologica Sinica 8: 25–34.

Zhou LW, Cao Y, Wu SH, Vlasák J, Li DW, Li MJ, Dai YC. 2015. Global diversity of the *Ganoderma lucidum* complex (*Ganodermataceae, Polyporales*) inferred from morphology and multilocus phylogeny. Phytochemistry 114: 7–15. https://doi.org/10.1016/j.phytochem.2014.09.023

MYCOTAXON

ISSN (print) 0093-4666 (online) 2154-8889 Mycotaxon, Ltd. ©2022

January–March 2022—Volume 137, pp. 153–169

https://doi.org/10.5248/137.153

Marasmius tageticolor and *M. tucumanus* from the Dominican Republic

Nicolás Niveiro[1*], Natalia A. Ramírez[1], Claudio Angelini[2,3]

[1] *Instituto de Botánica del Nordeste, IBONE (UNNE–CONICET), Facultad de Ciencias Exactas y Naturales y Agrimensura, Universidad Nacional del Nordeste (FACENA-UNNE), Sargento Cabral 2131, CC 209 Corrientes Capital, CP 3400, Argentina*

[2] *Via Cappuccini 78/8, I-33170 Pordenone, Italy*

[3] *National Botanical Garden of Santo Domingo, Santo Domingo, Dominican Republic*

[*] Correspondence to: *niconiveiro@gmail.com*

Abstract—Two purple *Marasmius* species from the Dominican Republic are described and illustrated. *Marasmius tageticolor* is characterized by its radially striped pileus, distant lamellae, and elongated spores, and *M. tucumanus* is characterized by its purple to dark red pileus, fragile basidioma, and small spores. Both species were sequenced for the first time and phylogenetically resolved to *Marasmius* sect. *Globulares,* closely related to species of *M.* ser. *Haematocephali* + *M.* ser. *Leonini.*

Key words—*Agaricales*, ITS, *Marasmiaceae*, mushroom, diversity

Introduction

Marasmius tageticolor and *M. tucumanus* are members of *M.* sect. *Globulares* (Antonín & Noordeloos 2010, Oliveira & al. 2020), characterized by the purple coloration of their pileus surface (Singer 1976). *Marasmius tageticolor* is a relatively well-known species from the Caribbean and northern South America, but there are no complete modern descriptions or publicly available sequences. On the other hand, *M. tucumanus* has been found only once, as the type material from northwestern Argentina that has not been illustrated or sequenced. The aim of this work is to describe and

illustrate both species, evaluate their phylogenetic relationship, and expand their range of distribution to the Dominican Republic.

Materials & methods

Morphological studies

The specimens, which were collected on litter from man-made lowland deciduous woods in the Dominican Republic, were photographed and described macroscopically in situ. The specimens were analyzed macro- and microscopically following the criteria and terminology proposed by Vellinga (1988) and Lodge & al. (2004). Color terminology follows Kornerup & Wanscher (1978). For microscopic analysis, tissue sections were made freehand and mounted in a solution of 5% KOH (v/w) with 1% phloxine aqueous solution. Melzer's reagent (Wright & Albertó 2002) was used to verify amyloidity. The microscopic structures were measured directly through a 1000× oil-immersion objective or photographs taken with a Leica EC3 built-in camera using ImageJ software (Schneider & al. 2012). The notation "L" refers to the number of true lamellae (extending from the stipe insertion to the pileus margin) counted at the margin of the pileus. The minimum-maximum interval was provided for the different microscopic structures. For basidiospores, n = number of spores measured, x = mean spore length × width, Q= length / width ratio, and Qx = mean Q value. The authors of scientific names agree with Index Fungorum (2020), and herbarium acronyms follow Thiers (2020). The collected material was dried at 40 °C and stored in a freezer for a week before being deposited in the Jardín Botánico Nacional Dr. Rafael M. Moscoso (JBSD) and in the Instituto de Botánica del Nordeste herbaria (CTES).

DNA extraction, amplification, sequencing

Genomic DNA was extracted from dried specimens implementing a modified CTAB protocol based on Murray & Thompson (1980). For PCR reactions, we followed the recommended cycling condition by Mullis & Faloona (1987). Primers ITS1F and ITS4 (White & al. 1990, Gardes & Bruns 1993) were employed to amplify the ITS rDNA region. PCR products were checked in 1% agarose gels and positive reactions were sequenced with one or both PCR primers. DNA extraction, amplification, and sequencing were performed by Alvalab (Spain). Sequences were edited using BioEdit 7.2.5 (Hall 1999).

Phylogenetic analysis

The nrITS dataset compiled included our three new sequences and 44 *Marasmius* sequences selected from GenBank based on BLAST results and previous studies (Table 1). *Crinipellis zonata* (Peck) Sacc. was used as outgroup (Aime & Phillips-Mora 2005). Sequences were aligned with MAFFT 7 (Katoh & Standley 2013) under the Q-INS-i criteria. The alignment was manually adjusted with MEGA 5 (Tamura & al. 2011). Potential ambiguously aligned ITS1-ITS2 segments were detected and deleted using Gblocks 0.91b (Castresana 2000).

Table 1: *Marasmius* and outgroup sequences used in the phylogenetic analyses. Sequences obtained in this study are in bold.

Species	Series	Voucher	GenBank #	Reference
Crinipellis zonata		VPI3355	AY916692	Aime & Phillips-Mora 2005
M. sect. *Marasmius*				
M. rotalis	*Marasmius*	JES145	KX149000	Shay & al. 2017
		JES141	KX148999	Shay & al. 2017
M. cf. *subruforotula*	*Sicciformes*	JES186	KX149017	Shay & al. 2017
		JES192	KX149018	Shay & al. 2017
M. tubulatus	*Marasmius*	TYS502	FJ431280	Tan & al. 2009
		TYS518	FJ431279	Tan & al. 2009
M. sect. *Globulares*				
M. maximus	*Globulares*	KG224	FJ904974	Antonín & al. 2010
		BRNM714571	FJ904977	Antonín & al. 2010
M. nivicola	*Globulares*	BRNM714575	FJ904972	Antonín & al. 2012
		BRNM714572	FJ904970	Antonín & al. 2010
M. pseudo-purpureostriatus	*Globulares*	NW286	EU643513	Wannathes & al. 2009
M. purpureostriatus	*Globulares*	BRNM714566	FJ904978	Antonín & al. 2010
M. corrugatiformis	*Atrorubentes*	DED8233	KX953757	Shay & al. 2017
		DED8326	KX953756	Shay & al. 2017
M. cystidiatus	*Atrorubentes*	1672	MH2160421	Sharafudheen & Manimohan 2018
		CAL1669	MH216191	Sharafudheen & Manimohan 2018
M. ochroleucus	*Atrorubentes*	LE 295978	KF912952	Kiyashko & al. 2014
M. strobiluriformis	*Atrorubentes*	BRNM714914	GU266263	Antonín & al. 2012
		BRNM714915	GU266264	Antonín & al. 2012
M. bondoi	*Haematocephali*	NW320	EU935474	Wannathes & al. 2009
M. confertus var. *tenuicystidiatus*	*Haematocephali*	BRNM718808	HQ607374	Antonín & al. 2012
M. haematocephalus	*Haematocephali*	NW434	EU935529	Wannathes & al. 2009
		NW430	EU935535	Wannathes & al. 2009
M. magnus	*Haematocephali*	ICN179252	KX228848	Magnano & al. 2016
		FLOR55963	KX228846	Magnano & al. 2016
M. siccus	*Haematocephali*	BRNM552709	HQ607384	Wannathes & al. 2009
		LE295980	KF774130	Kiyashko & al. 2014
M. sullivantii	*Haematocephali*	MO218479	MK607492	Russell & Grootmyers (unpub.)

Species	Series	Voucher	GenBank #	Reference
M. acerosus	*Leonini*	TYS427	FJ431214	Tan & al. 2009
		TYS458	FJ431213	Tan & al. 2009
M. adhaesus	*Leonini*	TYS467	FJ431216	Tan & al. 2009
		TYS464	FJ431217	Tan & al. 2009
M. olivascens	*Leonini*	TYS424	FJ431266	Tan & al. 2009
		TYS426	FJ431265	Tan & al. 2009
M. plicatulus	*Leonini*	NW439	EU935480	Wannathes & al. 2009
M. tageticolor	***Leonini***	**JBSD130776**	**MT260146**	**This paper**
		JBSD130775	**MT260147**	**This paper**
M. tucumanus	***Leonini***	**JBSD130778**	**MT260145**	**This paper**
M. dendrosetosus	*Spinulosi*	JES205	KX148995	Shay & al. 2017
		JES211	KX148996	Shay & al. 2017
M. longisetosus	*Spinulosi*	JO248	JX424040	Oliveira & al. 2014
M. neotrichotus	*Spinulosi*	CTES0568167	MF683958	Niveiro & al. 2018
M. nummularius	*Spinulosi*	NW266	EU935492	Wannathes & al. 2009
		NW396	EU935493	Wannathes & al. 2009
M. paratrichotus	*Spinulosi*	DED8248	KX953749	Grace & al. 2019
M. trichotus	*Spinulosi*	NW262	EU935490	Wannathes & al. 2009
		NW263	EU935491	Wannathes & al. 2009

Phylogenetic reconstruction was inferred using Maximum Likelihood (ML) and Bayesian Inference (BI). Maximum likelihood was carried out in RAxML-HPC v.8 (Stamatakis 2014), employing the GTRGAMMA model for the entire dataset. The analyses first implemented 1000 ML independent searches, each one starting from one randomized stepwise addition parsimony tree. Only the best scored ML tree was kept, and node reliability was accessed through nonparametric Bootstrap (BS) pseudoreplicates under the same model, allowing the program to halt bootstrapping automatically using the autoMRE option.

Bayesian Inference was performed in MrBayes 3.2.6 (Ronquist & al. 2012). The evolutionary model for BI was estimated using Akaike Information Criterion (AIC) as implemented in jModelTest2 v.1.6. (Guindon & Gascuel 2003, Darriba & al. 2012). We implemented two independent runs, each one beginning from random trees, with four simultaneous independent chains. A total of 2×10^7 generations was carried out, sampling one tree every 1×10^3 generation. All phylogenetic analyses were conducted via CIPRES Science Gateway (Miller & al. 2010). Both analyses (ML and BI) produced similar topology trees. Only the BI 50% majority-rule consensus tree is shown, indicating support values Bayesian posterior probabilities (BPP) / rapid bootstrapping (BS) of each node. A node is considered strongly supported if it showed a BPP ≥0.98 and/or BS ≥90%; moderate support is indicated by BPP ≥0.95 and/or BS ≥70%.

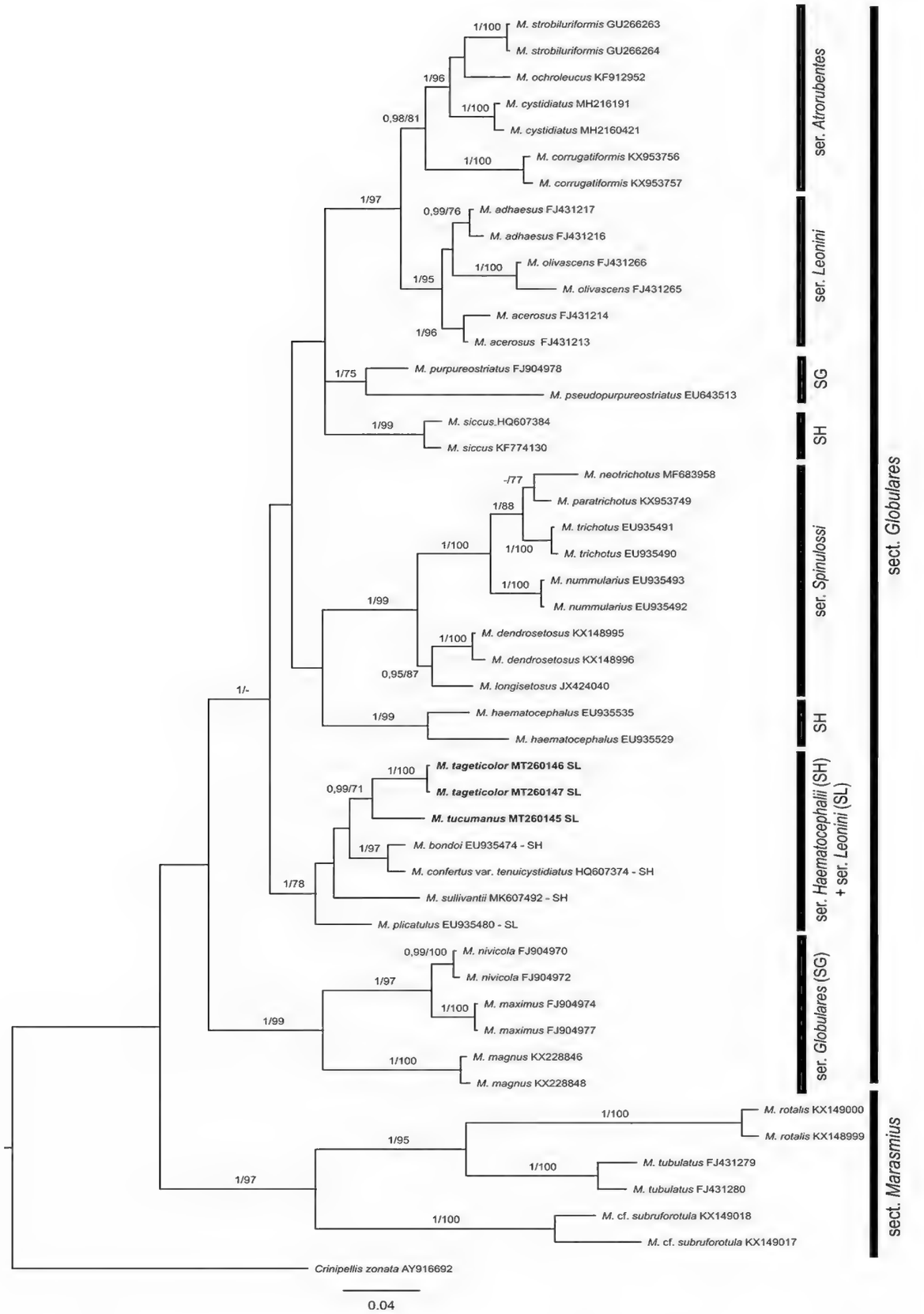

Fig. 1: 50% majority-rule consensus tree from Bayesian Inference based on a dataset of nrITS sequences of *Marasmius* taxa. Bayesian posterior probability BPP ≥0.9, and Bootstrap value, BS ≥70% are shown.

Phylogenetic results

The nrITS dataset included 48 sequences from 29 *Marasmius* taxa plus the outgroup, resulting in an alignment with 728 characters, of which 296 are parsimony informative.

Our phylogenetic inference (Fig. 1) recovered two major, well-defined clades: *M.* sect. *Marasmius* (BPP = 1; BS = 97%) and *M.* sect. *Globulares* (BPP = 0.93). Within *M.* sect. *Globulares*, five moderately to highly supported subclades are recognized: *M.* ser. *Globulares* (BPP = 1; BS = 99%), *M.* ser. *Atrorubentes* (BPP = 0.98; BS = 81%), *M.* ser. *Leonini* (BPP = 1; BS = 95%), *M.* ser. *Spinulosi* (BPP = 1; BS = 99%) and *M.* ser. *Haematocephali* + *M.* ser. *Leonini* (BPP = 1; BS = 78%).

Our target species, *M. tageticolor* and *M. tucumanus*, are sisters (BPP = 0.99; BS = 71%) and closely related to *M. bondoi* Wannathes & al. and *M. confertus* var. *tenuicystidiatus* Antonín within the subclade of *M.* ser. *Haematocephali* + *M.* ser. *Leonini*.

Taxonomy

Marasmius tageticolor Berk.,
Hooker's J. Bot. Kew Gard. Misc. 8: 136. 1856. Figs 2, 3

Basidiomata gregarious, in small groups. Pileus ≤20 mm broad, campanulate to convex when young, then convex to broadly convex, umbonate or with depressed center, sulcate up to the center in all stages of development, with slightly crenate edge; surface striped in pigmentation (the colored stripes correspond to the lamellae and lamellulae lines), center and radial stripes purple (13E8 "deep magenta" to 13F8 "dark magenta") usually with lighter marginal zones (13C6–7 "greyish magenta"), and white (1A1), pinkish-white (13A2) to pinkish (13A3) between stripes, brown (7E5) to dark brown (7F5) with light yellow (4A4) to light orange (5A4) stripes in dehydrated specimens; dry, subvelutinous, dull. Context thin, whitish (13A1), odor and taste not distinctive. Lamellae free to narrowly adnexed, broadly ventricose, ≤5 mm, distant, L = 8–9, white (13A1) at the marginal edge, pink (13A3) to purplish red (13A6) towards the pileus; usually with one series of lamellulae between lamellae. Stipe 15–45 × 1–1.5 mm, central, cylindrical thin, flared upwards, hollow, surface reddish purple brown (9D7–9E7 "reddish-brown"), lilac (13C7, "purplish red") towards the apex, blackish (8F4 "greyish brown to 14F8 "dark purple") towards the base, glabrous, dry, with a whitish ochre (5B3–4 "greyish orange") basal mycelial patch. Annulus absent. Spore-print not observed.

Fig. 2: *Marasmius tageticolor,* macroscopic views: a. JBSD130776; b. JBSD130775; c. Detail of basal mycelial patch. Scale bars: a, b = 10 mm. (Photo by C. Angelini).

Basidiospores 14–21.8 × 3–4(–4.5) µm, x = 18.8 × 3.4 µm, Q = 3.5–7.1, Qx = 5.5, n = 25; oblong, acicular to narrowly clavate, with suprahilar depression, inamyloid, hyaline, smooth, thin-walled. Basidia 22–25 × 5–6.5 µm, clavate, 4-spored, hyaline, thin-walled. Basidioles 15–25 × 5–6.5 µm, narrowly clavate to fusoid, hyaline, thin-walled. Pleurocystidia absent. Cheilocystidia in form of *Siccus*-type broom cells, hyaline, with main body claviform, 9–15 × 4.5–6 µm, setulae ≤6 µm long, and base 1 µm diam. Hymenophoral trama subregular, hyphae 3–5(–9) µm diam., hyaline, thin-walled, dextrinoid. Pileipellis hymeniform, comprising *Siccus*-type broom cells with main body claviform, 9.5–11.5 × 5–7 µm, setulae ≤7 µm long, and bases 1.5 µm diam.; hyaline in lighter or discolored interlamellar region, stramineous in the pigmented region. Pileocystidia absent. Stipitipellis a cutis of smooth hyphae, stramineous, appressed, 3–4 µm diam. Caulocystidia absent. Clamp connections present.

Ecology— Forming small groups on dried dicotyledonous twigs and leaves in the litter.

Specimens examined—**DOMINICAN REPUBLIC: Puerto Plata Province, Sosua,** Puerto Chiquito, on the litter of an anthropized plain forest with broad-leaved trees, 8/8/2011, leg. C. Angelini 714 (JBSD130775!, GenBank MT260147; CTES!); 5/12/2013, leg. C. Angelini 291 (JBSD130776!, GenBank MT260146; CTES!).

Distribution—Originally described from northwestern Amazonas State, Brazil (Berkeley 1856); also known from Venezuela, Mexico (Singer 1976), Panama (Desjardin & Ovrebo 2006), Colombia (Vasco-Palacios & al. 2005), and USA, Trinidad and Tobago, St. Vincent and the Grenadines (GBIF 2020). Newly recorded from the Dominican Republic.

Comments—*Marasmius tageticolor* is characterized by its pileus surface, which is conspicuously radially striped with a purple-red to purple center and lamellar stripes, interspersed with lighter interlamellar regions, distant lamellae, and elongated spores (Singer 1976). The *Siccus*-type broom cells of the pileipellis and the absence of pleurocystidia place this species in *M.* sect. *Globulares* (Antonín & Noordeloos 2010) and *M.* ser. *Leonini* (Singer 1976).

A striped pileus is not a frequent feature in *M.* ser. *Leonini* (Antonín 2007). *Marasmius poecilus* Berk., found in Bolivia, Brazil, and Venezuela, is the closest species and occasionally considered a synonym (Singer 1965). However, Singer (1976) highlighted fine differences to separate these two species, such as the more darkly colored pileus (purplish brown to fulvous with white to yellow stripes), and longer (35–80 mm) stipe in *M. poecilus* (Singer 1976).

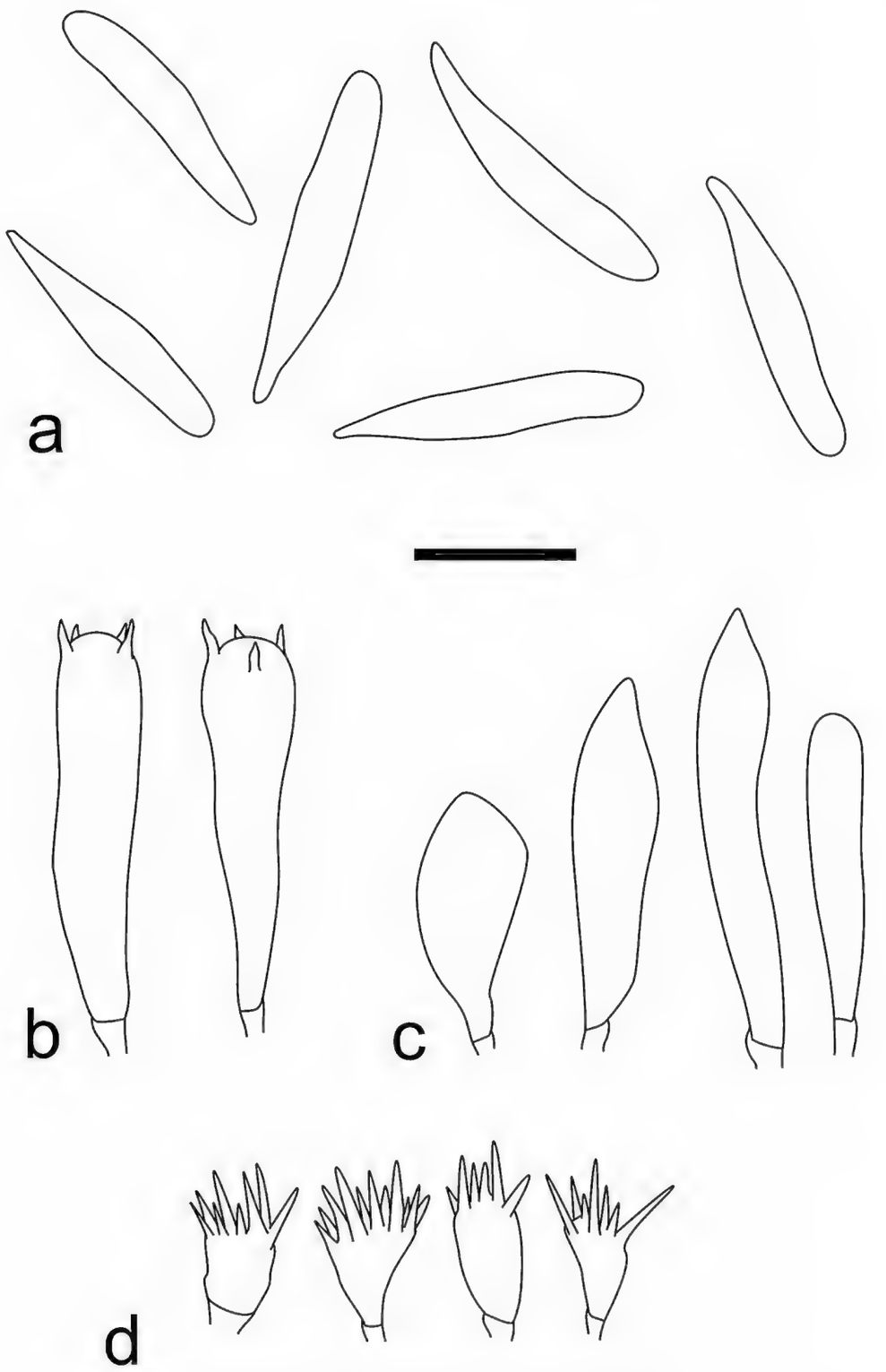

Fig. 3: *Marasmius tageticolor* (JBSD130775).
a. Basidiospores; b. Basidia; c. Basidioles; d. Cheilocystidia. Scale bar = 10 μm.

Another striped Neotropical species is *M. phaeus* Berk. & M.A. Curtis, but it clearly differs by its dark reddish-brown coloration, lacking a purple hue (Singer 1976). Some African striped taxa such as *M. lilacinoalbus* Beeli var.

lilacinoalbus and *M. lilacinoalbus* var. *lilacinocarmineus* Singer are similar to *M. tageticolor* but differ in their yellowish pileus center and broader spores (4–5 µm; Antonín 2007). *Marasmius striipileus* Antonín has orange brown (6C8) to brown (6D8) tints with paler stripes (Antonín 2004), but differs in the absence of marked streaks with white, yellowish or with pink tints (Antonín 2007).

Berkeley (1856) described *M. tageticolor* (based on dehydrated material and black and white drawings submitted by Spruce from Brazil) as "convex, membranaceus, umbonate, varying from reddish-brown to deep crimson, adorned with from eight to ten yellow rays, very minutely wrinkled… Gills narrow, ventricose, attenuated behind and free, yellow like the rays." Over a century later, Singer (1965) reported specimens of *M. tageticolor* having brown pileus with deep cream radial stripes and lamellae based on the type material (Spruce 37 K) and additional material from Bolivia (Singer B 1981 LIL) that was later identified as *M. poecilus* (Singer 1976). In that same work and with additional material from Mexico and Venezuela, Singer (1976) described *M. tageticolor* with red pileus and white to ochraceous-whitish stripes and white lamellae. More recently, Desjardin & Ovrebo (2006) described *M. tageticolor* based on specimens from Panama having a light buff pileus surface with beet red (11–12E–F–8) stripes. The specimens analyzed here agree with those described by Desjardin & Ovrebo (2006), but they present some minor differences compared with the protologue (Berkeley 1856) and descriptions made by Singer (1965, 1976), primarily regarding the color of the pileus and lamellae. Pigment variations may be due to different developmental stages, humidity, or observations based on dehydrated materials in which the lamellae and pileus stripes have yellowed. Despite these variables, the remaining characteristics agree with the concept of *M. tageticolor*. Likewise, the pigmentation of the specimens studied here and those described by Desjardin & Ovrebo (2006) are similar to *M. haematocephalus* var. *pseudotageticolor* Singer, with which they could easily be confused, although the *M. haematocephalus* variety differs by the presence of pleurocystidia and the insititious or subinsititious stipe base (Singer & Digilio 1952 as "*M. tageticolor*"; Singer 1959, 1965, 1976).

Marasmius tucumanus Singer,
Lilloa 25: 206. 1952. Figs 4, 5

Basidiomata solitary or in small groups. Pileus ≤15 mm broad, campanulate to convex with papillate center, striate-sulcate up to the center,

Fig. 4: *Marasmius tucumanus,* macroscopic views: a, b. JBSD130777; c. JBSD130778; d. Detail of basal mycelial patch. Scale bars: a–c = 10 mm. (Photo by C. Angelini).

with entire to crenate edge, dark purple (11E7, 11F7 "violet brown") at the center, lighter towards the margin, from vivid purple red (11A8, "vivid red") to dark red (11C8); dry, subvelutinous, sometimes pruinose, mostly dull or semi-translucent at the margin. Context thin, whitish (13A1), odor and taste not distinctive. Lamellae free to narrowly adnexed, ventricose, ≤2 mm, distant, L = 11–15, white (11A1) at the marginal edge, pink (12A3–4) towards the pileus; with 3–4 series of lamellulae. Stipe 20–40 × 1.5 mm, central, cylindrical, equal, hollow, surface purple red (10A8 "vivid red") when young, to violet brown (10F8) when mature, glabrous, dry, with a tomentose, whitish ochre (5B3–4, "greyish orange") basal mycelial patch. Annulus absent. Spore-print not observed.

Basidiospores 10–15 × 3–4.5 µm, x = 13.2 × 3.7 µm, Q = 3.0–4.0, Qx = 3.5, n = 15; oblong, subclavate, with attenuated suprahilar depression, inamyloid, hyaline, smooth, thin-walled. Basidia 22–27 × 6–7.5 µm, clavate, 4-spored, hyaline, thin-walled. Basidioles 15.5–34.5 × 4–6 µm, narrowly clavate to fusoid, hyaline, thin-walled. Pleurocystidia absent. Cheilocystidia in form of *Siccus*-type broom cells, stramineous colored with main body claviform, 11–19 × 5–9.5 µm, setulae ≤7 µm long, and base 1.5 µm diam. Hymenophoral trama subregular, hyphae 1.5–3.5 µm diam., thin-walled, dextrinoid. Pileipellis hymeniform, comprising *Siccus*-type broom cells with main body claviform, 15–22 × 6–7.5 µm, hyaline with ≤7 µm long setulae and base 1.5 µm diam. with stramineous coloration. Pileocystidia absent. Stipitipellis an appressed cutis of smooth stramineous hyphae, 3–6 µm diam. Caulocystidia absent. Clamp connections present.

Ecology—Solitary or forming small groups on dried leaves or small twigs of dicotyledonous litter.

Specimens examined—**DOMINICAN REPUBLIC, Puerto Plata Province, Sousa,** Vertedero, on the litter of an anthropized hill forest with broad-leaved trees, 6/12/2013, leg. C. Angelini 136 (JBSD130777!; CTES!); Puerto Chiquito, on the litter of an anthropized plane forest with broad-leaved trees, 13/12/2014, leg. C. Angelini 503 (JBSD130778!, GenBank MT260145; CTES!). **ARGENTINA, Tucumán Province, Tafí,** Parque Aconquija, 13/03/1951, leg. R. Singer T1460 (holotype, LIL!).

Distribution—Previously known only from the type locality, in Argentina (Singer & Digilio 1952). Newly recorded from the Dominican Republic.

Comments—*Marasmius tucumanus* is characterized by its relatively fragile basidiome, purple to dark red coloration, and spores smaller than those of its most closely related taxa: *M. tageticolor* or *M. haematocephalus* complex (Singer & Digilio 1952). The type specimen (Singer T1460 LIL!) consists of

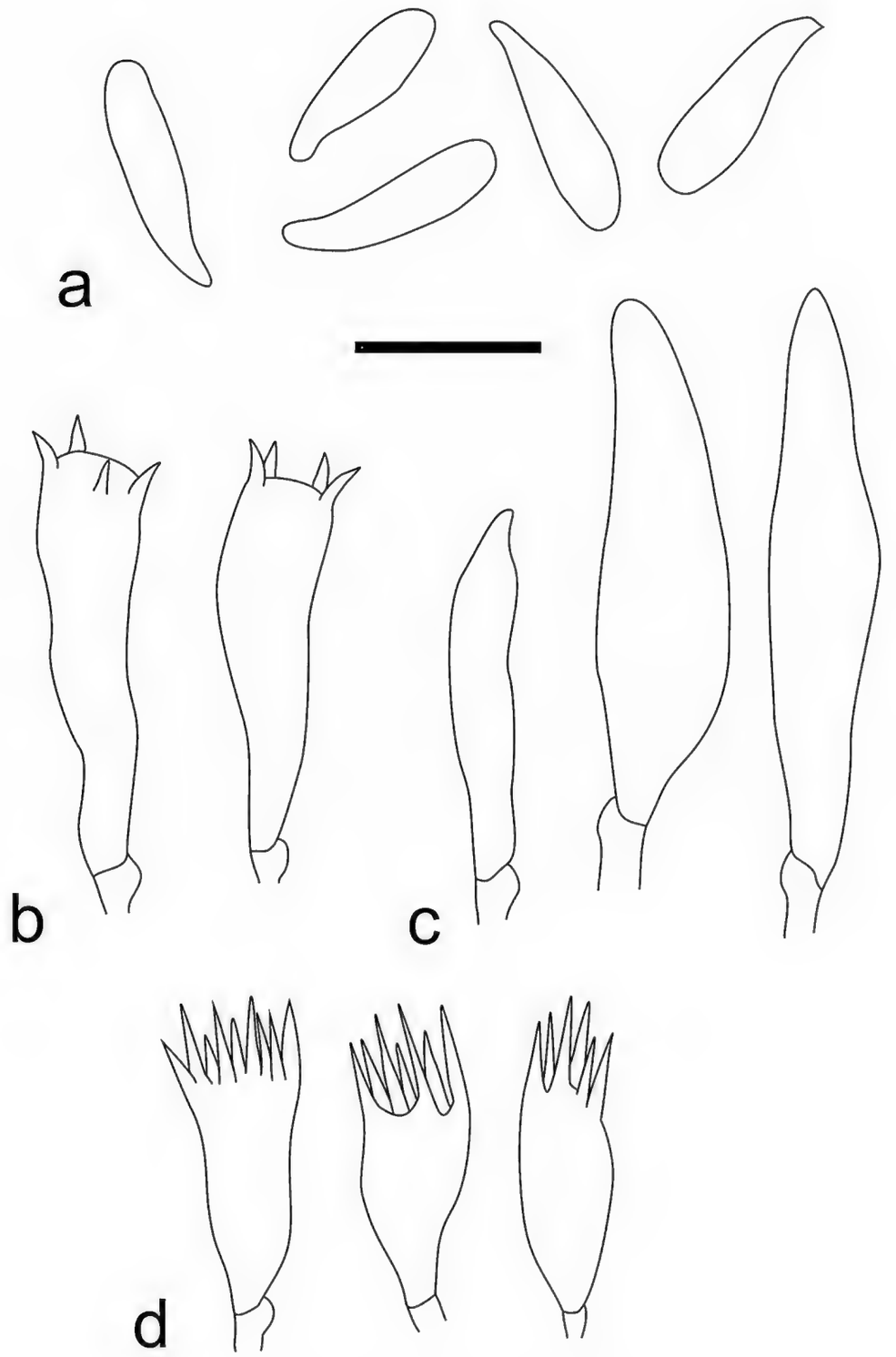

Fig. 5: *Marasmius tucumanus* (JBSD130777).
a. Basidiospores; b. Basidia; c. Basidioles; d. Cheilocystidia. Scale bar = 10 µm.

a single, well-preserved specimen with macroscopic features that agree with the characters cited in its protologue. Unfortunately, it was not possible to

determine whether the microscopic structures are the same, as destructive sampling of the type specimen is not allowed.

The presence of purple pigment in the pileus is considered an important feature by different authors in delimiting groups of species (Singer 1976, Desjardin & al. 2000, Tan & al. 2009, Wannathes & al. 2009, Shay & al. 2017). Species with similar pigmentation in *M.* ser. *Leonini* are: 1) *M. tageticolor*, which differs by its peculiar striped pileus and elongated basidiospores (Singer 1976, Desjardin & al. 2000); 2) *M. amazonicus* Henn., known from Bolivia and Brazil, which is distinguished by its larger (16–58 mm) pileus with oval to irregularly rounded buff-colored dots (Oliveira & al. 2008); 3) *M. purpureotinctus* Antonín & P. Roberts, an African species, which differs by its larger (17.5–20 × 4.5–5.7 µm) basidiospores and its pileipellis with thick-walled broom-cells (Antonín 2013); and 4) *M. aratus* Massee [≡ *M. masseei* Tkalčec & Mešić] from southeastern Asia, which differs by larger spores (22–32 × 3.5–5 µm; Tan & al. 2009). The *M. haematocephalus* complex also resembles *M. tucumanus* in pileal shape and coloration. However, all its taxa have well differentiated pleurocystidia and larger spores (14–25 × 3.5–6 µm; Singer 1976, Tan & al. 2009, Wannathes & al. 2009, Shay & al. 2017).

Discussion

Marasmius tageticolor and *M. tucumanus* are sister species in the phylogenetic tree (Fig. 1) and closely related to some species belonging to the traditional *M.* ser. *Haematocephali* + M. ser. *Leonini*. This clade has been consistently recovered in different papers (Wannathes & al. 2009, Magnano & al. 2016, Shay & al. 2017, Grace & al. 2019). Among the other species in this clade included in our analyses, *M. bondoi, M. confertus* var. *tenuicystidiatus,* and *M. sullivantii* Mont. lack a purple pileus and have pleurocystidia (Antonín 2004, Wannathes & al. 2009), while *M. plicatulus* Peck has more robust basidiomata, a dark reddish brown, minutely velutinous pileus surface, and wider basidiospores (4.8–6.3 µm; Desjardin 1987).

Acknowledgments

The authors wish to thank J.J.S. Oliveira (Instituto Nacional de Pesquisas da Amazônia, Rio de Janeiro) and R.A. Koch (University of Nebraska at Lincoln, USA) for their critical revision of the manuscript, C. Salvador Montoya for his advice on phylogenetic analysis, A. Michlig for a preliminary manuscript revision, and A. Hladky and P. Medina from LIL for photographs of the *M. tucumanus* type specimens. CA wishes to thank Ricardo G. García, Francisco Jiménez, Brígido

Peguero (Jardín Botánico Nacional) and Dr. Rafael M. Moscoso (Santo Domingo, Dominican Republic) for their interest and encouragement in studying fungi of the Dominican Republic and for their active cooperation in providing herbarium material preserved in their institution. NN acknowledges the support of the Consejo Nacional de Investigaciones Científicas y Técnicas (CONICET) from Argentina (PIP 2014-0714), the Secretaría General de Ciencia y Técnica, Universidad Nacional del Nordeste (SGCyT-UNNE - PI19-P001), and the Agencia Nacional de Promoción Científica y Tecnológica (PICT 2016-2529) that made this work possible with their funding.

Literature cited

Aime MC, Phillips-Mora W. 2005. The causal agents of witches' broom and frosty pod rot of cacao (chocolate, *Theobroma cacao*) form a new lineage of *Marasmiaceae*. Mycologia 97(5): 1012–1022. https://doi.org/10.1080/15572536.2006.11832751

Antonín V. 2004. New species of marasmioid genera (*Basidiomycetes*, *Tricholomataceae*) from tropical Africa III. *Marasmius* sect. *Globulares*. Mycotaxon 89: 399–422.

Antonín V. 2007. Fungus flora of tropical Africa. Vol. 1. Monograph of *Marasmius*, *Gliocephala*, *Palaeocephala* and *Setulipes* in tropical Africa. Meise Botanical Garden. Available in: https://www.ffta-online.org/ffta1/

Antonín V. 2013. Supplements to the monograph of tropical African species of *Marasmius* (*Basidiomycota, Marasmiaceae*). Cryptogamie, Mycologie 34(2): 113–135. https://doi.org/10.7872/crym.v34.iss2.2013.113

Antonín V, Noordeloos ME. 2010. A monograph of marasmioid and collybioid fungi in Europe. IHW-Verlag, Eching. 480 p.

Antonín V, Ryoo R, Shin HD. 2010. Marasmioid and gymnopoid fungi of the Republic of Korea. 2. *Marasmius* sect. *Globulares*. Persoonia 24: 49–59.

Berkeley MJ. 1856. Decades of fungi. Decades LL–LIV. Rio Negro fungi. Hooker's Journal of Botany and Kew Garden Miscellany 8: 129–144

Castresana J. 2000. Selection of conserved blocks from multiple alignments for their use in phylogenetic analysis. Molecular Biology and Evolution 17: 540–552. https://doi.org/10.1093/oxfordjournals.molbev.a026334

Darriba D, Taboada GL, Doallo R, Posada D. 2012. jModelTest 2: more models, new heuristics and parallel computing. Nature Methods 9(8): 772. https://doi.org/10.1038/nmeth.2109

Desjardin DE. 1987. New and noteworthy marasmioid fungi from California. Mycologia 79: 123–134. https://doi.org/10.1080/00275514.1987.12025378

Desjardin D, Ovrebo CL. 2006. New species and new records of *Marasmius* from Panamá. Fungal Diversity 21: 19–39.

Desjardin D, Retnowati A, Horak E. 2000. *Agaricales* of Indonesia. 2. A preliminary monograph of *Marasmius* from Java and Bali. Sydowia 52(2): 92–193.

Gardes M, Bruns TD. 1993. ITS primers with enhanced specificity of basidiomycetes: application to the identification of mycorrhizae and rusts. Molecular Ecology 2: 113–118. https://doi.org/10.1111/j.1365-294X.1993.tb00005.x

Grace CL, Desjardin DE, Perry BA, Shay JE. 2019. The genus *Marasmius* (*Basidiomycota*, *Agaricales*, *Marasmiaceae*) from Republic of Sao Tomé and Principe, West Africa. Phytotaxa 414(2): 55–104. https://doi.org/10.11646/phytotaxa.414.2.1

GBIF. 2020. *Marasmius tageticolor* Berk. In GBIF backbone taxonomy. Checklist dataset. https://doi.org/10.15468/39omei. Accessed on 2020-03-03.

Guindon S, Gascuel O. 2003. A simple, fast and accurate algorithm to estimate large phylogenies by maximum likelihood. Systematic Biology 52: 696–704. https://doi.org/10.1080/10635150390235520

Hall TA. 1999. BioEdit: a user-friendly biological sequence alignment editor and analysis program for Windows 95/98/NT. Nucleic Acids Symposium Series 41: 95–98.

Index Fungorum. 2020. Authors of fungal names. Accessed April 2020: http://www.indexfungorum.org/Names/NAMES.ASP

Katoh K, Standley DM. 2013. MAFFT Multiple sequence alignment software version 7: improvements in performance and usability. Molecular Biology and Evolution 30: 772–780. https://doi.org/10.1093/molbev/mst010

Kiyashko AA, Malysheva EF, Antonín V, Svetasheva TY, Bulakh EM. 2014. Fungi of the Russian Far East 2. New species and new records of *Marasmius* and *Cryptomarasmius* (*Basidiomycota*). Phytotaxa 186: 1–28. https://doi.org/10.11646/phytotaxa.186.1.1

Kornerup A, Wanscher JH. 1978. Methuen handbook of colour, Eyre Methuen Publishers, London. 252 p.

Lodge DJ, Ammirati JF, O'Dell TE, Mueller GM, Huhndorf SM, Wang CJ & al. 2004. Terrestrial and lignicolous macrofungi. 127–172, in: GM Mueller & al. (eds) Biodiversity of fungi, inventory and monitoring methods. Elsevier Academic Press, San Diego. https://doi.org/10.1016/B978-012509551-8/50011-8

Magnano AC, Oliveira JJS, Neves MA. 2016. *Marasmius magnus* (*Marasmiaceae*), a new species from the southern Atlantic Forest of Brazil. Phytotaxa 266(4): 271–281.

Miller MA, Pfeiffer W, Schwartz T. 2010. Creating the CIPRES Science Gateway for Inference of large phylogenetic trees. 1–8, in: Proceedings of the Gateway Computing Environments Workshop (GCE). New Orleans, LA.

Mullis K, Faloona FA. 1987. Specific synthesis of DNA in vitro via a polymerase-catalyzed chain reaction. Methods in Enzymology 155: 335–350. https://doi.org/10.1016/0076-6879(87)55023-6

Murray MG, Thompson WF. 1980. Rapid isolation of high molecular weight plant DNA. Nucleic Acids Research 8(19): 4321–4325. https://doi.org/10.1093/nar/8.19.4321

Niveiro N, Michlig A, Ramírez N, Salvador-Montoya C, Pérez L, Albertó E, Antonín V. 2018. Two new setose species of *Marasmius* from the Paraná riparian forest in Argentina. Cryptogamie, Mycologie 39: 483–506. https://doi.org/10.7872/crym/v39.iss4.2018.483

Oliveira JJS, Puccinelli C, Capelari M, Baseia IG. 2008. Neotypification of *Marasmius amazonicus*. Mycotaxon 106: 227–232.

Oliveira JJS, Moncalvo JM, Margaritescu S, Capelari M. 2020. A morphological and phylogenetic evaluation of *Marasmus* sect. *Globulares* (Globulares-Sicci complex) with nine new taxa from the Neotropical Atlantic Forest. Persoonia 44: 240–277.

Ronquist F, Teslenko M, Van der Mark P, Ayres DL, Darling A, Höhna S & al. 2012. MrBayes 3.2: efficient Bayesian phylogenetic inference and model choice across a large model space. Systematic Biology 61: 539–542. https://doi.org/10.1093/sysbio/sys029

Schneider CA, Rasband WS, Eliceiri KW. 2012. NIH image to ImageJ: 25 years of image analysis. Nature Methods 9(7): 671–675. https://doi.org/10.1038/nmeth.2089

Sharafudheen SA. Manimohan P. 2018. A new species of *Marasmius* section *Globulares* from Kerala State, India. Phytotaxa 364: 92–100. https://doi.org/10.11646/phytotaxa.364.1.6

Shay JE, Desjardin DE, Perry BA, Grace CL, Newman DS. 2017. Biodiversity and phylogeny of *Marasmius* (*Agaricales*, *Basidiomycota*) from Madagascar. Phytotaxa 292(2): 101–149. https://doi.org/10.11646/phytotaxa.292.2.1

Singer R. 1959 Studies toward a monograph of the South American species of *Marasmius*. Sydowia 12: 54–145.

Singer R. 1965 Monographic studies on South American basidiomycetes, especially those of the east slope of the Andes and Brazil. 2. The genus *Marasmius* in South America. Sydowia 18: 106–358.

Singer R. 1976. *Marasmiae* (*Basidiomycetes – Tricholomataceae*). Flora Neotropica 17. 347 p.

Singer R, Digilio APL. 1952 ["1951"]. Pródromo de la flora agaricina Argentina. Lilloa 25: 6–461.

Stamatakis A. 2014. RAxML version 8: a tool for phylogenetic analysis and post-analysis of large phylogenies. Bioinformatics 30: 1312–1313. https://doi.org/10.1093/bioinformatics/btu033

Tamura K, Peterson D, Peterson N, Stecher G, Nei M, Kumar S. 2011. MEGA5: molecular evolutionary genetics analysis using Maximum Likelihood, evolutionary distance, and maximum parsimony methods. Molecular Biology and Evolution 28: 2731–2739. https://doi.org/10.1093/molbev/msr121

Tan YS, Desjardin DE, Perry BA, Vikineswary S, Noorlidah A. 2009. *Marasmius* sensu stricto in Peninsular Malaysia. Fungal Diversity 37: 9–100.

Thiers B. 2020. Index herbariorum: a global directory of public herbaria and associated staff. New York Botanical Garden's Virtual Herbarium. http://sweetgum.nybg.org/ih/ [accessed April 2019].

Vasco-Palacios AM, Franco-Molano AE, Lopez-Quinteros CA, Boekhout T. 2005. Macromicetes (*Ascomycota, Basidiomycota*) de la región del medio Caquetá, departamentos de Caquetá y Amazonas (Colombia). Biota Colombiana 6: 127–140.

Vellinga EC. 1988. Glossary. 54–64, in: C Bas & al. (eds). Flora Agaricina Neerlandica, vol. 1. A.A. Balkema Publisher, Rotterdam.

Wannathes N, Desjardin DE, Hyde KD, Perry BA, Lumyong S. 2009. A monograph of *Marasmius* (*Basidiomycota*) from Northern Thailand based on morphological and molecular (ITS sequences) data. Fungal Diversity 37: 209–306.

White TJ, Bruns T, Lee S, Taylor J. 1990. Amplification and direct sequencing of fungal ribosomal RNA genes for phylogenetics. 315–322, in: MA Innis & al. (eds). PCR protocols: a guide to methods and applications. Academic Press, San Diego CA. https://doi.org/10.1016/B978-0-12-372180-8.50042-1

Wright JE, Albertó EO. 2002. Guía de hongos de la región pampeana I. Hongos con laminillas. Literature of Latin America (LOLA), Buenos Aires. 278 p.

MYCOTAXON

ISSN (print) 0093-4666 (online) 2154-8889 Mycotaxon, Ltd. © 2021

January–March 2022—Volume 137, p. 171

https://doi.org/10.5248/137.171

Regional annotated mycobiota new to the Mycotaxon website

Abstract—The 14-page mycobiota reporting on new records of *Chaetomium* and *Chaetomium*-like species on *Syagrus coronata* from the Caatinga in Bahia, Brazil by Fortes & Vitória may now be downloaded from Mycotaxon's mycobiota webpage. This well-illustrated range extension, which includes a key to 8 species, brings to 153 the number of free-access fungae uploaded or linked to

http://www.mycotaxon.com/mycobiota/index.html

SOUTH AMERICA

Brazil

Nilo Gabriel Soares Fortes & Nadja Santos Vitória. New records of *Chaetomium* and *Chaetomium*-like species (*Ascomycota, Chaetomiaceae*) on *Syagrus coronata* from the Raso da Catarina Ecological Station (ESEC), Caatinga, Bahia, Brazil. 14 p.

Abstract—Studies on the mycobiota associated with the plants of family *Arecaceae* are scarce in Brazil, especially in semiarid ecosystems within the Caatinga domain, which comprises a unique biodiversity. During field expeditions to the Raso da Catarina Ecological Station, we found six new records of *Chaetomium* and *Chaetomium*-like species for the Caatinga domain in the State of Bahia. These fungi were colonizing vegetative and reproductive structures of *Syagrus coronata* (Mart.) Becc., a palm tree endemic to the Caatinga and particularly important for animals and people from this region. We present morphological descriptions, illustrations, comments, and distribution maps for the fungal species associated with *S. coronata.*

Key words—*Arecaceae,* biodiversity, fungi, licuri, semiarid, taxonomy

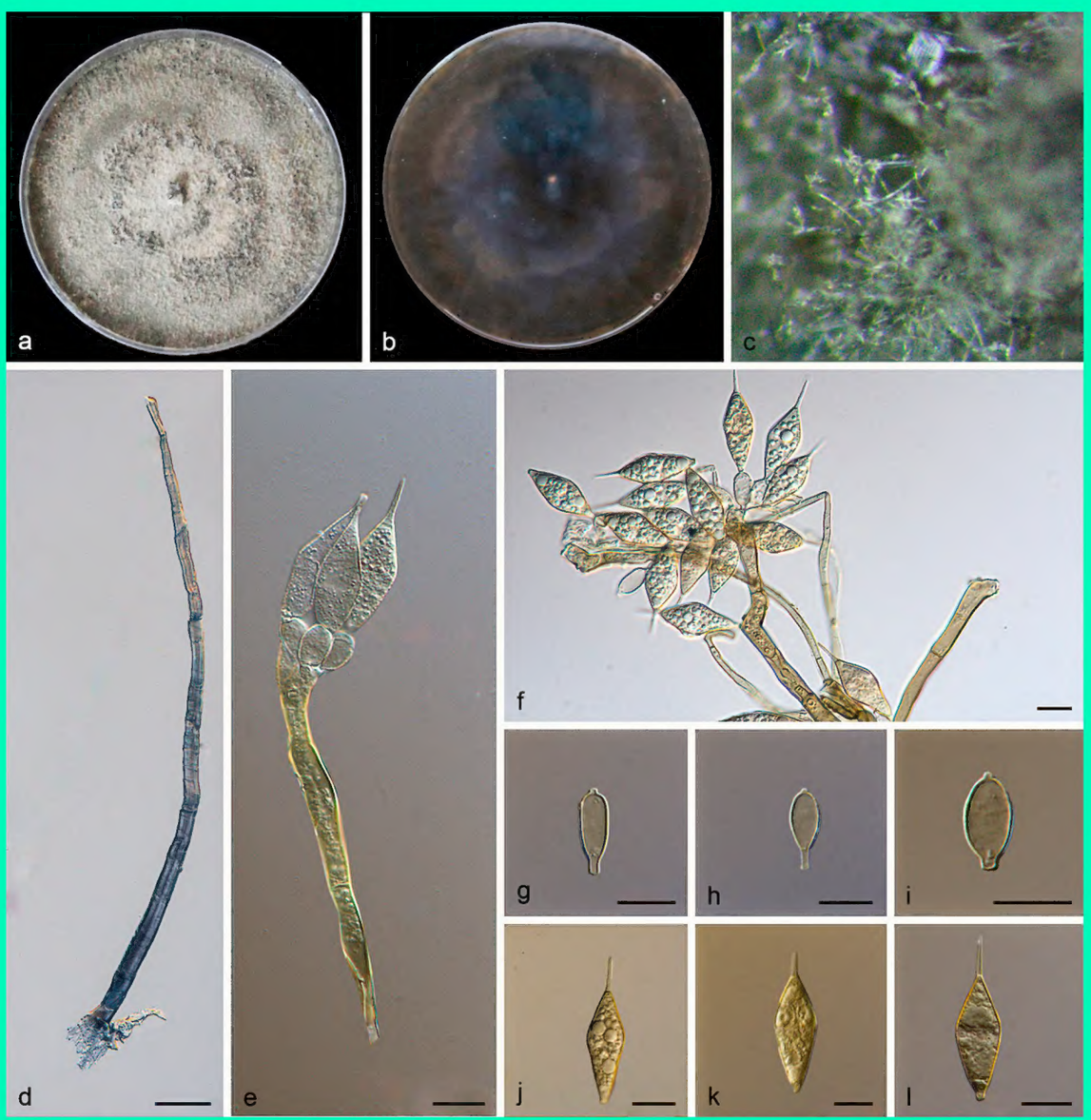

Beltrania shenzhenica sp. nov.

(Zhang & al.— Fig. 2, p. 37)